ABSTRACT

HAMZA, MOSTAFA. Causal Framework for Modeling Dependencies of Human Failure Events in Nuclear Power Plants: Single-Unit, Multi-Unit, and Multi-Module Perspectives (Under the direction of Dr. Mihai A. Diaconeasa).

The impact of human intervention has been recognized in probabilistic risk assessment (PRA) ever since its inception in the 1960s. The first reactor safety study, WASH-1400, highlighted the significance of human actions in nuclear power plant (NPP) accident scenarios. For instance, sequence $AH - \varepsilon$'s frequency, a potential source of radioactive releases, heavily relies on the probability of operators properly aligning systems. Even within WASH-1400's human reliability analysis (HRA) model, human failure events (HFE) are not deemed independent, highlighting the risks of assuming such independence, which may lead to unrealistically small human error probabilities (HEP). The technique of human error-rate prediction (THERP) further emphasizes that one human action failure may increase the subsequent failure probabilities. Consequently, subsequent HRA methodologies have integrated modeling approaches to assess dependencies between HFEs within the PRA model.

Despite numerous HRA methodologies, dependency analysis modeling progress has been slow since THERP's dependence model. Current HRA methodologies generally adopt one of two approaches for modeling dependencies: a multi-point continuum with varying levels of dependency or linked Bayesian networks. While differing significantly, both holistically model HFEs as basic events, quantifying their HEPs and adjusting them to reflect the impact dependency. Alongside other methodology-specific limitations, this holistic treatment of HFEs presents a shortcoming of the state-of-the-art dependency analysis. In Generation IV NPPs, the reliance on human intervention in safety-related actions is expected to decrease significantly, reducing the number of operators required within a shared control room of multi-module small modular reactors

(SMR). By reducing the number of operators needed per module of SMR, the operation and maintenance (O&M) cost can be significantly reduced compared with current multi-unit light-water reactors (LWR) that integrate several units with their control room into a single complex. In multi-unit and multi-module NPPs, the impact of HFEs and their dependencies becomes more extensive and interconnected. However, limited efforts have been made to model dependencies between HFEs in multi-unit NPPs, while multi-module dependency analysis for advanced NPPs is almost non-existent.

This study proposes a framework to explicitly model dependency between HFEs within the PRA model, aiming to overcome the limitations in dependency modeling techniques. Building on the Integrated Human Event Analysis System (IDHEAS) HRA methodology, this framework incorporates explicit dependency links in the PRA model. The framework includes a screening process to identify key HFE combinations, build corresponding human failure trees (HFT), employ IDHEAS' cognitive failure modes (CFM), and identify dependency links. Bayesian networks are used to quantify the impact of dependencies on HFEs, CFMs, and performance-influencing factors (PIF). The modified probabilities associated with CFMs and HFEs can be linked in the PRA model, showcasing clear dependency links while mitigating any under/overestimation.

Moreover, this study extends the dependency analysis framework to multi-unit and multi-module PRA models. The explicit modeling of dependency between HFEs allows for the link between a post-initiator HFE of one module and an at-initiator HFE of another, modeling the impact of a shared control room. Moreover, the HFTs allow for the separation between diagnosis, decision-making, and action-taking failure modes of the operating and maintenance crews, modeling the dependency of shared resources in multi-unit NPPs. A case study using the modular high-temperature gas-cooled reactor (MHTGR) is conducted to demonstrate the framework. The PRA model of the MHTGR is replicated, identifying key HFE combinations, building their corresponding HFTs, and finally incorporating the HFTs within the model. The model is then expanded to a multi-module MHTGR site with a shared control room and extended to a generic pressurized water reactor (G-PWR) PRA model for multi-unit considerations, simulating independent operating crews with shared resources.

Causal Framework for Modeling Dependencies of Human Failure Events in Nuclear Power Plants: Single-Unit, Multi-Unit, and Multi-Module Perspectives

by
Mostafa Hamza

A thesis submitted to the Graduate Faculty of
North Carolina State University
in partial fulfillment of the
requirements for the degree of
Doctor of Philosophy

Nuclear Engineering

Raleigh, North Carolina
2024

APPROVED BY:

Dr. Maria Avramova	Dr. Nam Dinh
Dr. Haufei Liao	Dr. Minh Tang

Dr. Mihai A. Diaconeasa
Committee Chair

DEDICATION

To over 37 thousand pure souls, Hind Ragab, Refaat Alareer, and all who we know and those we do not. May your martyrdom usher in a just world.

To my colleague, friend, love, and wife, Nermeen. You are my everything; thank you for just being you.

To my mom, Walaa, my dad, Mohamed, and my brother, Mahmoud. Thank you for supporting my dreams with your prayers and efforts.

To all my aunts. May Allah bless you with prolonged, joyful, and healthy lives.

To my little nephew, you are loved more than you know. May your future be full of joy and achievements.

"إِنۡ أُرِيدُ إِلَّا ٱلۡإِصۡلَٰحَ مَا ٱسۡتَطَعۡتُۚ وَمَا تَوۡفِيقِيٓ إِلَّا بِٱللَّهِۚ عَلَيۡهِ تَوَكَّلۡتُ وَإِلَيۡهِ أُنِيبُ"

هود ٨٨

"I only intend reform as much as I am able. And my success is not but through Allāh. Upon Him I have relied, and to Him I return"

Hūd 88

BIOGRAPHY

Mostafa Hamza was born in Alexandria, Egypt's second-biggest city, on March 19, 1993. He received his bachelor's degree in nuclear engineering from the Nuclear and Radiation Engineering Department at Alexandria University in 2016. He received his master's degree in nuclear engineering from the Department of Nuclear Engineering at North Carolina State University in 2022. Mostafa's passion is supporting the design of advanced reactors, leading the Renaissance era of the safe and reliable utilization of the power of atoms. His short-term goals are to support the licensing, construction, and operation of advanced (Gen-IV) nuclear power plants. His long-term goal is a lifelong research journey to push the field of probabilistic risk assessment to its frontiers, standing on the shoulders of giants.

ACKNOWLEDGMENTS

I am so grateful to Dr. Mihai A. Diaconeasa for guiding my research and graduate journey as an advisor and friend. Also, I appreciate the valuable comments from my colleagues in the Probabilistic Risk Assessment Group at NCSU. Further, I thank X-energy's probabilistic risk assessment team for their insights, expertise, and guidance.

My committee members, Dr. Maria Avramova, Dr. Nam Dinh, Dr. Huafei Liao, and Dr. Minh Tang, have provided invaluable insights and guidance in developing and finalizing this work.

I thank Dave Blanchard for his insights, comments, and support. This study would have been challenging to complete without his help.

Moreover, I am grateful to Dr. Abdel Fattah Solyman and Dr. Yousry Azmy for their continuous and unconditional support and guidance throughout the most challenging times.

Finally, I thank everyone who taught me a single word. Without you all, I would not have been here. Thank you.

TABLE OF CONTENTS

LIST OF TABLES

LIST OF FIGURES

LIST OF ACRONYMS

ADS	Accident Dynamics Simulator
AGR	Advanced Gas-Cooled Reactor
ANS	American Nuclear Society
AOO	Anticipated Operational Occurrences
API	Application Programming Interface
AR	Alarm Response
ASEP	Accident Sequence Evaluation Program
ASME	American Society of Mechanical Engineers
ATHEANA	A Technique for Human Error Analysis
ATRS	Anticipated Transient Requiring Scram
ATWS	Anticipated Transient Without Scram
AVR	Arbeitsgemeinschaft Versuch Reaktor
BBA	Basic Belief Assignments
BBN	Bayesian Belief Network
BDBE	Beyond Design Basis Event
BHEP	Basic Human Error Probability
CAFTA	Computer Aided Fault Tree Analysis System
CD	Complete Dependence
CDF	Core Damage Frequency
CFM	Crew/Cognitive Failure Mode
CFR	Code of Federal Regulations
CHEP	Conditional Human Error Probability

CP	Type C Procedural Based Human Failure Event
CPT	Conditional Probability Table
CR	Type C Recovery Action Human Failure Event
CRD	Crew Response Diagram
CRT	Crew Response Tree
CRW	Control Rod Withdrawal
DAG	Directed Acyclic Graph
DBE	Design Basis Event
DSET-AHP	Dempster-Shafer Evidence Theory and Analytic Hierarchy Process
DT	Decision Tree
EOC	Error of Commission
EOO	Error of Omission
EPRI	Electric Power Research Institute
ES	Event Sequence Analysis
ESQ	Event Sequence Quantification
F-C	Frequency-Consequence
FSV	Fort St. Vrain
G-PWR	Generic Pressurized Water Reactor
HD	High Dependence
HEP	Human Error Probability
HFE	Human Failure Event
HFT	Human Fault Tree
HRA	Human Reliability Analysis

HTS	Heat Transfer System
HUNTER	Human Unimodel for Nuclear Technology to Enhance Reliability
IDAC	Information, Decision, and Action in a Crew Context Cognitive Model
IDHEAS At-power	Integrated Human Event Analysis System for Nuclear Power Plant Internal Events At-Power Application
IDHEAS-ECA	Integrated Human Event Analysis System for Event and Condition Assessment
IDHEAS-G	General Methodology of An Integrated Human Event Analysis System
IE	Initiating Event Analysis
IJS-HRA	Institute Jozef Stefan Human Reliability Analysis
INL	Idaho National Laboratory
LB-LOCA	Large Break Loss of Coolant Accident
LBE	Licensing Basis Event
LD	Low Dependence
LERF	Large Early Release Frequency
LMP	Licensing Modernization Project
LOCA	Loss of Coolant Accident
LOIA	Loss of Instrument Air
LOOP	Loss of Offsite Power
LOSP	Loss of Offsite Power
LWR	Light Water Reactor
MAE	Mean Absolute Error
MD	Moderate Dependence

MHTGR	Modular High-Temperature Gas-cooled Reactor
MS	Moderate Steam Generator Tube Leak
MU	Multi-unit
NPP	Nuclear Power Plant
NRLE	Normalized Relative Logarithmic Error loss
O&M	Operation and Maintenance
OA	Operator Action
PC	Primary Coolant Leak
PIF	Performance Influencing Factor
PRA	Probabilistic Risk Assessment
PSF	Performance Shaping Factor
RHR	Residual Heat Removal
RI	Risk Integration
RIL	Research Information Letter
RP	Response Planning
RT	Reactor Trip
SA	Situation Assessment
SAPHIRE	Systems Analysis Programs for Hands-on Integrated Reliability Evaluations
SB-LOCA	Small Break Loss of Coolant Accident
SCS	Shutdown Cooling System
SGTR	Steam Generator Tube Rupture
SHARP	Systematic Human Action Reliability Procedure

SMR	Small Modular Reactor
SPAR-H	Standardized Plant Analysis Risk – Human Reliability Analysis
SPV	Staffing Plan Validation
SS	Small Steam Generator Tube Leak
THERP	Technique for Human Error-Rate Prediction
THTR	Thorium Hochtemperatur Reaktor
TMI	Three Mile Island
U.S. DOE	United States Department of Energy
U.S. NRC	United States Nuclear Regulatory Commission
ZD	Zero Dependence

CHAPTER 1. INTRODUCTION

1.1.Background and Motivation

Early in its development, probabilistic risk assessment (PRA) identified the importance of the human element in accounting for the reliability of any complex system. Human input is crucial not just in the nuclear industry but also in all complex systems during all life stages, starting from the initial development, deployment, operation, maintenance, and decommissioning. In WASH-1400, the first reactor safety study [1], the impact of human actions was identified, assessed, and quantified as part of the human reliability analysis (HRA) using a methodology developed by Swain over a decade [2]-[4].

Starting with Swain's Technique for Human Error Rate Prediction (THERP), multiple HRA methodologies surfaced to address the need to assess the impact of human actions. These methodologies cross fields ranging from transportation [5] to oil and gas industries [7], and medicine [8][9]. As many as 72 methods and/or tools can be considered partially or totally related to the field of HRA [9]. This myriad of HRA methodologies either built on, improved, and expanded previous methodologies, like Accident Sequence Evaluation Program (ASEP), A Technique for Human Error Analysis (ATHEANA), and SPAR-H, or presented a new approach to quantifying the impact of human actions, like Accident Dynamics Simulator - Information, Decision, And Action in A Crew Context Cognitive Model (ADS-IDAC) and Human Unimodel for Nuclear Technology to Enhance Reliability (HUNTER).

In the nuclear industry, both the American Society of Mechanical Engineers/American Nuclear Society (ASME/ANS) PRA standard for light-water reactor (LWR) [10] and for advanced non-light-water reactor (non-LWR) [11] nuclear power plants (NPP) consider the HRA element an integral part of the PRA model. Both standards list multiple high-level and supporting requirements that are expected from the HRA element of a PRA model; moreover, all other elements of the PRA model include supporting requirements that capture the impact of human actions within them.

The United States Nuclear Regulatory Commission (U.S. NRC), along with the nuclear industry, issued multiple guidance reports for good practices while implementing HRA and PRA in LWRs and non-LWRs [12][13]. The primary purpose of these guidance reports is to ensure a systematic, replicable, and reproducible assessment of human actions. To limit the analysis differences due to the different analysts and methodologies, the U.S. NRC also funded a project in which 10 HRA methodologies were compared against good practices issued in NUREG-1792, and the underlying model, strengths, and limitations associated with each method were identified [12][14][14].

However, human actions do not happen in a vacuum and cannot be considered, at least initially, as fully independent. If an operator fails to perform an action within a sequence of actions, the failure of subsequent actions may, and most probably would, be impacted by the previous failure. The potential of such a dependence between human actions was identified and captured in the first safety study [1][1] under what was termed "coupling." The methodology to address "coupling" was later developed further and incorporated in the "dependence" analysis of the pioneer HRA methodology, THERP [15].

Within the HRA supporting requirements of the PRA standard, for LWRs and Non-LWRs, the dependencies between multiple human failure events are required to be identified, assessed, and quantified. The good practices for implementing HRA, presented in NUREG-1792 [12], require using a default assumption in its screening analysis of high dependence between multiple human failure events within the same event sequence. This somewhat conservative assumption tries to avoid the overoptimism associated with assuming independence between human actions. Failure to make a realistic dependence assessment may lead to a grossly unrealistic failure probability of a specific action.

Even though the importance of dependency analysis was identified early on, more improvement was needed in this field. The dependency analysis methodology developed over 65 years ago, presented in WASH-1400, and later implanted by THERP was, in some way, the central methodology adopted by many subsequent HRA methodologies. ASEP [16] and Standardized plant analysis risk human reliability assessment (SPAR-H) [17] present an example of widely used HRA methodologies that implement a version of THERP's dependence analysis.

Furthermore, due to the simplicity of the design and the push for economic competitiveness, advanced NPPs are expected to have limited required operator actions. However, accompanied by that reduced human workload, fewer licensed control room staff are expected compared to LWRs. The effort to obtain approval for reduced control room staffing, under Conditions of Licenses Title 10 of the Code of Federal Regulations (10 CFR) 50.54, is currently underway, with NuScale Power, LLC, the first to submit a topical report to justify their control room staffing plan of only three operators operating up to 12 modules from a single control room [18].

Having a single control room that operates multiple modules further complicates the assessment of operator action dependencies. The complication stems from the fact that, following an incident within one of the modules, an operator is expected to ensure regular operation of the unaffected modules while enacting the necessary actions for the modules where the incident occurred. Moreover, a site-wide incident, like an external hazard, would require the operator to manipulate multiple modules simultaneously to ensure their safe operation.

1.2.Probabilistic Risk Assessment

Since the start of the commercial use of nuclear power plants, multiple studies have been conducted investigating the potential of reactor accidents. The "Theoretical Possibilities and Consequences of Major Accidents in Large Nuclear Power Plants," or WASH-740, investigated "[s]ome of the worst possible combinations of circumstances that might conceivably occur" to assess their consequences [19]. Whereas the "Technical Report on Anticipated Transients Without Scram for Water-Cooled Power Reactors," or WASH-1250, specifically investigated the frequency of having a transient for which the protection system fails to trip the reactor, i.e., Anticipated Transient Without Scram (ATWS) [20]. Both WASH-1250 and NUREG-0460 suggested requirements for the reliability and testing of the scram systems [20][21].

It was not until 1975 that a full assessment of the risk associated with nuclear power plants was conducted in the "Reactor Safety Study – An Assessment of Accident Risks in U.S. Commercial Nuclear Power Plants," or WASH-1400 [1]. In WASH-1400, a comprehensive and realistic assessment of the risk associated with different accident scenarios was conducted, pioneering the PRA field. The definition of "risk" in WASH-1400 was similar to the most widely accepted definition presented by Kaplan and Garrick [22]. Under that definition, risk can be understood as the answer to three fundamental questions: what can go wrong, how likely can it happen, and what are the consequences? [23] In quantitative terms, risk is defined as the complete set of three parameters and any associated uncertainty represented formally in Equation (1).

$$R = \{< s_i, p_i, x_i >\}_c, \quad i = 1,2,\dots,N \qquad (1)$$

In Equation (1), s_i presents the description of scenario i, answering the "what can go wrong?", p_i presents the scenario probability estimation, answering the "how likely can it happen?", and x_i presents the scenario consequence, answering the "what are the consequences?" [22].

The nuclear engineering community heavily contested the results of WASH-1400. It was the consensus that “the experts all agree that the chances that major accidents might occur are exceedingly small” [19] due to the fact of ensuring the emergency cooling for large-break loss of coolant accidents (LB-LOCA) which was deemed as the most risk-significant accident. So, after WASH-1400 concluded that small-break loss of coolant accident (SB-LOCA) poses a higher risk than LB-LOCA, the results were considered to overestimate the likelihood of accidents [24].

Following the definition presented in Equation (1), the conclusion of WASH-1400 can be put in context. Since the risk of any scenario (SB-LOCA vs. LB-LOCA) is a combination of its likelihood and consequences, SB-LOCA presents a higher risk than the more infrequent LB-LOCA. These results were later supported by the Three Mile Island (TMI) accident, where an SB-LOCA resulted in the melting of two-thirds of the second unit’s core. Due to misdiagnosing the incident, the operators incorrectly throttled off the emergency core cooling system pumps to avoid the pressurizer going solid. Their decision uncovered the core due to a lack of coolant inventory [25]. The operators’ response supported the findings of WASH-1400 regarding the importance of the human elements in operating and mitigating adverse incidents [1]. Ever since WASH-1400 and TMI, the field of PRA has become an integral part of the commercial nuclear power plants industry. PRA was expanded further to support different regulatory activities supported by the U.S. NRC through different implementation plans [26]-[28].

Any PRA model starts by investigating potential initiating events (IE), their associated plant responses, public doses, and environmental damage. For LWRs, this complete analysis is divided into three levels [23][29]: level 1 PRA, which starts with IEs and estimates the core damage frequency (CDF); level 2 PRA, which begins from core damage and estimates the large early release frequency (LERF), and finally level 3 PRA, which starts from environmental release and assess the public dose and environmental damage. Whereas the proposed approach for non-LWR PRA in the Licensing Modernization Project (LMP) [30][31], endorsed by the NRC in the Regulatory Guide 1.233 [32], is to combine all three levels of PRA, as defined for LWRs, and assess the aggregate plant risk starting from IEs and ending with public doses.

1.3.Human Reliability Analysis

The impact of operator actions was captured early in the nuclear industry, even before WASH-1400. The insights implemented in WASH-1400 relied on previous work developed over a decade [2]-[4]. The concepts developed by Swain et al. were fully implemented in WASH-1400 in an entire section in Appendix III, titled "Human Reliability Analysis," that focused on quantifying the impact of operator actions [33]. This section captures the "human interaction with the system in routine plant operation, testing and maintenance" and "human intervention […] required in case of malfunction of automatic systems" [33]. As indicated in [1], "The inclusion of human failures and test and- maintenance contributions was an important reason for the rather high values predicted for system failure probabilities," capturing the value of HRA within any PRA model.

Just as TMI cemented the value of PRA in general, all three major nuclear accidents clearly indicated the importance of human actions. Operators can initiate an incident with significant consequences similar to how the initiation of a test by the operators disregarding procedures and safe practices caused the Chernobyl accident [34]. Operators can also exacerbate the situation by failing to implement correct actions or implementing incorrect actions, similar to how the operators throttling off the emergency core cooling system pumps worsened the situation during TMI [25]. Finally, operators can improve the situation by implementing correct procedures or achieving general guidelines during severe accidents, similar to how the valiant efforts of the operators significantly reduced the consequences of the Fukushima Daiichi accident [35].

The main goal of the HRA element of the PRA model is to identify and describe potential human failure events (HFE), which is “a basic event that represents a failure or unavailability of a component, system, or function that is caused by human inaction, or an inappropriate action” [11], and to estimate the human error probability (HEP) associated with these HFEs. In general, HFEs can be categorized into pre-initiator, at-initiator, and post-initiator HFEs. According to [11], these categories can be defined as follows:

- Pre-initiator (or category A) HFEs: human failure events that represent the impact of human errors committed during actions performed prior to the initiation of an event (e.g., during maintenance or the use of calibration procedures).
- At-initiator (or category B) HFEs: a type of initiating event; a human failure event that causes or contributes to an initiating event (e.g., the human failure event that directly involves plant personnel actions at the time of the initiating event, including actions correctly performed but which are based on erroneous indications).
- Post-initiator (or category C) HFEs: human failure events that represent the impact of human errors committed during the response to abnormal plant conditions.

To showcase the expectation of the HRA element in any PRA model, both standards of the LWR PRA [10] and Non-LWR PRA [11] list high-level and supporting requirements expected to be met by the PRA model. Both the requirements of the HRA element and other different elements require the identification, assessment, and estimation of dependencies between different HFEs. Event sequences that include multiple HFEs should be assessed to ensure that any dependencies between HFEs are captured. Failing to capture dependencies would result in over-optimistic results, especially for those actions that rely on shared resources. The importance of dependency between HFEs was identified early on within WASH-1400 and the subsequent HRA methodologies.

Multiple good practices for implementing HRA ensure that dependencies among multiple HFEs in the same sequence are captured and conservatively accounted for [12].

1.4.Research Objectives

Despite being a requirement of the HRA element in the PRA model, limited achievements were made in the field of dependency analysis among HFEs. Multiple HRA methodologies were developed through the years since WASH-1400 that differed in their approaches. However, most of these methodologies relied on an approach similar to the one implemented by WASH-1400 in the mid-1970s. Dependency analysis saw fragmented efforts to be updated and to investigate different techniques; however, the nuclear industry has yet to adopt any of these efforts. Moreover, with the current push towards reducing the operational and maintenance costs, reducing the number of crew members operating multiple modules introduces another complexity that needs to be captured by any current dependency analysis methodology.

Hence, the work presented in this study assesses existing HRA methodologies to stand on the state of the art of HFE dependency analysis along with the gaps and limitations. Multiple HRA and dependency-analysis-specific methodologies are chosen based on their wide use in the industry or academia, which can be deemed a representative set of most approaches. A framework to conduct dependency analysis for the Integrated Human Event Analysis System (IDHEAS) HRA methodology is then developed. This framework is expanded to include the dependency analysis of HFEs in multi-unit NPPs. For multi-unit NPPs, each unit would have its main control room with its operating crew; however, multiple units may share resources with the maintenance crew. Finally, the framework is expanded further to include the dependency analysis of HFEs in multi-module NPPs. For multi-module NPPs, multiple modules would be controlled from a single control room, sharing an operating crew, resources, and maintenance crew.

1.5.Overview of Thesis

Following the introductory chapter, which provides a general overview of this work's motivation, contribution, and background, CHAPTER 2 studies the dependency analysis developed and adapted by different HRA methodologies. Also, in CHAPTER 2, an overview of the methodology history, its adapted dependency analysis, and the advantages and limitations of the dependency analysis are presented. This chapter analyzes a representative set of the most widely used HRA methodologies to cover different generations of HRA methodologies. CHAPTER 3 gives detailed attention to the IDHEAS HRA methodology, presenting a high-level discussion of the various versions of the methodology along with a thorough assessment of the dependency model utilized by each version.

CHAPTER 4 presents the framework developed to incorporate dependency analysis in the IDHEAS HRA methodology. Moreover, CHAPTER 4 presents how to expand the dependency analysis framework to incorporate multi-unit and multi-module NPPs. CHAPTER 5 showcases the implementation of the framework for a single-unit, single-module NPP. The PRA model for the Modular High-temperature Gas-cooled Reactor (MHTGR) demonstrates the implementation for non-LWRs. The generic Pressurized Water Reactor (G-PWR) PRA model is used to illustrate the implementation of the framework for LWRs. The steps to assess the dependency analysis in multi-control-room multi-unit NPPs are presented using the generic PWR model. The steps to determine the dependency analysis in shared-control-room multi-module NPPs are presented using the MHTGR model. Finally, CHAPTER 6 summarizes the research conducted in this study along with recommendations for future work.

.

CHAPTER 2. LITERATURE REVIEW

A myriad of HRA methodologies were developed over the lifetime of the PRA field. Starting with the work presented by Swain in the 1960s, the development of the HRA methodology can be categorized based on different criteria, such as modeling approach, cognitive model, etc. Based on the modeling approach, the first category of HRA methodologies divides the human failure event into smaller subtasks that are assessed to determine the failure probability associated with each subtask. The failure probability associated with the human failure event is then quantified as the amalgamation of the failure of different subtasks. On the other hand, the second category of HRA methodologies probabilistically models human behavior during the accident progression. Depending on the transient, the probability distribution of human failures changes, and a sampling is performed to determine whether the human failure event happened.

Generally, the first category of HRA methodologies is associated with the so-called static PRA models, whereas the second category is more compatible with dynamic PRA models. The second category, which includes ADS-IDAC and HUNTER, presents an objective approach that avoids direct influence from the analysts. However, due to the resources required to conduct such an analysis explicitly modeling time, the second category is conducted through lengthy resource-intensive simulations. On the other hand, the first category, which includes THERP and IDHEAS, presents a somewhat less-objective approach that is more appropriate with static PRA models that implicitly consider time. Depending on the specific methodology, the resources the analysts require to perform vary; However, all first-generation HRA methodologies are less resource-intensive than the second-generation.

In this chapter, a sample of HRA methodologies is chosen to investigate the different approaches to dependency analysis. A brief history is presented for each method, along with an overall description of its basic structure. The dependency analysis approach associated with each HRA methodology is presented in detail, with discussions of its limitations. Due to the similarity in the approaches, some methodologies are combined and discussed together. Finally, the individual efforts conducted by different scholars are presented, and their prospects and limitations are discussed.

2.1. Multi-Point Dependency Continuum

2.1.1. THERP

The technique for human error prediction (THERP) was developed based on the human reliability analysis conducted in WASH-1400. Developed by Swain in Sandia National Laboratory, THERP presents the amalgamation and improved version of the work done in WASH-1400 and other projects [1]-[4]. The basic assumption of THERP is that human errors, like misreading or skipping a step, occur at a constant rate. Hence, by decomposing a task into its low-level elementary subtasks, HEPs can be quantified using the estimated nominal probability of failure in each subtask [36]. Associated with these nominal probabilities are multiple performance shaping factors (PSFs), stress, etc., that impact human performance and HEPs and are accounted for using multipliers [15]. The steps in THERP follow the conventional reliability assessment approach with modifications to account for the higher unpredictability and interdependence in human actions. These steps can be summarized in the following:

- Familiarization: In this step, the analyst gathers information about the plant, system, and event. This is done by visiting the plant to become aware of different PSFs, reviewing maintenance and testing policies, and reviewing the procedures associated with each event.

- Qualitative assessment: In this step, the analyst investigates the event progression and identifies the performance requirements. Based on these requirements, the analyst can identify potential human errors and any associated subtasks.
- Quantitative assessment: In this step, the analyst develops estimates for the failure probability of each of the identified human failure events. These estimates consider factors impacting human performance and/or possible recovery actions.
- Incorporation: In this step, the analysts integrate the HRA results with other elements of the PRA model. Different sensitivity analyses can be performed to assess the impact of different assumptions made during the HRA.

Although THERP is considered the earliest full HRA methodology, the impact of dependency between different HFEs was identified in the development of the THERP methodology. In fact, in the dependence chapter, the THERP guidance states that complete independence in human actions is uncommon, but instead, the dependence can be considered “so slight that we assume [zero dependence] for purposes of analysis” [15]. Hence, assessing dependence between different actions is essential due to the over-optimism accompanying any independence assumption. Two types of dependence were identified by THERP: positive dependence, where the failure of the first action increases the failure probability of the following action, and negative dependence, where the failure of the first action decreases the failure probability of the following action. The dependence model of THERP deals mainly with positive dependence.

In WASH-1400 [1], a similar dependence, called coupling, analysis model to that of THERP was employed. The dependence between human actions is assessed between two tasks only, whereas for more than two tasks, the conditional probabilities of subsequent tasks are derived by attributing all the effects of dependence to the immediately preceding task. Between two subsequent tasks, THERP's dependence model can be represented as a continuum, as seen in Figure 1, between 5 points representing zero, low, moderate, high, and complete dependence. In assessing a nonzero level of dependence, making an error on any task in the sequence implies that the operator is in an error-likely state at the time of the error and that this state carries over to the performance of the next task in the sequence. By investigating only subsequent tasks, the assumption becomes that the error-likely state terminates when a task within a sequence is performed correctly.

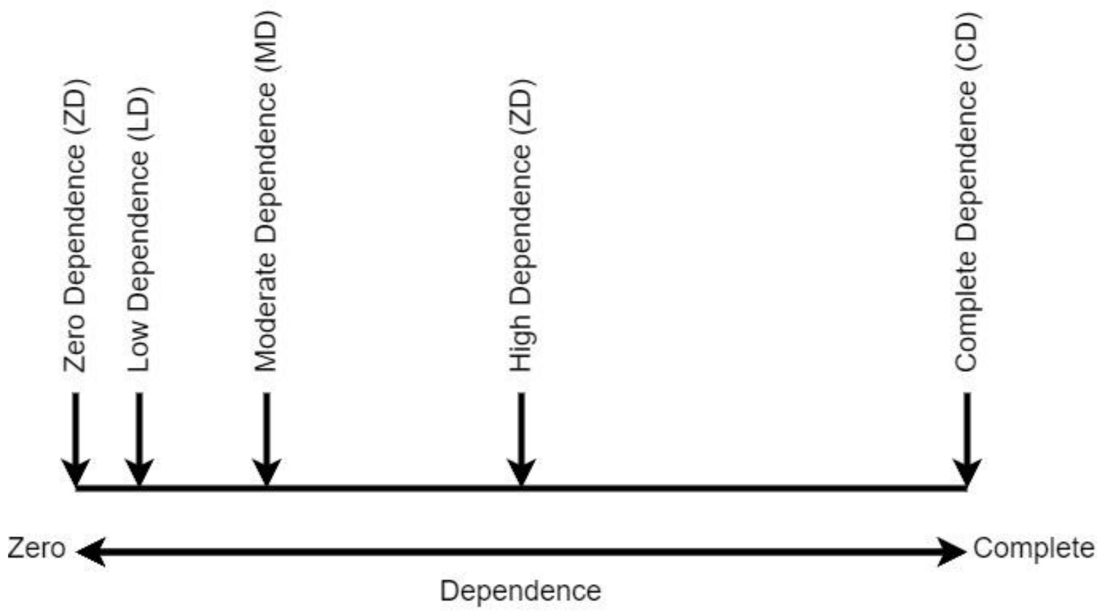

Figure 1. THERP's Positive dependence continuum (reproduced from [15]).

For tasks with zero dependence (ZD), one task's performance, or failure, does not impact the other task. Periodic scanning of displays during normal operation is an example of tasks that can be assumed to be with zero dependence if these scans are separated enough in time. Also, executing individual steps in a written procedure can be assumed with zero dependence, given that the operator properly follows the procedures. However, even these examples can easily have none ZD either by making the tasks closer in time or location. Hence, as can be seen, although occasionally the dependence is judged to be so slight that we assume ZD, complete independence is uncommon between human tasks. The conditional failure probability of an HFE following the failure of a previous HFE can be calculated as shown in equation (2), where $\Pr(F_N|F_{N-1}|ZD)$ presents the conditional human error probability (CHEP) of task N following the failure of task N-1 assuming zero dependence between both tasks. Pr (F_N), on the other hand, presents the basic human error probability (BHEP) of task N.

$$Pr(F_N|F_{N-1}|ZD) = Pr\ (F_N) \tag{2}$$

Low dependence (LD) can be considered the default assumption whenever ZD is not guaranteed. By ensuring that LD is the default, any unforeseen sources of dependence can be incorporated into the model, accounting for any completeness uncertainty. The tasks that rely on interactions between new crewmates, where the confidence in each other is low, can be considered an example of LD. This example raises the importance of specifying the direction of crew interaction during the assessment because a shift supervisor checking an operator would not have the same dependence if flipped. The conditional failure probability of an HFE following the failure of a previous HFE can be calculated as shown in (3), where $\Pr(F_N|F_{N-1}|LD)$ presents the CHEP of task N following the failure of task N-1 assuming low dependence between both tasks. Due to the qualitative difference between zero and nonzero dependence, even assuming low dependence would substantially change the CHEP.

$$Pr(F_N|F_{N-1}|LD) = \frac{1 + 19 \times Pr(F_N)}{20} \tag{3}$$

Moderate dependence (MD) can be considered the default assumption whenever there is an obvious relationship between the performance of different tasks. Tasks collaborating between the shift supervisor and the operators during normal conditions can be assumed to have MD. Equation (4) presents the quantification of the CHEP under the assumption of MD, where $\Pr(F_N|F_{N-1}|MD)$

presents the CHEP of task N following the failure of task N-1 assuming moderate dependence between both tasks.

$$Pr(F_N|F_{N-1}|MD) = \frac{1 + 6 \times Pr(F_N)}{7} \quad (4)$$

Midway on the dependence continuum, as seen in Figure 1, falls the high dependence (HD) level. The HD level represents a substantial impact from a task's performance, or failure to perform, on subsequent tasks. Due to the quantification method of CHEP assuming HD, as seen in Equation (5), the assumption of HD would yield a high CHEP, over 0.5, approaching the value of a complete dependence. This dependence level can be exemplified by the tasks that involve multiple people, among whom a person has a significant influence. In other words, even though a shift supervisor checking an operator's performance in a newly formed crew can be assumed to be LD, an operator checking the shift supervisor's performance may be considered HD. This stems from the tendency to avoid questioning supervisors, especially during off-normal situations with high-stress levels.

$$Pr(F_N|F_{N-1}|HD) = \frac{1 + Pr(F_N)}{2} \quad (5)$$

Although ZD is rare, complete dependence (CD) is not as unusual to be the case. Although CD between actions performed by multiple people is rare, it is not uncommon because some failures (for example, calibration) would directly result in the inability to perform the following actions. Moreover, CD within actions performed by the same person can be exemplified by errors of omission (EOO), where the operator skips a step, failing all the following steps that rely on the performance of the first step. The CHEP associated with this dependence level, as shown in Equation (6), represents that the failure of the preceding task ensures the failure of the task under assessment.

$$Pr(F_N|F_{N-1}|CD) = 1.0 \quad (6)$$

The failure equations, listed in (2) through (6), to quantify the CHEP are chosen to provide conditional probabilities of failure of about 5%, 15%, and 50% of the distance between the BHEP 0.0 (ZD) and 1.0 (CD), for the low, moderate, and high levels of dependence, respectively. This is true for all tasks for which the BHEP is .01 or smaller; however, for BHEPs < .01, the CHEP becomes unaffected by the value of the BHEP. As the BHEP's value becomes smaller, the CHEP reaches the asymptotic value of 0.05, 0.15, and 0.5 for LD, MD, and HD, respectively. This stems from the judgment of THERP’s developers that the behavioral phenomena related to dependent tasks are substantially different from those related to independent tasks; that is, the dependent behavior induced by the contributing factors is a class of behavior in itself.

Multiple HRA methodologies employed the dependence analysis developed in THERP, or a slightly modified version of it, as their dependency analysis method of choice. In the following sections, some of these methodologies and their specific variation of THERP’s dependency analysis are listed.

2.1.2.SPAR-H

In the early 1990s, the U.S. NRC contracted Idaho National Laboratory (INL) to develop an improved, traceable, easy-to-use HRA methodology. In that effort, the Standardized Plant Analysis Risk HRA (SPAR-H) methodology was developed to account for contextual and environmental factors. Within SPAR-H, human actions are subdivided into action tasks, including carrying out one or more activities, and diagnosis tasks, including understanding plant conditions. The SPAR-H methodology consists mainly of identifying nominal HEP, 1.0E-03 and 1.0E-02, for action and diagnosis tasks, respectively, and modifying those nominal HEPs based on PSFs and dependence. SPAR-H captures the impact of environmental factors utilizing nine PSFs developed from psychological research on human errors. Out of the nine PSFs, only available time, stress, and complexity can be assessed agnostic of the plant design, whereas the remaining five, experience, procedures, ergonomics, fitness for duty, and work processes, can only be evaluated using a plant-specific model [17][37].

The steps in SPAR-H follow a systematic worksheet process to quantify human errors. The steps of this process can be summarized in the following:

- Entering header information about the plant, initiating event, analyst, context, and general task description.
- Identifying the appropriate type of task, i.e., either diagnosis, action, or both.
- Rate the associated PSFs and identify the multiplier associated with each PSF.
- Quantify the HEP without dependency ($P_{w/od}$) using the diagnosis, action, of joint HEP.
- Determine the level of dependency.
  - If there are no dependencies, the final HEP value is quantified from the previous step.
  - If there are dependencies, quantify the task failure probability using the level of dependency identified in the previous step.

Dependencies are modeled, to some level, in SPAR-H by a dependency model that mimics THERP's that ranges from zero to complete dependence (Gertman et al., 2055). SPAR-H, however, presents a systematic process to define the dependency level between tasks. Similar to the worksheet approach of SPAR-H in quantifying the failure probabilities without formal dependency, a worksheet presented in Figure 2 is used to identify the dependency level. Following the identification of the dependency level, SPAR-H utilizes the same formula presented by THERP, equations (2) to (6), to adjust $P_{w/od}$ obtaining the failure probability with formal dependency $P_{w/d}$.

Crew	Time	Location	Cues	No.	Dependency Level
Same Crew	Close in Time	Same Location	No Additional Cues	1	CD
			Additional Cues	2	CD
		Different Location	No Additional Cues	3	HD
			Additional Cues	4	HD
	Not Close in Time	Same Location	No Additional Cues	5	HD
			Additional Cues	6	MD
		Different Location	No Additional Cues	7	MD
			Additional Cues	8	LD
Different Crew	Close in Time	Same Location	No Additional Cues	9	MD
			Additional Cues	10	MD
		Different Location	No Additional Cues	11	MD
			Additional Cues	12	MD
	Not Close in Time	Same Location	No Additional Cues	13	LD
			Additional Cues	14	LD
		Different Location	No Additional Cues	15	LD
			Additional Cues	16	LD
				17	ZD

Figure 2. SPAR-H Dependency Condition Table

It should be noted that, within the SPAR-H worksheet, no pathways would result in zero dependency. In other words, from SPAR-H's perspective, zero dependency is outside of the scope of the analysis and would be decided separately from this worksheet. Moreover, the worksheet investigates the dependency among multiple tasks, which could be over 2, unlike THERP, in a series. During the assessment of more than two tasks in a series, the least dependency level that can be assumed for the 3rd error is moderate, whereas the least dependency level that can be assumed for the 4th error is high.

2.1.3.ASEP

Due to THERP being a resource-intensive methodology, the Accident Sequence Evaluation Program (ASEP) methodology was developed as a simplified screening methodology that requires fewer resources to implement. A detailed screening and nominal methodology are presented in ASEP for pre- and post-accident tasks. Incorporating multiple simplifications within ASEP increases the speed of the analysis at the expense of accuracy and having more conservative error estimation. This speed, however, allows for combining both ASEP and THERP in the analysis where ASEP is used for screening and THERP is used for risk-significant human errors [16][36].

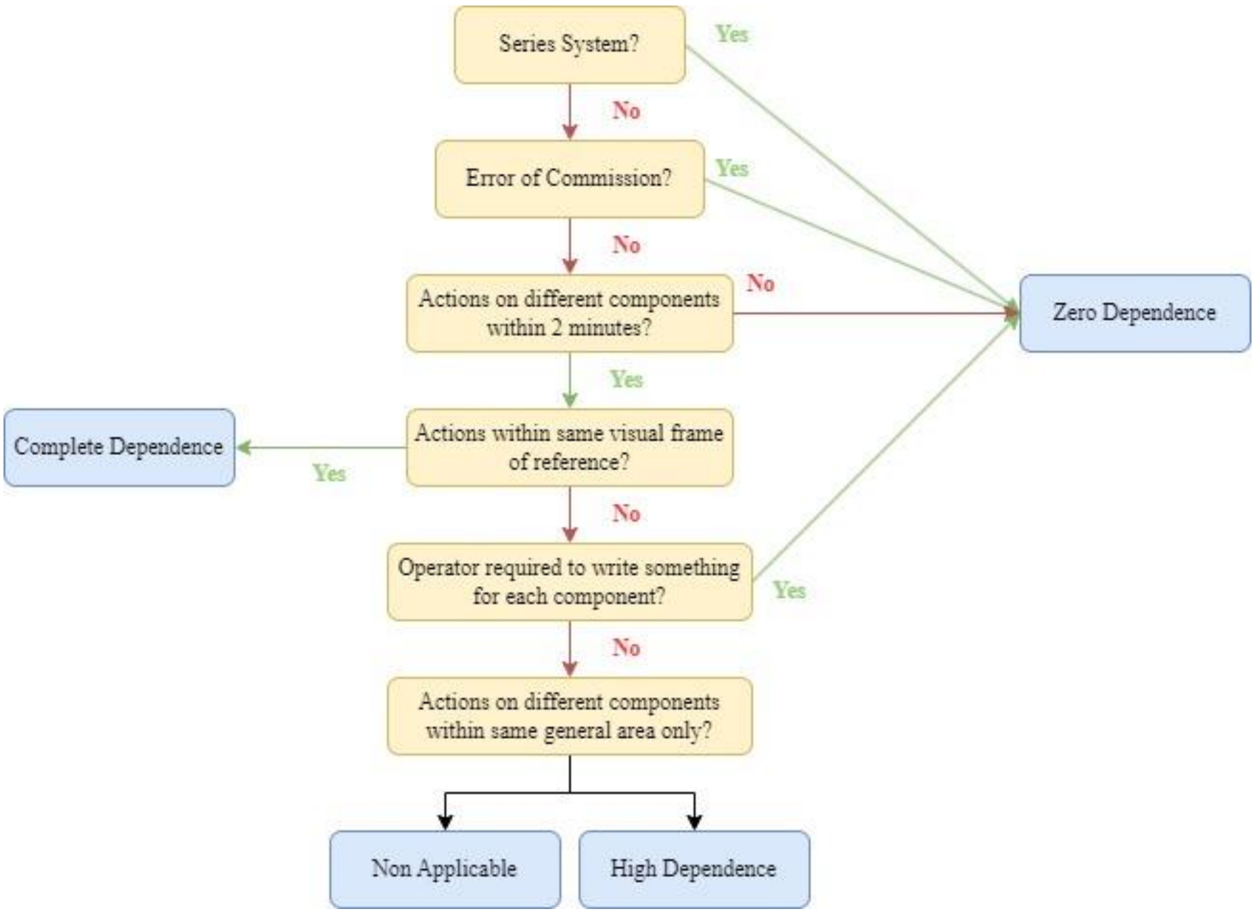

Figure 3. ASEP within-person positive dependence levels for pre-accident tasks.

Since ASEP can be considered a smaller version of THERP, it is understood that ASEP implements a similar dependency analysis to THERP's. However, the dependency analysis of ASEP consists of 3 dependency levels: ZD, HD, and CD. For pre-accident errors, a decision tree is developed by ASEP and presented in Figure 3 to identify the dependency level between tasks. It should be noted that, despite having a decision tree for deciding the dependency level of pre-accident tasks, ASEP does not provide guidance on assessing the dependency level of post-accident tasks.

2.1.4.SHARP1

In 1984, the Electric Power Research Institute (EPRI) developed the initial revision of the Systematic Human Action Reliability Procedure (SHARP) HRA methodology widely used by the industry and NRC. Improving on the fundamental framework presented by SHARP, a revised methodology, fittingly called SHARP1, is developed to enhance user-friendliness, provide additional guidance on human action logic modeling and quantification, and incorporate comparative evaluation with existing HRA methodologies [40]. The SHARP1 approach, which is the basis of EPRI's HRA calculator, consists of four main stages that can be subdivided into multiple steps and can be crudely summarized as follows [40]:

- Stage 1: human interaction definition and integration into plant logic model: this step aims to define human interaction events in sufficient detail with clear boundaries that allow for the quantification of their associated HEPs. This stage represents a culmination of different pieces of the PRA model and can be subdivided into five steps: definition, qualitative screening, subtask breakdown, impact assessment, and logic model integration.
- Stage 2: human interaction event quantification: The goal of this step is to quantify the human interaction basic event, i.e., the HEP associated with each HFE. This stage can represent an input to stage 1 if the results require altering the logical representation and can be subdivided into five steps: qualitative screening, influence factor identification, representation, human interaction quantification, and reassessing the logic model.
- Stage 3: recovery analysis: This stage deals with recovery actions that are not driven by procedure but rather by the inventiveness of the staff. This stage represents an effort to realistically capture the impact of recovery actions instead of conservatively not accounting for them; this stage can be subdivided into six steps: definition, feasibility-based screening,

logic model integration, influence factors, representation, and human interaction quantification.

- Stage 4: Internal review: This stage represents an effort to thoroughly document and review all the assumptions and subjective analyses. It can be subdivided into four steps: review of stage 1, stage 2, and stage 3 and documentation of the process.

In SHARP1, dependencies associated with different HFEs can be grouped into four classes. Class 1 dependencies represent the dependency of different post-initiator HFEs, type C, on their respective scenario. Type C events, subdivided into procedural-based (CP) and recovery actions (CR), are highly dependent on the conditions associated with their respective scenarios, including available time, procedures, control room environment, etc. Class 1 dependencies are usually well understood by the analysts and accounted for by the appropriate PSFs. On the other hand, class 2 and class 3 dependencies represent the interdependencies between different type C and type A HFEs, respectively. These dependencies arise due to, for example, cognitive dependencies in the case of type C actions, and common procedures, personnel, and administrative environment in the case of type A actions. Finally, Class 4 dependencies capture those dependencies, for both types A and C, that arise from factors that are not scenario-dependent, e.g., action complexity [41].

Where stage 1 addresses class 1 dependencies within the model logic and class 4 dependencies are treated internally in the quantification model, class 2 and class 3 dependencies are accounted for by assigning different HEP values for a specific HFE depending on the success/failure of previous HFEs. Though the dependency model presented by SHARP1 relies heavily on THERP's model, qualitative suggestions are given by SHARP1 to determine the degree of dependency. These qualitative suggestions, presented in Table 1, can be considered complementary to the guidance provided by THERP.

Table 1. SHARP's Conditions for Different Dependence Levels

Complete or High Dependence	Medium Dependence	Low or Zero Dependence
Actions represent multiple approaches to the same goal.	Actions represent multiple approach to the same goal in the same time interval but by different people.	Actions are committed to memory and performed by different people.
Actions are initiated by the same cue.	Distinct cues trigger the second action at the same goal.	Actions with distinct cues and low burden
The requirement of starting an action is the failure of previous action and the time interval between them is short.	Increased time separation from CD/HD	Actions are separated by a long interval with low stress.
Actions are directed by one person in a short time.		Actions are guided by the same procedures and separated by successful action.
The actions are the same function.		

2.1.5.IJS-HRA & Depend-HRA

The Institute Jozef Stefan (IJS-HRA) methodology is developed to integrate features from state-of-the-art methodologies and new features such as simulator experience to be up to date with modern computerized PRA models. The IJS-HRA high-level framework, presented in Figure 4, closely resembles other methodologies where the primary inputs are the PRA model, plant information, standards, guides, and good practice. The IJS-HRA consists of scoping, identification, task analysis, evaluation, dependency analysis, and result interpretation steps. The identified human failure events with the most prominent risk factors are reported to simulator training management to prioritize simulator training.

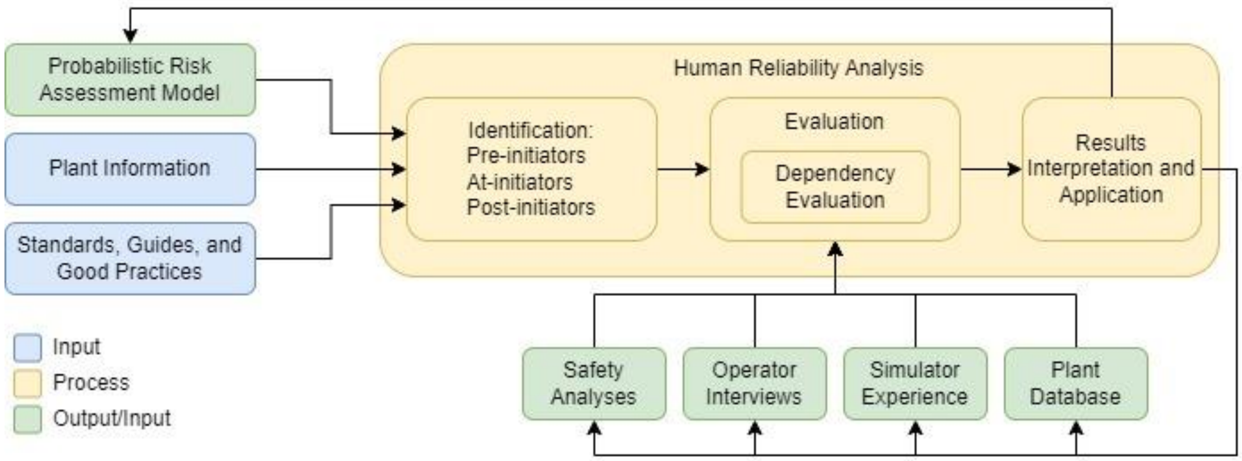

Figure 4. Scheme of IJS-HRA Methodology

Similar to THERP, the dependency analysis model of IJS-HRA relies on a five-point dependency continuum. Not only are similar dependency points used by IJS-HRA, ZD, LD, MD, HD, and CD, but the same formulae are also used to quantify the joint human error probabilities as generalized in equation (9). In equation (9), $P_{XD}(\mathrm{P_B}|\mathrm{P_A})$ is the probability that both human failure events in one sequence, $\mathrm{P_A}$ is the human error probability of the first event, $\mathrm{P_B}$ is the human error probability of the second event, and k is a dependency factor dependent on the dependency level.

$$P_{XD}(P_B|P_A) = \frac{P_A(1 + K * P_B)}{K + 1}, where\ k = \begin{cases} 0, & for\ ZD \\ 1, & for\ LD \\ 6, & for\ MD \\ 19, & for\ HD \\ \infty, & for\ CD \end{cases} \qquad (7)$$

IJS-HRA presented a framework to identify the dependency level of pre- and at-initiators using multiple parameters. The parameters used to determine the dependency level of pre-initiators include task type (calibration vs. alignment), procedures (same vs. different), time interval (less vs. more than 10 minutes), task performer (same vs. different), and task similarity (similar vs. different visual cues or tools). At-initiators' and post-initiators' dependency levels are decided, according to IJS-HRA, based on the diagnosis function (common vs. different), time interval (less than 5 minutes vs. less than 30 minutes vs. more than 30 minutes), task performer (same vs. different), stress level (low vs. medium vs high), and task complexity (simple vs complex) [42].

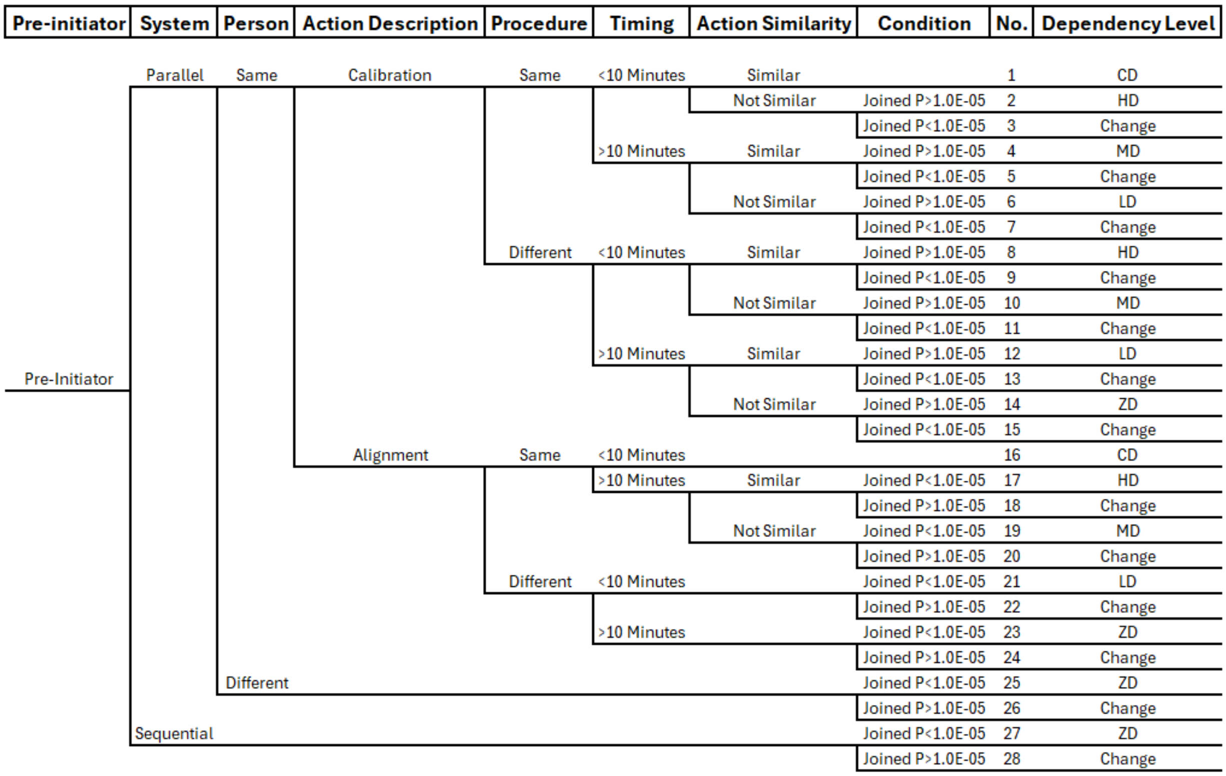

Figure 5. Pre-initiator Dependency Level Decision Tree

The dependency analysis methodology associated with IJS-HRA was initially introduced as an integrated step within the IJS-HRA methodology [42][43]. However, the dependency analysis step was then extracted and presented as its dependency analysis framework, Depend-HRA [44]. In Depend-HRA, however, the assumption is that pre-initiators are independent of at- and post-initiators. Moreover, the dependency between at- and post-initiators is assumed to be inapplicable and is only left as an option for further analysis [44]. During this literature review, IJS-HRA/Depend-HRA is the only methodology to present an explicit separate decision tree to identify the dependency levels of pre-initiators, as seen in Figure 5. It should be noted that the IJS-HRA methodology requires changing, i.e., increasing, the dependency level in the cases where the joint HEP is unjustifiably low, as can be seen in Figure 5 and Figure 6.

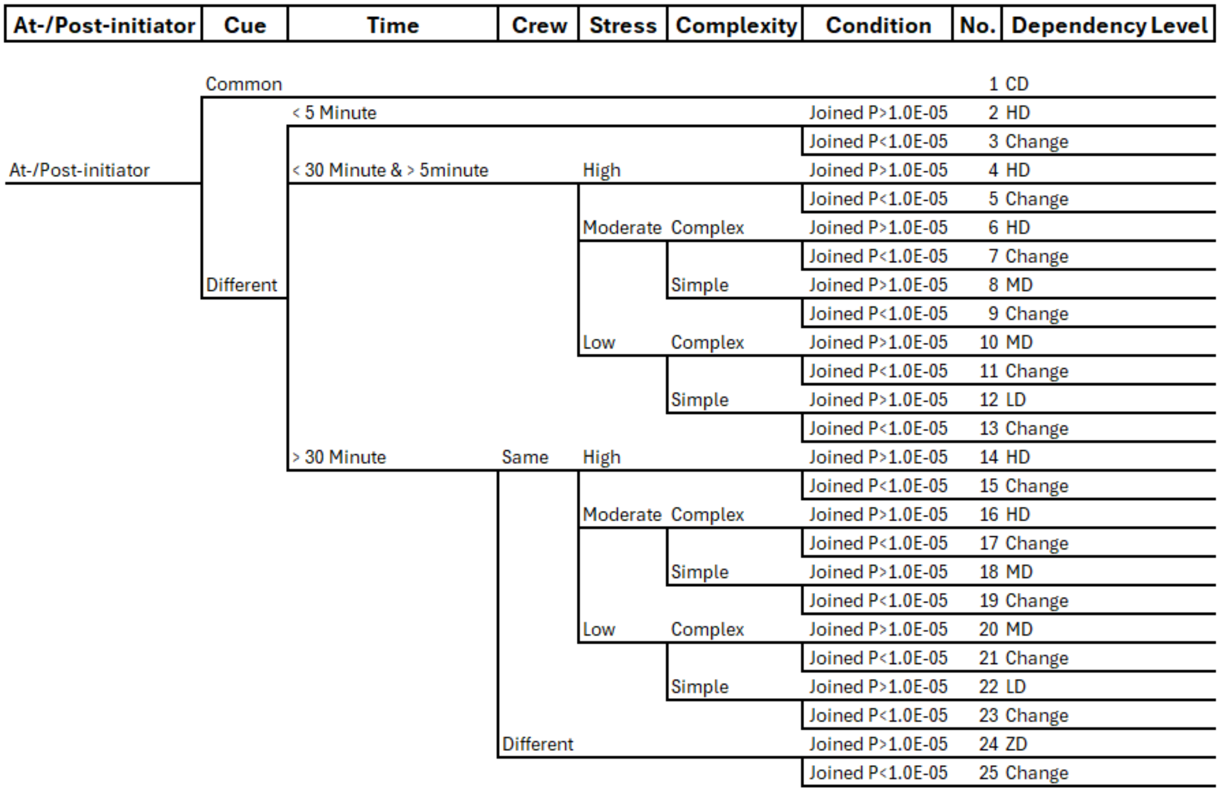

Figure 6. At-/Post-initiator Dependency Level Decision Tree

2.1.6.DSET-AHP

The Dempster-Shafer evidence theory and analytic hierarchy process (DSET-AHP) framework was developed to overcome the subjectivity of selecting the dependence level within the THERP methodology. The methodology's authors argue that the decision trees associated with subsequent HRA methodologies, some of which presented in sections 2.1.2 to 2.1.5, are not flexible due to the analyst's judgment being constrained to extreme situations [46][47]. Hence, DSET-AHP allows for representing the analyst's judgment more flexibly, incorporating both the ambiguity and the confidence of the judgment. Moreover, DSET-AHP quantifies the conditional HEP among human tasks using a predefined computational model, reducing the subjectivity associated with THERP [45].

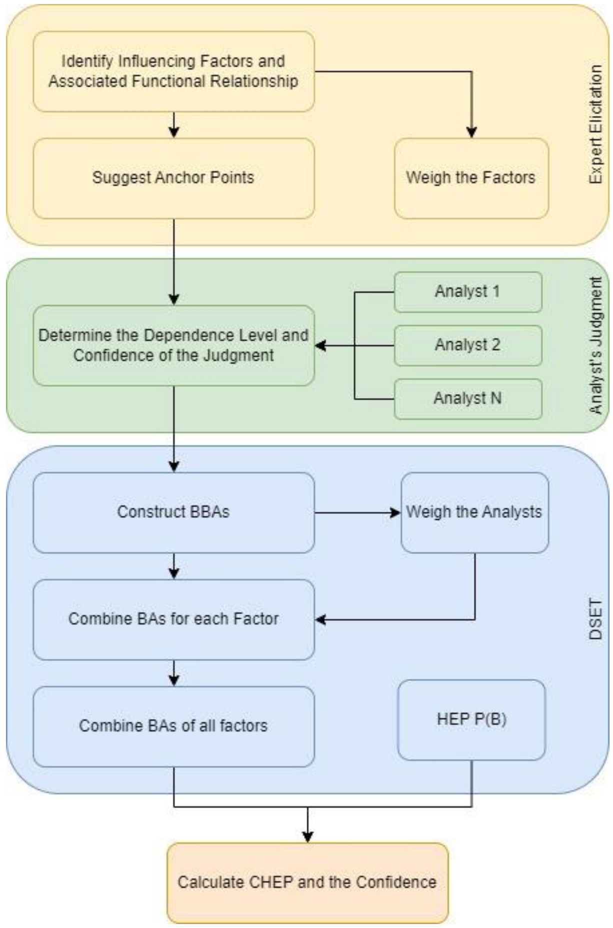

Figure 7. High-level Structure of DSET-AHP Methodology

The high-level structure of DSET-AHP, as illustrated in Figure 7, can be divided into four main parts: expert elicitation, analyst judgment, DSET process, and calculation steps. During the expert elicitation step, experts identify the input factors related to the dependence, select anchor points corresponding to five dependence levels, and evaluate the relative importance of the input factors. The analyst judgment step allows the analyst to assess the input factors according to actual situations, including their confidence judgment. The DSET process constructs basic belief assignments (BBA), which map the input factors set to a number between 0 and 1 for each of the judgments and their confidence. These BBAs are combined using a weighted average into a fused BBA. Finally, the calculation step quantifies the conditional HEP and its associated confidence based on the fused BBA.

Despite introducing multiple new concepts and incorporating multiple expert elicitations, the formula for quantifying the conditional HEP between the two actions, introduced in equation (10), is nothing but a superposition of the weighted formulae for all the dependency levels defined in THERP. The DSET-AHP builds the matrix of those weights that gives the probability that the dependence level between two actions is a certain level. In equation (10), Bet $P(XD)$ presents the pignistic probability function (weight) of a certain (X) dependence level, and $P_{XD}(B|A)$ is the conditional probability of the X dependence level as introduced by THERP presented in equations (3) to (6).

$$\begin{aligned} P(B|A) &= \sum_{XD} Bet\ P(XD) * P_{XD}(B|A) \\ &= Bet\ P(LD) * P_{LD}(B|A) + Bet\ P(MD) * P_{MD}(B|A) \\ &\quad + Bet\ P(HD) * P_{HD}(B|A) + Bet\ P(CD) * P_{CD}(B|A) \end{aligned} \tag{8}$$

2.2. Linked Bayesian Networks

2.2.1. Phoenix

The Phoenix HRA methodology was developed as part of an effort to overcome the limitations of HRA methodologies. According to Phoenix [38], the limitations of conventional HRA methodologies include the lack of theoretical basis, experimental validation, causal models, and sophisticated approaches to implement performance influence factors (PIFs). In Phoenix, PIFs are factors that, similar to THERP's PSFs, impact the failure probability of a specific task. The Phoenix methodology consists of two integrated, qualitative and quantitative, analyses. The qualitative analysis delves into the PRA scenarios to extract potential HFEs. Different crew response trees (CRT) are then developed for each potential HFE, identifying possible crew/cognitive failure modes (CFM). A failure logic model (i.e., fault tree) is built using the PIFs associated with each CFM. Within the quantitative analysis, tables of conditional probabilities are developed that estimate the success/failure probabilities of different CFMs conditional on the various states of PIFs. By implementing the conditional probability tables in the model, the analysts can quantify the HEPs associated with different HFEs.

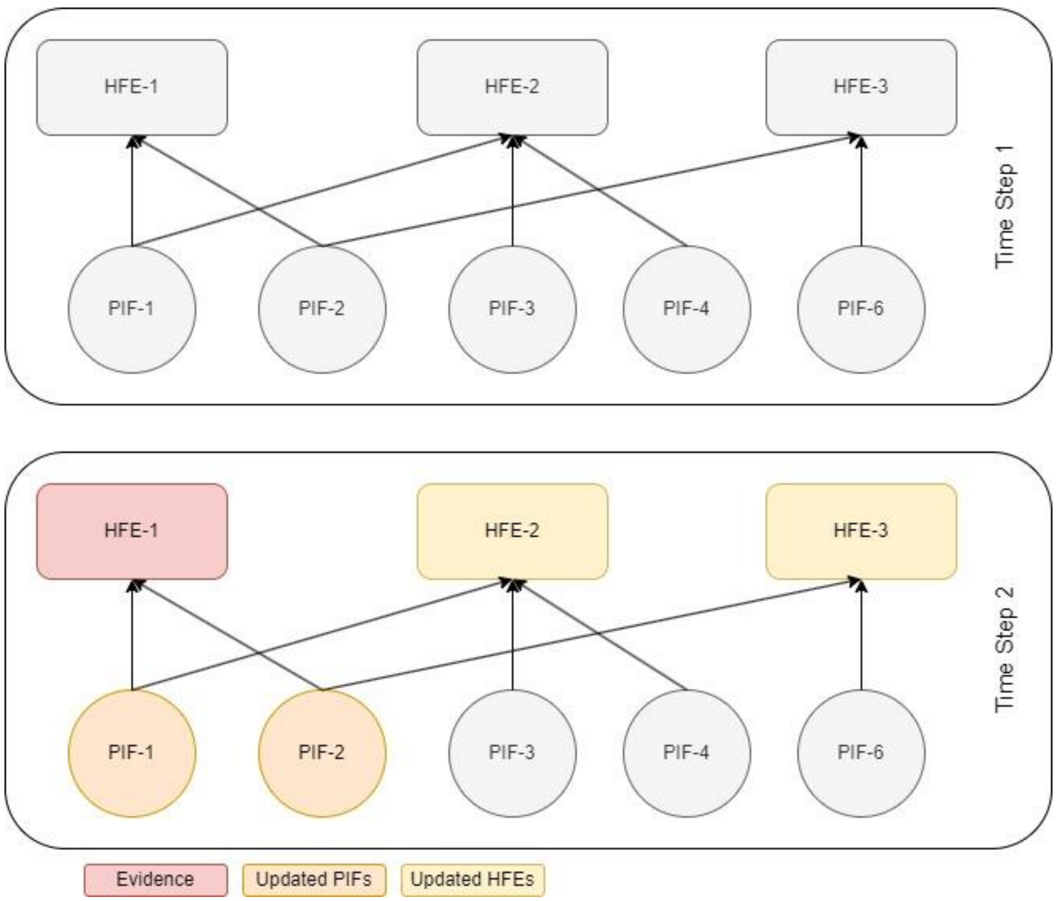

Figure 8. Phoenix's dependency analysis model.

Phoenix's dependency model heavily utilizes Bayesian belief networks (BBN), building on previous efforts to use BBN in a so-called "explicit treatment" of dependency [38][39]. According to the method's developers, the Phoenix implementation of dynamic BBNs allows for the capture of dynamic effects like changes in PIFs and the ordering of HFEs. Generally, BBNs are a-cyclic graphical models of stochastic processes. Dynamic BBNs, according to Phoenix's developers, are multiple BBNs that reflect different time steps of a specific sequence. The model developed by Phoenix can be expanded to include various nodes or levels. Horizontal expansion by adding multiple additional HFE nodes allows for modeling dependencies among multiple HFEs. Moreover, vertical expansion by adding multiple levels allows for evidential reasoning and capturing dependencies between different tasks. To model dependencies, Phoenix proposes the following steps, as illustrated in Figure 8:

- Identify the BBN nodes associated with HFEs, CFMs, and PIFs, the links/relationships between these nodes, and the different states related to each node.
  - Build the conditional probability tables associated with each node and estimate/quantify the initial probability values of each node.
- Identify the temporal ordering and time steps and build the corresponding BBNs associated with each time step.
- Incorporate the necessary evidence, i.e., HFE failures, in their appropriate time steps to update and quantify the conditional failure probability of other HFEs.

2.2.2.Other Linked Bayesian Network Methods

Using Bayesian networks to represent and quantify human failure events has been incorporated by multiple different HRA methodologies, as can be seen in [39],[48]-[52]. Despite having slight variations in their overall HRA framework, all implementations of the Bayesian networks rely on Bayesian networks to capture the one-directional impact of different performance influencing/shaping factors on human error. Such a modeling approach, illustrated in Figure 8, implicitly assumes that performance-influencing factors are external to human error. Such an implicit assumption, though it might be correct for some factors like time, may not appropriately capture dependency links from

2.3.State-of-the-art Limitations

2.3.1.Multi-Point Dependency Continuum

This can be seen in the brief review presented in section 2.1, the multi-point continuum methodologies share some characteristics that, regardless of their specific implementation, lead them to suffer from the same limitations. The formulae developed in the THERP and reused in all subsequent methodologies are based on the assumption that the current HFE only depends on the immediately preceding HFE. This approach considers only pairs of HFEs where dependency can only be assessed between two consecutive events. This limitation means that concurrent HFEs or scenarios involving more than a pair of HFEs cannot be analyzed using this methodology unless they are broken down into pairs. This simplification can lead to an incomplete understanding of dependencies in more complex situations where multiple HFEs interact simultaneously.

Also, the formulae and instructions introduced to identify and quantify the dependency level in these methodologies are based on ad-hoc operational experience rather than grounded in a cognitive framework. As a result, there needs to be more traceability or rationale provided for the cognitive reasons behind the dependency links between two actions. For instance, Figure 2 illustrates that sharing the same crew could result in various levels of dependency (Complete, High, or Moderate), but the reasoning behind these distinctions needs to be clarified. This lack of a cognitive basis means that the methodology may need to accurately reflect the true nature of human cognitive processes and the impact of these cognitive links on dependencies.

Moreover, because THERP did not present clear guidance on defining dependency levels, subsequent methodologies had to address this limitation by developing their guidance. This has resulted in inconsistency between methodologies regarding defining and quantifying dependency levels. Without standardized definitions and association rules, practitioners may interpret and apply dependency analysis differently, as can be seen in Figure 2, Figure 3, and Figure 6, reducing the reliability and comparability of results across different studies and applications.

Finally, all methodologies treat human failure as basic events, where the dependency affects the failure probability of that basic event, i.e., conditional HEP. This holistic treatment can obscure the specific links between dependencies and potential paths for improvement. For example, treating a human failure to read procedures correctly only by quantifying the failure probability of a single event (random failure) does not consider the underlying reasons, such as procedural ambiguity, which could lead to consistent failures across different tasks. This approach can lead to overestimation or underestimation of the dependency impact, as it does not capture the nuanced ways multiple factors contribute to human error. Understanding the specific causes of dependency is crucial for developing targeted interventions to reduce human error rates.

The limitations of the multi-point continuum methodologies highlight the need for more sophisticated approaches that consider multiple HFEs simultaneously, are based on a solid cognitive framework, provide clear and consistent guidance, and address the specific causes of human failures rather than treating them as holistic events. Addressing these limitations can lead to more accurate and effective human reliability analysis, improving safety and performance.

2.3.2.Linked Bayesian Networks

This can be seen in the brief review presented in section 2.2, the linked Bayesian network methodologies share some characteristics that, regardless of their specific implementation, lead them to suffer from the same limitations. Numerous conditional probabilities are required to construct a Bayesian network, many of which can only be obtained through expert elicitation. This process involves gathering judgments from experts to estimate probabilities for various conditional dependencies within the network. However, the quality and reliability of the elicited probabilities heavily depend on the expertise and subjective opinions of the individuals involved. Moreover, the impact of PIFs on CFMs is poorly understood, making it challenging to ensure the validity of the elicited probabilities. This uncertainty can lead to inaccuracies in the Bayesian network, potentially compromising the integrity of the risk assessment.

When considering links, as illustrated in Figure 8, there is an inherent assumption that the state of PIFs is consistent across both CFMs and independent of any failure. This implies that PIFs are considered external to the specific situation and unaffected by the event's progression or the failure of other HFEs. Such an assumption leads to an incomplete modeling of dependencies by overlooking the potential impact of HFEs on the PIFs. For instance, the failure of an action could introduce a new level of stress, thereby increasing the conditional probability of subsequent failures. Neglecting these dynamic interactions results in a less accurate representation of the real-world dependencies and can lead to underestimating the impact of dependency links.

Moreover, the Bayesian networks methodology needs to provide a streamlined approach to reduce the resources required for analysis. This lack of a reduction strategy means that all potential HFEs are analyzed in exhaustive detail, regardless of their significance to overall risk. This comprehensive approach can be resource-prohibitive, requiring extensive time, effort, and expertise. As a result, analysts may refrain from using Bayesian networks due to the high costs and resource demands. The detailed analysis of risk-insignificant HFEs can detract from focusing on more critical areas, leading to inefficient allocation of resources in the risk assessment process.

Despite expanding human failure analysis into a Bayesian network, most methodologies use this step primarily to quantify the failure probability of the human failure basic event for insertion into the PRA model. While more sophisticated in its initial analysis, this approach ultimately shares the same limitation as the multi-point dependency continuum methodologies. By treating human failures as basic events, the methodology overlooks the complex interdependencies and nuances of human error. This holistic treatment can obscure specific dependency links and potential improvement paths, leading to potential overestimation or underestimation of the impact of dependencies. It needs to traceably capture the detailed cognitive dependency links that contribute to human error, resulting in a less insightful risk assessment.

The limitations of Bayesian network methodologies highlight the need for more refined approaches that efficiently conduct expert elicitation, fully account for the dynamic interactions between PIFs and CFMs, develop strategies to reduce resource demands and move beyond the holistic treatment of human failures. Addressing these limitations can enhance the effectiveness of Bayesian network methodologies in human reliability analysis, leading to more effective human reliability analysis.

2.3.3.Multi-unit and Multi-module Nuclear Power Plants

The current generation of LWRs is a multi-unit project where multiple units, each with its primary loop, secondary loop, turbine, and main control room, share a single nuclear power plant site. Different units may share specific systems and resources like diesel generators, maintenance crew, and security crew. Two types of initiating events may occur for such sites: single-unit initiating events or site-wide multi-unit initiating events. Assessing the uncertainty associated with the plant/site response following an initiating event has been identified as a critical area for further improvement. Dependency analysis between HFEs is crucial as it significantly affects the overall PRA results for multi-unit NPPs. Improvements to conventional dependency analysis methods have been suggested, yet none specifically apply to MU scenarios. Key areas are tackling the complexities of human actions and emergency response prioritization in multi-unit severe accident scenarios [53][54].

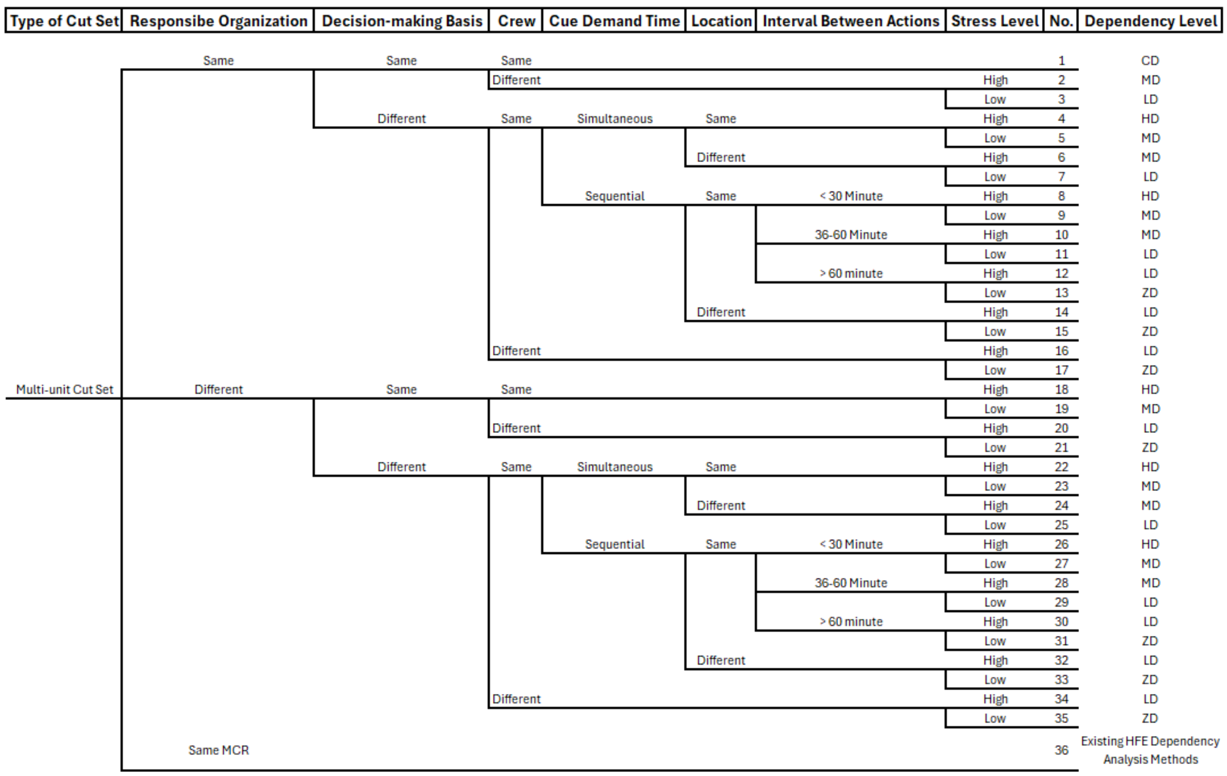

Figure 9. Multi-unit Dependency Analysis Decision Tree

Despite various efforts to address dependencies in a multi-unit site [55]-[61], most are restricted to providing additional guidance on assigning dependency levels, as seen in Figure 9. Following the assignment of the appropriate dependency level, formulae similar to those presented in equations (2) to (6) are used to quantify the conditional HEP [55]. Even those efforts face the limitation of requiring significant resources to build a causal-based parametric dependency model [58]. Even efforts of explicitly modeling multi-unit event sequences, like those presented in [56], only actions performed within the main control rooms are identified, which were subsequently assumed to be independent. Moreover, existing HRA methodologies incorporate the assumption that pre-, at-, and post-initiators are inherently independent. This assumption, even if appropriate for single-unit assessments, is never scrutinized from the perspective of multi-unit assessments.

For future generations of advanced NPPs, however, a push for reducing the operating and maintenance (O&M) costs combined with the inherent safety features of new NPP designs led to the consideration of sharing a single control room between multiple modules within the same site [18]. Moreover, a remote control/monitoring center is presented as an option for supervising mostly autonomous micro-reactor operations [62]-[64]. Within the scope of the current study, the term “multi-module” represents any advanced reactor that shares, among other resources and systems, a single control room with a single operating crew. Despite the many challenges such an environment presents to the dependency assessment of operator actions within a multi-module site, limited literature has been found to include such challenges [65][66].

During its design certification process, NuScale Power proposed a staffing plan for six licensed operators to manage up to twelve power modules from a single control room, complying with 10 CFR part 50 § 50.54(k) but not with §§ 50.54(m)(2)(i) and (iii) [67]. To address this, NuScale requested NRC approval for design-specific control room staffing requirements, providing a technical basis aligned with SECY-11-0098, which the NRC deemed acceptable. This technical basis, however, is based on a staffing plan validation (SPV) test by having trained personnel perform preplanned, challenging, and high-workload scenarios in the 12-module control room simulator [68][69]. By pursuing this approach, NuScale avoided the need to assess dependencies between operator actions by reducing all potential actions to only two [70]. However, any pursuer of licensing using the LMP methodology and the non-LWR PRA standard would be required to assess the impact of intra-module operator actions, which, as it stands, does not yet have a systematic methodology of incorporating.

2.4.Summary

Multi-point continuum methodologies, such as those developed in THERP, assume that each HFE depends only on the immediately preceding one, limiting the analysis to pairs of HFEs and neglecting concurrent or multiple interacting HFEs. This simplification can result in an incomplete understanding of dependencies in complex scenarios. Additionally, these methodologies rely on ad-hoc operational experience rather than a cognitive framework, leading to limited rationale for dependency levels and inconsistency between methods. Linked Bayesian network methodologies, on the other hand, require numerous conditional probabilities often obtained through expert elicitation, making them susceptible to biases and inaccuracies due to reliance on expert judgments. They assume that PIFs remain consistent and are unaffected by the progression of events or failures, leading to incomplete modeling of dependencies and neglecting dynamic interactions. Additionally, these methodologies need a more streamlined approach to reduce resource demands, making the analysis resource-intensive and potentially deterring their use.

Furthermore, in both dependency modeling approaches, human failures are treated as basic events, obscuring specific links between dependencies and potential improvements, which can result in overestimating or underestimating dependency impacts. Existing methodologies, moreover, provide limited guidance and widely assume independence between pre-, at-, and post-initiators. Future advanced reactors aim to reduce operating and maintenance costs with designs like shared control rooms and remote supervision of autonomous reactors, presenting new challenges in dependency assessment. The approach adopted by NuScale simplified dependency assessments, but future methodologies must address intra-module operator actions systematically, a need currently unmet by existing methodologies.

More sophisticated approaches are needed to address these limitations, which consider multiple HFEs simultaneously, are based on a solid cognitive framework, provide clear and consistent guidance, and address the specific causes of human failures rather than treating them as holistic events. Thus, they would improve the accuracy and effectiveness of human reliability analysis.

CHAPTER 3. IDHEAS DEPENDENCY MODELS

The proposed framework in this study can be considered as an expansion of the IDHEAS HRA methodology. So, in this chapter, the different versions of IDHEAS are presented along with their differences and respective dependency models. IDHEAS was developed by EPRI and the U.S. NRC, focusing on reducing the variability within HRA and increasing the consistency of the HEP estimates [71]. Within IDHEAS, a similar process to that of Phoenix is implemented in which HFEs are identified from the PRA scenario, a crew response diagram (CRD) is developed through which CFMs are identified, and decision trees (DT) are built to quantify the associated HEPs.

Despite having multiple variations [72]-[73], only the Event and Condition Assessment (IDHEAS-ECA) has a systematic approach for modeling dependencies. However, the general methodology of IDHEAS [71] identified a high-level framework of the expected dependency analysis module of the methodology. The general methodology identified the lack of cognitive foundation, explicit consideration of different parts of the HFE, and basis for dependency factors and probability adjustments as the shortcomings of the current dependency modeling and practices. The NRC staff recognized that improving individual parts of the current dependency approaches, such as providing detailed guidelines on assessing dependency factors, would not address the fundamental limitations in existing dependency approaches due to a lack of fundamental technical basis.

The guidance for conducting dependency analysis in the IDHEAS methodology [74] presents guidance for using the dependency model of the IDHEAS-ECA methodology. The full dependency analysis process in PRA begins by identifying minimal cut sets associated with an initiating event, determining which pairs of HFEs in a cut set require dependency analysis, and evaluating dependency between HFE pairs. The dependency model of IDHEAS-ECA can be broken down into three major steps: predetermination, screening, and detailed analyses. While the detailed analysis relies on IDHEAS-ECA, the predetermination and screening Analysis can be used for HFEs evaluated using other HRA methods [74].

This chapter presents a brief description of the different variation of the IDHEAS methodology and their associated dependency model. The limitations of the dependency model associated with each IDHEAS methodology are presented and discussed.

3.1.IDHEAS

The integrated human event analysis system (IDHEAS), developed by EPRI and the U.S. NRC, focuses on reducing the variability within HRA, hence increasing the consistency of the HEP estimates resulting from it [47]. Within IDHEAS, HFEs are identified from the PRA scenario, a CRD is developed through which CFMs are identified, and DTs are built to quantify the associated HEPs. Multiple variations of the general methodology (IDHEAS-G) [71] have been developed, including IDHEAS for NPP internal events at-power application (IDHEAS at-Power) [72], IDHEAS data collection effort (IDHEAS-DATA), and IDHEAS for event and condition assessment (IDHEAS-ECA).

The IDHEAS-G method consists of the following steps [71]:

- A scenario analysis step is when the PRA scenario is analyzed to identify possible HFEs.
- A task analysis step in which a CRD is developed for each HFE and the associated CFMs are identified.
- A CFM analysis step in which all associated PIFs that could impact the CFM are identified, and an associated DT is built.
- A quantification step in which the paths within DT that would result in CFM are identified and the associated HEP is quantified.

Despite sharing the overall methodology, different iterations of IDHEAS have been developed to improve certain aspects of the general methodology. The method presented in NUREG-2199, IDHEAS At-Power, offers guidance for the entire cycle of the HRA process for nuclear power plant internal events at-power applications. The guidance given by IDHEAS At-Power builds upon the guidance presented by IDHEAS-G for scenario analysis and HFE identification while presenting a more specified guidance for qualitative and quantitative analyses. Expanding on the macrocognitive functions adopted by IDHEAS-G, detection, understanding, decision-making, action execution, and teamwork, IDHEAS At-Power implements 15 CFMs that cover the status assessment, response planning, and execution phases of response. Depending on the status of different performance influencing factors (PIF), the failure probability of a specific CFM can be quantified using the appropriate DT. Finally, the IDHEAS At-Power methodology, illustrated in Figure 10, presents a method to quantify the HEP associated with a specific HFE, as stated in equation (9). In equation (9), $HEP(HFE|S)$ represents the HEP of a specific HFE given a specific scenario (S), where the outer sum is over the CRD that leads to the HFE. The inner sum is over the different CFMs applicable to that specific CRD sequence [72].

$$HEP(HFE|S) = \sum_{Critical\,Tasks} \sum_{CFM} Prob(CFM|CRD\ sequance, S) \qquad (9)$$

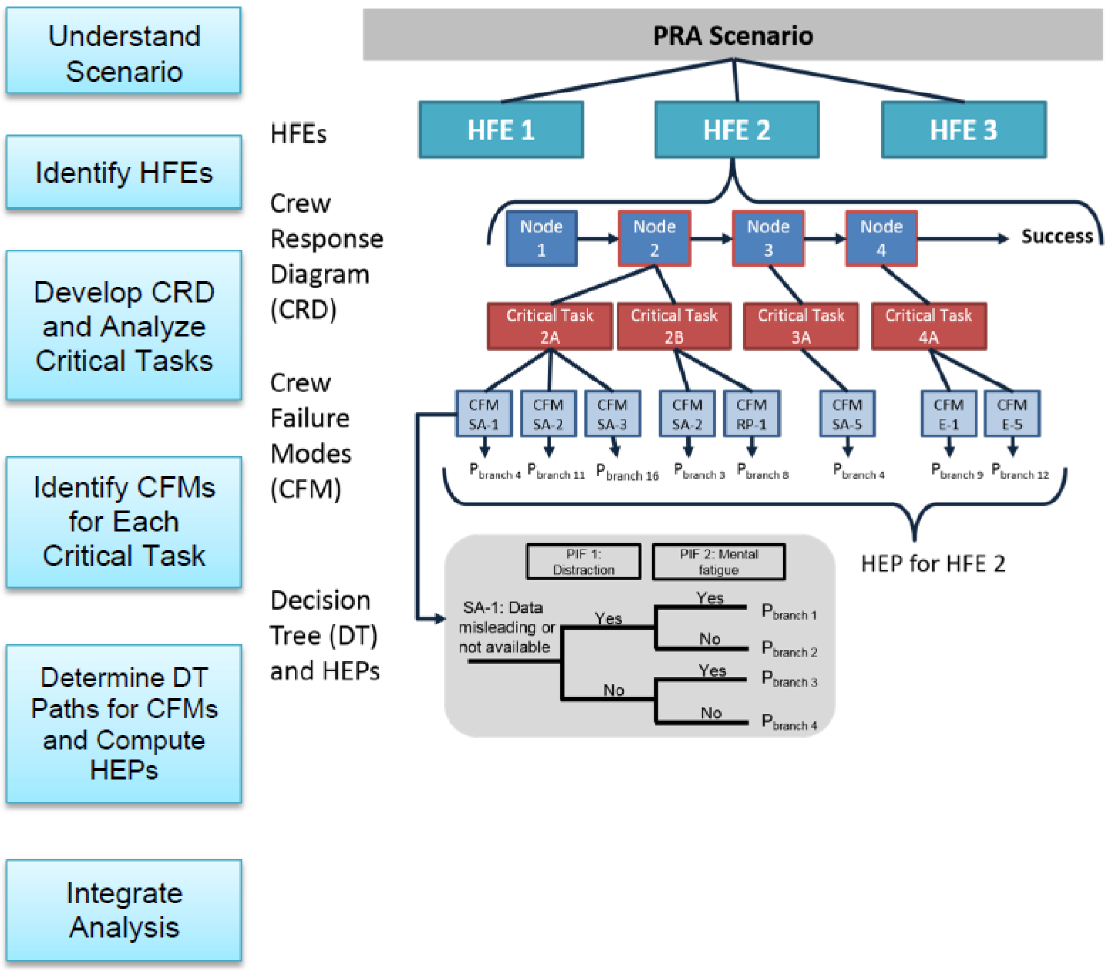

Figure 10. IDHEAS At-Power process [72].

As the name suggests, the IDHEAS At-Power methodology is developed for at-power internal events for human actions performed in the control room. On the other hand, IDHEAS-ECA is intended to be used in any HRA applications, including level 1 and level 2 PRA, internal and external hazards, at-power, low-power, and shutdown operations, etc. the IDHEAS-ECA methodology, as depicted in Figure 11, differs from IDHEAS At-Power in defining the CFMs assessed for each critical task. In IDHEAS-ECA, the generalized macrocognitive functions presented by IDHEAS-G are used as the general CFMs analyzed for each critical task. These CFMs, detection, understanding, decision-making, action execution, and interteam coordination, represent the high-level brain functions that must be successfully accomplished to perform a specific task. Associated with the methodology, the IDHEAS-ECA software package and a worksheet present a tool to conduct and streamline the quantification process of different HEPs. The probability of human failures can be quantified as depicted in equation (10), where P_c is the failure probability attributed to the CFM, and P_t is the failure probability attributed to the time uncertainty [73].

$$P(HFE) = 1 - (1 - P_c)(1 - P_t) \tag{10}$$

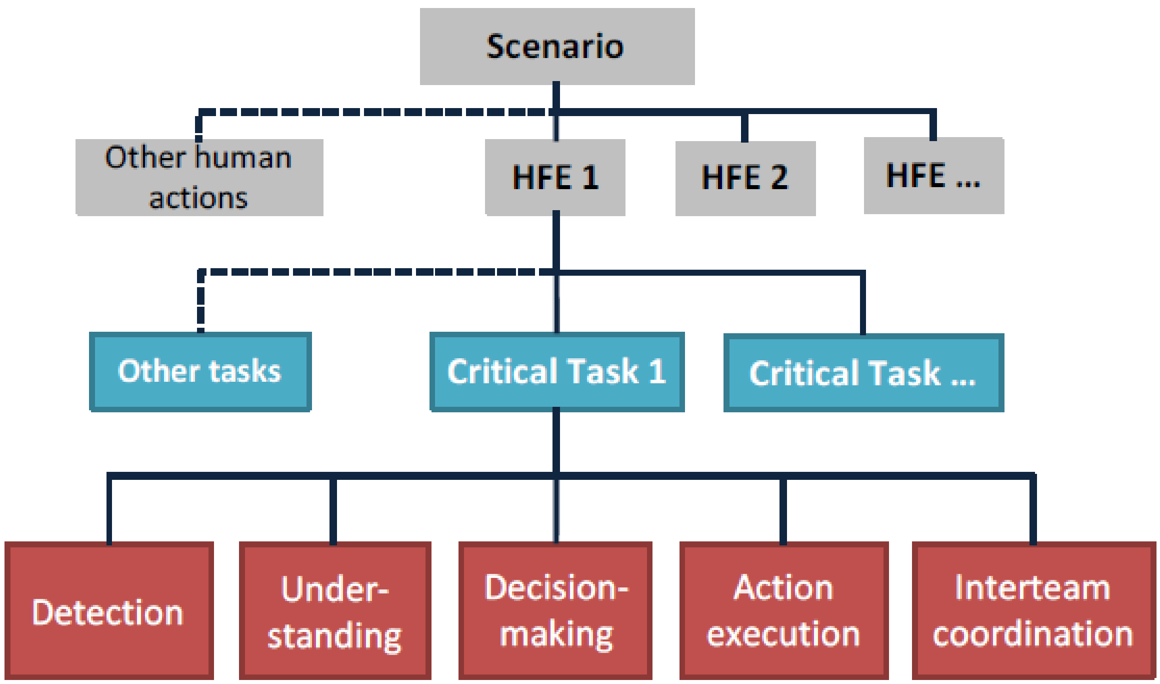

Figure 11. IDHEAS-ECA process [73].

Finally, associated documents will be published to address different parts of the IDHEAS-ECA process. These documents include NUREG-2257, NUREG-2259, NUREG-2260, IDHEAS-DATA, IDHEAS-TIME, and IDHEAS-REC, respectively. IDHEAS-DATA presents the method used to attain the data used in IDHEAS, whereas IDHEAS-TIME presents guidance for using the time uncertainty model to calculate HEPs, and IDHEAS-REC documents the guidance on evaluating and quantifying the impact of potential recovery actions from human errors. The following section discusses the dependency analysis models introduced in IDHEAS-G, IDHEAS At-Power, and IDHEAS-ECA and their limitations.

3.2.IDHEAS Dependency Model

Dependency among different HFEs is identified in all IDHEAS methodologies as having an important impact on the probability of human actions' success/failure. The context of an HFE may change significantly due to the performance of its preceding actions. In IDHEAS-G, the dependency between different HFEs is captured through the CFMs, enabling precise modeling of dependencies. According to IDHEAS-G, the dependency context categorizes dependencies into consequential, resource-sharing, and cognitive dependencies. Consequential dependencies are those where the failure of a human action directly affects various aspects of subsequent actions. Resource-sharing dependencies result from multiple tasks sharing the same resources; hence, an action taking more than the allocated resources may result in fewer resources for the subsequent actions. Finally, cognitive dependency results from a lapse in one of the cognitive activities of a task that results in incorrect action execution. The dependency model of IDHEAS-G, depicted in Figure 12, assesses the second (dependent) HFE, HFE-2, in the context of the failure of the first HFE, HFE-1. To evaluate the changes in HFE-2 in the context of the failure of HFE-1, the analyst investigates the following questions:

- Are there changes to HFE-2’s definition?
- Does the failure of HFE-1 make HFE-2 infeasible?
- Does the failure of HFE-1 change the time availability for HFE-2?
- Are the critical tasks of HFE-2 different after the failure of HFE-1?
- Are there new CFMs for the critical tasks?

- Are there changes in PIF attributes applicable to the CFMs?

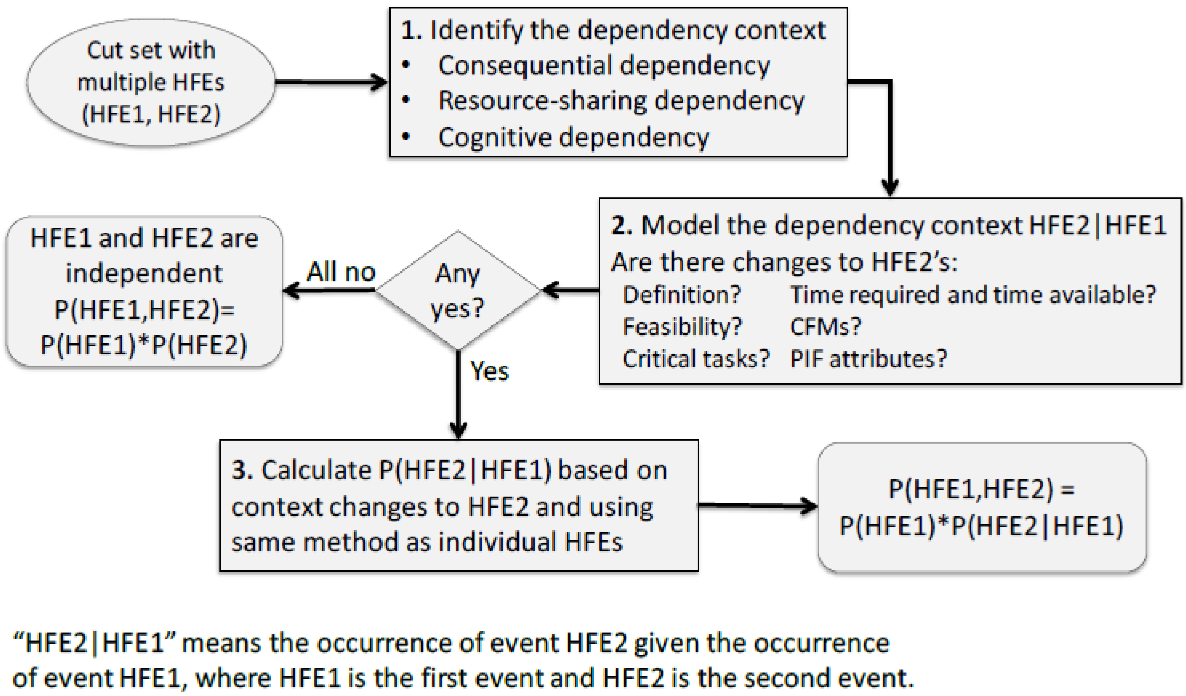

Figure 12. Overview of IDHEAS-G Dependency Model [71].

If the answers to all the questions are no, then HFE-1 and HFE-2 are deemed independent. Otherwise, the changes to HFE-2 are documented, and the HEP associated with HFE-2 is quantified in the light of the updated definition, feasibility, time availability, critical tasks, CFMs, and/or PIFs [71].

In IDHEAS At-Power, the dependency model is considered part of the HRA model integration with the PRA model, and a dependency analysis guidance still needs to be fully developed. Despite having more explicit treatment of the cognitive activities, IDHEAS At-Power utilizes the same dependency model as THERP's [15] 5-point dependency spectrum. Although IDHEAS has the potential to elucidate the dependency mechanisms because it allows human events to be analyzed while considering the underlying cognitive processes and the causal, the current version of IDHEAS At-Power does not include a method for the treatment of dependency. When performing dependency analysis between HFEs, IDHEAS allows the analysts to follow their state of practice with the existing dependency models, such as those described in NUREG-1921 or the dependency models in other HRA methods, such as SPAR-H [72].

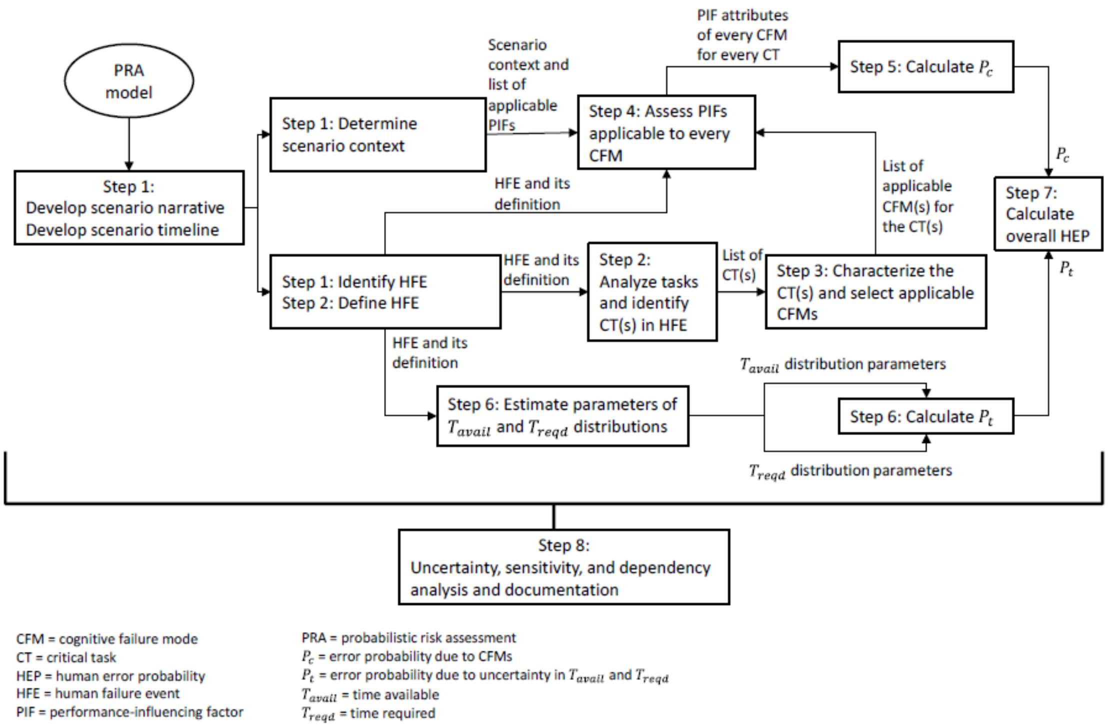

Figure 13. IDHEAS-ECA HRA process [73].

For IDHEAS-ECA, the dependency analysis is part of step 8 of the methodology, which, as can be seen in Figure 13, spans all the other steps. To describe the dependency analysis model, the model structure associated with the process is documented in a Research Information Letter (RIL) [74][74]. The model structure can be summarized in the following steps that are illustrated in Figure 14:

- Predetermination Analysis: This step identifies the relationship between the two HFEs. This relationship can either be no dependency, complete dependency, or something in between.

- Screening Analysis: In this step, potential factors applicable to the dependency are identified and assessed using a set of discount factors. The impact of each undiscounted factor is classified into low, medium, and high.
- Detailed Analysis: This step identifies the critical tasks, CFMs, PIFs, and changes in time availability due to the dependency relationship. The probability of the second (dependent) HFE is then recalculated to incorporate the dependency impact.

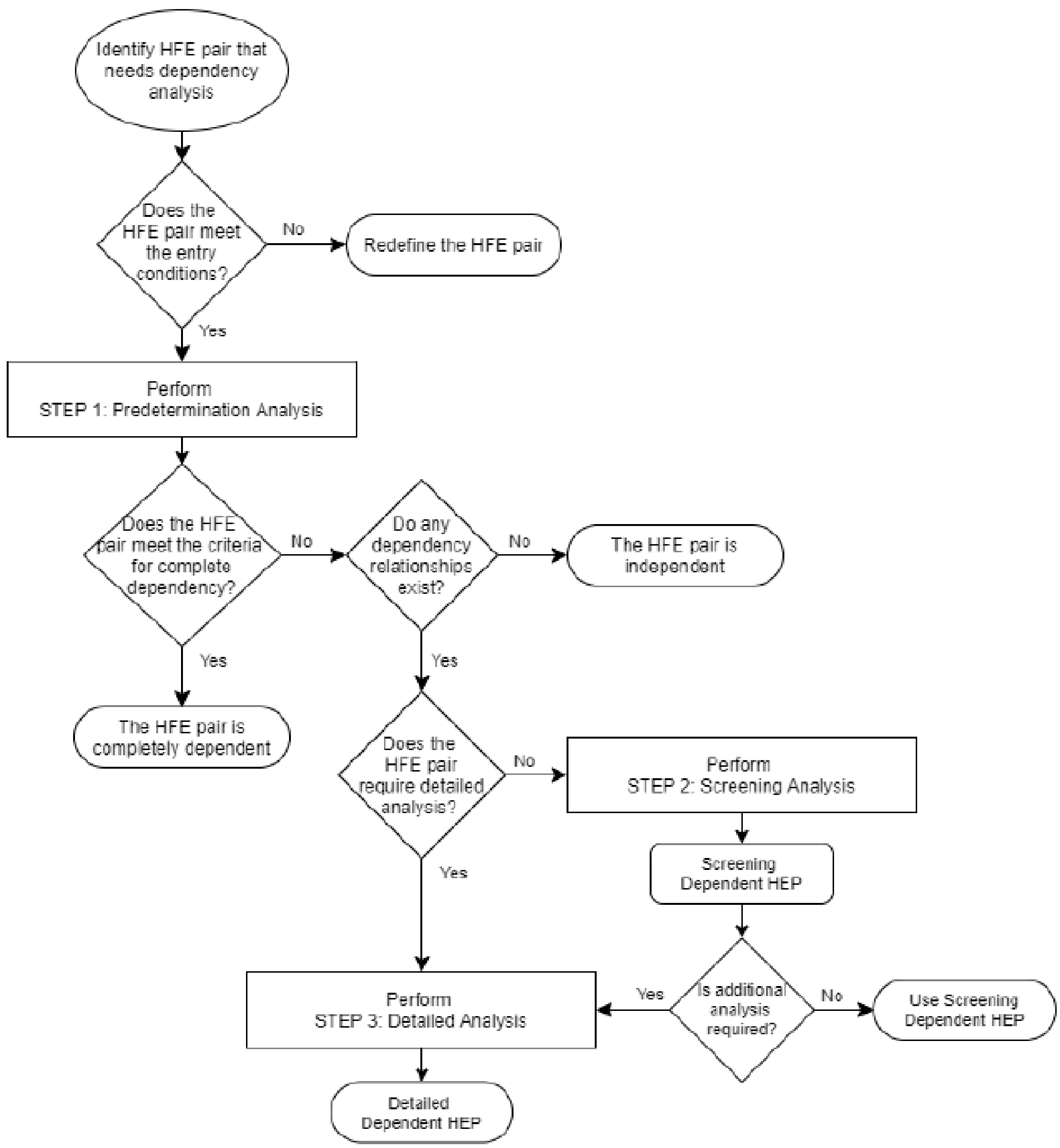

Figure 14. IDHEAS-ECA Dependency Analysis Model [74].

As shown in Figure 14, to start the dependency analysis in IDHEAS-ECA, the HFE pair needs to meet some entry conditions. These entry conditions can be summarized as either:

- The HFE pair is in the same PRA event sequence or minimal cut set, AND there are no relevant human action successes occurring between them, OR
- The first HFE is an at-initiator HFE, i.e., causing the initiating event, and the subsequent HFEs need to be assessed for dependency.

Table 2. IDHEAS-ECA Predetermination Analysis

Dependency Relationship	Assessment Guidelines	
Complete Dependency	(1) HFE1 and HFE2 use the same procedure, AND (2) HFE1 is likely to occur because of issues associated with the common procedure (such as having an ambiguous or incorrect procedure), AND (3) There is no opportunity to recover from the issue with the procedure between HFE1 and HFE2 Note: opportunity for recovery may exist if there is adequate time to recover. AND steps are in the procedure to recover, AND additional personnel outside the crew, such as a shift technical advisor (STA), are available to identify the need to recover.	- Yes - No
R1 – Functions or Systems	(1) HFE1 and HFE2 have the same functions or systems, OR (2) HFE1 and HFE2 have coupled systems or processes that are connected due to automatic responses or resources needed.	- Yes - No
R2 – time proximity	(1) HFE1 and HFE2 are performed close in time, OR (2) The cues for HFE1 and HFE2 are presented close in time.	- Yes - No
R3 – Personnel	HFE1 and HFE2 are performed by the same personnel	- Yes - No
R4 – Location	(1) HFE1 and HFE2 are performed at the same location, OR (2) The workplace for HFE1 and HFE2 are affected by the same condition (such as low visibility, high temperature, low temperature, or high radiation)	- Yes - No
R5 – Procedure	HFE1 and HFE2 use the same procedure	- Yes - No

If the HFE pair meets the entry conditions, the Predetermination Analysis step is conducted to assess the appropriate relationship between these two HFEs. First, the HFE pair is evaluated against the complete dependency criteria. If they are met, the probability of the second (dependent) HFE is adjusted to 1.0, and the dependency analysis is complete. If the complete dependency criteria are not met, the dependency relationships are assessed against a set of criteria, R1 through R5, that are evaluated in isolation. If the answer to all the dependency relationship criteria is no, then the HFE pair can be deemed independent. Otherwise, the analyst may choose to perform the Screening Analysis or the Detailed Analysis step. Table 2 illustrates the worksheet expected to be used during the Predetermination Analysis step.

CHAPTER 4. FRAMEWORK DESCRIPTION

As can be seen in CHAPTER 2 and CHAPTER 3, limited innovation is presented in the dependency analysis of HFEs. Despite the myriad of HRA methodologies, all associated dependency analysis methodologies fall under one of two broader categories: multi-point dependency continuum or Bayesian networks. In this chapter, the proposed framework for dependency analysis is presented, building on the causal framework of IDHEAS at-power. Section 4.1 briefly introduces some of the tools used in the proposed framework. Section 4.2 presents a high-level overview of the framework, whereas section 4.3 delve into the details of each associated step. It should be noted that, despite being developed using the causal model of IDHEAS at-power, the proposed framework is methodology-independent, allowing for implementation with various HRA methodologies. Section 1.1 and 4.5 present guidelines on how to incorporate multi-unit and multi-module impacts within the dependency model, respectively. Finally, section 4.6 presents the limitations associated with the proposed framework and other source of uncertainties.

4.1.Backgrounder

4.1.1.Bayesian Networks

In the proposed framework, Bayesian networks, or directed acyclic graphs (DAG), quantify the failure probability of different CFMs. Bayesian networks are directed acyclic graphs where random variables are represented by nodes connected by links presenting the probabilistic dependencies. As shown in Figure 15, two types of nodes exist within a Bayesian network: parent and descendant/child. Parent nodes are those nodes with outgoing links, whereas descendant/child nodes are those with incoming links; links represent the conditional causal dependence between two nodes. It should be noted that node types relate to the relationship between two specific nodes; in other words, a single node can be the descendant/child of some nodes while simultaneously being the parent of different nodes. However, the acyclic nature of the Bayesian networks prohibits a node from being the parent and descendent of the same node [84]-[86].

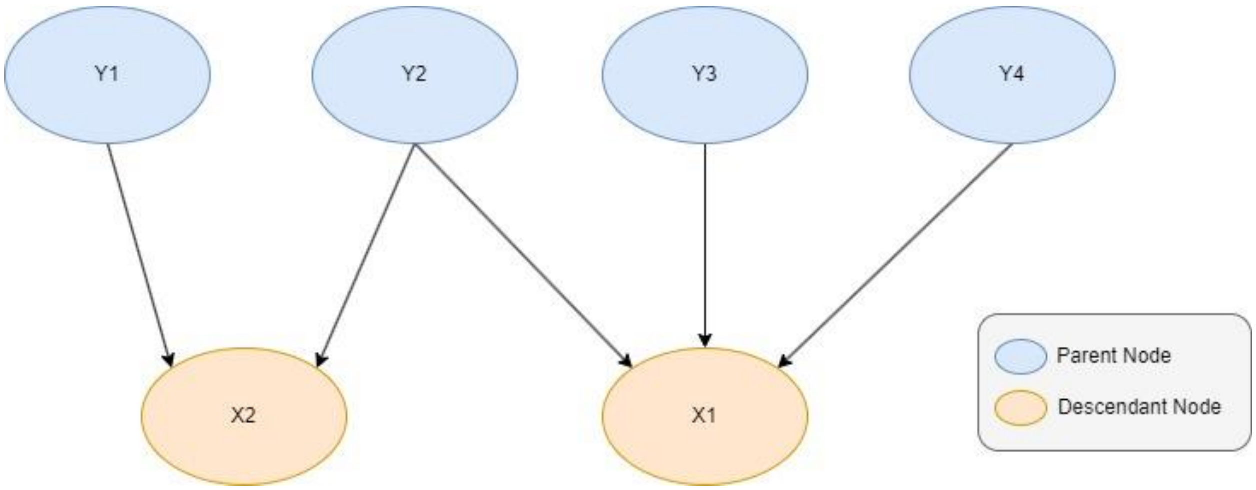

Figure 15. Bayesian Network Example

Since a Bayesian network for any event, X, determines a joint probability distribution for X, any probability can be computed using the Bayesian network. For example, the Bayesian network presented in Figure 15 can be used to calculate the probability of event X_1 given observation of the other variables as shown in equation (11). Conditional independencies can be encoded in the Bayesian network to make the computation of probabilities more efficient, resulting in the reduced form shown in equation (12) [90].

$$P(Y_1|X_1,Y_2,Y_3,Y_4,X_2) = \frac{P(Y_1,X_1,Y_2,Y_3,Y_4,X_2)}{P(X_1,Y_2,Y_3,Y_4,X_2)} = \frac{P(Y_1,X_1,Y_2,Y_3,Y_4,X_2)}{\sum_{Y_1'} P(Y_1',X_1,Y_2,Y_3,Y_4,X_2)} \quad (11)$$

$$P(Y_1|X_1,Y_2,Y_3,Y_4,X_2)$$

$$= \frac{P(Y_1)P(Y_2)P(Y_3)P(Y_4)P(X_1|Y_2,Y_3,Y_4)P(X_2|Y_1,Y_2)}{\sum_{Y_1'} P(Y_1')P(Y_2)P(Y_3)P(Y_4)P(X_1|Y_2,Y_3,Y_4)P(X_2|Y_1,Y_2)} \quad (12)$$

$$= \frac{P(Y_1)P(X_2|Y_1,Y_2)}{\sum_{Y_1'} P(Y_1')P(X_2|Y_1',Y_2)}$$

For a specific operator action, a Bayesian network, like the example given in Figure 8, can represent the ability of the operator to perform a particular task. The parent nodes to this operator action are the different environmental factors that impact the performance of this action. This Bayesian network aims to quantify the failure probability of that operator action given a specific set of environmental factors states. The dependency links, however, encode the conditional probability that the parent node and only the parent node impact the operator action—such conditional probabilities—are discussed in Section 2.3.2, grow in number quickly with each link and node state added. The number of conditional probabilities required for a Bayesian network with binary nodes is $N = 2^i$ conditional probabilities.

Moreover, isolating the impact of a single environmental factor requires an unattainable understanding of the different cognitive functions and their intricate connections. Such complexity cannot be addressed simply by eliciting experts due to the biases and uncertainties associated with each elicitation, nor by simulation due to the inability to isolate the impact of a single factor. Hence, to utilize the benefits of Bayesian networks in this framework, the limitations are presented in section 2.3.2 need to be addressed to allow building the conditional probability table. The approach utilized is inverse estimation of conditional probabilities using IDHEAS' decision trees, as presented in section 4.3.9.

4.1.2.Inverse-Canopy

Developed by the North Carolina State University PRA group, Inverse-Canopy is an inverse estimation tool that quantifies the system's unavailability margins in event sequences where only the end state frequencies are available. The tool employs a normalized relative logarithmic error loss (NRLE) within a gradient-based non-convex constrained optimization process to establish reliability bounds. Event trees graphically represent a set of event sequences where a split fraction represents each top event's success/failure. The frequency of a specific end state is then the initiating event frequency multiplied by the product of the split fractions that constitute this path. The split fractions can be considered as a set of conditional probabilities that a state of the top event can occur given a specific event sequence path, i.e., given the success/failure of previous top events [87].

Within Inverse-Canopy, a non-negative truncated log-normal distribution is enforced when quantifying the conditional probability of a particular top event. The gradients of the loss function are calculated in each iteration, refining the estimates of the conditional probability that could result in the end-state frequency. The loss function calculated in each iteration and presented in equation (13) integrates discrepancies in the probability density functions and the parameters of the log-normal distributions into a single metric. Different iterations use automatic differentiation for gradient computation to minimize the loss function until the NRLE converges to a predefined threshold or a maximum number of iterations is reached.

$$NRLE = \frac{1}{N}\sum_{i=1}^{N}\left(\frac{1}{2}\Big(MAE\big(log\big(y_{obs,i} + \epsilon\big), log\big(y_{pred,i} + \epsilon\big)\big) + MAE\big(\sigma_{obs,i}, \sigma_{pred,i}\big)\Big)\right) \tag{13}$$

Where N represents the number of end states, MAE is the mean absolute error defined for a vector of x and y of length n as $\mathrm{MAE}(x, y) = \frac{1}{n}\sum_{i=1}^{n} |x_i - y_i|$. On the other hand, y_{obs} and y_{pred} are the observed and predicted end state frequencies, respectively, and σ_{obs} and σ_{pred} represent the standard deviation of the log-normal distributions associated with y_{obs} and y_{pred}, respectively. Finally, ϵ is a small constant added to prevent the logarithm from diverging for values of y that approach zero.

In the proposed framework, Inverse-Canopy is used to quantify the conditional probability tables needed to build the Bayesian networks. To quantify the conditional probabilities, the decision trees constructed by the IDHEAS at-power methodology are used along with the expert-elicited values of the human failure probability conditional a specific path in the decision tree. This step, discussed in section 4.3.9, eliminates the limitations of implementing Bayesian networks to quantify the human failure probability while keeping the number of parameters manageable.

4.1.3.DepHep

Developed by Applied Reliability Engineering, Inc., DepHep is a Visual Basic program that identifies focus points within the dependency analysis of human actions. DepHep utilizes the EPRI's application programming interface (API) to identify potential human error combinations within the PRA model and prioritize, or rather order them, in terms of impact on the PRA model. By ordering different potential human error combinations, the analyst can determine which combinations contribute the most to a change in the cut set frequency, focusing only on those impactful combinations. DepHep utilizes a user-generated list of post-initiator HFEs included in the PRA to identify all combinations of HFEs within a specific cut set. These combinations are then listed in descending order based on their importance; within DepHep, a modified version of Birnbaum's measure of importance is used [88].

$$I_B = P(S|E_i = 1) - P(S|E_i = 0) \tag{14}$$

Birnbaum's importance measure, listed in equation (14), represents a partial derivative of the accident sequence frequency with respect to the frequency of a specific event. As can be seen in equation (14), Birnbaum importance measure, I_B, represents the failure probability of a system, S, given the success of an event, E_i, subtracting from it the failure probability of S given the failure of E_i. Unlike Fussell-Vesely, risk reduction ratio, and risk increase ratio, Birnbaum's importance measure is not a relative ratio. It is often known to overestimate the importance of events with small frequencies [24]. Within DepHep, Birnbaum's importance measure is calculated for each pair of human actions, $\mathrm{E}_1 and\ \mathrm{E}_2$, restricting the result to only where both actions appear and excluding cut sets where only one action appears. Birnbaum's importance measure is then multiplied by the probability of failure of one of the two events, $\mathrm{P}(\mathrm{E}_1)$, crediting only one operator action in the combination and assuming complete dependence of the second action on the first action. The modified version of Birnbaum's importance measure is listed in equation (15) [89]. Within this framework, DepHep is used as an automated way of identifying and ordering different combinations of operator actions within the PRA model.

$$I_{B\ Modified} = P(E_1) * [P(S|E_1 = 1, E_2 = 1) - P(S|E_1 = 0, E_2 = 0)] \tag{15}$$

4.2.Framework Overview

As with other elements, the proposed framework is connected to different elements within the PRA model. The proposed framework builds on the cognitive model developed in the IDHEAS HRA methodology. As presented in section 3.1, the IDHEAS HRA framework assesses the PRA model, including initiating event, event sequence, and systems analyses, to identify potential operator actions. Following identifying operator actions, a CRD is developed to track/identify the critical tasks required to perform the corresponding operator action. Each critical task presents a failure point, an HFE, broken down into its associated applicable CFMs. The PIFs for each CFM are identified based on the event progression. However, during the early design stages, the PRA model may not be developed enough to support a complete HRA analysis. For cases with limited HRA analysis, high-level operator actions are identified with screening values for HEPs. The proposed framework is structured such that it can support both model fidelity levels.

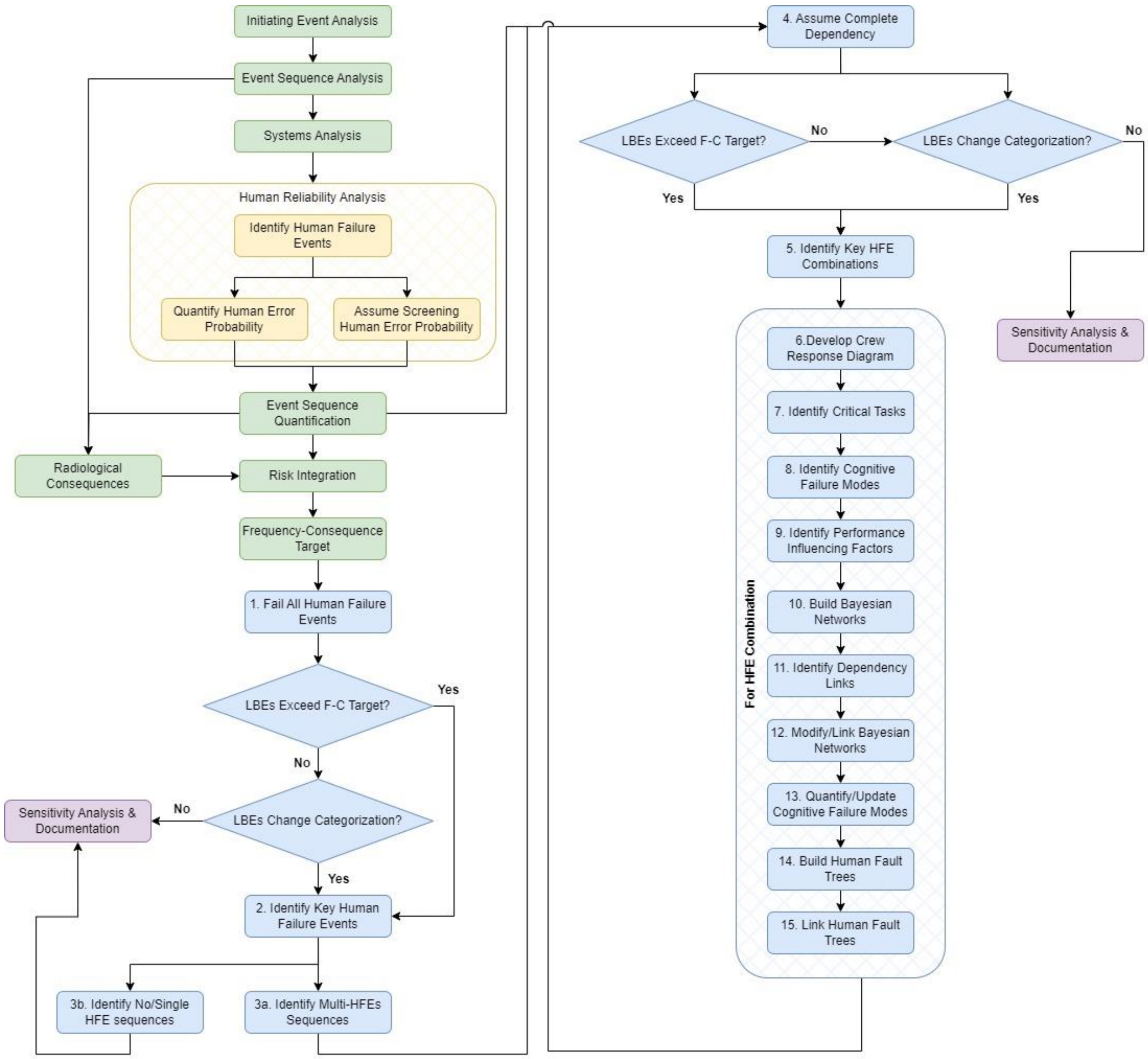

Figure 16. Framework High-level Overview

The proposed framework starts, as can be seen in Figure 16, with inputs from the PRA model that either feed directly into the framework, including Events Sequence Quantification (ESQ) and Risk Integration (RI)/Frequency-Consequence (F-C) Curve, or feed into the HRA model itself, including Initiating Event (IE), Event Sequence (ES), and Systems analyses (SA). The steps of the framework, discussed in detail in section 4.3, can be summarized as follows:

- Step 1 (Fail all HFEs): In this step, the ESQ results are used along with the F-C curve produced in RI. Initially, the HEPs associated with all HFEs, whether screening or quantified, are artificially set to a high probability (1 or close to 1). The PRA model, i.e., ESQ, is then re-quantified with the new HEP values to emphasize the impact of different HFEs within the PRA model.
- Step 2 (Identify Key HFEs): In this step, the updated results of the ESQ model are used to identify sequences whose frequencies had significant changes from the baseline model. These sequences, or licensing basis events (LBE) in the LMP methodology, heavily rely on operator actions, and the associated HFEs can be considered as key HFEs, eliciting further detailed analysis. LBEs whose frequency (mean or 95th percentile) does not show significant changes compared with the baseline are insensitive to operator actions, and the detailed assessment of their associated HFEs will result in a negligible impact on the risk profile of the PRA model.
- Step 3 (Identify Multi-HFE Sequences): LBEs with cut sets incorporating more than one HFE are identified in this step. These cut sets could include pre-, at-, and post-initiator HFE combinations. The remaining sequences that include single or no HFEs can then be easily identified as the remainder. Single HFE sequences can be used for further sensitivity analyses since this single HFE significantly impacts the risk profile of the PRA model.
- Step 4 (Assume Complete Dependency): In this step, sequences that contain multiple HFEs are modified by setting the HEP of the initial HFE to its original (screening/quantified) value while setting the HEPs associated with all following HFEs to unity. This assumes complete dependency between multiple HFEs within the same sequence, where the failure of the first HFE guarantees the failure of all subsequent HFEs.

- Step 5 (Identify Key HFE combinations): In this step, by re-quantifying the ESQ model, key HFE combinations can be identified, which are those combinations that result in significant changes in LBE frequencies. The remaining HFE combinations can then be screened out of any further detailed analysis since even a conservative assumption of complete dependency shows minimal impact on the risk profile of the PRA model.
- Step 6 (Develop Crew Response Diagram): In this step, starting with the top key HFE combination, a CRD is developed for each associated HFE. Depending on the maturity of the HRA model, CRDs may already be developed for each HFE. A CRD is a graphical representation whose nodes represent sequential critical high-level steps or tasks. Within a CRD, the failure of a critical task would result in the failure of the HFE.
- Step 7 (Identify Critical Tasks): In this step, critical tasks are identified corresponding to the tasks associated with the significant transition points in a crew's response, such as entering a procedure, transitioning to another procedure, and deciding to begin implementation and execution. Hence, the identified critical tasks can be considered a decomposition of the high-level HFE into its subtasks. It should be noted that, depending on the maturity of the HRA model, critical tasks may already be identified for each HFE.
- Step 8 (Identify Cognitive Failure Modes): In this step, for each critical task identified in Step 7, the CFM, which correspond with different sources of failure within a task, are identified. Depending on the maturity of the HRA model, CFMs may already be identified for each HFE. The IDHEAS at-power and IDHEAS ECA methodologies have a set of pre-defined CFMs, which are assessed during this step to identify applicable CFMs for each critical task.

- Step 9 (Identify Performance Influencing Factors): In this step, each applicable CFM identified in Step 8 is assessed to decide the status of each PIF. Each CFM is impacted by multiple PIFs that, depending on the status of those PIFs, change the failure probability associated with each CFM. It should be noted that, depending on the maturity of the HRA model, critical tasks may already be identified for each HFE.
- Step 10 (Build Bayesian Networks): A Bayesian network is built for each critical task, linking it with its associated CFM and PIFs. The framework presents guidance on quantifying the required conditional probabilities to construct the Bayesian network. The failure probability of each critical task can be quantified by linking the applicable CFMs, along with the appropriate PIFs, with their associated critical task. For those PIFs whose status is unknown, the framework presents a way of incorporating a non-informed impact on the failure probability of the associated HFE.
- Step 11 (Identify Dependency Link): In this step, the Bayesian networks are assessed to identify the dependency links among HFEs, critical tasks, or CFMs. The dependency links are those links between the Bayesian networks that represent the points where the failure of an HFE, a critical task, or a CFM would impact other HFEs, critical tasks, or CFMs. These links could be between HFEs and critical tasks, HFEs and CFMs, critical tasks and CFMs, and CFMs and CFMs. A link between two HFEs would represent the dependency that the framework is quantifying.
- Step 12 (Modify/Link Bayesian Networks): In this step, the Bayesian network is modified to represent the impact of the dependency. This impact is defined by changes in the conditional probability in the proceeding critical task, CFMs, or PIFs due to the failure of the preceding HFE, critical task, or CFMs. It should be noted that the failure probabilities

of the proceeding critical tasks, CFMs, or PIFs conditional on the success of the preceding HFE, critical tasks, or CFMs is simply the independent failure probability quantified in Step 10. By doing this, it is assumed that only the failure of the previous HFEs impacts the current HFE, i.e., positive dependency. However, the framework also allows for modeling negative dependency, where the success of prior HFEs impacts the current HFE.

- Step 13 (Quantify Crew Failure Modes): In this step, the linked Bayesian networks are quantified with the updated conditional probabilities to obtain the value of each CFM's failure probability. The quantified failure probability in this step represents the conditional failure probability of a CFM conditional on the failure of previous HFEs or CFMs. For the failure probability of a CFM conditional on the success of the previous HFEs or CFMs, the probability quantified in Step 10 is used.
- Step 14 (Build Human Fault Trees): In this step, a human fault tree is built for the HFE combination to be considered. A human fault tree (HFT) represents a decomposition that replaces the HFE basic event in the PRA model, merging all applicable critical tasks and CFMs under appropriate AND or OR gates. Within the HFT, all basic events represent CFMs where the failure probabilities quantified in step 13 are used.
- Step 15 (Link Human Fault Trees): In this step, the HFTs for the combination in consideration are linked within the PRA model using appropriate linking rules and flags. These links could be between specific CFMs, critical tasks, or HFTs, and they represented the change in probability in an HFT due to the failure of previous actions. These links model an if/then logic within the PRA model where if the initial action shows up in the cut set (failure), then the new probabilities of the preceding actions are used.

After modeling the first key HFE combination, the PRA model is quantified by repeating steps 4 through 15 until the change in LBE frequencies becomes insignificant. For the remaining HFE combinations that do not significantly impact the risk profile, they can be screened out of further analysis and assumed to be completely dependent on any previous HFEs.

4.3.Framework Detailed Steps

4.3.1.Step 1 Fail All Human Failure Events

The initial step in the dependency analysis methodology of any HRA methodology is to identify the HFE pairs whose dependencies will be assessed. Because, in general, multiple human actions within a single sequence are very reliable if assumed independent, cut sets with multiple human actions are almost always obscured by other cut sets that are more probable. Moreover, identifying the sensitivity of LBE frequencies relative to the failure probability of different HFEs is the initial step of multiple sensitivity analyses. Hence, to determine the most impactful HFEs on the risk profile, the HEP value associated with all HFEs is assumed to be high. An easy assumption is to assume the failure of all HFEs, i.e., assuming HEP values of 1.0E+00. However, to avoid any mathematical quirks that may result in obscuring some cut sets, another approach would be assuming a HEP value of almost, but not exactly, 1.0E+00.

After artificially increasing the impact of all HFEs within the ESQ model, the model is quantified with the new HEP values to update the frequency associated with all LBEs. Following this step, three possible outcomes will be noticed:

- Outcome 1: After assuming high HEP values, the mean or 95th percentile frequency of one or more event sequence, or LBE, exceeds the F-C target, as defined in the LMP and shown in Figure 17.

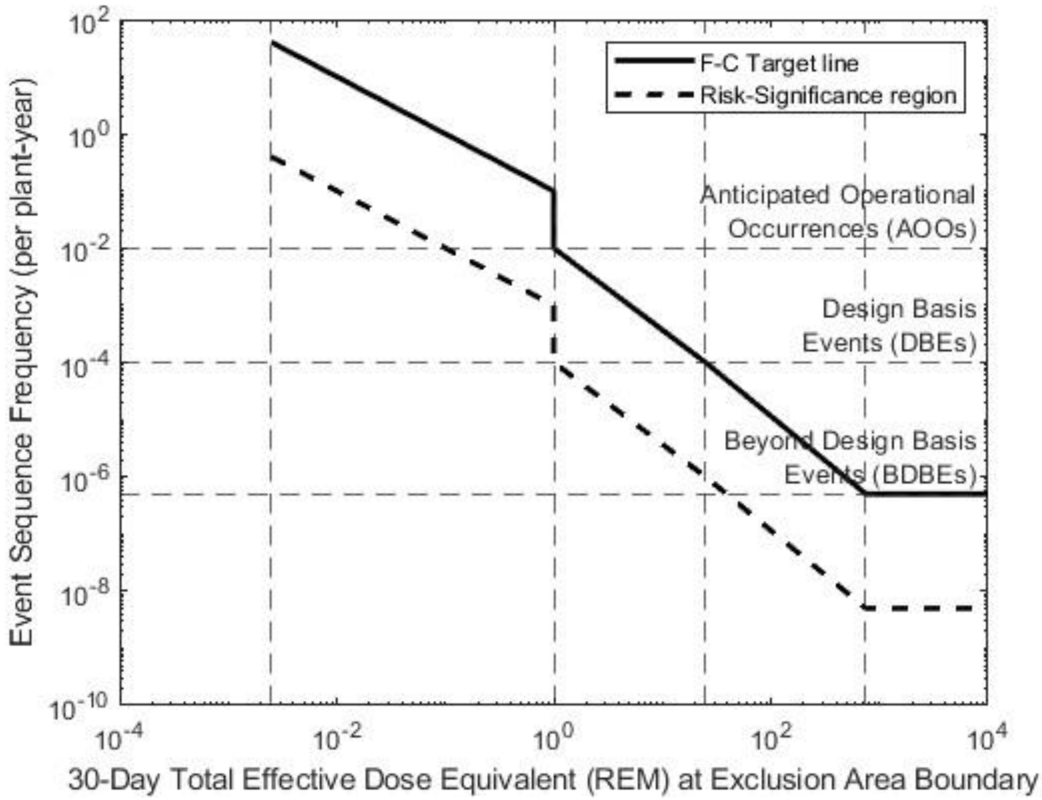

Figure 17. Frequency-Consequence Target

- Outcome 2: the mean and 95th percentile frequency of all LBEs remain within the F-C target; however, the mean or 95th percentile frequency of one or more event sequences, or LBEs, change categorization as defined in the LMP. This could happen in many ways where the frequency of an LBE:
    - Increase from the uncategorized rare events (< $5.0E-07$ per plant calendar year) into the beyond design basis event (BDBE). Design basis event (DBE) or the anticipated operational occurrences (AOO) regions.
    - Increase from the BDBE region ($< 1.0E-04\ AND > 5.0E-07$ per plant calendar year) into the DBE or AOO regions.

    - Increase from the DBE region ($< 1.0E-02\ AND > 1.0E-04$ per plant calendar year) into the AOO region ($> 1.0E-02$ per plant calendar year).

- Outcome 3: No changes in the categorization of all event sequences, or LBEs, or their 95th percentile frequency.

All these changes are documented and used in the following step.

4.3.2.Step 2 Identify Key Human Failure Events

Within this step, the results of the screening analysis conducted in 4.3 is used to identify a list of key HFEs. Key HFEs are those whose failure probabilities significantly impact the frequency of their associated LBEs. The three outcomes resulting from 4.3 are assessed to identify key HFEs as follows:

- Key HFEs are those whose assumed guaranteed failure, either independently or combined with other HFEs, results in:
    - An LBE mean or 95th percentile frequency increase exceeds the F-C target.
    - The increase of an LBE mean or 95th percentile frequency exceeding the initial LBE categorization, i.e., AOO, DBE, or BDBE.
    - The increase of an LBE mean or 95th percentile frequency exceeds the risk-significance region, even if no alternative change in categorization is quantified.
- Insignificant HFEs are those whose assumed guaranteed failure, either independently or combined with other HFEs, results in:
    - The mean and 95th percentile frequency have no change in the LBE categorization, and the LBE does not exceed the risk-significance region of the F-C curve.

The outcome of this step is a list of key HFEs that constitute the basis of further detailed analysis. The remaining insignificant HFEs present minimal/no impact on the risk profile and have limited risk insights that warrant any detailed analysis.

4.3.3.Step 3 Identify Multi-HFEs Sequence

This step uses the list of key HFEs to identify cut sets with multiple HFEs, including pairs, triplets, quadruples, or more HFE combinations. It should be noted that, in general, any m HFE combination includes k combinations of n size, where $k = {}^{m}C_{n}$; for example, a triplet HFE combination $(m = 3)$ includes $k = 3$ pairs $(n = 2)$ of HFE combinations. This step can be automated by a script scanning through different cut sets using the list developed in 4.3.2, to extract cut sets that contain more than one HFE from the list. Moreover, it should be noted that this step can be performed using the complete set of HFEs within the PRA model. However, minimal benefit is expected from identifying HFE combinations that have minimal impact on the risk profile.

4.3.4.Step 4 Assume Complete Dependency

Within this step, all cut sets identified in 4.3.3 are modified where the HEP value of the initial HFE in the sequence is set to its original HEP value, i.e., pre-Step 1 value, while all the remaining HFEs within the sequence are set to 1.0E+00. By doing this, a complete dependency between all the HFEs within the same sequence is assumed, where the failure of the first HFE results in a guaranteed failure of all subsequent HFEs. The ESQ model, or specific LBE frequency, is then re-quantified to capture the change in frequency due to the assumption of complete HFE dependency. Similar to 4.3, the possible outcomes of this step are:

- Outcome 1: the mean and 95th percentile frequency of the LBE exceeds the F-C target, as defined in the LMP and shown in Figure 17.

- Outcome 2: the mean and 95th percentile frequency of the LBE remain within the F-C target; however, the LBE changes categorization as defined in the LMP.
- Outcome 3: No changes in the categorization of the LBE.

This step's result is a list of HFE combinations and their associated impact on the risk profile of assuming complete HFE dependency, which is then fed into the following step.

It should be noted that this step constitutes the start of an iterative process where detailed analysis is conducted on a specific HFE combination, then complete dependency between the remaining HFEs is assumed, and the impact on the risk profile is reassessed to decide whether further detailed analysis is needed. If no LBE categorization change occurs (mean or 95th frequency) nor the LBE does not exceed the F-C curve's risk-significance region (mean or 95th frequency) following the assumption of complete dependency, limited risk insight is expected by conducting any further detailed analysis. Hence, for such insignificant HFE combinations, a conservative assumption of complete dependency can be used and documented for any sensitivity analyses.

4.3.5.Step 5 Identify Key HFE Combinations

This step identifies key HFE combinations within LBE cut sets using appropriate importance measures. The result of the importance measure is then used to arrange the HFE combinations in descending order for further analysis. The proposed framework leaves the choice of the appropriate importance measure up to the analysts; however, an example of a potential importance measure is given in the demonstration presented in CHAPTER 5. Step 5 presents another iterative step where, for each iteration starting from Step 4, HFE combinations are arranged to decide the order of combinations considered for the detailed analysis.

4.3.6.Step 6 Develop Crew Response Diagram

For the first key HFE combination identified in 4.3.5, a CRD is developed for each HFE within the combination. Depending on the maturity of the HRA model itself, CRDs may be available for all HFEs within the PRA model. However, the proposed framework allows for using a low-fidelity HRA model during the early design stages. Hence, the CRD associated with the HFEs within the first key HFE combination is developed for those low-fidelity HRA models. The CRD is an illustrative decomposition of the subtasks associated with an HFE. Building the CRD allows for identifying which procedures are applicable and in play in this scenario context, the decisions that must be reached and the execution tasks that must be performed to achieve the functional goal, the critical activities, and what must be done to complete the critical tasks, and the timeline of cues and the estimated time to reach specific points in the PRA scenario.

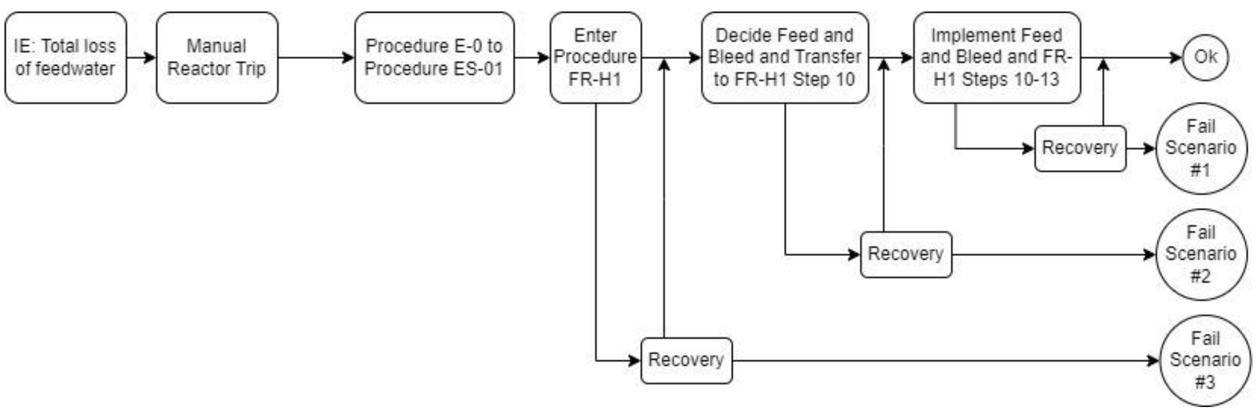

Figure 18. Example of Crew Response Diagram (reproduced from [72])

By developing the CRD of a specific HFE, as seen in Figure 18, the critical tasks associated with that HFE can be identified along with potential recovery paths. The CRD can be seen as a combination of sequential and parallel failure nodes that collectively model the failure of the main HFE.

4.3.7.Step 7 Identify Critical Tasks

Within this step, the nodes of the CRD developed in 4.3.6 are assessed as failure points, the failure of which would result in the failure of the main HFE. Depending on the type of the critical task, the logic of connecting these critical tasks can be either by OR or AND gates. Generally, sequential tasks are connected by OR gates, whereas recovery actions are connected by AND gates with their associated tasks. Critical tasks identified in this step are the middle level, which connects the top level, the HFE, with all the associated subtasks. Identifying critical tasks is the first step in building the qualitative part of the HFT presented in 4.3.14. For instance, building HFT of the failure presented in Figure 18, and simplified in Figure 19, can be seen in Figure 20.

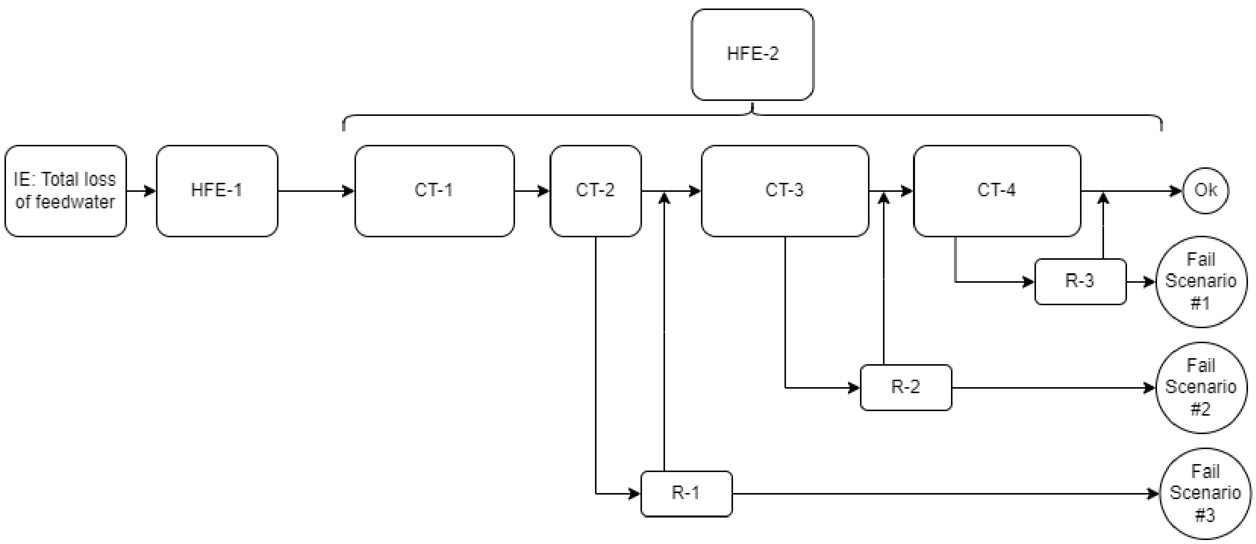

Figure 19. Simplified Crew Response Diagram

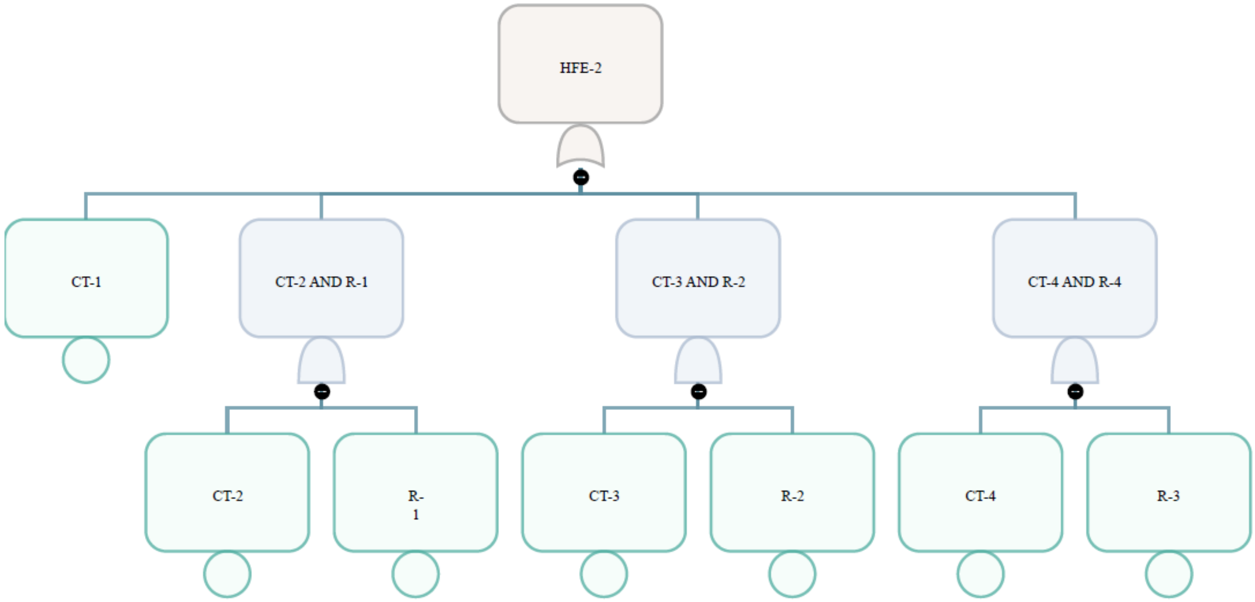

Figure 20. Initial Qualitative Human Fault tree for Example CRD

It should be noted that the basic events within the HFT in Figure 20, representing critical tasks and recovery points, will be replaced by appropriate gates in later steps.

4.3.8.Step 8 Identify Cognitive Failure Modes

Within this step, pre-defined CFMs are assessed to identify all applicable CFMs for each critical task of the HFE. These pre-defined CFMs represent how failure to perform specific tasks within operating procedures could occur. Within IDHEAS At-power, the CFMs summarize the failure of basic tasks within different response phases, status assessment, planning, and execution. The CFMs, listed in Table 3, constitute the low-level part, basic events, of the HFT developed in later steps. Since the failure of any of these CFMs represents a failure of the critical task, all applicable CFMs are connected to their respective critical tasks as part of an OR gate. All the applicable CFMs and any additional information/assumptions are listed for each critical step. Table 3 presents an example of an analysis sheet used to identify the applicability of a specific CFM to a critical task. It should be noted that some of these CFMs are mutually exclusive, E-4 and E-5, and cannot be both applicable to the same critical task.

Table 3. CFMs Identification Analysis Sheet (IDHEAS At-Power)

CFM	Applicable	Not Applicable	Notes
AR: Key alarm not attended to			
SA-1: Data misleading or not available			
SA-2: Wrong data source attended to			
SA-3: Critical data incorrectly processed/misperceived			
SA-4: Critical data dismissed/discounted			
SA-5: Premature termination of critical data collection			
RP-1: Misinterpret procedures			
RP-2: Choose inappropriate strategy			
E-1: Delay implementation			
E-2: Critical data not checked/monitored with appropriate frequency			
E-3: Fail to initiate execution			
E-4: Fail to execute simple response correctly			
E-5: Fail to execute complex response correctly			
MP: Misread or skip critical step(s) in procedure			
C-1: Miscommunication			

It should be noted that IDHEAS At-power, as described in section 3.1, is applicable for at-power operator actions within the control room. Pre-initiators, at-initiators, and post-initiators performed outside the control room all fall outside IDHEAS At-power's scope. Hence, the proposed methodology incorporates IDHEAS-ECA for operator actions that fall outside the scope of IDHEAS At-power. For IDHEAS-ECA, the five high-level cognitive failure modes introduced in the general methodology are implemented: Detection, Understanding, Decision Making, Action Execution, and Interteam Coordination. Like the treatment of at-power control-room actions, IDHEAS-ECA’s CFMs constitute the low-level part, basic events, of the HFT developed in later steps. Since the failure of any of these CFMs represents a failure of the critical task, all applicable CFMs are connected to their respective critical tasks as part of an OR gate. All the applicable CFMs and any additional information/assumptions are listed for each critical step. Table 4 presents an example of an analysis sheet used to identify the applicability of a specific CFM to a critical task.

Table 4. CFMs Identification Analysis Sheet (IDHEAS-ECA)

CFM	Applicable	Not Applicable	Notes
Detection			
Understanding			
Decision Making			
Action Execution			
Interteam Coordination			

4.3.9.Step 9 Identify Performance Influencing Factors

Within this step, the PIFs associated with each CFM identified in 4.3.8 are assessed to determine the status of each PIF within the PRA scenario. It should be noted that, within IDHEAS at-power, decision trees, shown in Appendix A, are used to assess the status of each PIF and the associated CFM failure probabilities. However, the proposed framework utilized the decision trees to identify conditional probabilities that link PIFs with their CFMs. To conduct this analysis, inverse estimation of the conditional probabilities is quantified based on the failure probabilities of the different crew failure scenarios. The inverse-canopy tool, developed by A. Earthperson et al. [87], is used to quantify the conditional probability associated with each split question in the decision trees. To avoid introducing any constraints, each split question within the event tree is assessed as its conditional probability, meaning that no assumption on the independence between PIFs is made. The results, illustrated in Figure 21 to Figure 34, present the quantitative basis of the Bayesian networks and subsequent HFTs.

It should be noted that, despite not making any assumptions regarding the independence between PIFs, the conditional probability of some PIFs remains constant regardless of the status of previous PIFs, like recovery PIFs, which indicates the independence of this PIF. Moreover, the proposed approach to quantifying PIF conditional probabilities mitigates one of the limitations of previous

HRA methodologies. HRA methodologies that rely on Bayesian networks require many conditional probabilities that require lengthy expert elicitation without any verification path.

In this methodology:

- A decision tree is built for each CFM with all its associated PIFs. Different crew failure scenarios are identified, and an exhaustive list of different PIF statuses is built.
- These crew failure scenarios are then described to the experts in a formal elicitation process where they are asked to quantify the failure probability associated with each scenario, i.e., $P(Failure|PIF_1, PIF_2, PIF_3 \ldots)$.
- The decision trees, along with the elicited failure probabilities associated with each crew failure scenario, are inserted in an inverse estimation tool, similar to inverse-canopy, to quantify the conditional probabilities associated with each PIF status. The inverse estimation tool quantifies the split fraction $P(PIF_i)$ such that $P(S_j) = \prod_{i=1}^{n} PIF_{i,j}$.

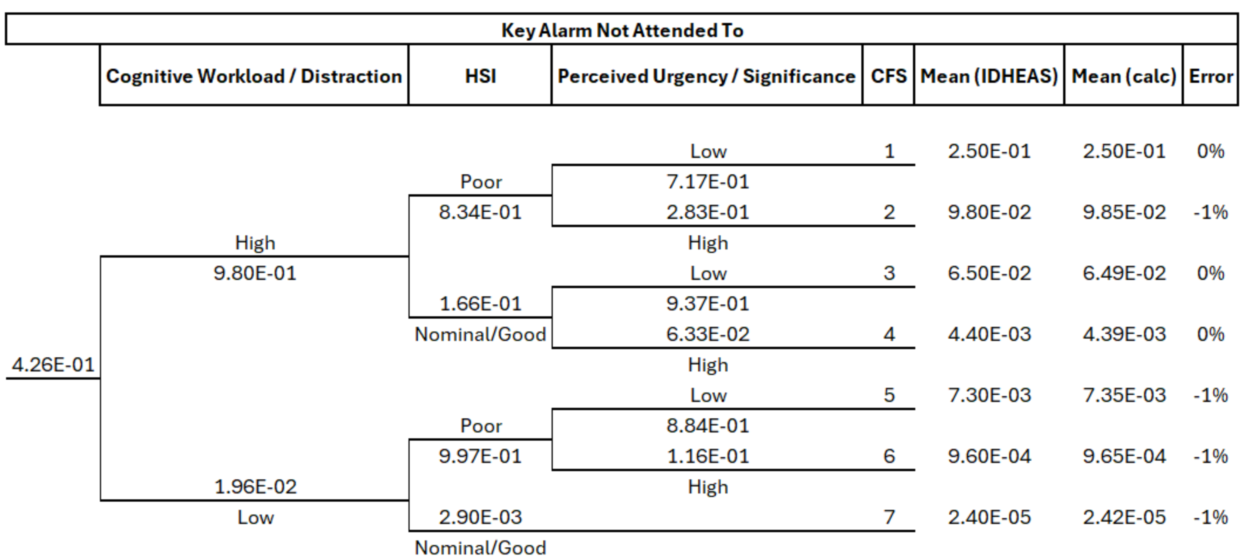

Figure 21. Conditional Probabilities for CFM AR

The proposed methodology allows for the inverse quantification of these conditional probabilities, which reduces the expert elicitation load and only estimates the failure probabilities associated with each crew failure scenario. Moreover, crew failure scenarios with a set of PIF statuses are more accessible to model using simulators than trying to model specific conditional probabilities between PIFs.

The scripts used to quantify the conditional probabilities for IDHEAS at-power decision trees are listed in Appendix B. The conditional probabilities quantified using inverse-canopy are listed in Figure 21 to Figure 34 and used in building the Bayesian networks in the following steps.

It should be noted that the conditional probabilities allow for an additional feature within the Bayesian networks compared to decision trees: modeling uninformed priors. For those PIFs whose statuses are unknown during the analysis, the conditional probabilities identified in this step allow for incorporating a state of uncertainty in the Bayesian network and the failure probability associated with the CFM.

For operator actions that fall outside the scope of IDHEAS At-power, however, the IDHEAS-ECA software is used to quantify the failure probability associated with each CFM. The failure probability of each CFM relies on multiple performance operating factors and attributes that modify the base HEP associated with each CFM by a pre-defined ad hoc factor. Quantified these factors relied on expert judgment and faced a similar limitation as the conditional probability table (CPT) values associated with linked Bayesian networks. However, due to the lack of additional resources that allow for building appropriate decision trees, this is identified as a limitation of the proposed network and suggested as future work for improvement.

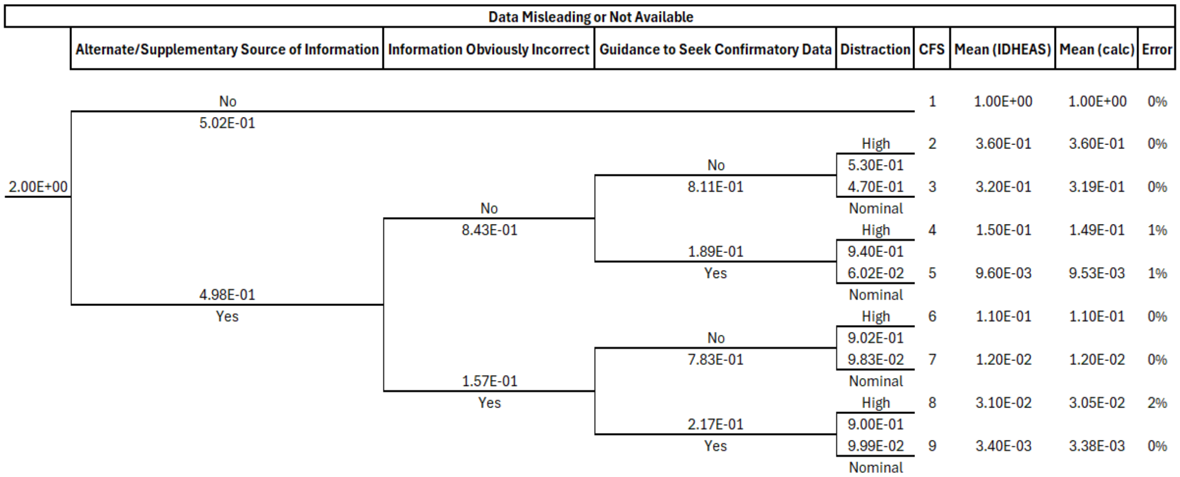

Figure 22. Conditional Probabilities for CFM SA-1

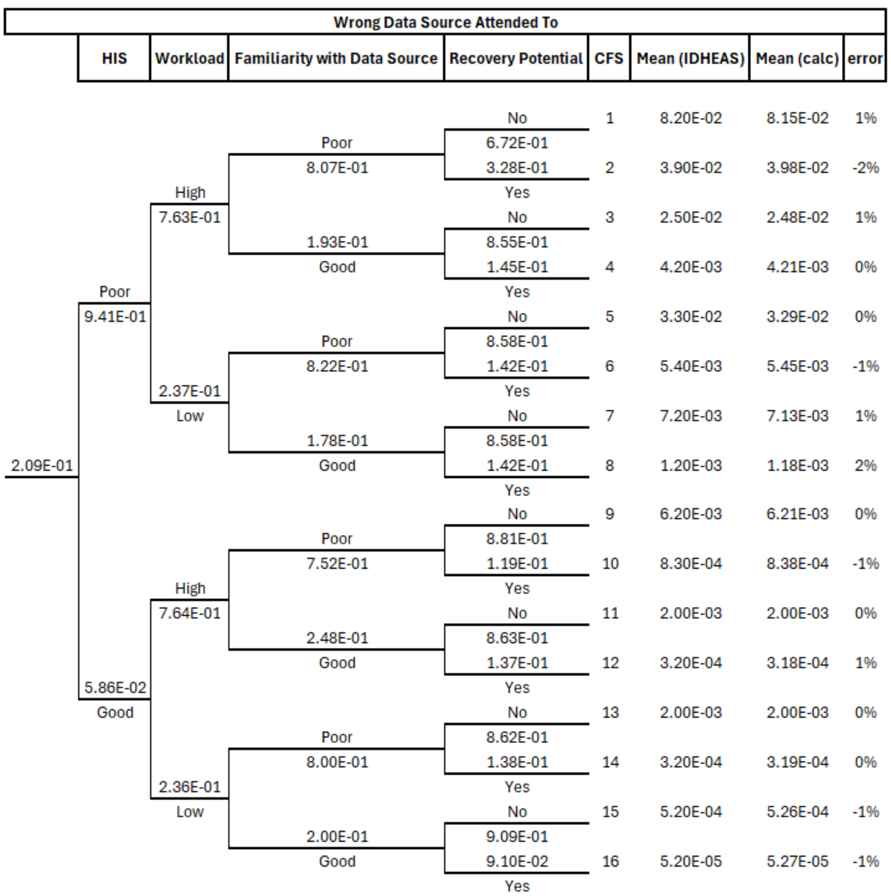

Figure 23. Conditional Failure probabilities for CFM SA-2

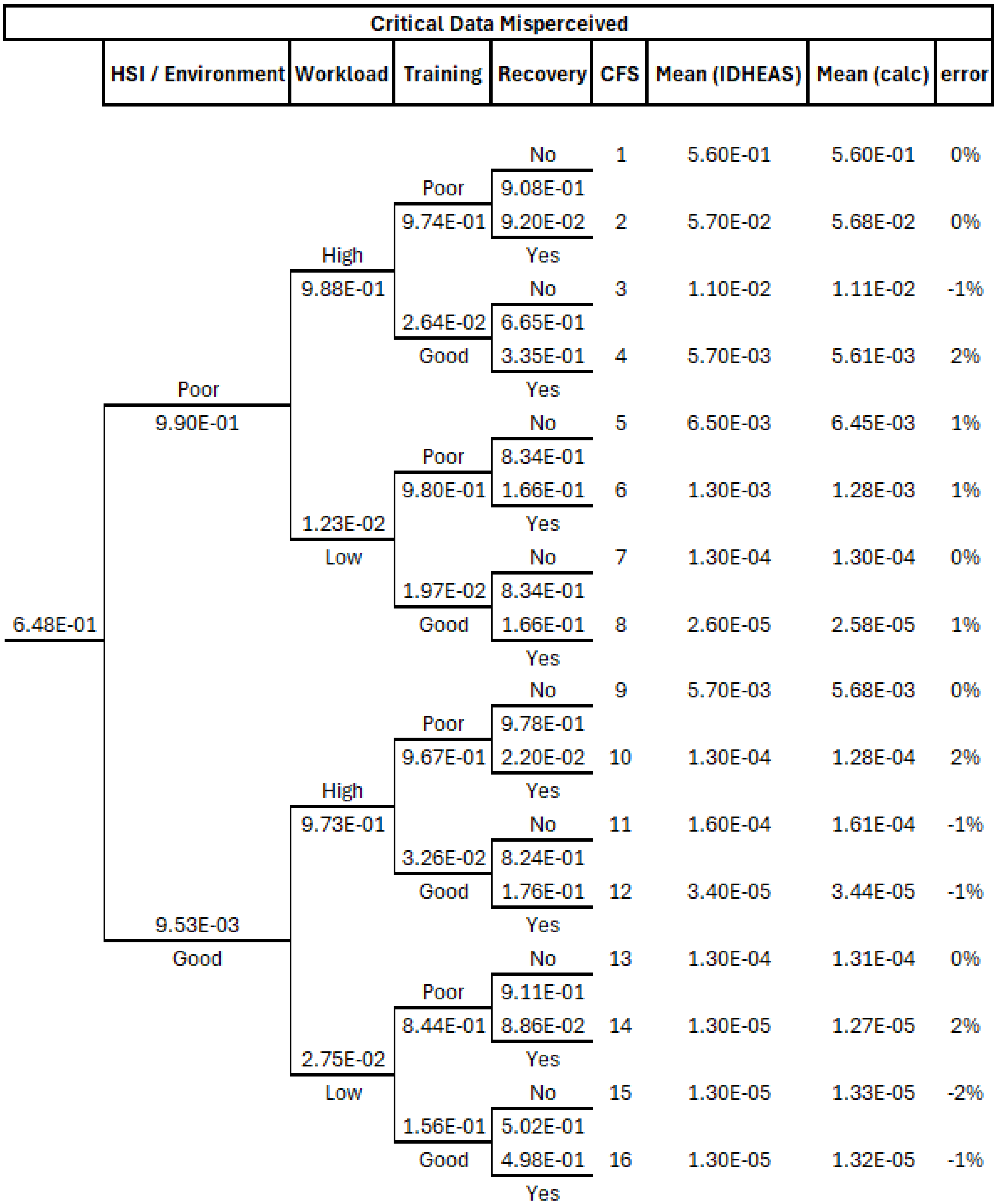

Figure 24. Conditional Probabilities for CFM SA-3

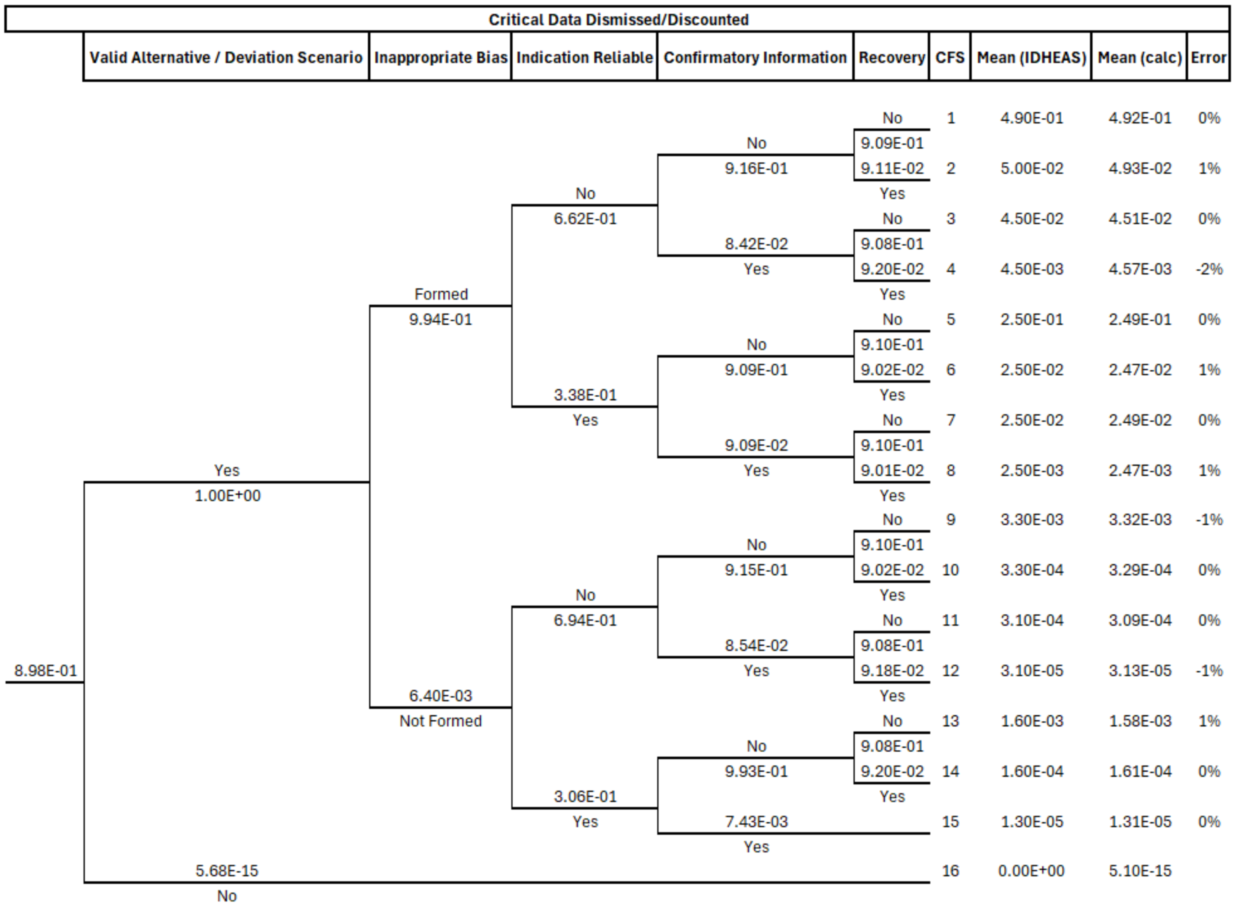

Figure 25. Conditional Probabilities for CFM SA-4

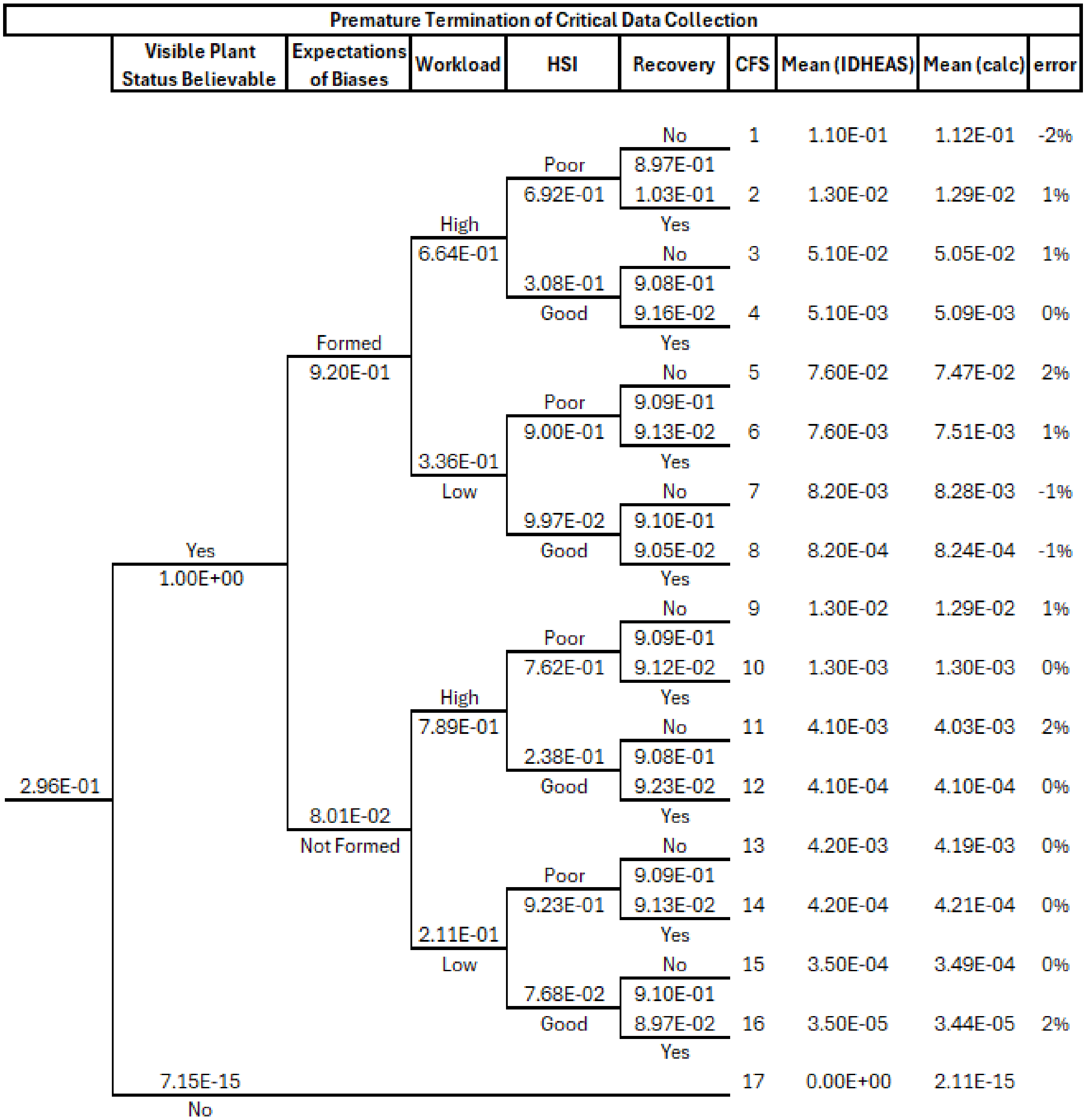

Figure 26. Conditional Probabilities for CFM SA-5

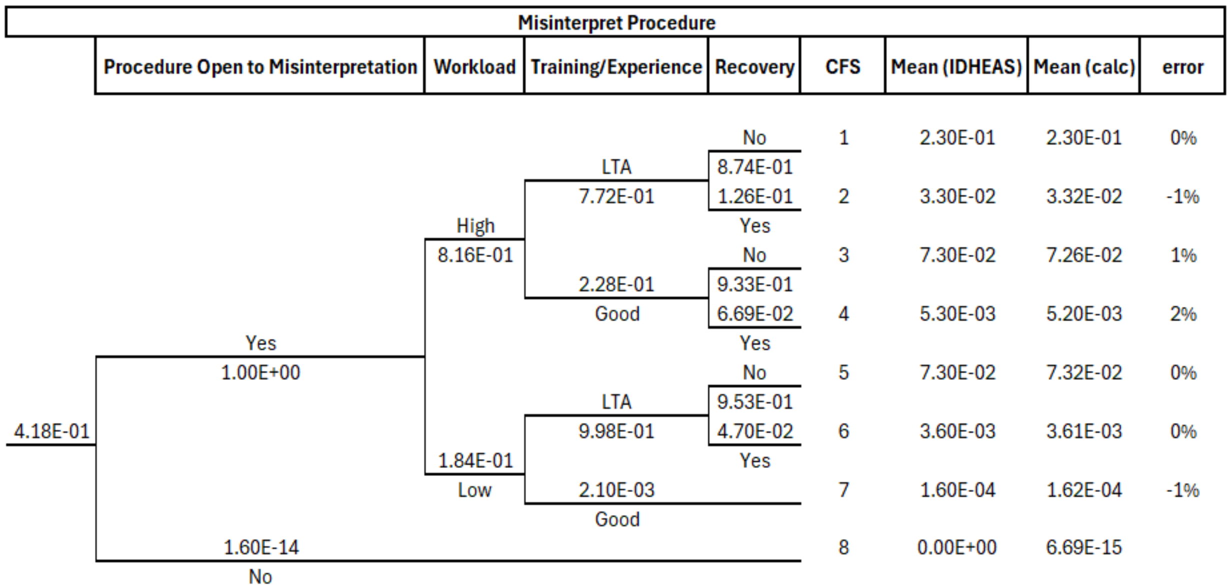

Figure 27. Conditional probabilities for CFM RP-1

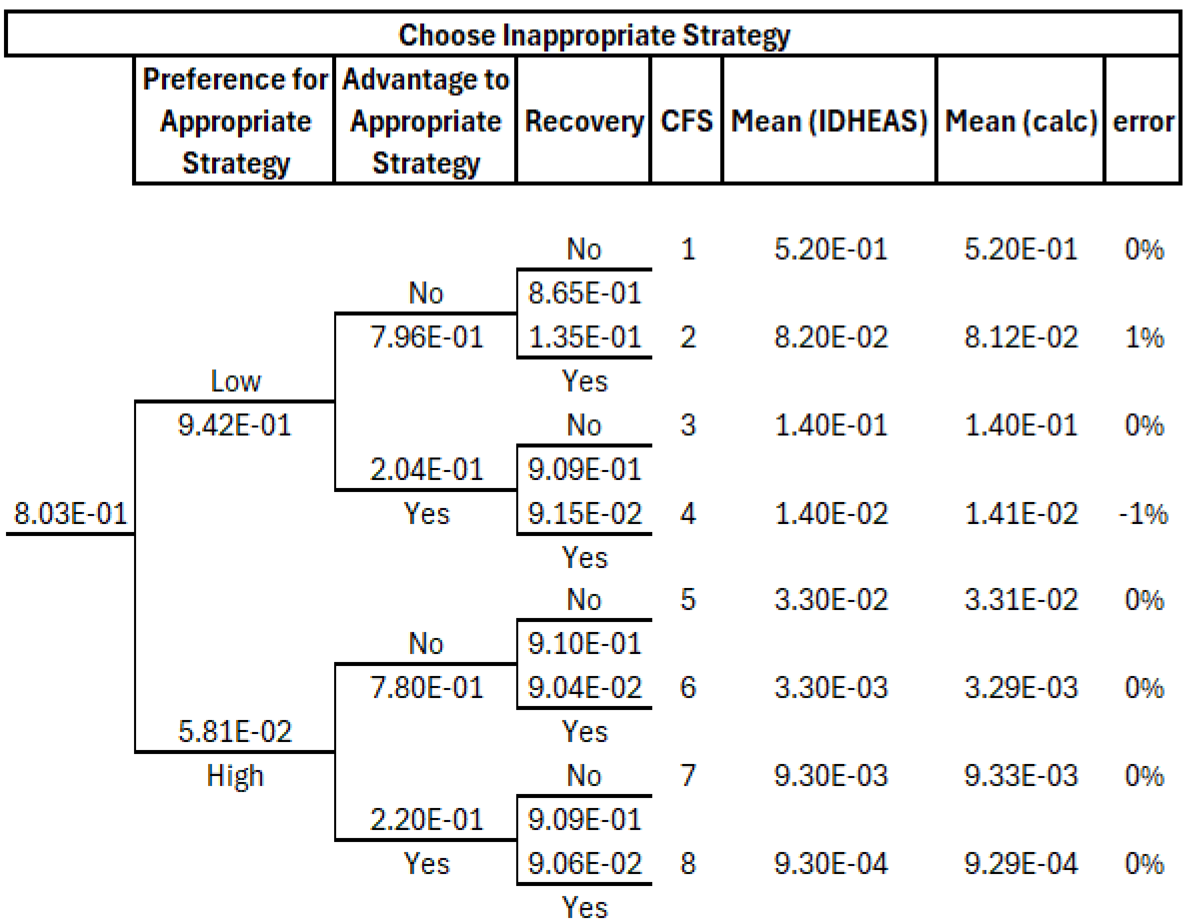

Figure 28. Conditional probabilities for CFM RP-2

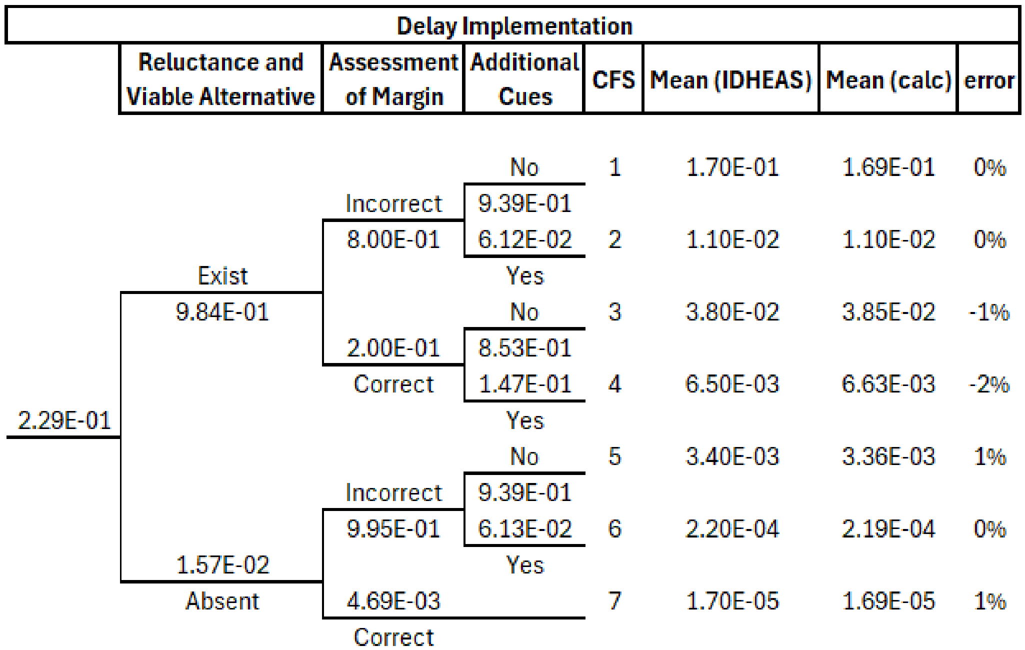

Figure 29. Conditional probabilities for CFM E-1

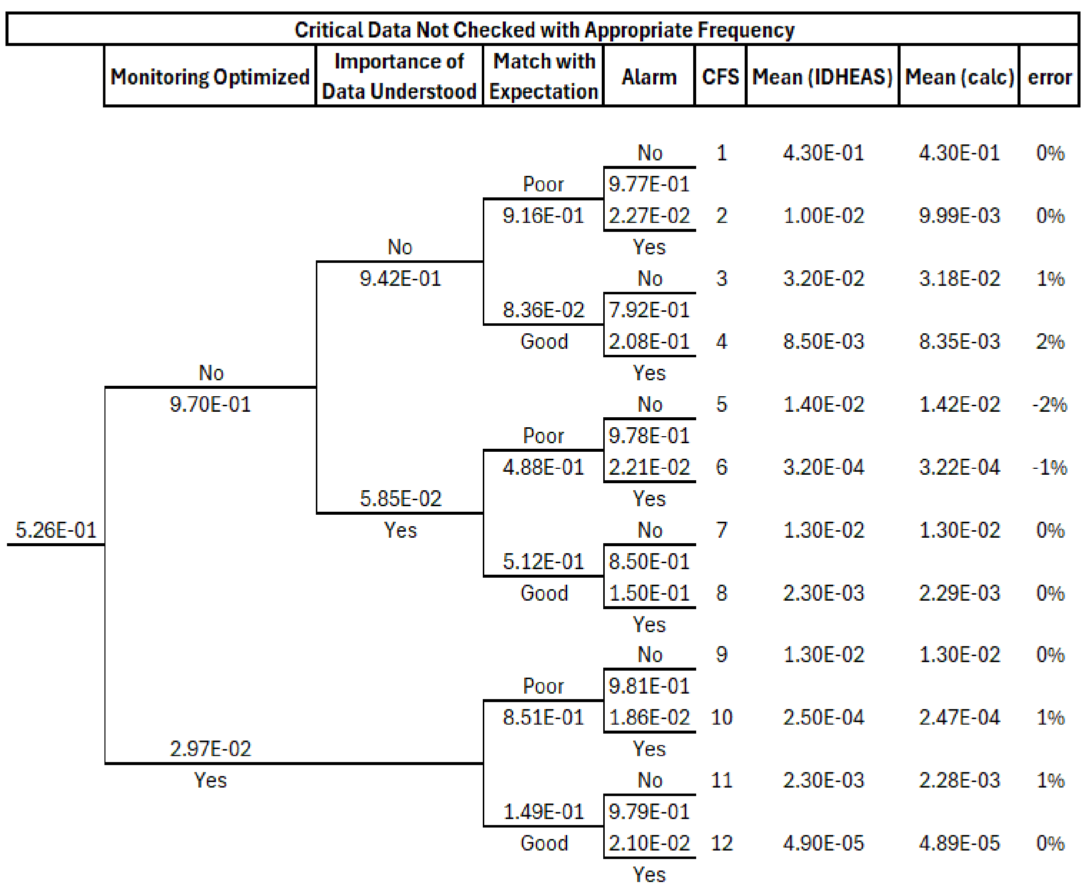

Figure 30. Conditional probabilities for CFM E-2

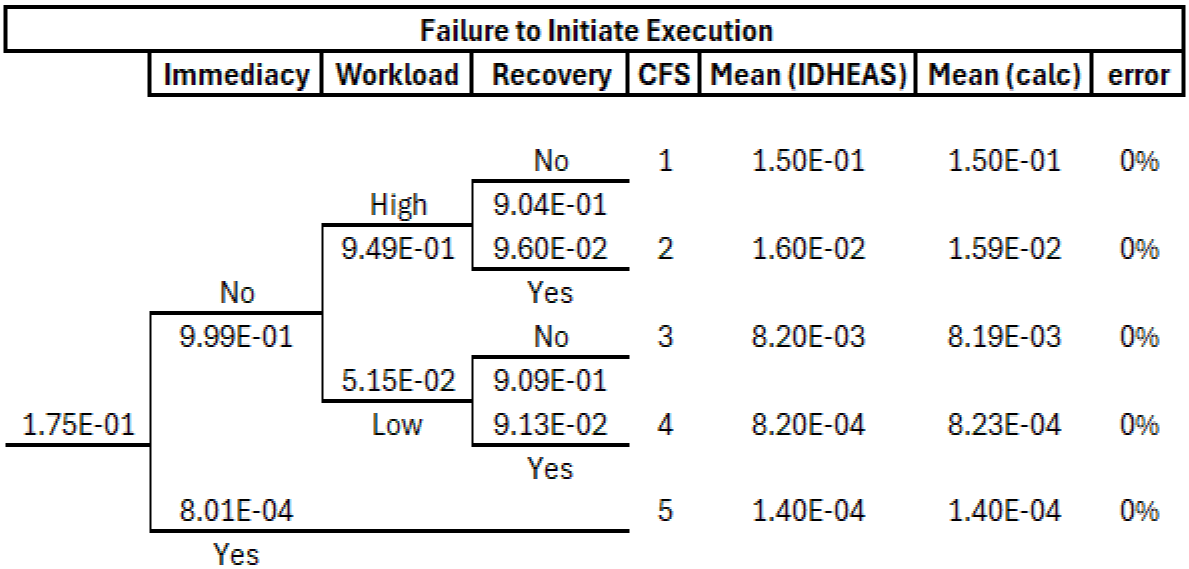

Figure 31. Conditional probabilities for CFM E-3

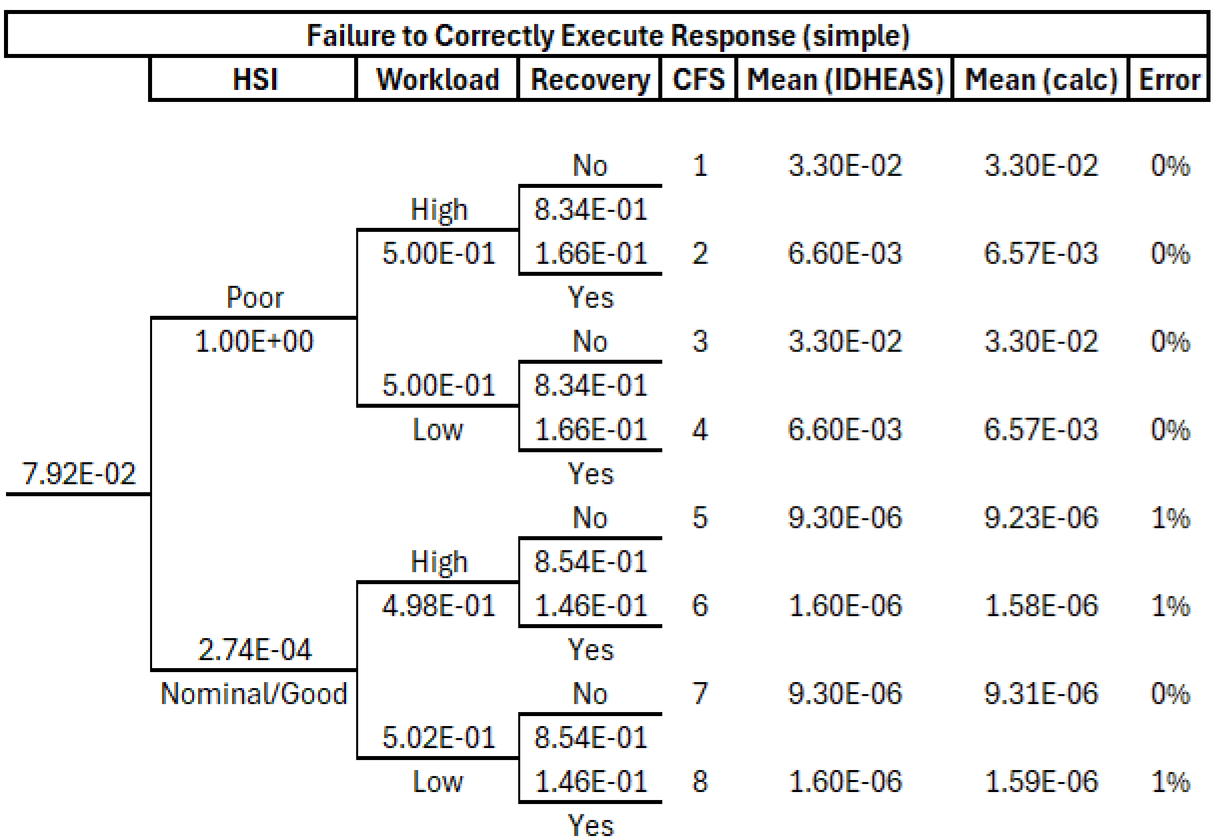

Figure 32. Conditional probabilities for CFM E-4

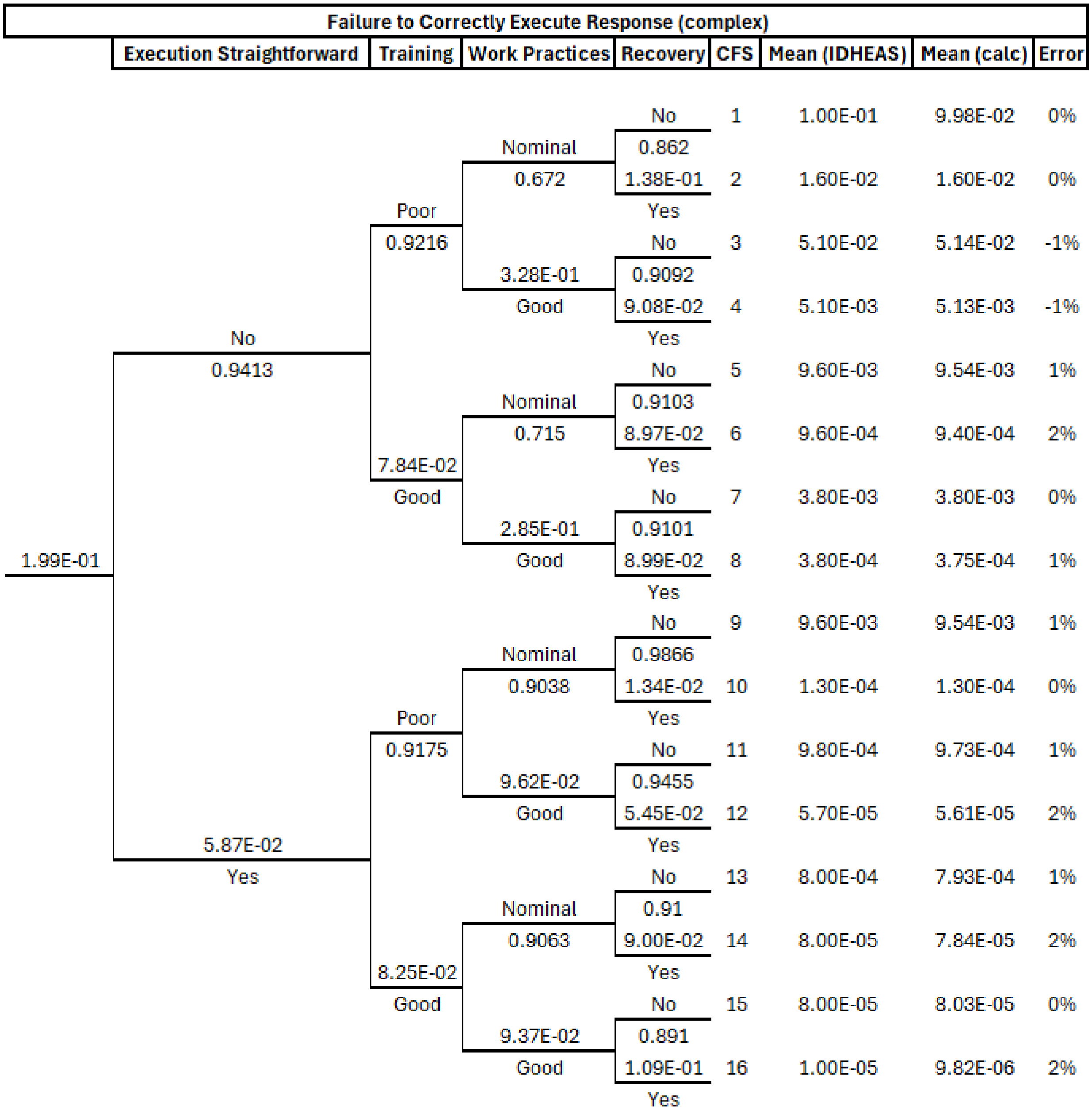

Figure 33. Conditional probabilities for CFM E-5

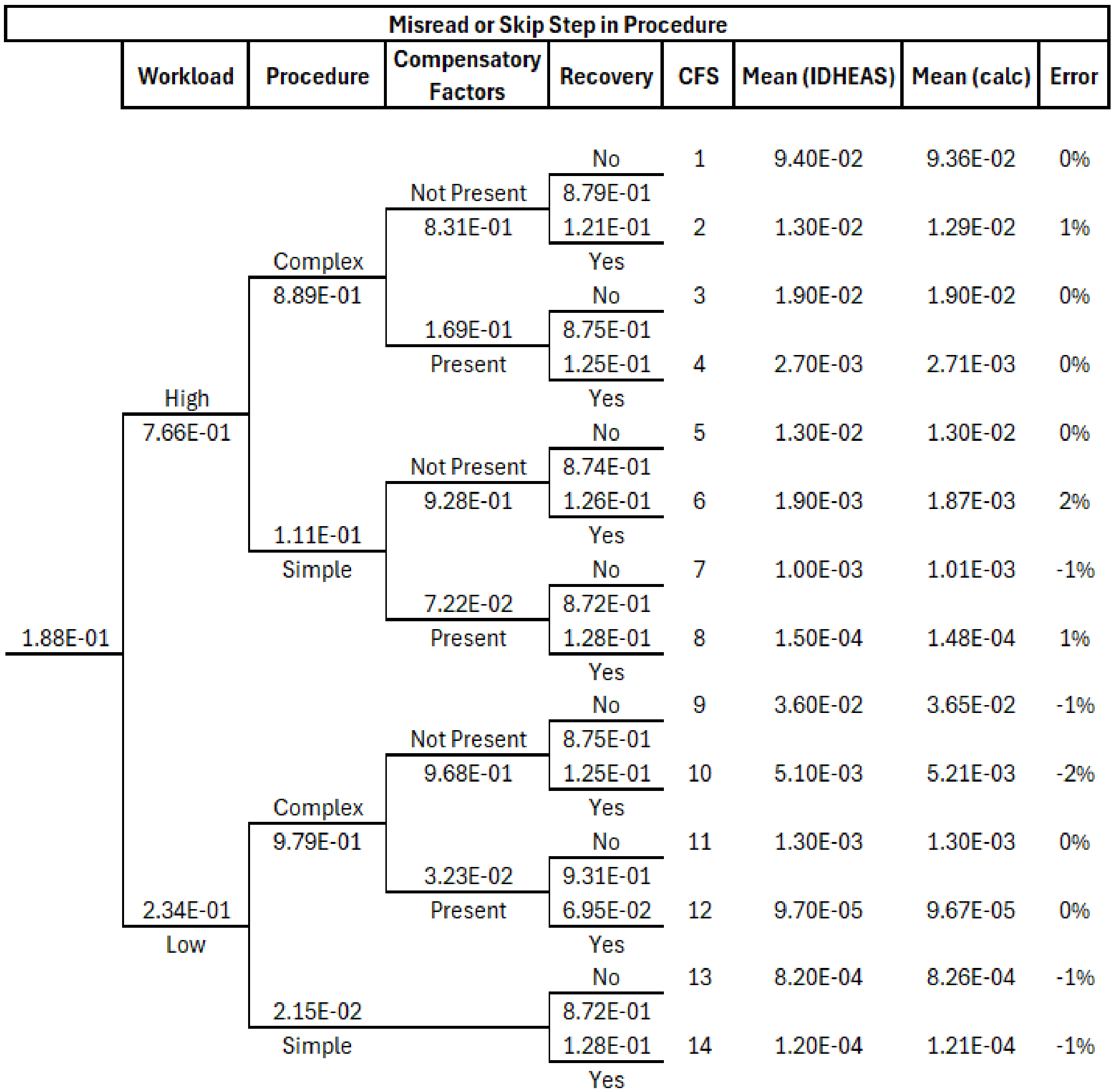

Figure 34. Conditional probabilities for CFM MP

4.3.10.Step 10 Build Bayesian Networks

Within this step, a Bayesian network is built for each critical task within the detailed analysis. To facilitate this step, the results of the 0 are used to construct individual Bayesian networks for each CFM and a combined Bayesian network for a generic HFE that incorporates all CFMs. To use the model developed in this step, analysts only need to set the status of PIFs within applicable CFMs as evidence within the Bayesian network. For CFMs that are not applicable, analysts only need to set their success as evidence in the Bayesian network. For those PIFs whose status is unknown, the analysts can leave its node with no evidence using prior conditional probabilities quantified from step 9. Alternatively, the analysts can use the prior conditional probabilities that are more suitable for their model. The Bayesian networks developed for all CFMs associated with IDHEAS at-power and a generic HFE are shown in Figure 35 to Figure 48 and Figure 49, respectively. All conditional probabilities used to build the Bayesian networks are listed in Appendix C.

It should be noted that similar to Step 9, no assumptions were made regarding the independence of PIFs, but rather, all possible links identified in the decision trees are modeled within the Bayesian network. For operator actions that fall outside the scope of IDHEAS At-power, the IDHEAS-ECA software can be directly used to quantify the failure probability associated with applicable CFMs. Hence, there is no need to build individual Bayesian networks for each CFM, and a single generic Bayesian network, illustrated in Figure 50, can be used to represent/quantify the failure of the operator action.

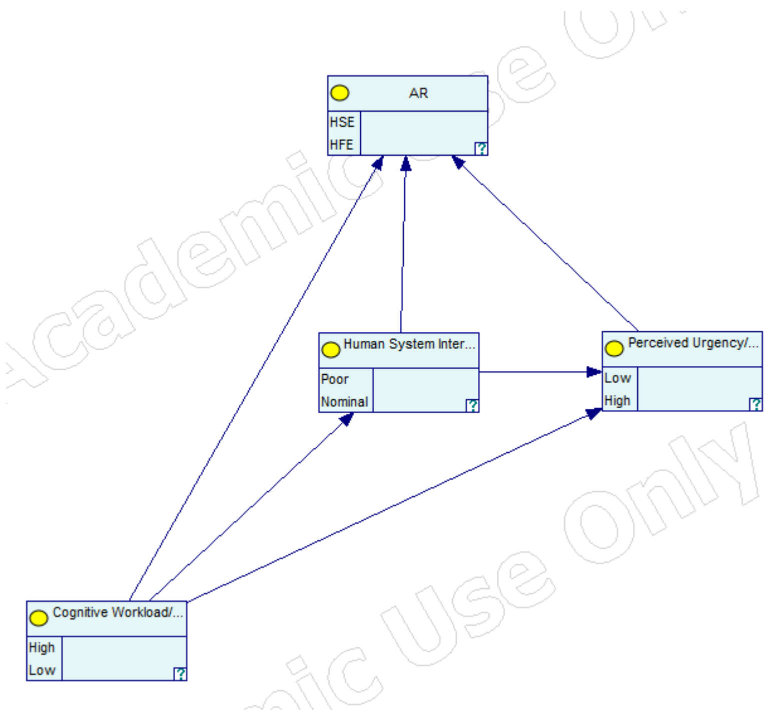

Figure 35. Bayesian network for CFM AR

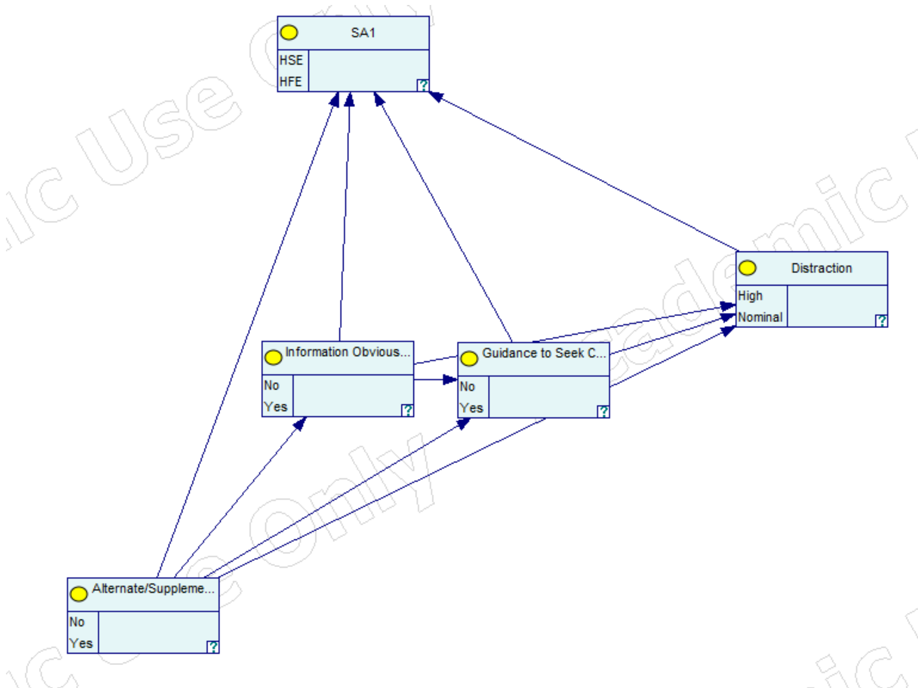

Figure 36. Bayesian network for CFM SA-1

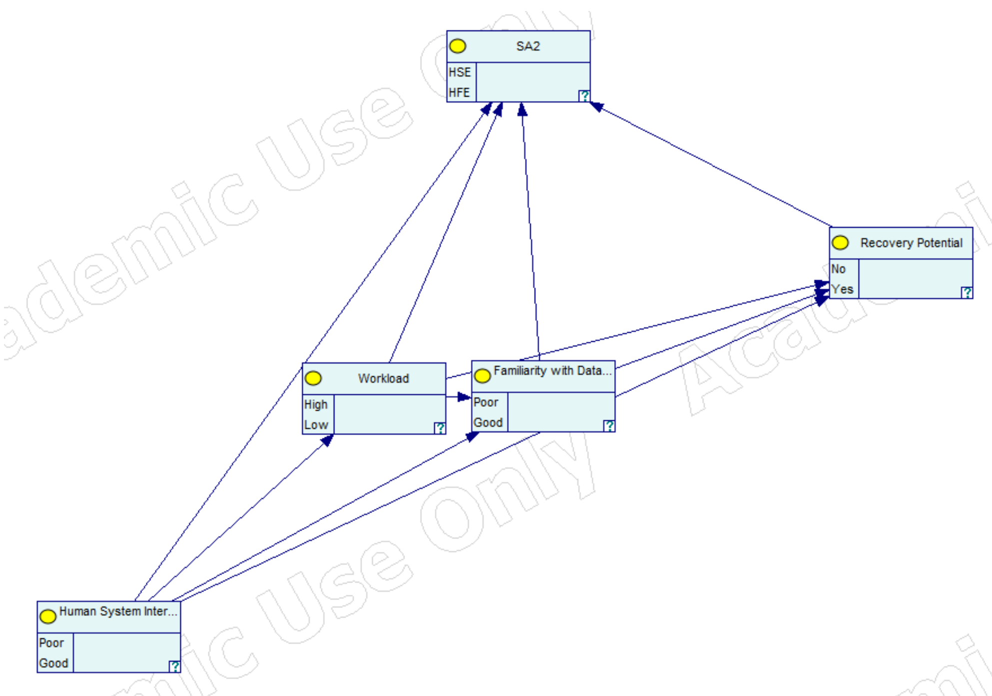

Figure 37. Bayesian network for CFM SA-2

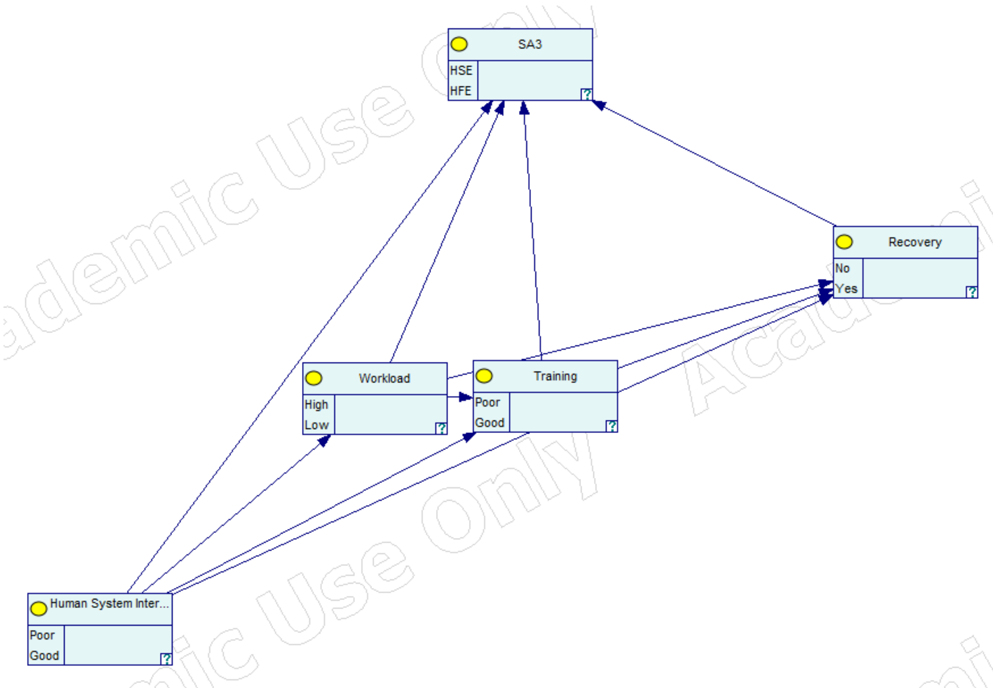

Figure 38. Bayesian network for CFM SA-3

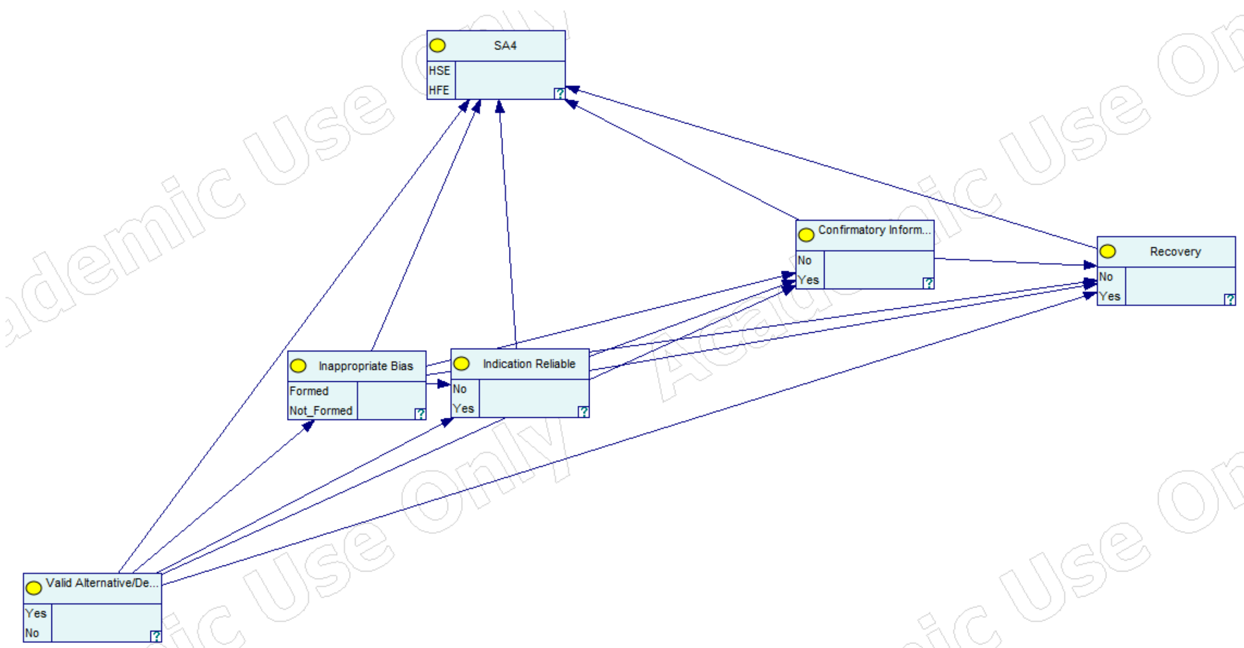

Figure 39. Bayesian network for CFM SA-4

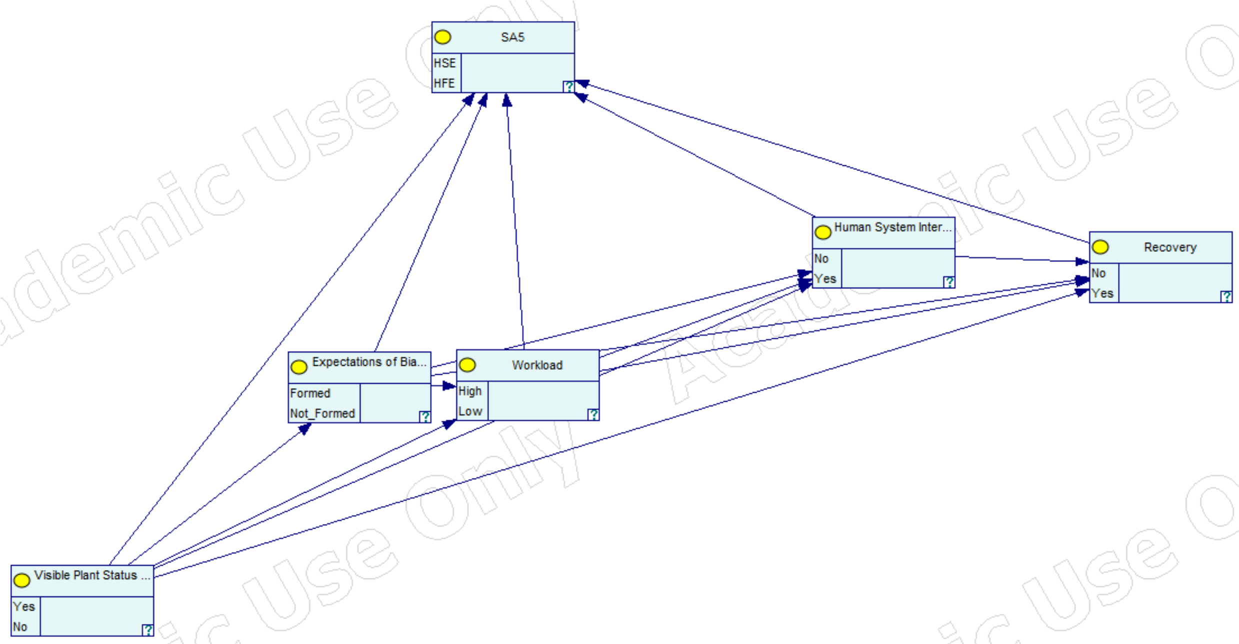

Figure 40. Bayesian network for CFM SA-5

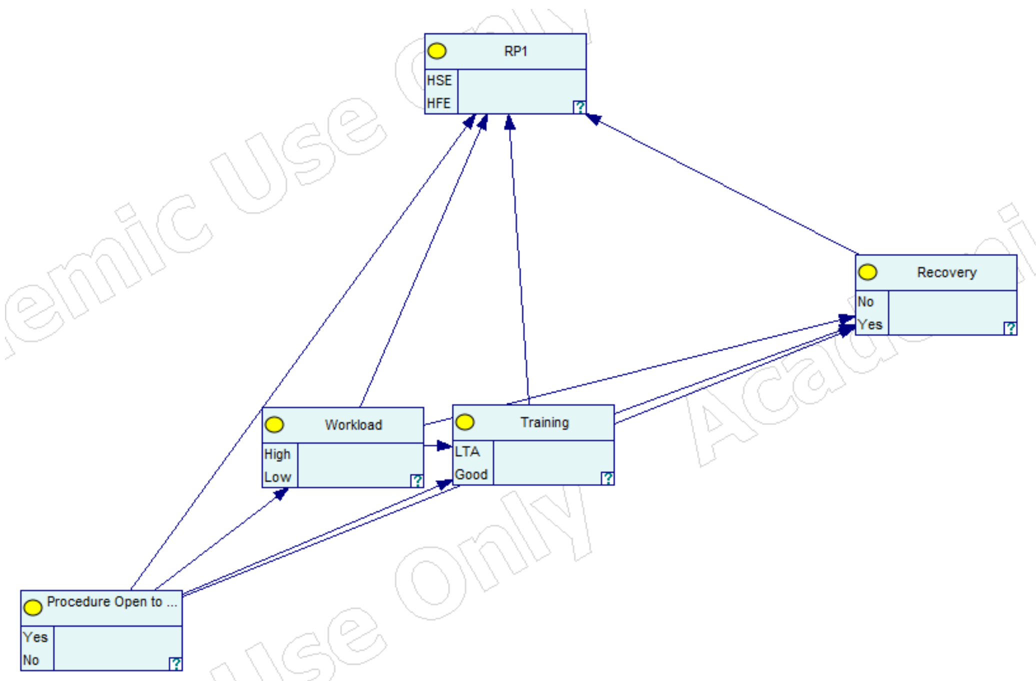

Figure 41. Bayesian network for CFM RP-1

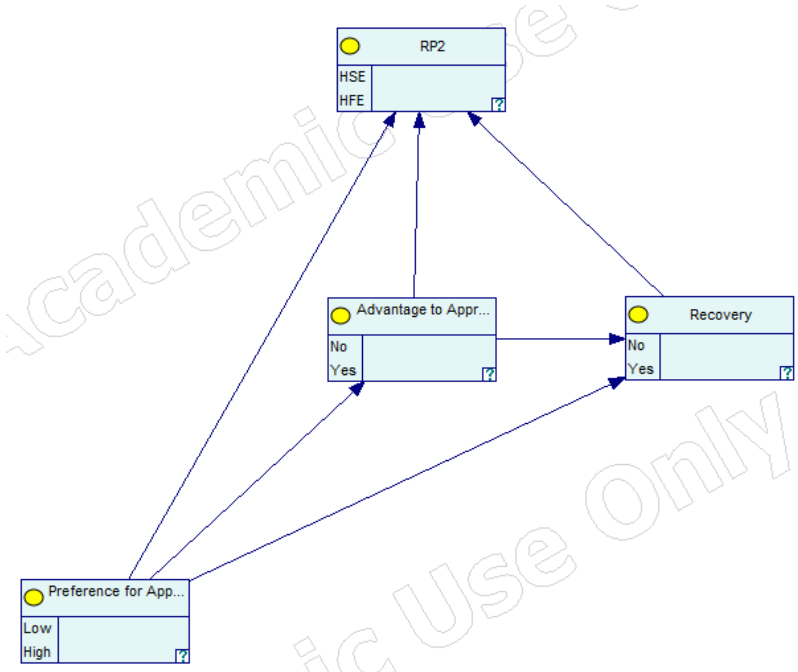

Figure 42. Bayesian network for CFM RP-2

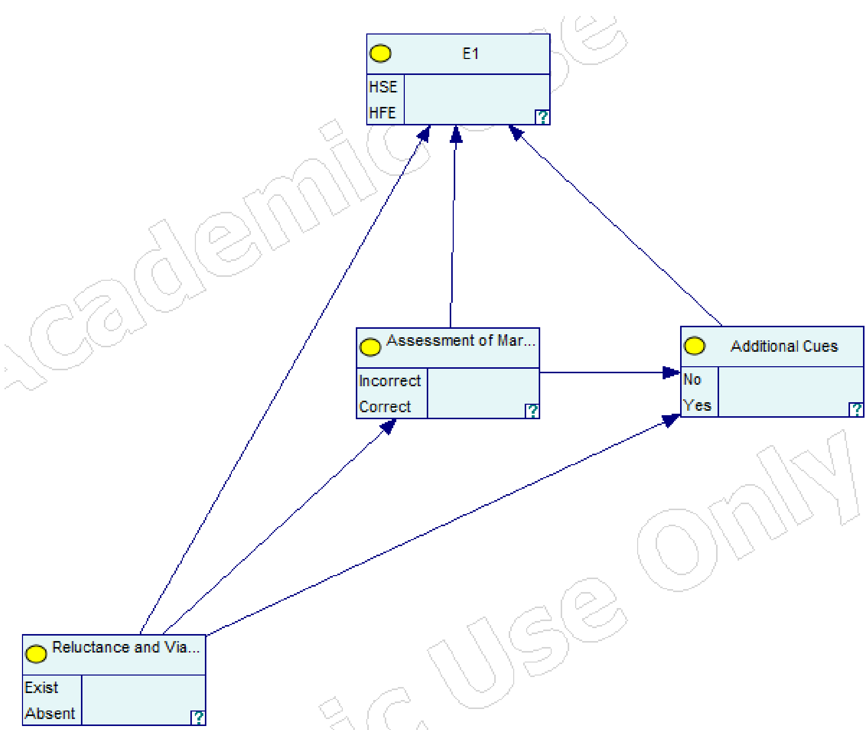

Figure 43. Bayesian network for CFM E-1

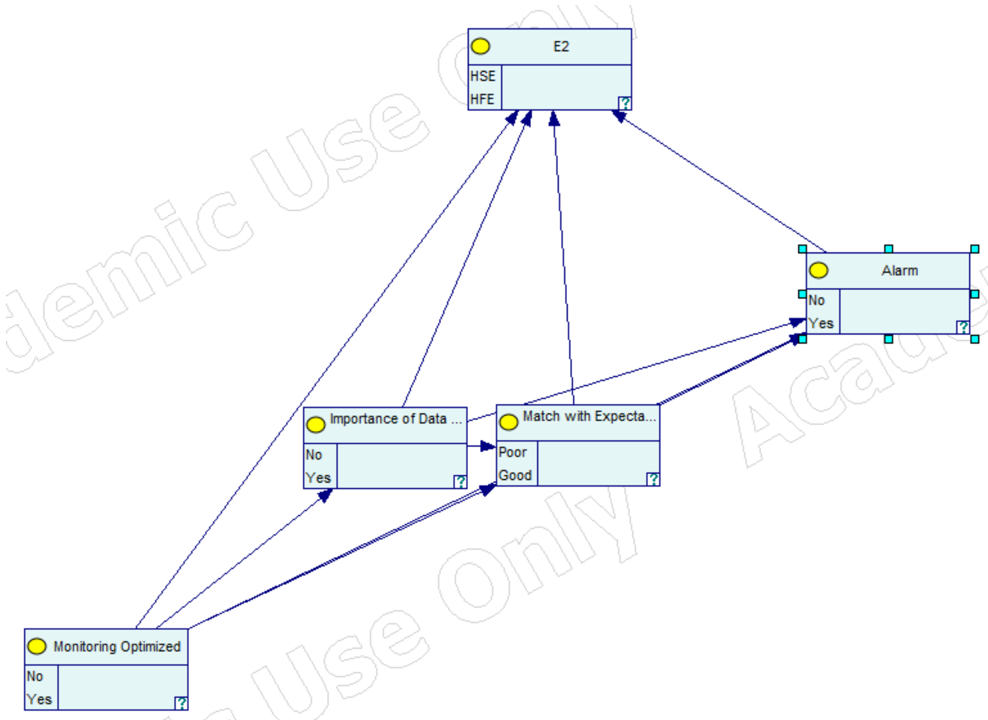

Figure 44. Bayesian network for CFM E-2

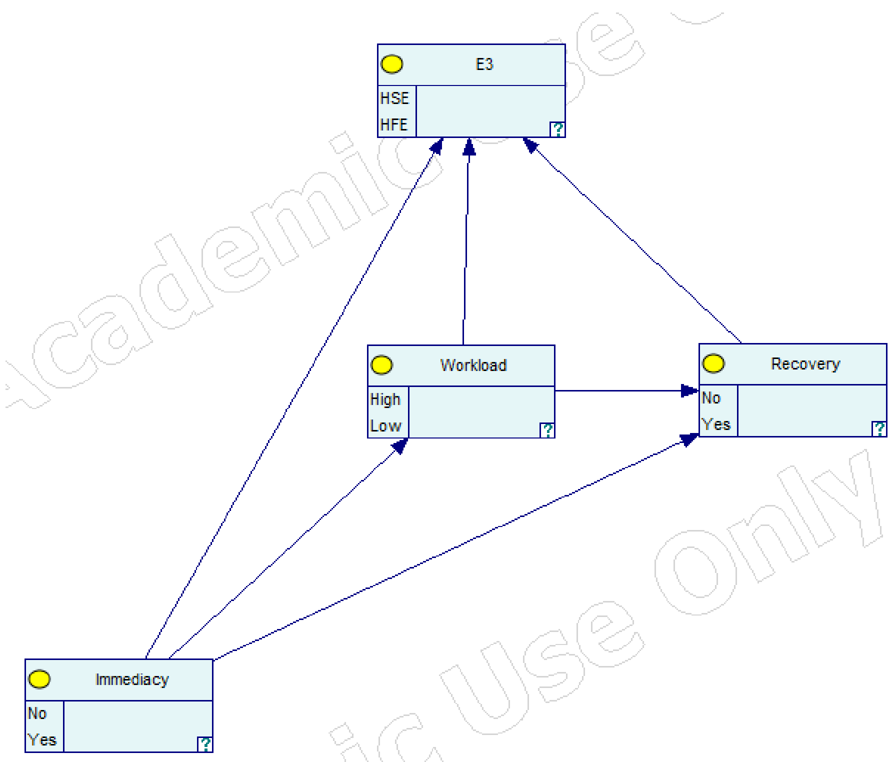

Figure 45. Bayesian network for CFM E-3

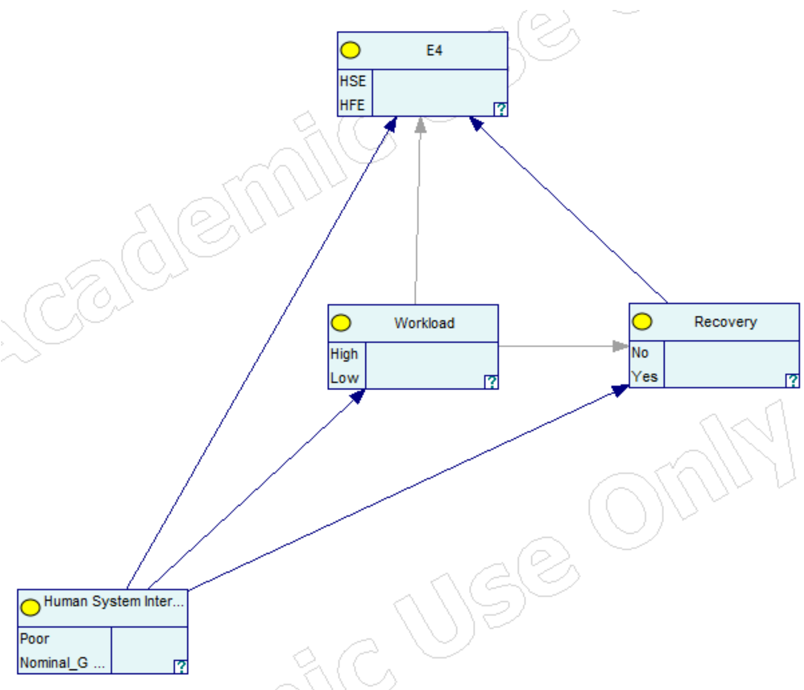

Figure 46. Bayesian network for CFM E-4

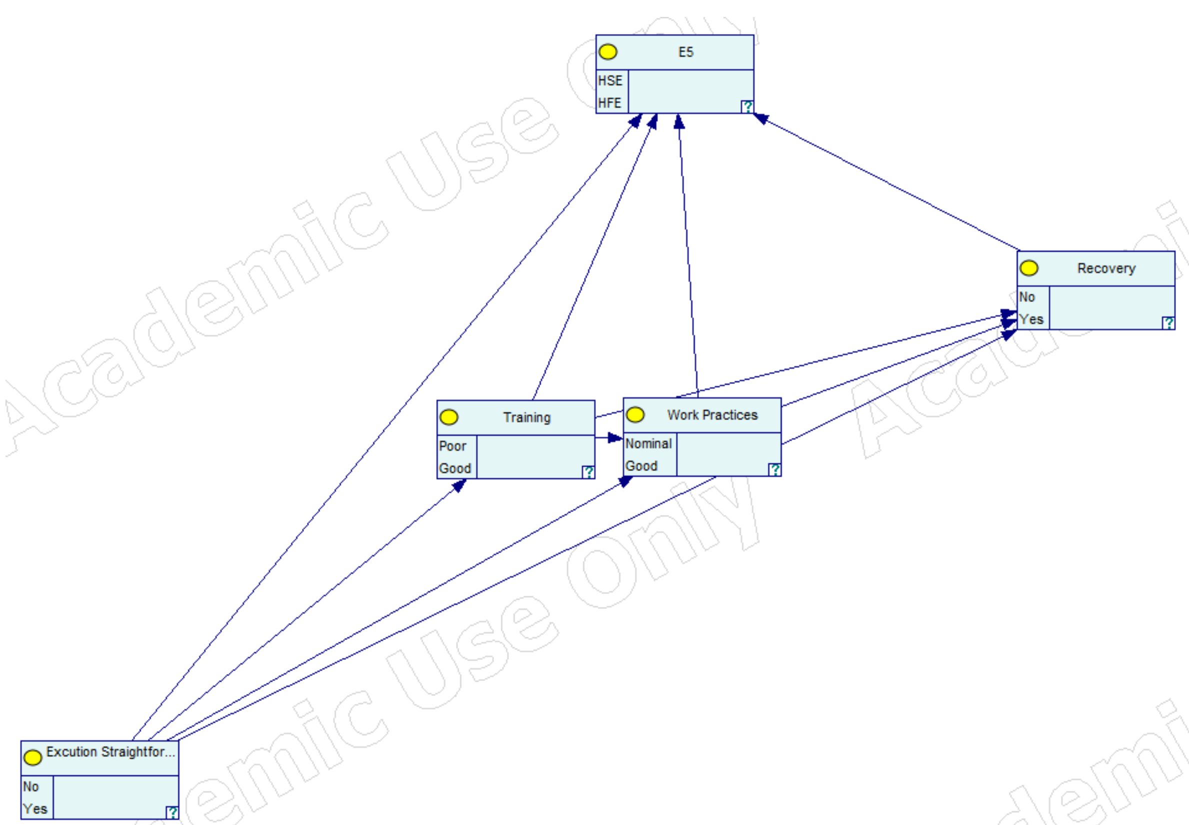

Figure 47. Bayesian network for CFM E-5

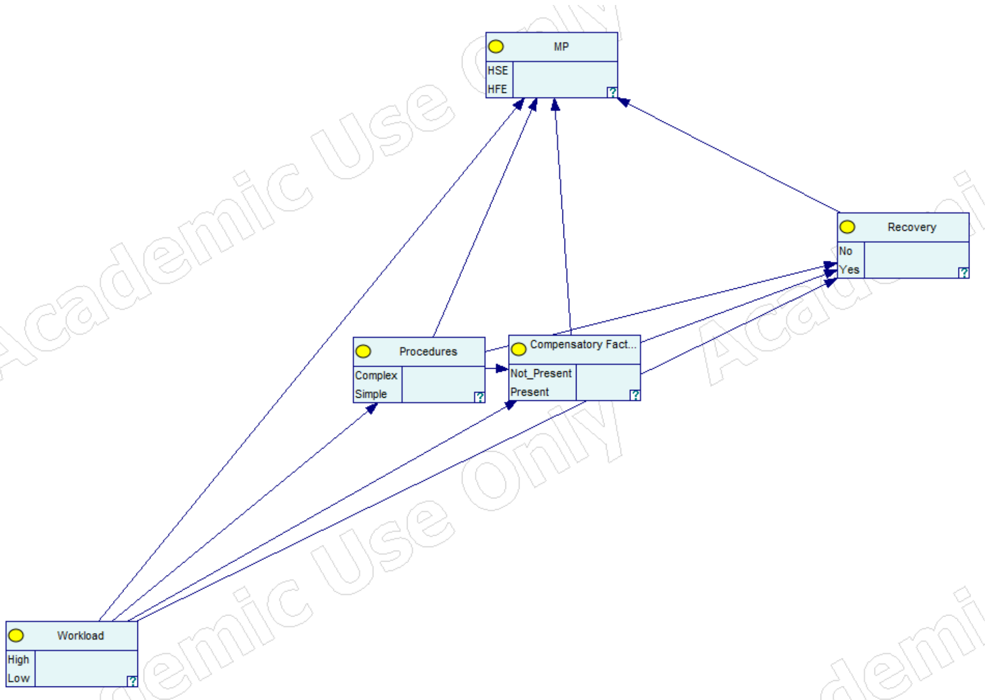

Figure 48. Bayesian network for CFM MP

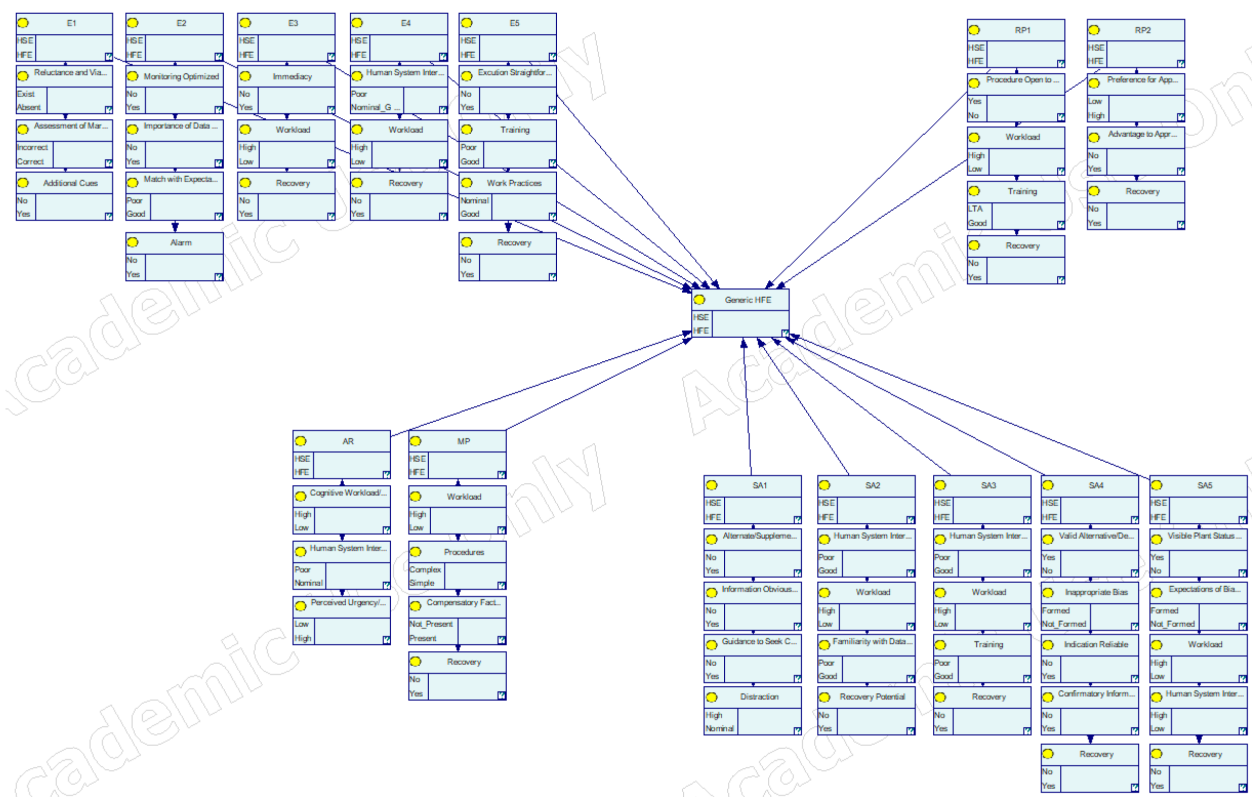

Figure 49. Bayesian network for a generic HFE (IDHEAS At-power)

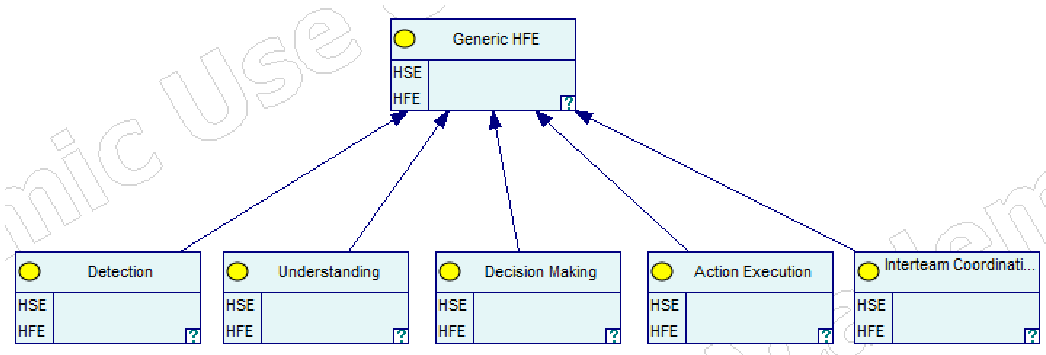

Figure 50. Bayesian network for a generic HFE (IDHEAS-ECA)

4.3.11.Step 11 Identify Dependency Links

This step identifies the HFE/CFM, CFM/CFM, CFM/PIF, and PIF/PIF dependency links. These links may be considered a different state of the same PIF, e.g., a different state of stress or a different instance of the same PIF. This step is essential in mitigating one of the limitations of Bayesian network methodologies, which stems from assuming that PIFs are external factors that are not impacted by the failure itself but rather whose probability increases by the evidence of the failure occurring. By introducing CFM/PIF and PIF/PIF links, the inherent assumption of externality is mitigated, and the failure of a CFM may have a direct impact on the PIFs while maintaining the acyclical nature of Bayesian networks, as can be seen in Figure 51 to Figure 53.

It should be noted that the dependency links between actions taken in the control room and actions taken outside the control room, as those illustrated in Figure 53, are restricted to the situation assessment, detection, and understanding. The communication between the operating crew in the control room and the field crew would impact their situational awareness only; the ensuing failures are then only restricted to the CFMs associated with this awareness. Hence, even though it is presented only as an example, Figure 53 intentionally does not include links between the first action, the decision-making, action execution, and interteam coordination CFMs of the second action.

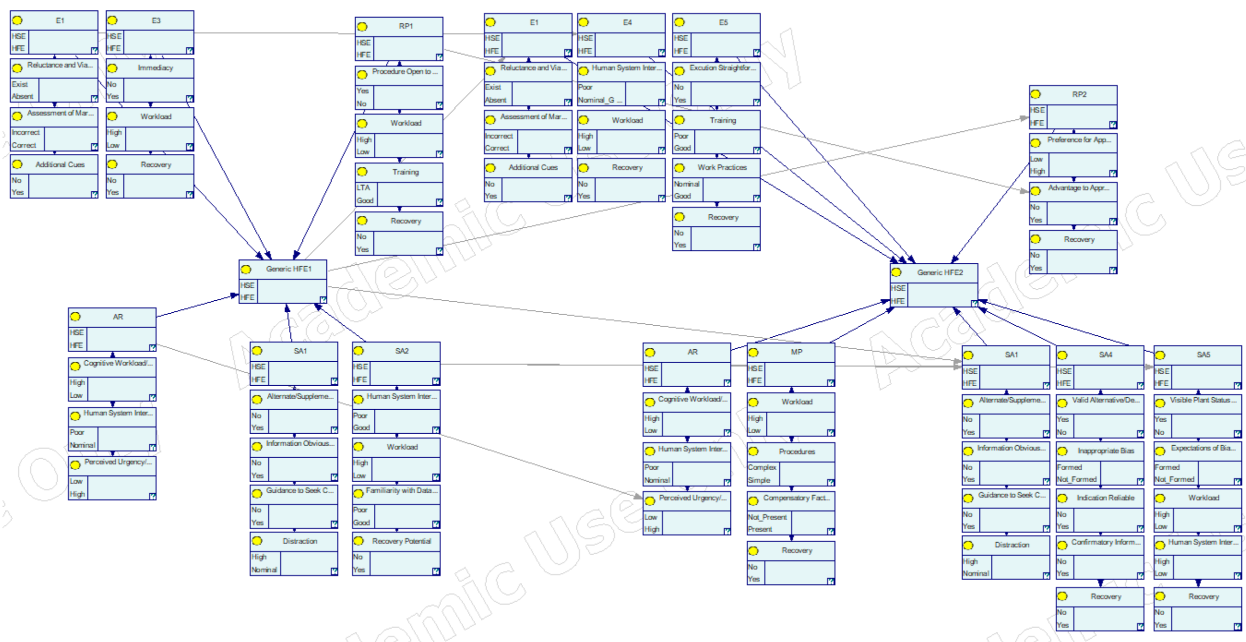

Figure 51. Example of Linked Bayesian Networks (IDHEAS At-Power & IDHEAS At-power)

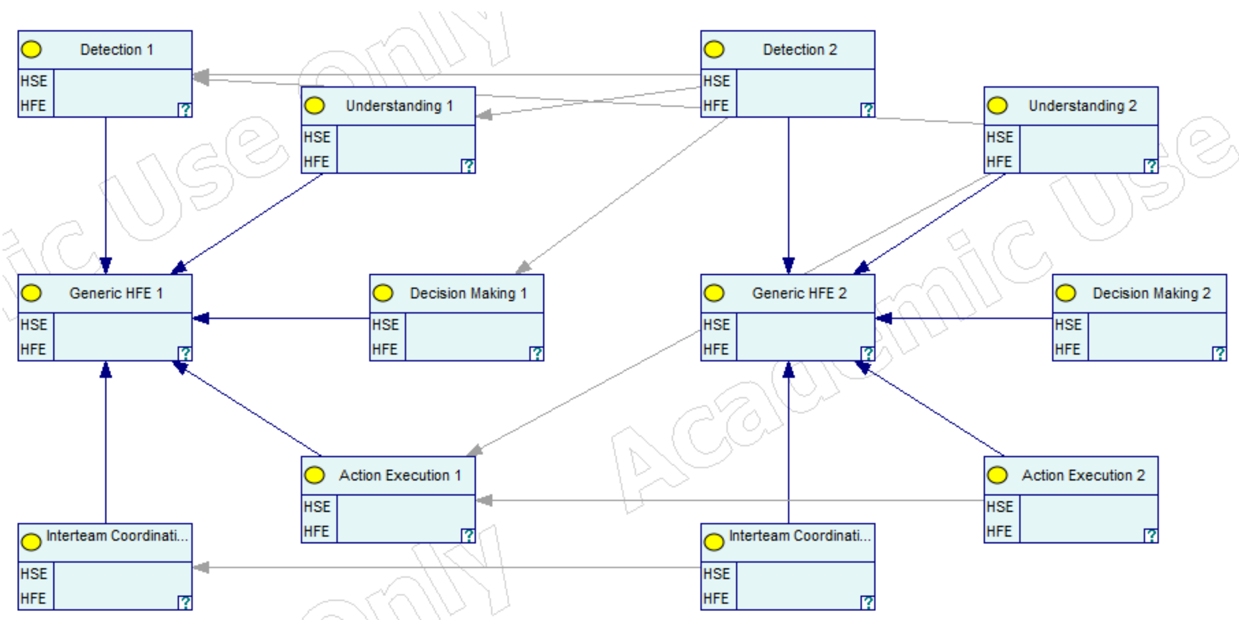

Figure 52. Example of Linked Bayesian Networks (IDHEAS-ECA & IDHEAS-ECA)

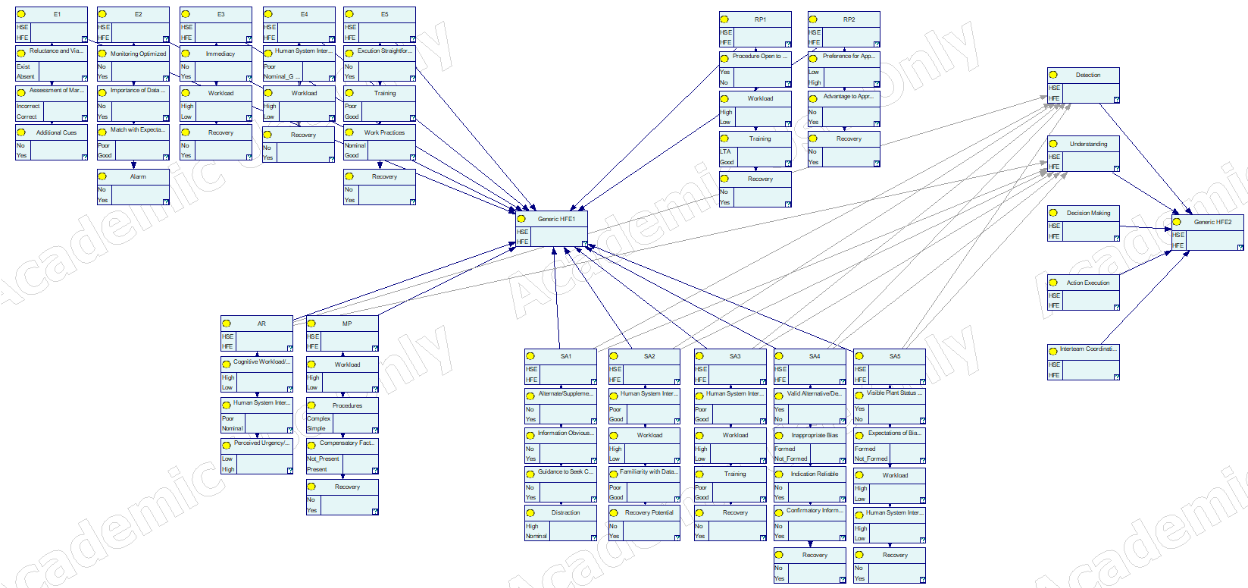

Figure 53. Example of Linked Bayesian Networks (IDHEAS At-power & IDHEAS-ECA)

4.3.12.Step 12 Modify/Link Bayesian Networks

Within this step, the conditional probabilities associated with linked critical tasks, CFMs, or PIFs are modified to incorporate the impact of the failure of preceding points. For PIFs, the effect can be quantified by enforcing a status, from low stress to high stress, for example. Another way of quantifying the impact on PIFs is by introducing a new state of the PIF itself, which is done by modifying the conditional probability of the CFM|PIF link, a higher failure probability for CFM|PIF conditional on the failure of a previous step. Finally, certain CFMs may be impacted by the same instance of a PIF; in other words, both CFMs are linked to the same PIF node, whose dependency impact is captured by setting the evidence of previous step failures.

The framework does not enforce specific modifications to the conditional probabilities. It is left to the analysts to decide on an appropriate change that reflects the dependency level; however, changes are recommended to be represented as percentage increases to the conditional probabilities rather than absolute changes. Initial percentage increases that may be considered are the asymptotic dependency values of the THERP dependence methodology of 5, 15, and 50%. It should be noted that, generally, the conditional probabilities associated with the success of the preceding step are the independent values extracted within this framework. The framework allows the analysts to modify the success conditional probabilities. However, a justification and documentation of the updated conditional probabilities are needed.

4.3.13.Step 13 Quantify/Update Cognitive Failure Modes

After modifying the Bayesian network in 4.3.12, the network is then quantified while setting the evidence of the failure of preceding critical task(s) or HFE(s). The updated failure probabilities of each CFM are then documented to be used during the quantification process of the detailed analysis. For each CFM, an independent failure probability along with a dependent failure probability are documented.

4.3.14.Step 14 Build Human Fault Trees

Within this step, the initial HFE combination is expanded into its appropriate HFT, where critical tasks are incorporated as OR gates that combine the CFM basic events. The HFT, an example of which can be seen in Figure 54 and Figure 57, presents a logical decomposition of the main HFE that allows tracking of the main causes of failures, significant CFMs, and potential paths of reducing their failure probabilities. Paths of improvement include identifying the main PIF conditions that lead to the high failure probabilities of the associated CFM and addressing them through the Human Factor Engineering program.

It should be noted that a specific CFM may impact multiple critical tasks simultaneously. This should not represent an issue except for recovery actions under an AND logic with other critical tasks; in this case, the same basic event is used within both the critical task and the recovery action gates.

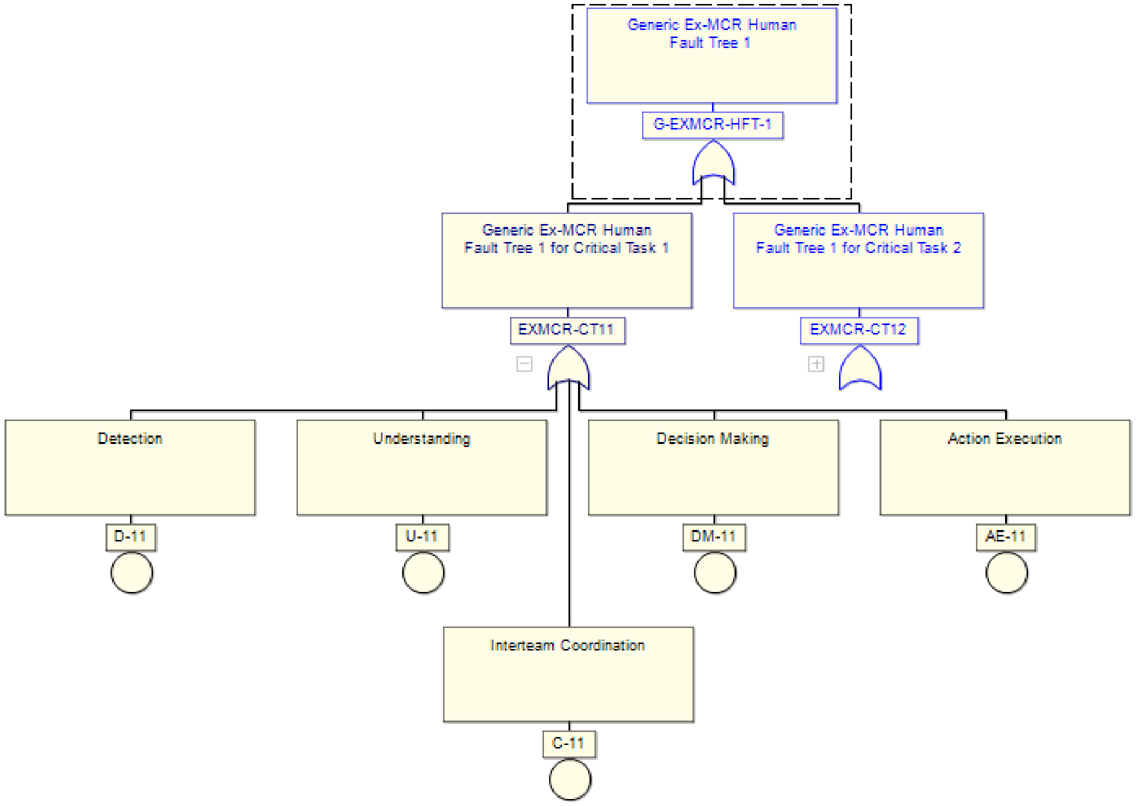

Figure 54. Example of Human Fault Tree (IDHEAS-ECA)

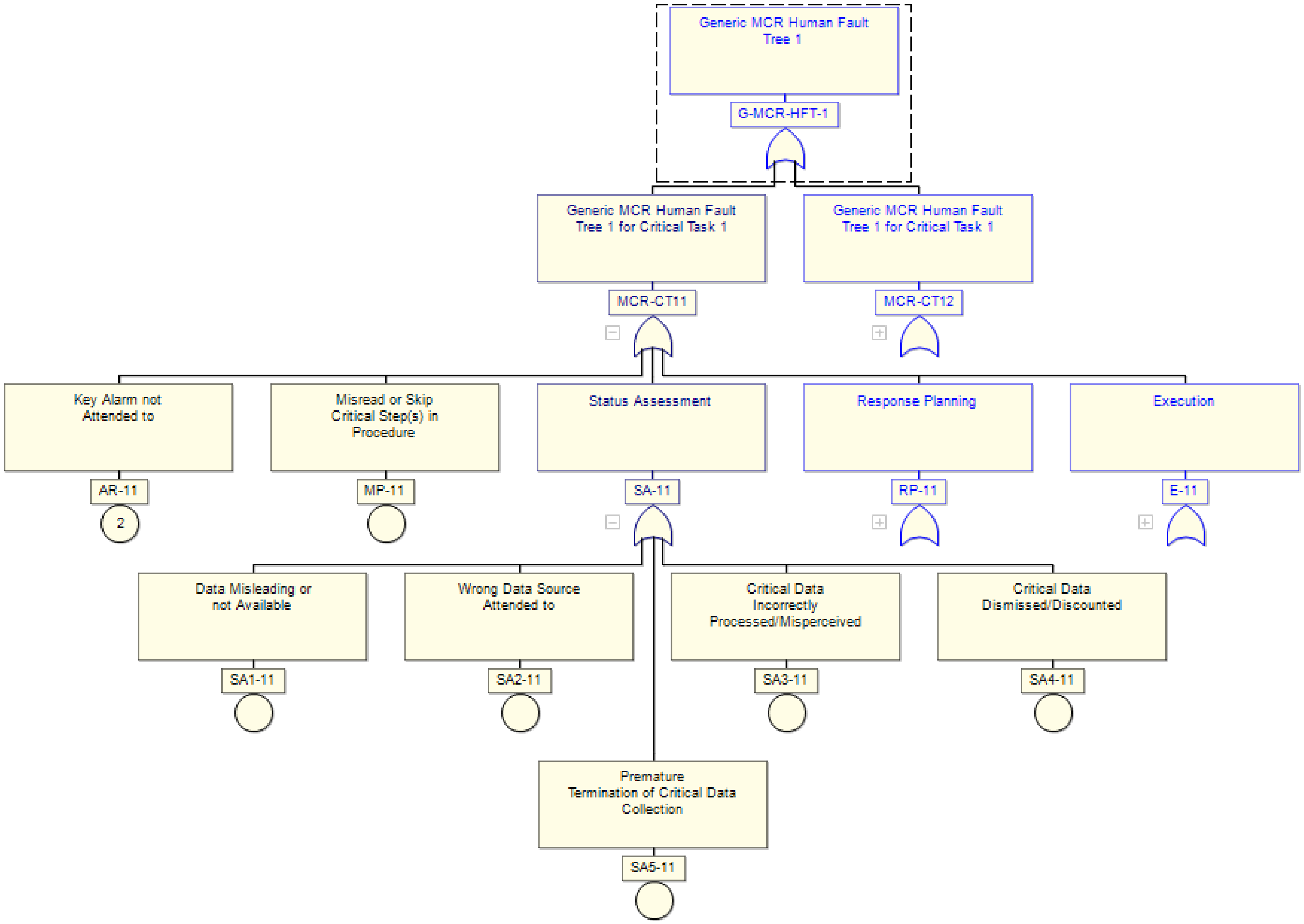

Figure 55. Example of Human Fault Tree (IDHAES At-Power) (1/3)

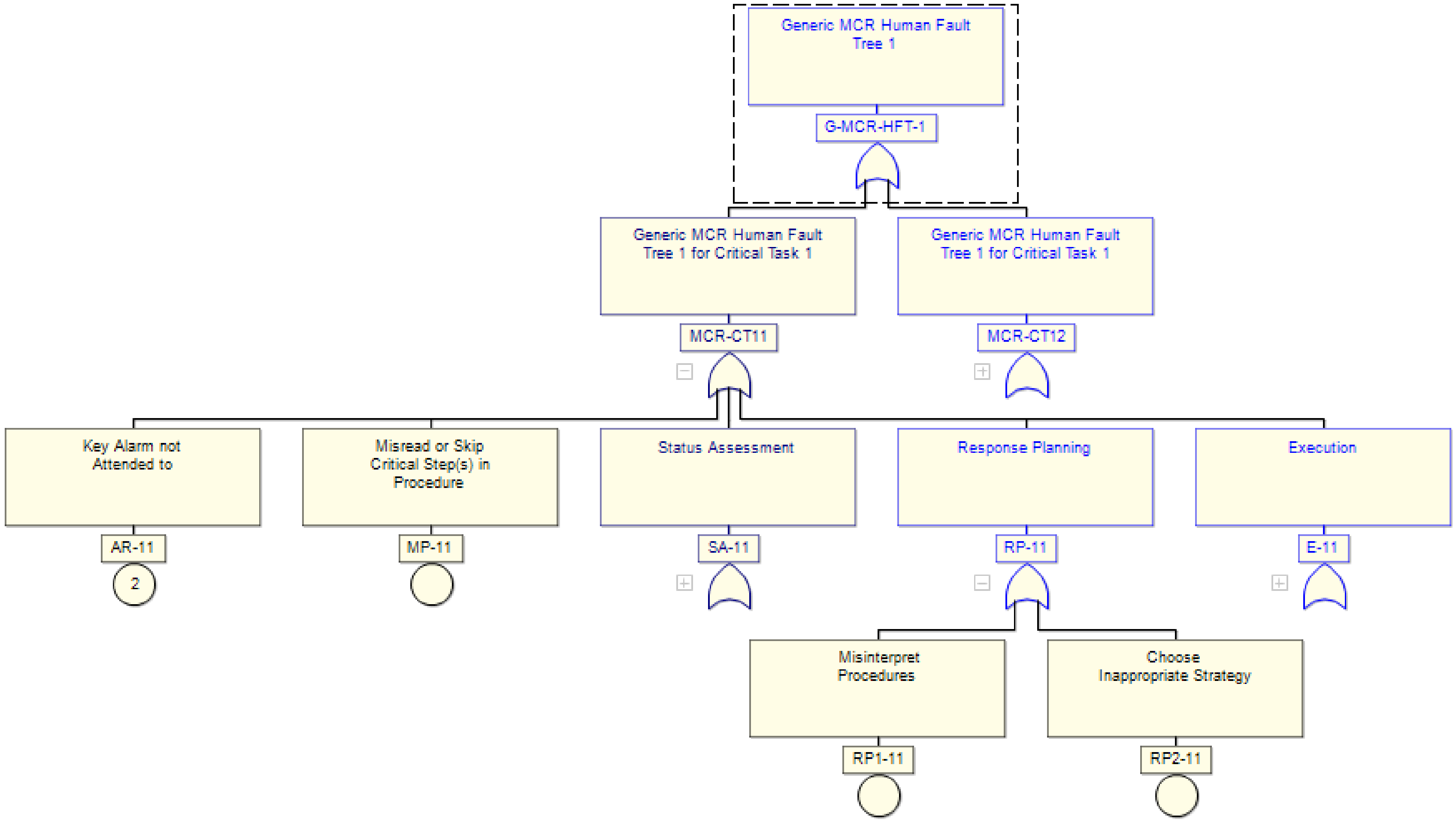

Figure 56. Example of Human Fault Tree (IDHAES At-Power) (2/3)

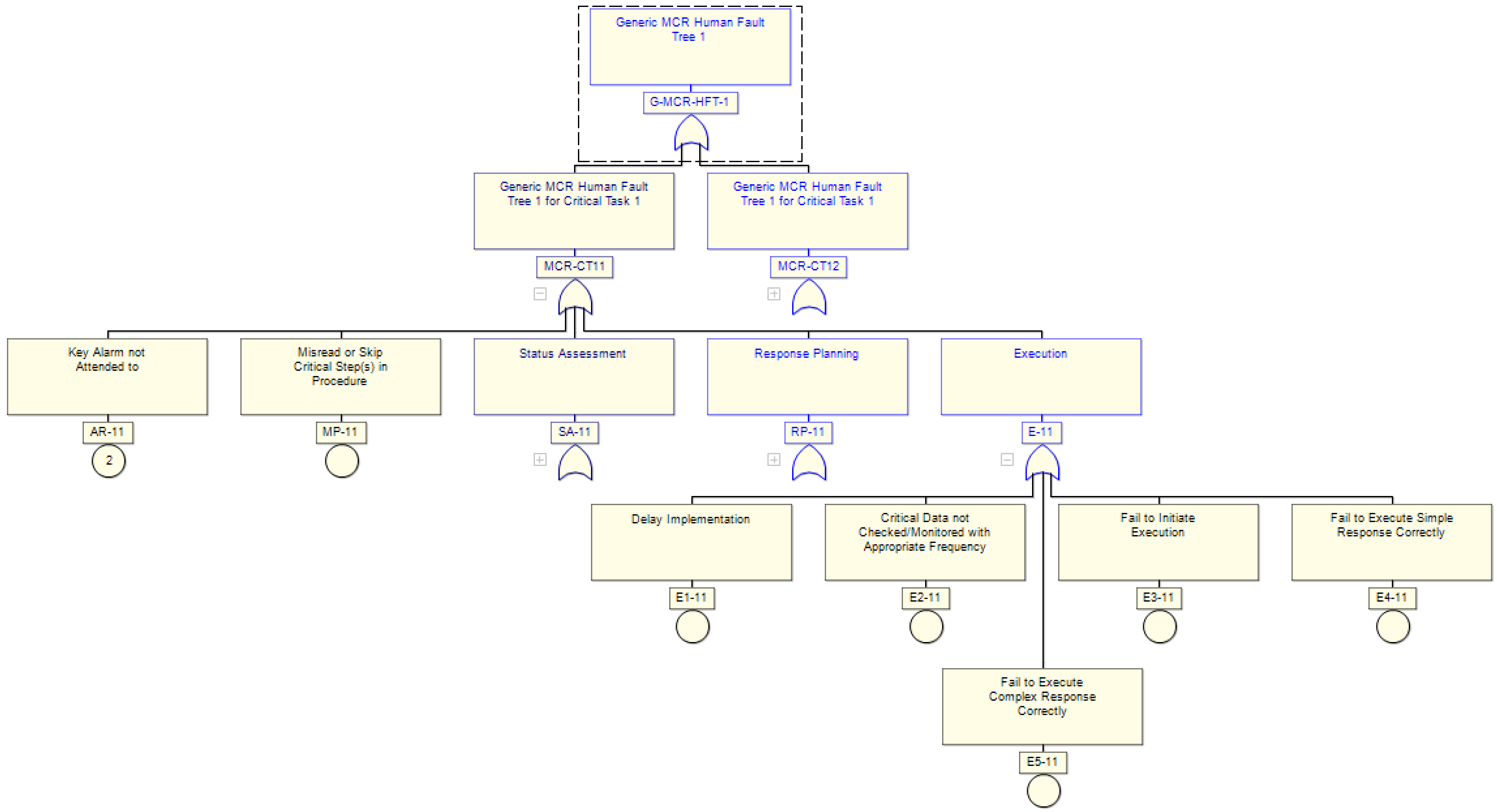

Figure 57. Example of Human Fault Tree (IDHAES At-Power) (3/3)

4.3.15.Step 15 Link Human Fault Trees

All HFTs are inserted into the ESQ model within this step, replacing their original HFE basic events. Dependent values are then inserted as their dependent HFTs linked to the preceding failures, as can be seen in Figure 58 to Figure 62. A flag is included within each instance of the HFT, whether independent or dependent, indicating which HFT instance shows up in the cut set. By setting the flag files as mutually exclusive events, i.e., independent and dependent HFTs can show up in the same cut set, all illogical cut sets can be removed from the ESQ model. The ESQ model is then quantified with the updated HFE list, and another iteration of detailed analysis starts from Step 4, introduced in 4.3.4.

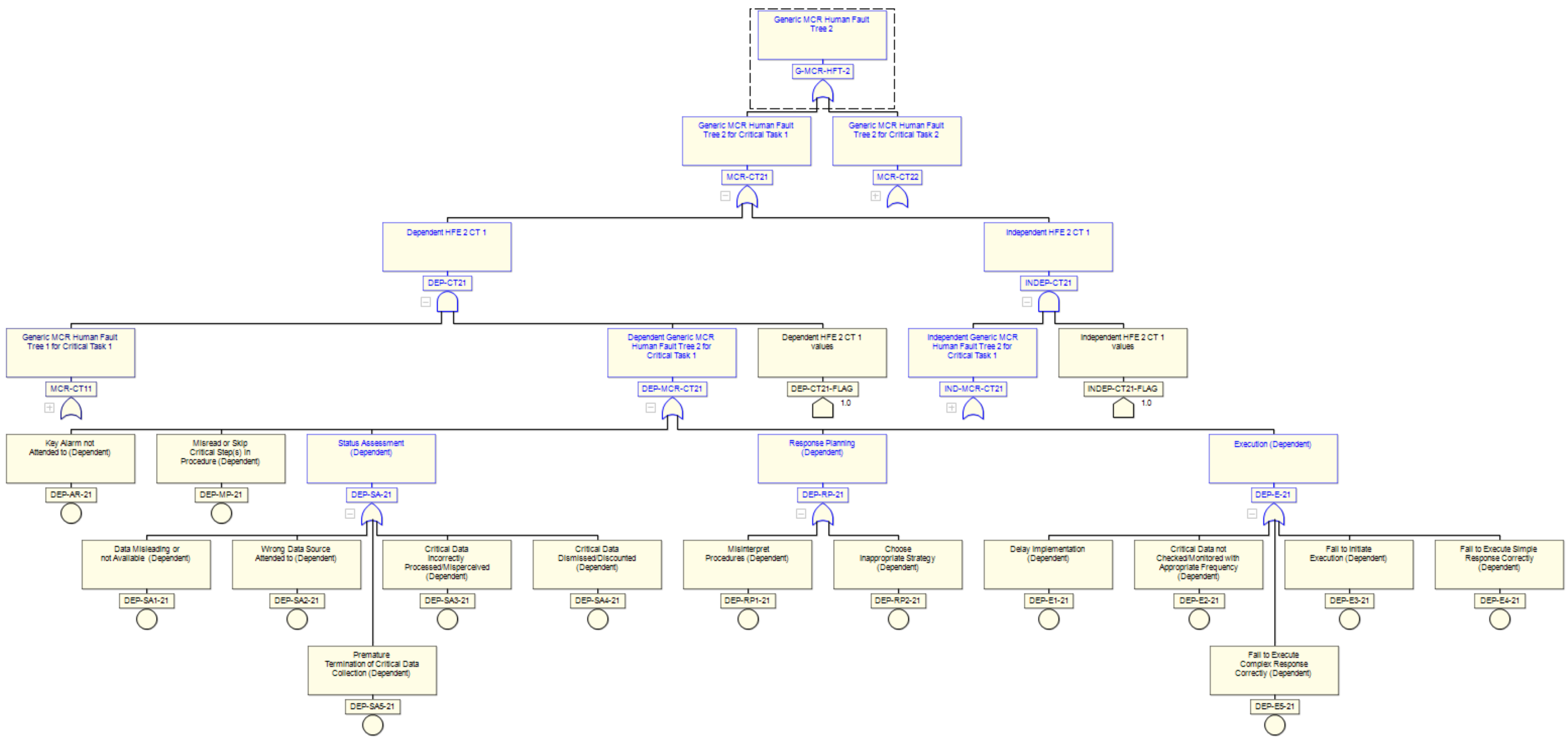

Figure 58. Example of linked Human Fault Tree (IDHEAS At-power & IDHEAS At-power) (1/2)

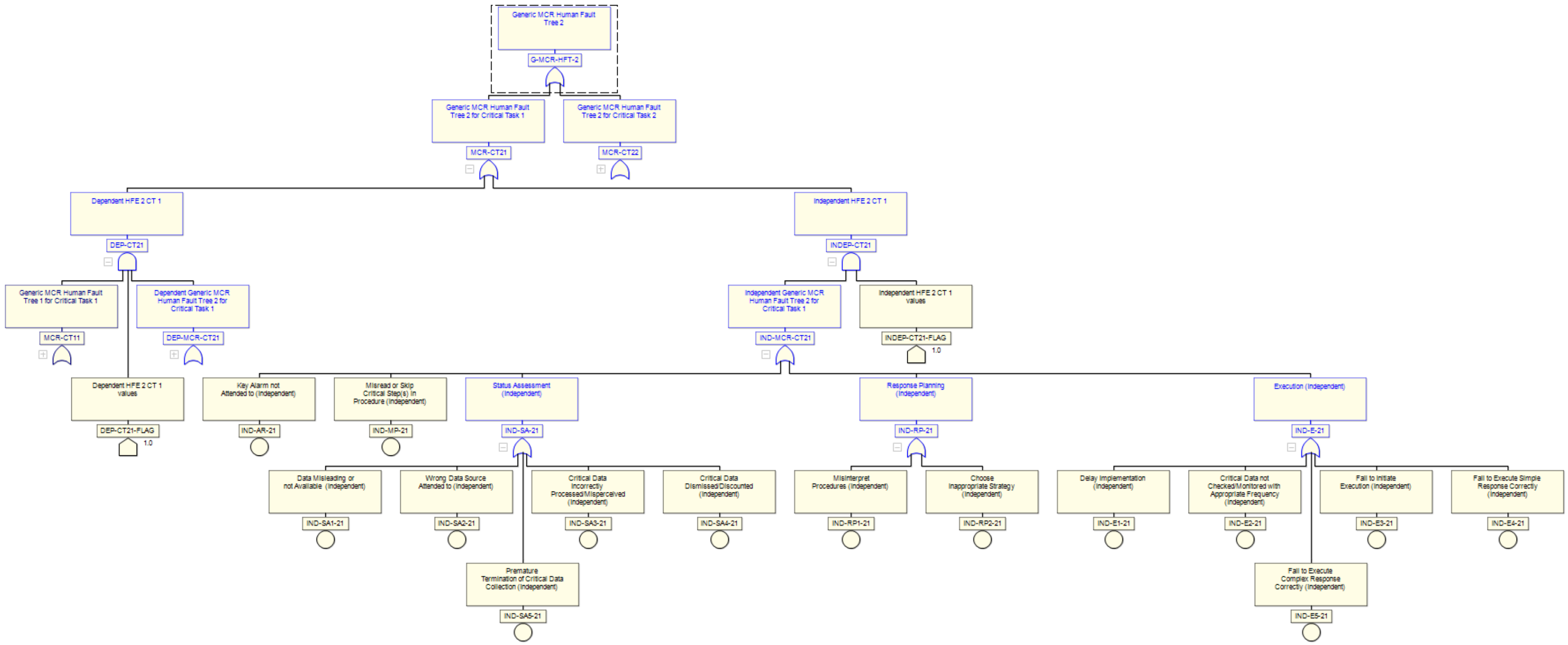

Figure 59. Example of linked Human Fault Tree (IDHEAS At-power & IDHEAS At-power) (2/2)

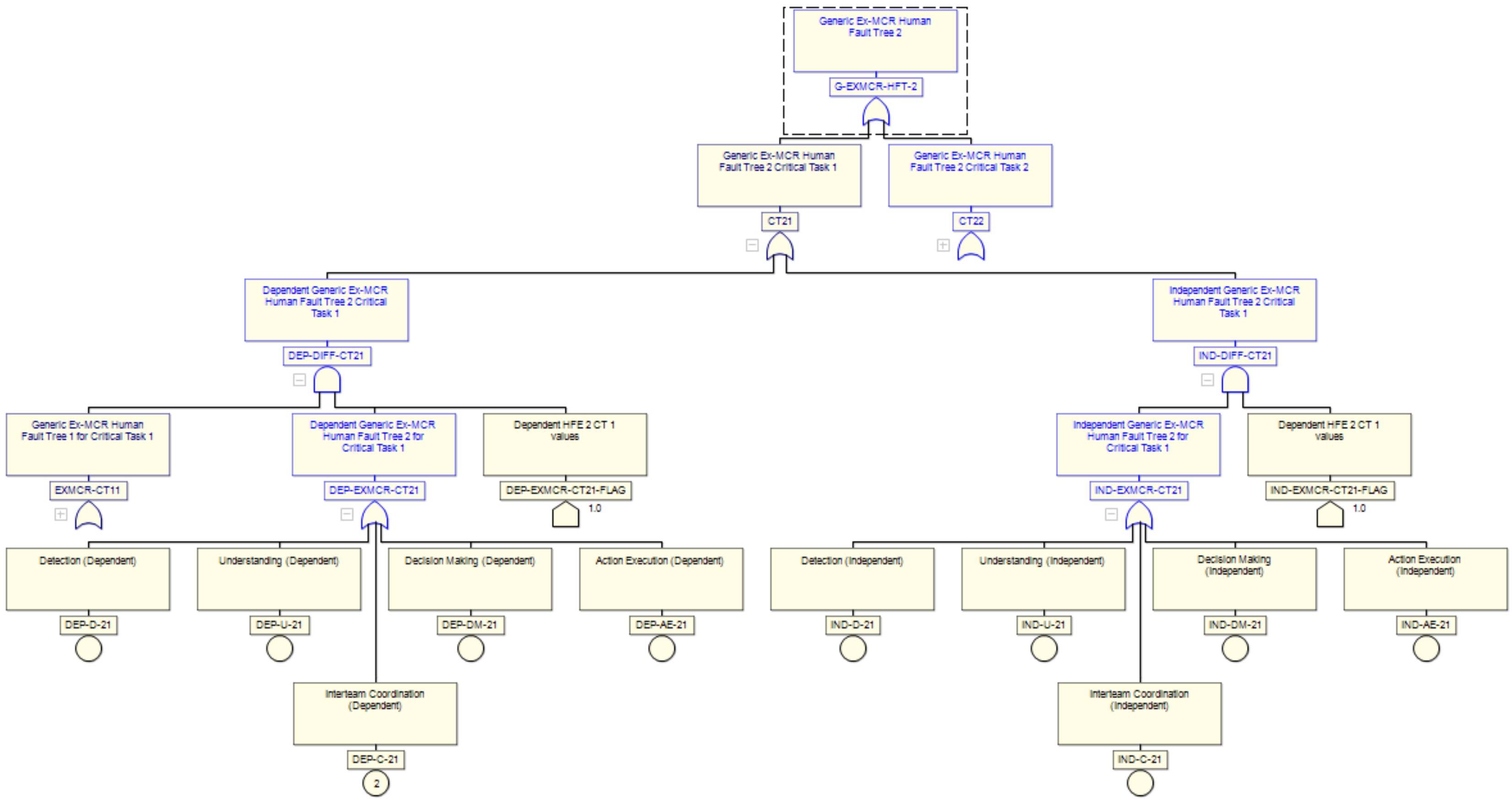

Figure 60. Example of linked Human Fault Tree (IDHEAS-ECA & IDHEAS-ECA)

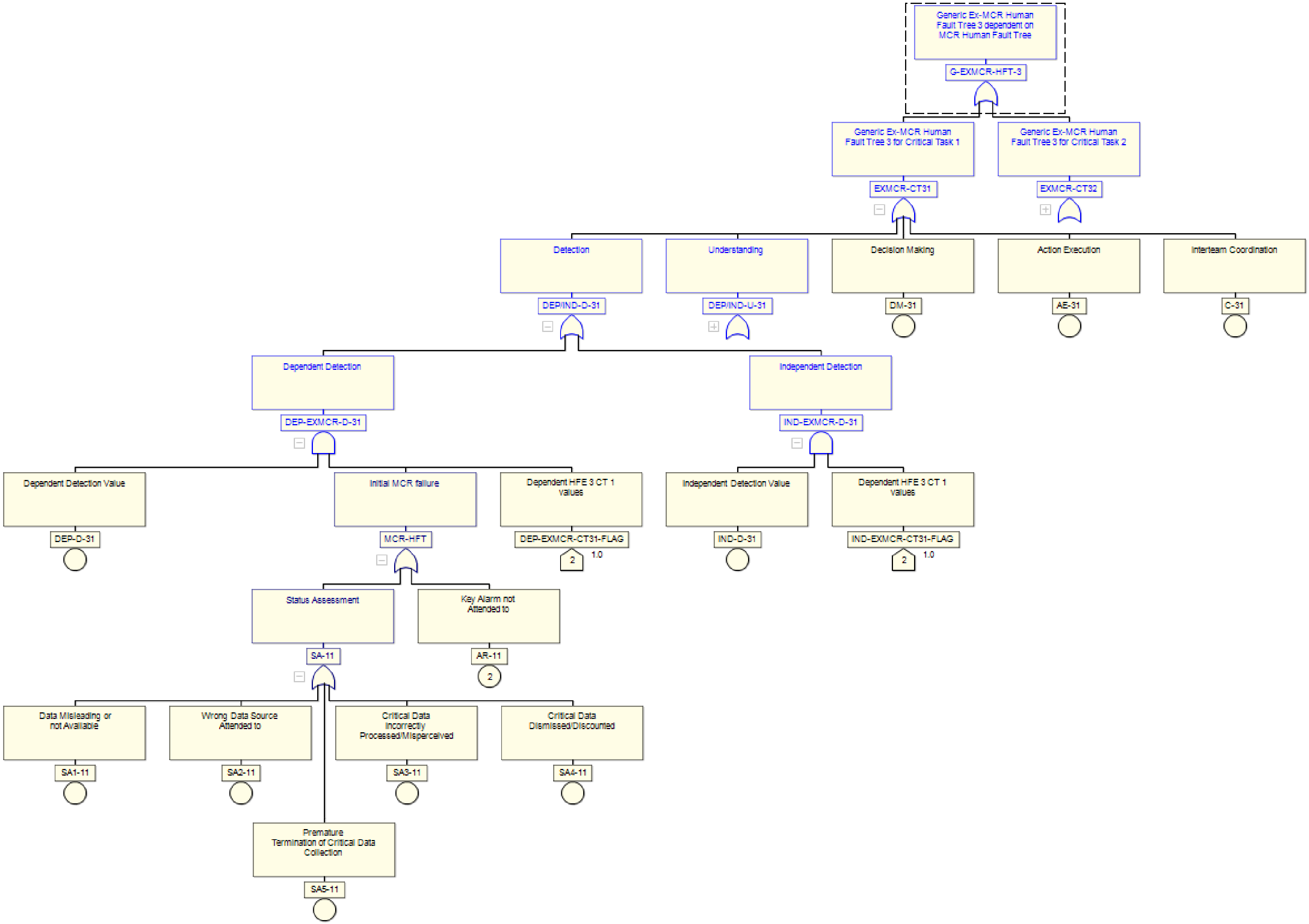

Figure 61. Example of linked Human Fault Tree (IDHEAS At-power & IDHEAS-ECA) (1/2)

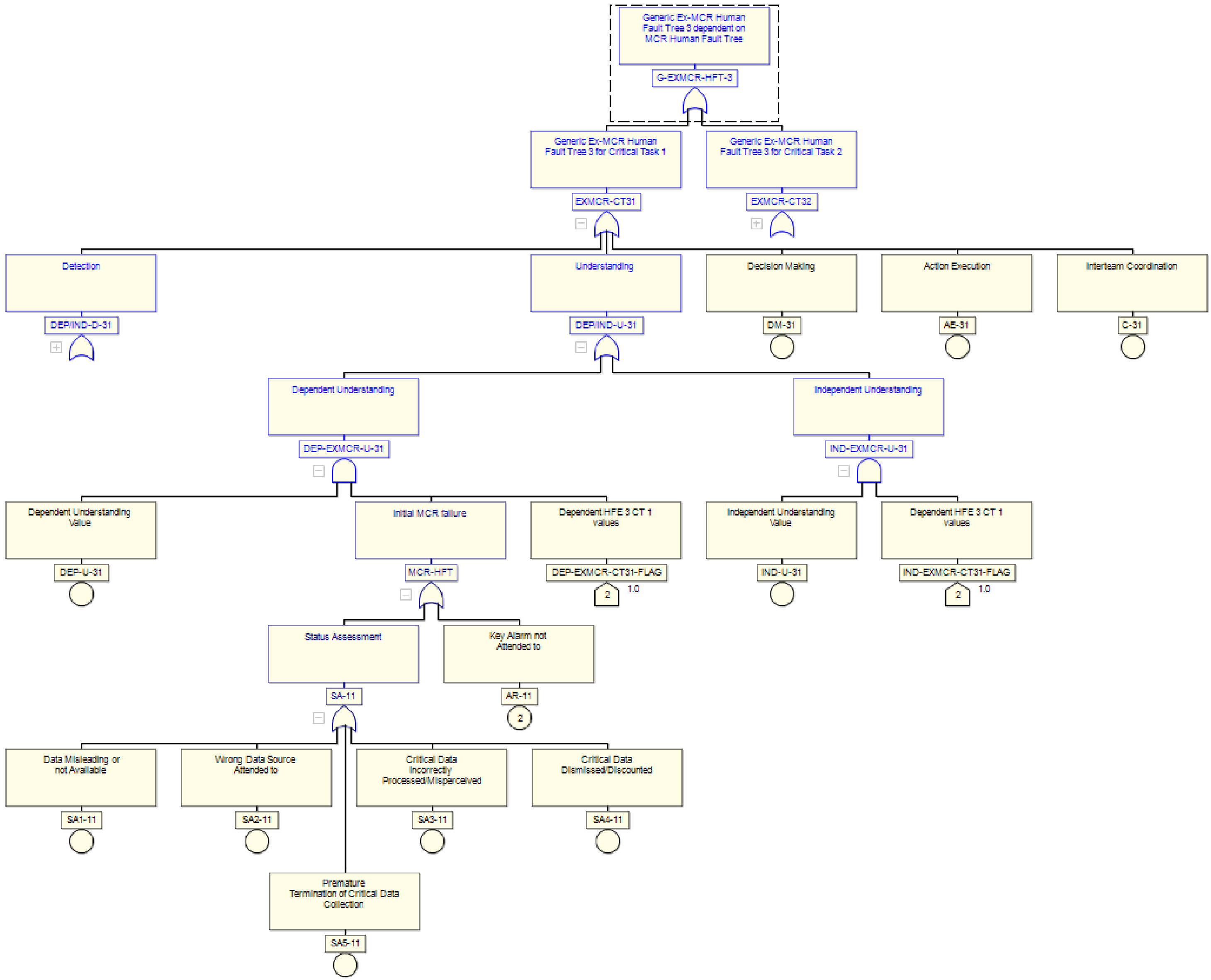

Figure 62. Example of linked Human Fault Tree (IDHEAS At-power & IDHEAS-ECA) (2/2)

4.4.Multi-Unit Considerations

Within a multi-unit site, two general types of initiating events impact the site: single-unit and multi-unit initiating events. Single unit initiating events impact one and only one unit while other units on the site continue normal operation without any impact on their operating states. An example of such single-unit initiating events includes loss of coolant accidents (LOCA), steam generator tube ruptures (SGTR), and loss of instrument air (LOIA). Site-wide multi-unit initiating events concurrently impact all units within the site, such as loss of offsite power (LOOP), seismic events, and other external hazards. It should be noted that some events included within the definition of LOOPs may be localized and impact only a single unit, such as plant-centered LOOPs. However, it is assumed that LOOPs, in general, impact all units on site within the current scope of this study [75].

For the current generation of reactors, even though multiple units may exist within the same site, each unit has a separate control room and frontline systems. However, some supporting systems may be shared among multiple units, such as diesel generators, whose failure would impact all units that rely upon them. The site may also share the same maintenance crew and the field crew associated with these shared systems; hence, identifying potential dependency links between their actions is critical to accurately building a multi-unit PRA model. Two approaches can be taken when creating a multi-unit PRA model; either a simplified single-unit PRA model is constructed and is adjusted to reflect the risk increase associated with having multiple units, or an explicit multi-unit PRA model is built that explicitly captures the response of all units.

Unlike the efforts presented in section 2.3.3, the proposed framework does not make any inherent assumptions regarding the dependence/independence of operator actions within a multi-unit site. However, by implementing the first steps of the proposed framework, the scope of detailed analysis may be significantly reduced to only impactful operator actions. The following guidelines are, however, presented to facilitate expanding the framework to both versions of multi-unit PRA models.

4.4.1.Explicit Multi-unit PRA Model

Pre-initiator HFEs: by definition, these events are related to testing and maintenance activities that may render a system unavailable when challenged. By sharing a maintenance crew, the dependency between pre-initiators throughout different systems and units should be assessed. A key area of consideration when determining the dependency between pre-initiators is the maintenance procedures and guidelines used within the site.

At-initiator HFEs: By definition, these events result in an initiating event occurring within the site. These include operator actions performed within the control room, an inadvertent reactor trip, or a frontline unit-specific system. Hence, these at-initiators are independent and unit-specific and do not impact other units. However, at-initiators may impact the following post-initiators due to high stress levels, misdiagnosis, or miscommunication.

Post-initiator HFEs: by definition, these are events that follow the occurrence of an initiating event. Depending on the type of HFE, this may impact the following post-initiator within the same unit or all units. Hence, the dependency between post-initiators throughout the systems and units should be assessed. Post-initiators can also render a shared system unavailable following a unit-specific initiating event. Such an HFE can be considered a pre-initiator for the other initially unimpacted units. However, such a scenario requires the occurrence of two consecutive initiating events (unit-specific followed by unit/site-specific initiating event), which renders this event mathematically unlikely; hence, the dashed line is used in Figure 63.

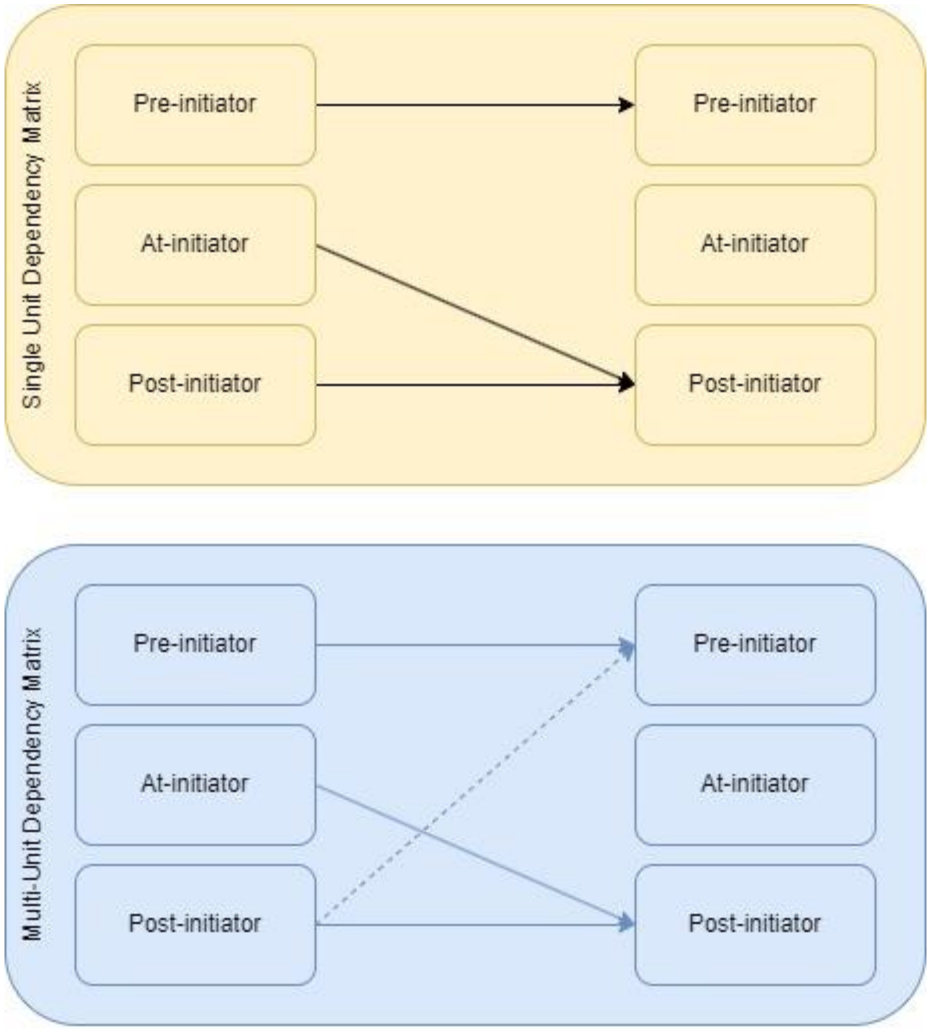

Figure 63. Single and Multi-Unit Dependency Matrix

4.4.2.Single-unit PRA Model with Multi-unit Consideration

For a simplified PRA model, a single-unit PRA model is developed with high fidelity, which is then modified to capture the risk increase due to having multiple units. For such models, the LBE frequencies associated with a single unit are multiplied by the number of units to represent the LBE frequencies associated with a multi-unit event. However, such an approach inherently assumes that all included systems and actions are independent, as shown in section 2.3.3, which is not the case. Hence, the suggested approach is to identify those multi-unit operator actions whose failure would impact all units on the site and isolate the impact of those actions before modifying the frequency.

To isolate the impact of a multi-unit operator action (MU), the following steps are followed:

- The operator action is assumed to fail (set the HFE to true).
- The ESQ model is quantified to calculate the LBE frequencies given the failure of MU.
- The operator action is assumed to succeed (set the HFE to false)
- The ESQ model is quantified to calculate the LBE frequencies given the success of MU.

The modified frequency of the LBEs can be computed using the formula presented in Equation (16) where $f_{MU}(LBE)$ is the multi-unit frequency of the LBE, $f_{SU}(LBE|MU_{Failed})$ is the single unit frequency of the LBE given the failure of MU, $f_{SU}(LBE|MU_{success})$ is the single unit frequency of the LBE given the success of MU, and N is the number of units within site.

$$f_{MU}(LBE) = N * f_{SU}(LBE|MU_{Failed}) + [f_{SU}(LBE|MU_{Success}) - f_{SU}(LBE|MU_{Failed})] \tag{16}$$

4.5.Multi-Module Considerations

Within a multi-module site, two general types of initiating events impact the site: single-module and multi-module initiating events. Single-module initiating events impact one and only one module while other modules on the site continue normal operation without any impact on their operating states. Examples of such single-module initiating events include a reactor trip (RT) or a primary side depressurization event. Multi-module initiating events concurrently impact all units within the site, such as loss of offsite power (LOOP) or loss of shared systems like turbines, instrument air, or feedwater systems.

For the advanced generation of reactors, some frontline and supporting systems may be shared among multiple units whose failure would impact all units that rely upon them. The site may also share the same control room, operating, maintenance, and field crew; hence, identifying potential dependency links between their actions is critical to accurately building a multi-module PRA model. Unlike multi-unit PRA models, a simplified single-module PRA model can no longer be used due to the complexity of the response, which depends on which operator failure occurs. A high-fidelity multi-module PRA model needs to be built explicitly modeling dependencies between operator actions following guidelines, presented in section 4.5.1.

4.5.1.Explicit Multi-module PRA Model

By definition, pre-initiator HFEs are events that are related to testing and maintenance activities that may render a system unavailable when challenged. By sharing a maintenance crew, the dependency between pre-initiators throughout different systems and modules should be assessed. A key area of consideration when determining the dependency between pre-initiators is the maintenance procedures and guidelines used within the site.

At-initiator HFEs, on the other hand, result in an initiating event occurring within the site. These include operator actions performed within the control room, an inadvertent reactor trip, or a frontline system. Hence, these at-initiators can be single- or multi-module events depending on the type of the HFE. Moreover, at-initiators may impact following post-initiators due to high levels of stress, misdiagnosis, or miscommunication.

Finally, post-initiator HFEs are events that follow the occurrence of an initiating event. Depending on the type of HFE, this may impact the following post-initiator within the same module or all modules. Hence, the dependency between post-initiators throughout the systems and units should be assessed. Post-initiators can also result in an at-initiator in other modules due to an error of commission by the operator or the crew, e.g., an operator inadvertently trips a module while navigating an event progression in another module. By sharing a control room and reducing staffing, such a scenario becomes a credible scenario that needs to be assessed, as illustrated in Figure 64.

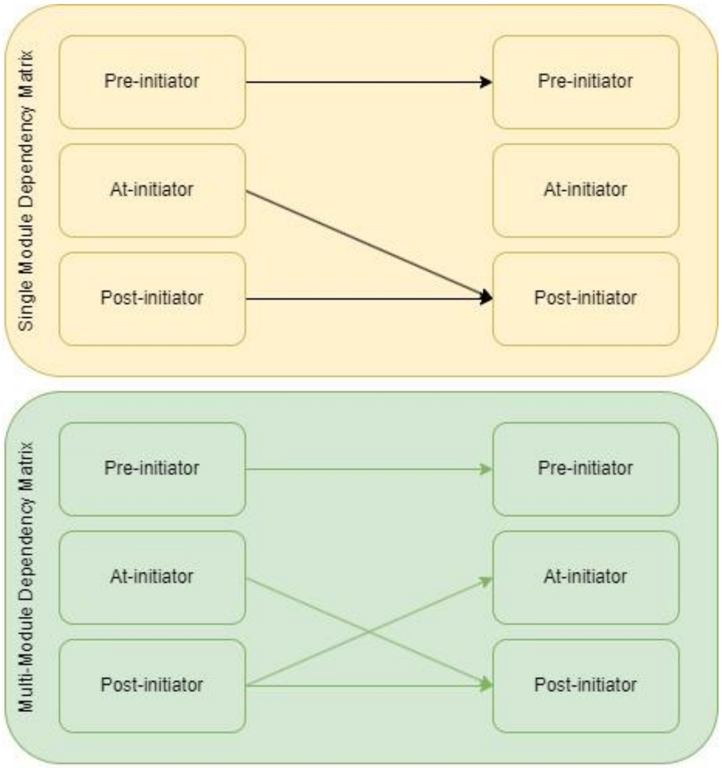

Figure 64. Single and Multi-module Dependency Matrix

4.6.Limitations and Sources of Uncertainty

This section identifies the primary sources of uncertainty associated with the proposed framework. The impact of each source of uncertainty is assessed, and whether or not it is accounted for in the framework. Sources of uncertainty whose influence is not accounted for are flagged as a limitation of the proposed framework, and an initial approach to address them is presented.

4.6.1.Conditional Failure Probabilities

The conditional failure probabilities used to build the Bayesian networks are usually elicited from experts, as presented in section 2.2. Since a similar approach to the linked Bayesian network methodologies is used in the proposed framework, the same uncertainty associated with the elicited values remains applicable. However, as presented in 4.3.9, by restricting the elicitation process to only the failure probability associated with specific crew failure scenarios, i.e., $P(CFM|PIF_1\&PIF_2 \ldots \&PIF_3)$ instead of $P(CFM|PIF_1)$, the number of elicited values a reduced significantly. The elicited values can then quantify the specific conditional probabilities needed for building the Bayesian networks.

The inverse estimation process used in this framework allows for quantifying a mean value of the conditional probabilities and estimating a distribution of each conditional probability. Moreover, the elicitation process could elicit uncertainty/confidence intervals associated with the experts, which can further be used to improve the uncertainty distribution quantified in the inverse estimation process. Such uncertainty distributions are already incorporated into IDHEAS At-power, where at least the mean, 5^{th} percentile, and 95^{th} percentile of each crew failure scenario probability are provided.

Finally, restricting the expert elicitation process to crew failure probabilities conditional on a set of performance influencing factors allows the incorporation of simulation and other data sources into the estimation. Since specific performance influencing factors cannot be studied in isolation, liberating the modeling and simulation from this restriction opens the possibility of designing experiments that incorporate different sets of the PIFs, such as high stress, short time, and adequate training.

4.6.2. Licensing Basis Event Frequency

The frequency associated with different LBEs incorporates multiple uncertainties associated with the parameters used, phenomena modeled, and responses assumed. Such uncertainties must be incorporated either quantitatively or qualitatively in the frequency-consequence results. By relying on the LBE frequency to identify key operator actions, the proposed framework needs to account for the uncertainty associated with these values. Hence, the proposed framework implemented an approach similar to that employed by the LMP methodology [30] where the mean and upper bound (95th percentile) of the LBE frequency are considered during evaluation.

During the 2nd and 4th steps of the framework, sections 4.3.2 and 4.3.4, a critical HFE pair is identified by considering its impact on the mean and 95th percentile of the LBE frequency. Hence, even if the mean value of an LBE frequency remains within the same LBE categorization, if the 95th percentile crosses into another LBE categorization, the framework requires a detailed analysis of any associated HFEs. By incorporating a similar approach to the LMP methodology, the proposed framework incorporates the quantitative uncertainty associated with the LBE frequencies.

4.6.3.IDHEAS-ECA and IDHEAS At-power

Unlike IDHEAS At-power, IDHEAS-ECA does not incorporate decision trees in its failure probability quantification. Instead, IDHEAS-ECA uses adjustment factors associated with each attribute state that modifies the basic HEP to incorporate influencing factors. Such values are expert elicited, reintroducing uncertainties similar to those associated with the conditional failure probability elicitation. Due to the lack of sources to construct the needed decision trees for this study, the software associated with IDHEAS-ECA is used to quantify CFM failure probabilities. However, the proposed framework presents a path to address this uncertainty whenever such decision trees become available. Hence, even if the proposed framework currently suffers from uncertainties associated with IDHEAS-ECA's factors, it can be deemed that these uncertainties are well addressed and have a clear path for closure.

4.6.4.Time and Feasibility Assessment

The proposed framework needs to address the uncertainty associated with the available time and feasibility of operator actions. The framework relies on feasibility analysis in the HRA model itself, evaluating whether operator actions can be realistically carried out. This assessment determines whether an operator action should be included and quantified in the model based on various performance factors. If an action is deemed unfeasible, it receives a HEP of 1.0. An initial feasibility assessment can occur during HRA's Identification and Definition phase, which screens out obviously unfeasible actions. Detailed assessment becomes necessary as more contextual and timing information becomes available during the analysis phases [72].

Moreover, both IDHEAS At-Power and IDHEAS-ECA incorporate a structured timeline to estimate time and quantify the time uncertainty for an individual HFE [72][73]. Both methodologies incorporate P_t, which represents the failure probability of an action due to time constraints. However, this was outside the scope of the current study, which only assessed cognitive failures. Hence, the time uncertainty impact on the dependency between two actions is a source of uncertainty in the proposed framework that is yet to be addressed.

4.6.5.Errors of Commission

Despite indicating the impact that errors of commission might have, especially in multi-module PRA models, the proposed framework needs to present an approach to assess and explicitly model errors of commission and their dependencies. Errors of commission would not only impact the frequency, but the operator may put the plant in a different state, depending on the human failure, which is different than simply the failure/success of a specific system. An example of that was given in section 4.5 an error of commission might convert a single-module initiating event to a multi-module complex initiating event. Hence, errors of commission present a significant source of uncertainty in the proposed framework that has yet to be addressed.

4.6.6.Cognitive Basis

Similar to all current HRA methodologies, the proposed framework lacks a cognitive basis for the dependency links and assumptions. The proposed framework incorporated the IDHEAS methodologies because they are judged to present a grounded cognitive basis for quantifying human failures. However, this remains an open area of research that would present a constant source of epistemic uncertainty.

CHAPTER 5. FRAMEWORK DEMONSTRATION

In this chapter, the proposed framework for dependency analysis, presented in CHAPTER 4, is implemented and demonstrated. Two PRA models demonstrate the framework: the G-PWR and the MHTGR PRA models. The G-PWR presents an example of legacy LWR that can be considered to represent a single unit within a multi-unit complex. The G-PWR is used to implement the multi-unit considerations presented in Section 1.1 identifying any limitations and shortcomings associated with the implementation. On the other hand, the MHTGR PRA model presents an example of an advanced multi-module design that is expected to incorporate multiple modules controlled through a single control room. Sections 5.1 and 5.2 present an overview of the PRA model for the MHTGR and the G-PWR, respectively. The models are described in Section 5.1.1 and 5.2.1 including different limitations and assumptions made when adopting the models. Sections 5.1.2 and 5.2.2 describe the implementation process of the proposed dependency framework for the MHTGR and G-PWR models, respectively. Addressing the impact of multi-module and multi-unit on the dependency model is addressed in sections 5.1.3 and 5.2.3, respectively. Finally, sections 5.1.4 and 5.2.4 lists the results of the framework implementation along with any limitations and shortcomings.

5.1.MHTGR PRA Model

The Modular High-Temperature Gas-cooled Reactor (MHTGR) was developed by a consortium consisting of five U.S. corporations – General Atomic Technologies Inc., Combustion Engineering, Inc., General Electric Company, Bechtel National, Inc., Stone & Webster Engineering Corporation – and Oak Ridge National Laboratory, sponsored by the U.S. Department of Energy (U.S. DOE). The MHTGR project aimed to create a nuclear reactor that is inherently safe and can provide power at a levelized 30-year bus-bar price that is less than 90% of that which can be supplied by a similarly sized coal-fired plant in the U.S. with a target cost of 45 mills/kW-hr.

The design of the MHTGR is based on previous experience with gas-cooled reactors, such as:

- In the United Kingdom:
    - The carbon dioxide-cooled Magnox, and
    - Advanced Gas-Cooled Reactor (AGR),
- In Germany:
    - The 15 MW(e) Arbeitsgemeinschaft Versuch Reaktor (AVR) development plant and
    - The 300 MW(e) Thorium Hochtemperatur Reaktor (THTR) demonstration plant,
- In the U.S.:
    - The 40 MW(e) Peach Bottom I, and
    - The 330 MW(e) Fort St. Vrain (FSV) plant.

The FSV facility has confirmed and demonstrated specific and generic HTGR design and operating characteristics.

The MHTGR was designed to meet the rigorous requirements established by the U.S. Department of Energy and the electric utility/user industry for a second-generation power source in the late 1990s. The plant was designed to be attractive for deployment and operation in the U.S., other major industrialized nations, and developing nations worldwide. The design of the MHTGR system includes four 350 MW(t) HTGR modules producing high-pressure, high-temperature steam to generate 538 MW(e) using two conventional turbine generators. The plant design uses high-level automation and passive safety systems, and control of all four reactors and the turbine plant is centralized in a common control room.

The consortium began developing the MHTGR in fiscal year 1984 and submitted a Preliminary Safety Information Document to the U.S. NRC in 1987 to receive a licensability statement. The MHTGR design has since evolved based on this effort and feedback from the NRC [78][79].

5.1.1.MHTGR Model Description

The MHTGR PRA model was developed over multiple years to provide a means of evaluating the safety of the conceptual design, providing the basis for the selection of LBEs, providing support of the emergency planning bases, and evaluating the risk to the public to show compliance with the NRC safety goals. Despite being developed in the 80s, the PRA model extends beyond the Level 1, 2, and 3 PRA aspects into a comprehensive PRA model that closely resembles the LMP methodology. The PRA model examined a broad event spectrum to identify events potentially dominant with respect to plant safety. Out of this wide spectrum, seven initiating events were selected for detailed evaluation:

- Primary coolant leaks.
- Loss of main loop cooling.
- Seismic activity.
- Loss of offsite power and inadvertent turbine trip.
- Anticipated transients requiring reactor scram.
- Control rod group withdrawal.
- Steam generator leaks.

The PRA model presented over two volumes [80][81] was recreated in EPRI’s Computer Aided Fault Tree Analysis System (CAFTA) to properly link different top events. The event trees associated with the seven initiating events within the scope of the MHTGR model are built and presented in Figure 65 to Figure 72. The fault trees associated with the top gates are also reproduced in CAFTA using the supplementary data included in [81] and [82]. The model includes three types of operator error basic events reflecting the pre-, at-, and post-initiator HFEs. Within the initiating event fault trees developed for all internal events, illustrated in Figure 65 to Figure 74, multiple operator errors were identified that could result in the loss of main loop cooling either during normal operation or during maintenance activities.

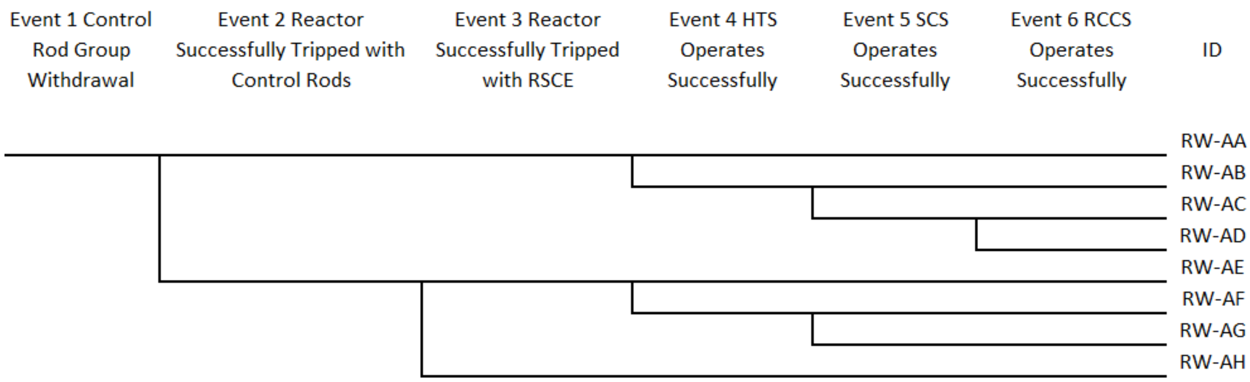

Figure 65. Event Tree for Control Rod Group Withdrawal Initiating Event

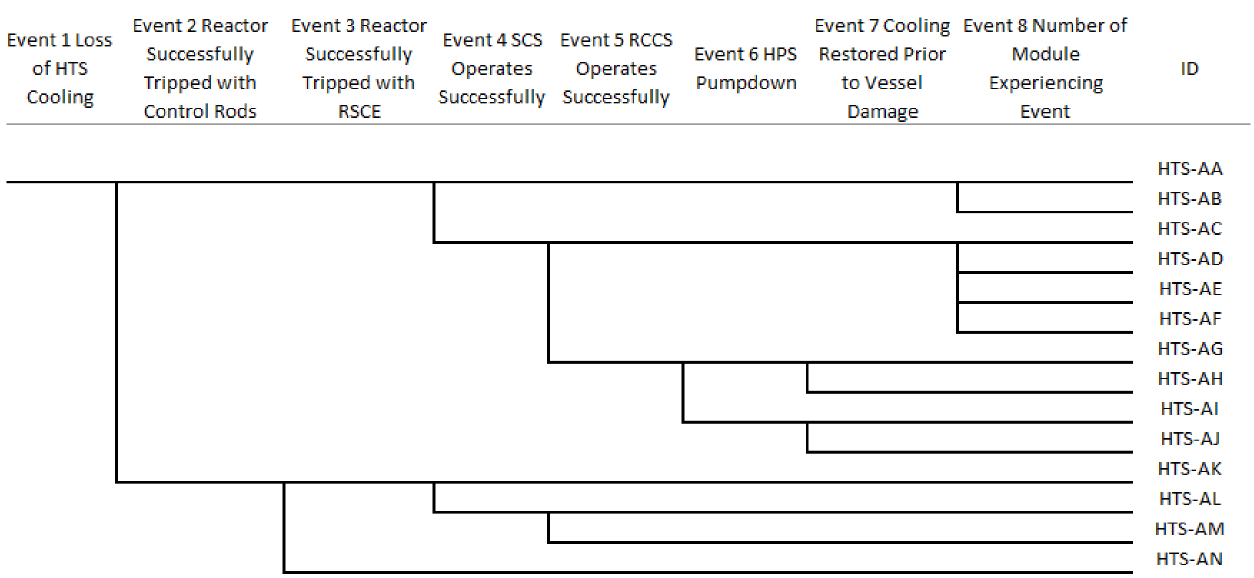

Figure 66. Event Tree for Loss of HTS Cooling Initiating Event

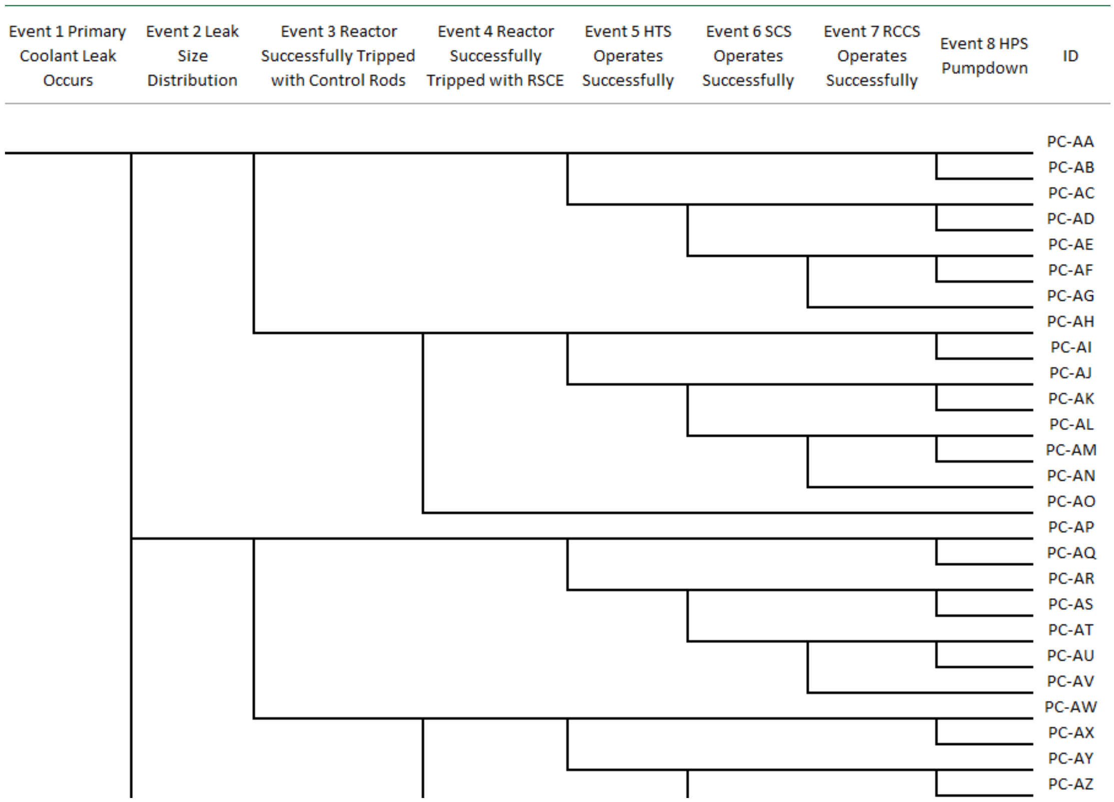

Figure 67. Event Tree for Primary Coolant Leak Initiating Event (1/2)

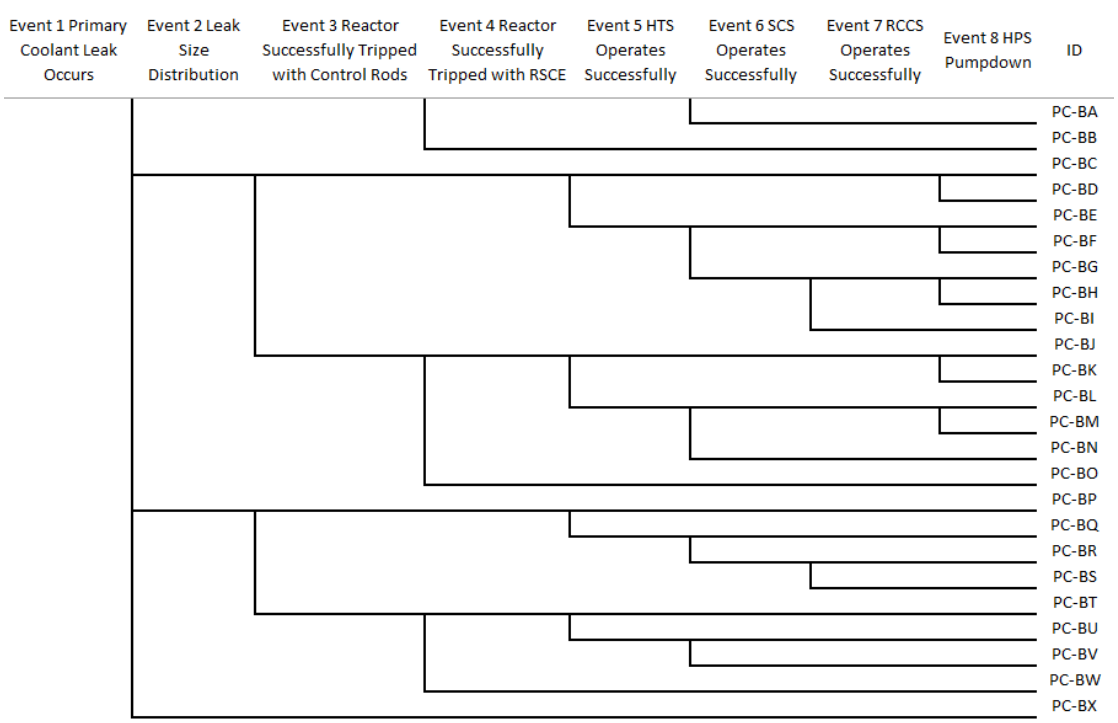

Figure 68. Event Tree for Primary Coolant Leak Initiating Event (2/2)

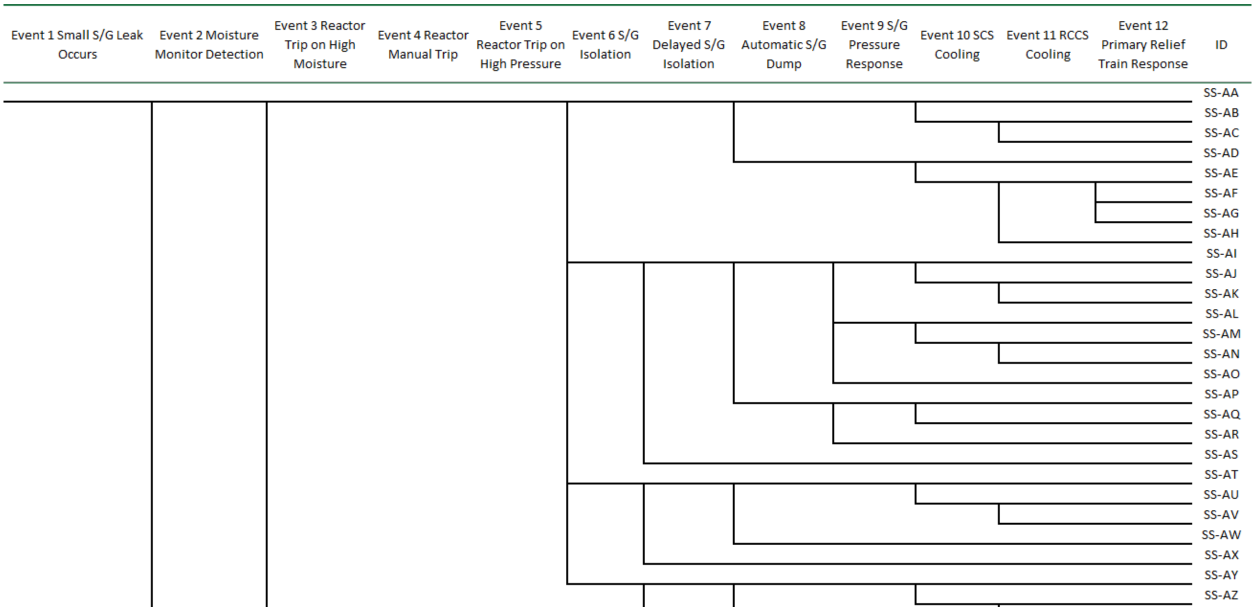

Figure 69. Event Tree for Small Steam Generator Tube Leak Initiating Event (1/2)

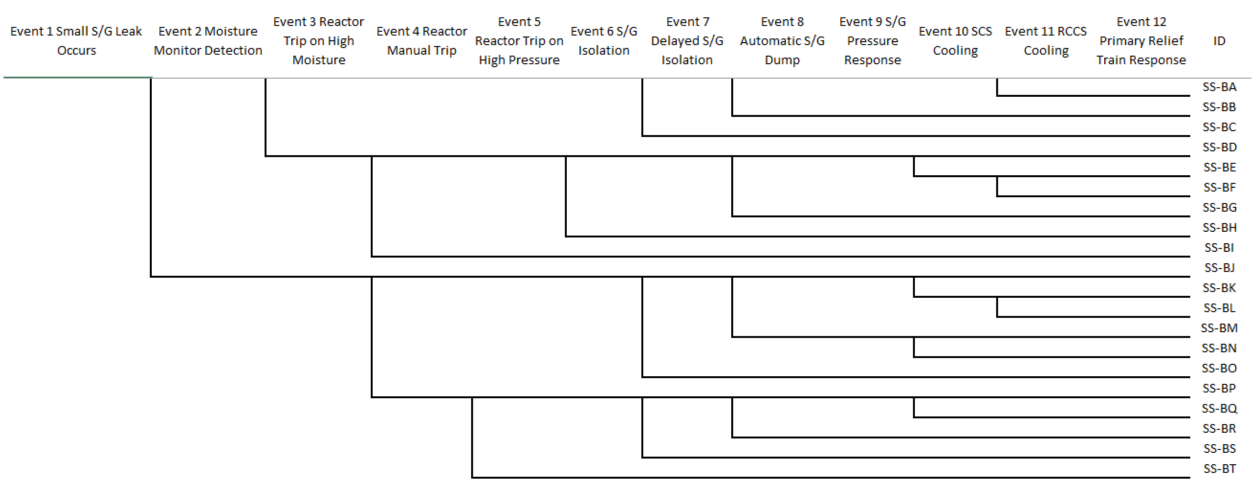

Figure 70. Event Tree for Small Steam Generator Tube Leak Initiating Event (2/2)

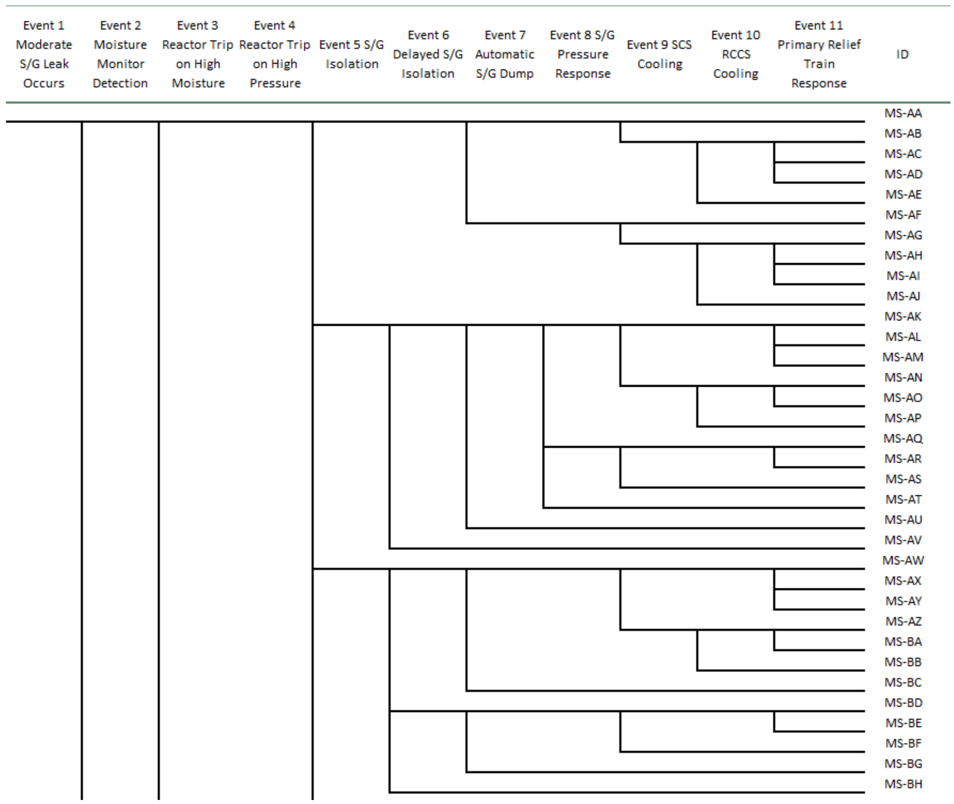

Figure 71. Event Tree for Moderate Steam Generator Tube Leak Initiating Event (1/2)

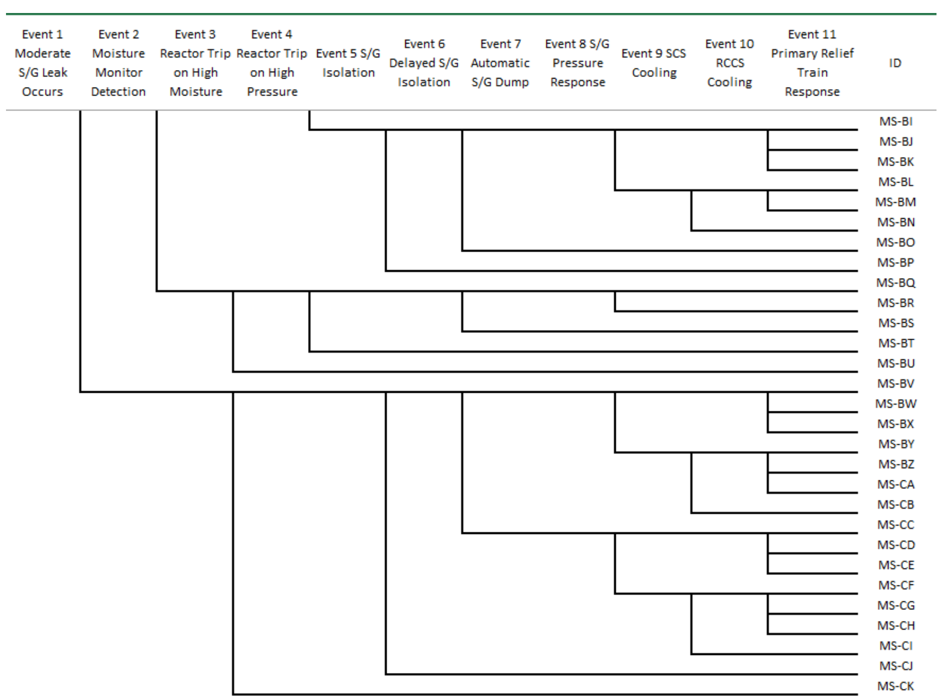

Figure 72. Event Tree for Moderate Steam Generator Tube Leak Initiating Event (2/2)

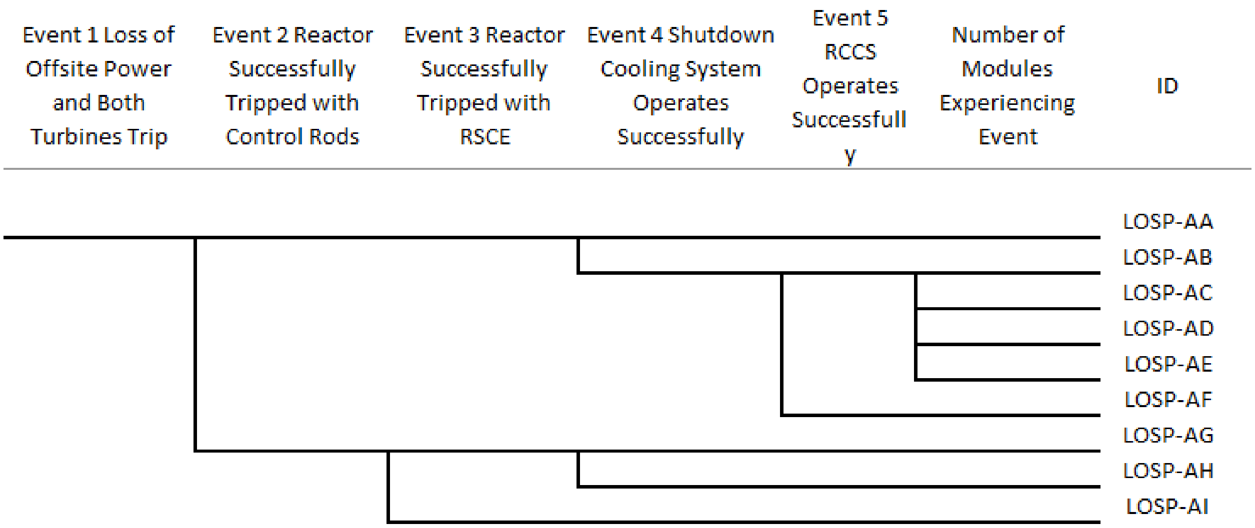

Figure 73. Event Tree for Loss of Offsite Power and Both Turbines Trip Initiating Event

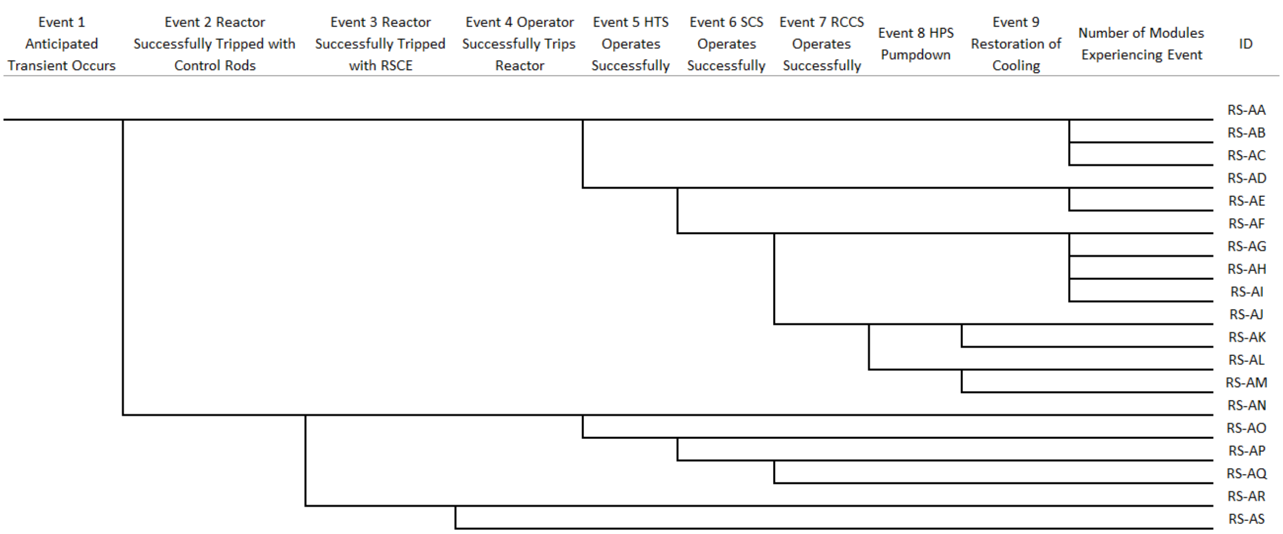

Figure 74. Event Tree for Anticipated Transient Requiring Scram Initiating Event

5.1.2.Framework Implementation

After building the PRA model for the MHTGR in CAFTA, the ESQ model is quantified to produce the baseline model for the framework implementation. The results of the baseline quantification, along with all following quantifications, are presented in Table 7. The framework starts by using the baseline quantification and conducts the following modifications:

- Step 1 → the failure probability of all pre-, at-, and post-initiator HFE basic events is modified from its original value to 9.9E-01. The modified ESQ model is then quantified to produce the first run of the framework, Run 0 in Table 7.
- Step 2 → the updated LBE frequencies are compared against their baseline values to identify the LBEs most impacted by HFEs. As can be seen in Figure 75 to Figure 83, most LBEs are insensitive to the changes in HFE probabilities; however, some LBEs experience increases in their frequency. Hence, the HFEs whose frequencies experience LBE categorization shifts associated with these LBEs are candidates for further detailed analysis. Those LBEs are extracted from Figure 75 to Figure 83 and listed in Table 5, along with their associated initiating event.

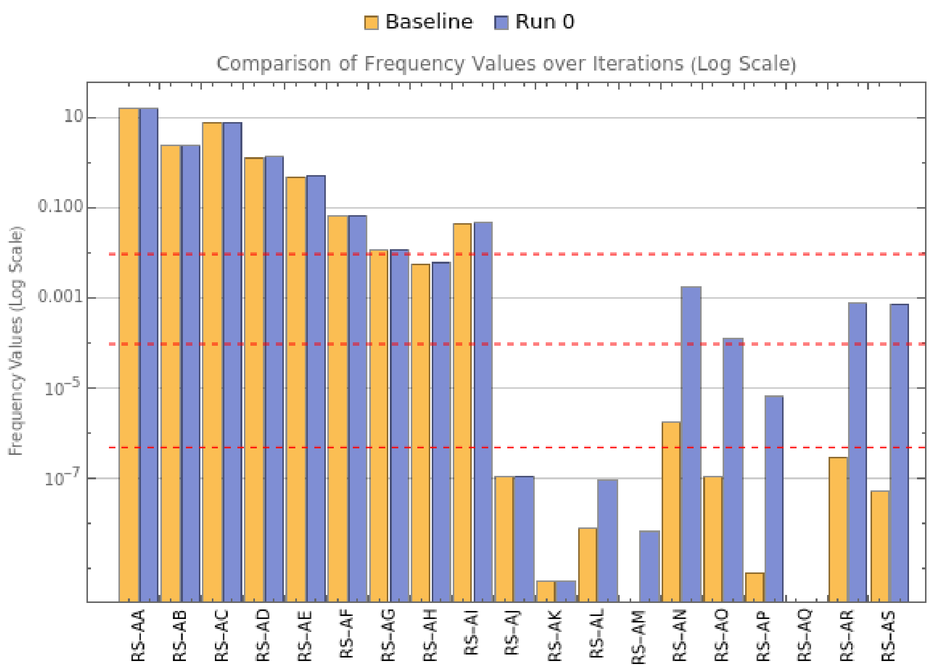

Figure 75. ATRS End State Frequency Comparison

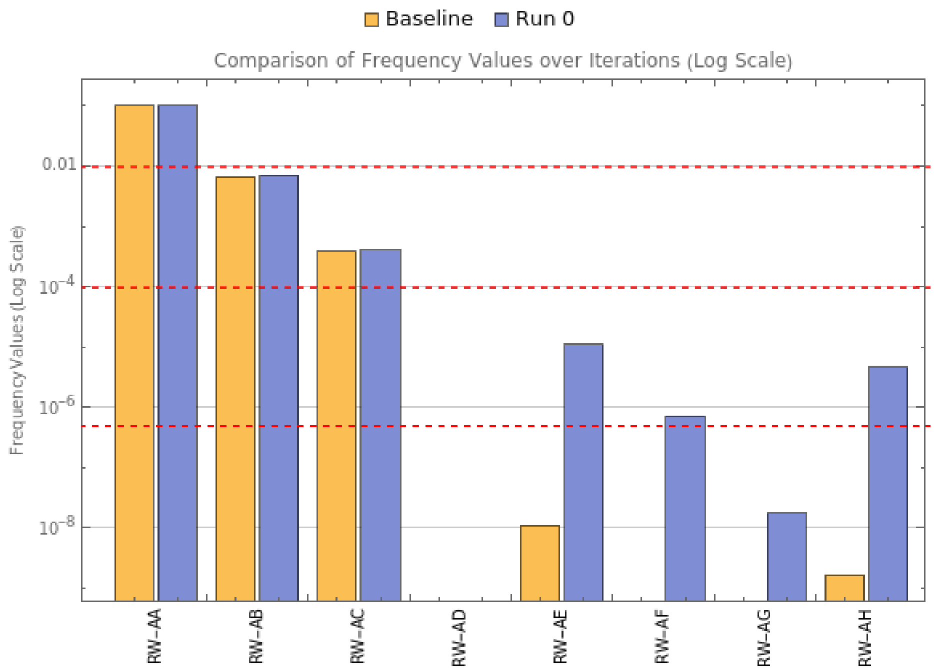

Figure 76. CRW End State Frequency Comparison

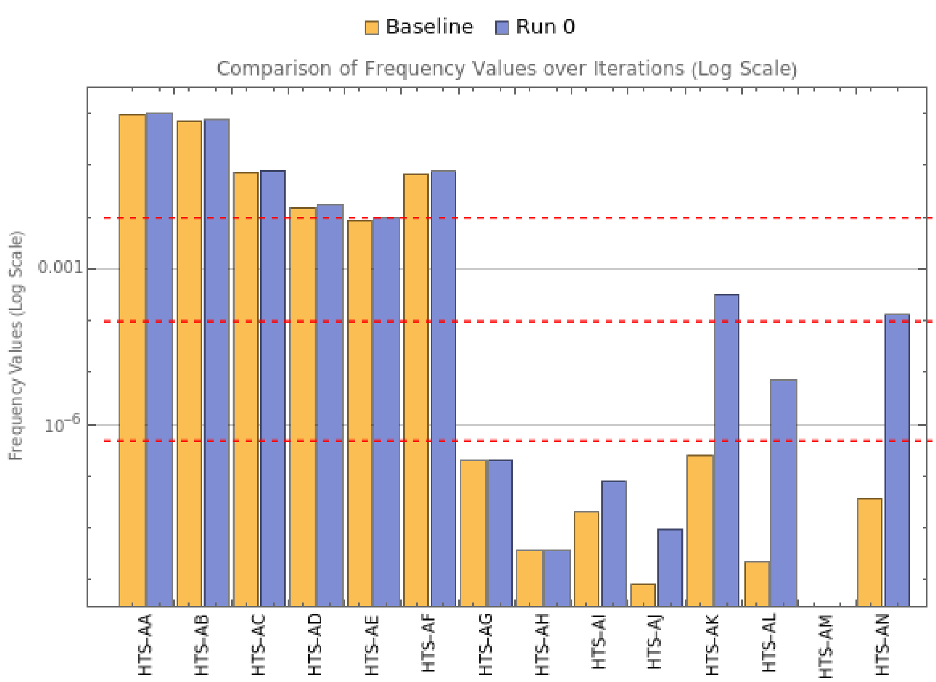

Figure 77. HTS End State Frequency Comparison

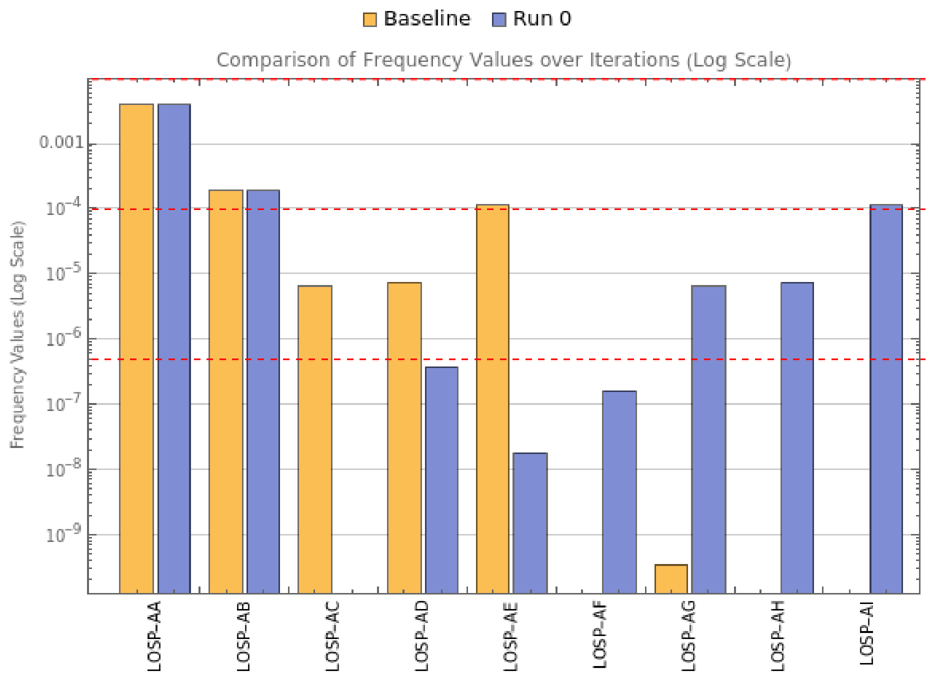

Figure 78. LOSP End State Frequency Comparison

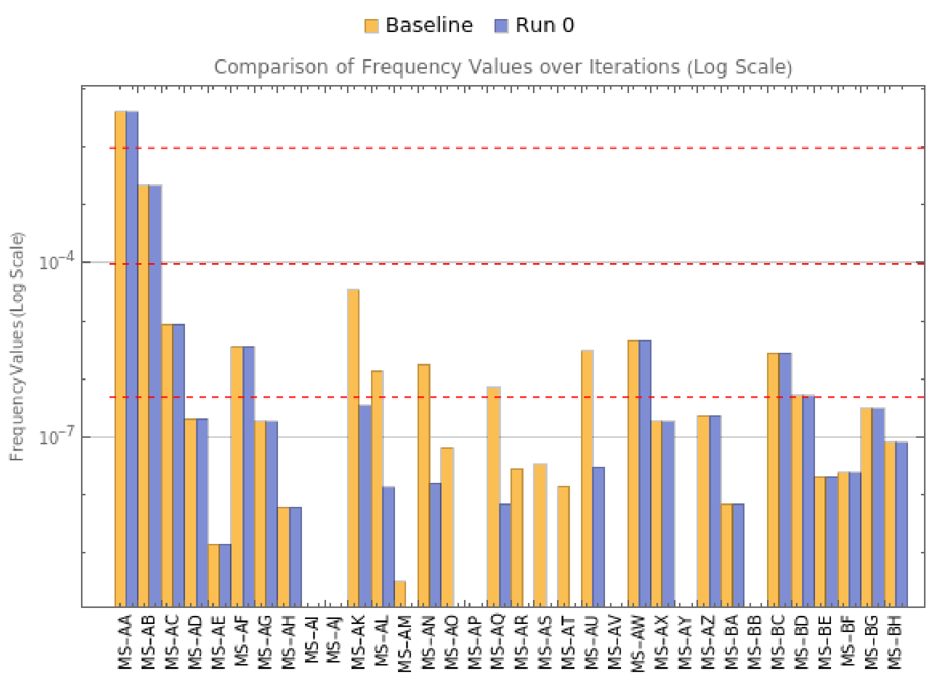

Figure 79. MS End State Frequency Comparison (1/2)

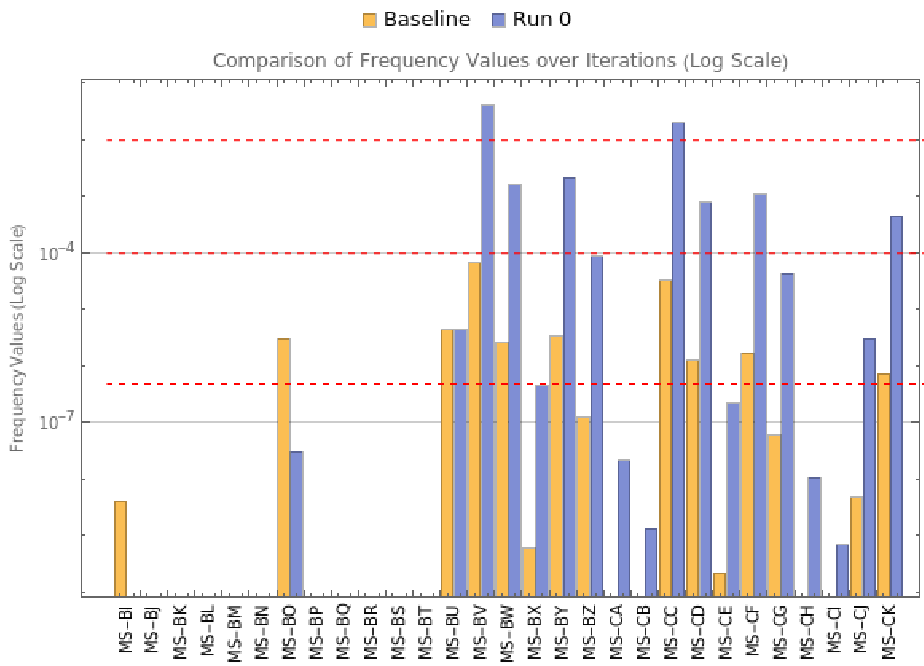

Figure 80. MS End State Frequency Comparison (2/2)

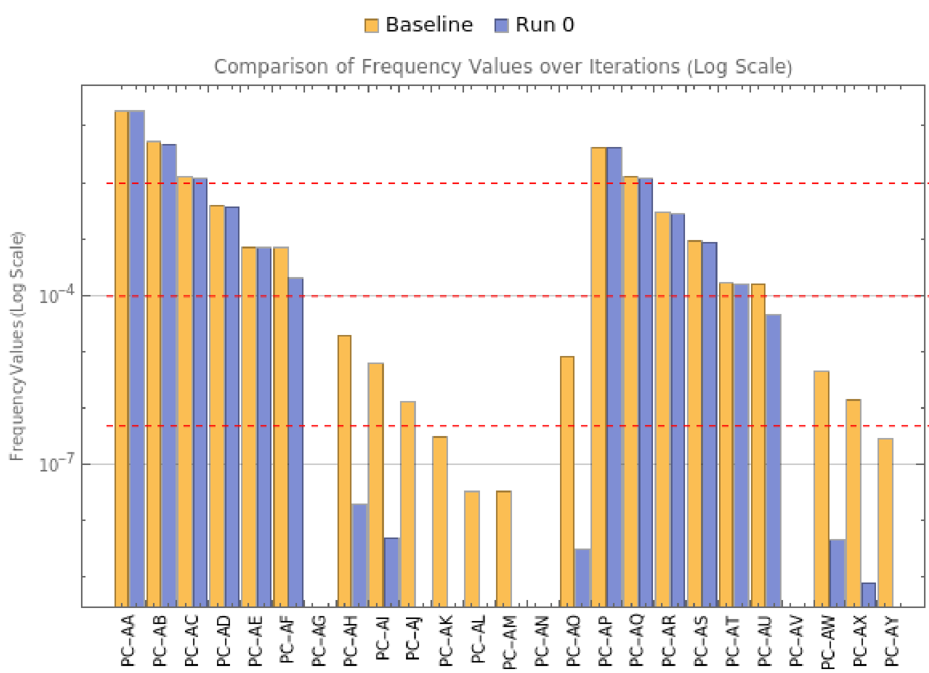

Figure 81. PC End State Frequency Comparison (1/2)

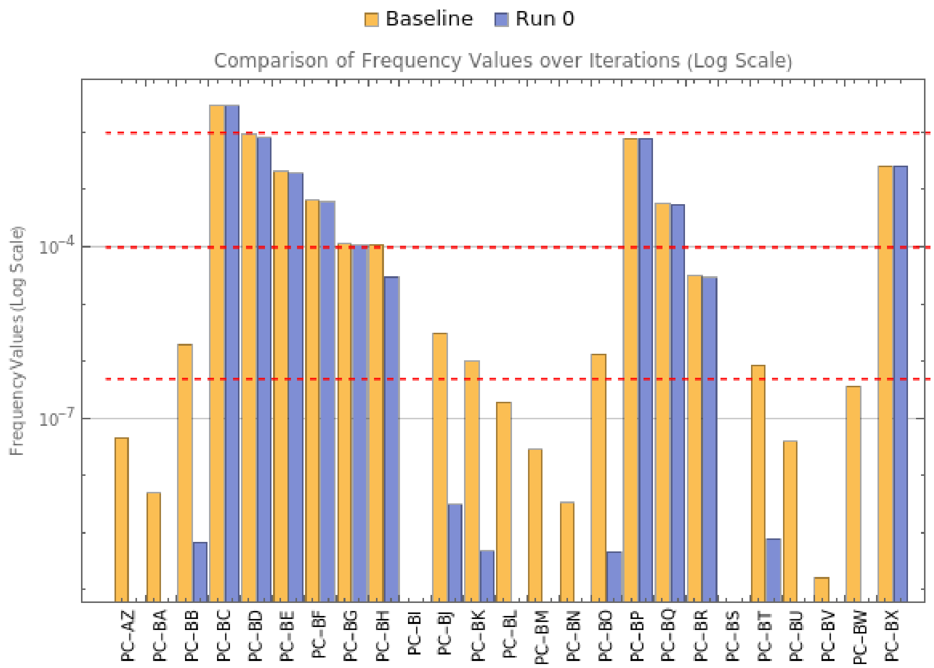

Figure 82. PC End State Frequency Comparison (2/2)

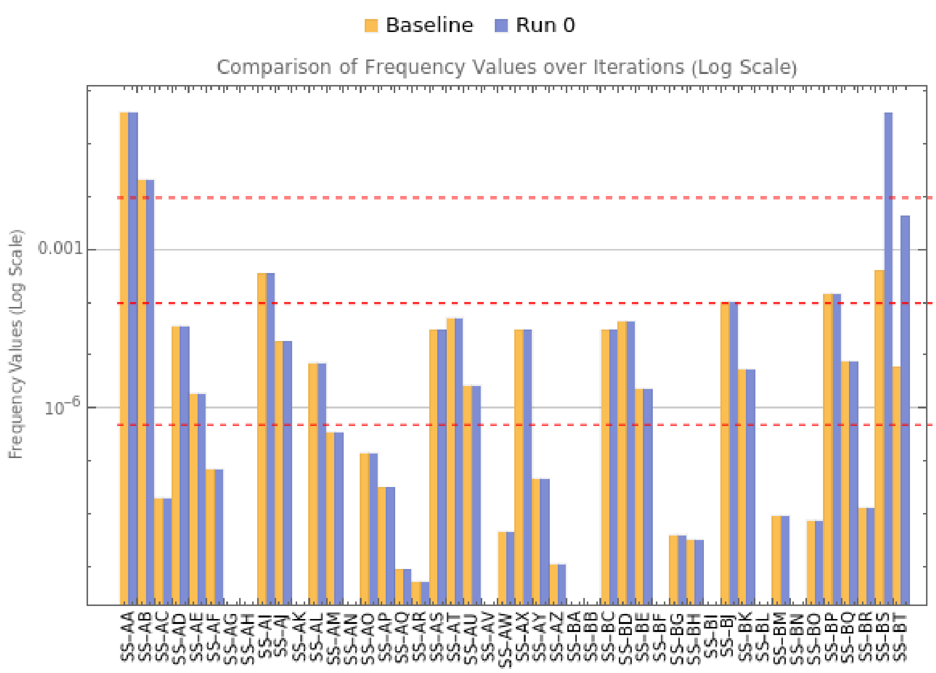

Figure 83. SS End State Frequency Comparison

- Step 3 → The cut sets associated with the LBEs listed in Table 5 are investigated to identify different HFE combinations. To conduct this part, the DepHep tool is used to extract all cut sets with one or more HFEs. The list of HFEs used in the MHTGR model, the cut set files, and the PRA model's database are used in this step. The results of the multi-HFE sequence identification are listed in Appendix D.

Table 5. List of Identified LBEs for Step 3

Initiating Event	Initiating Event ID	LBEs
Control Rod Group Withdrawal	RW	RW-AE
		RW-AF
		RW-AH
Primary Coolant Leak	PC	PC-AE
		PC-AF
		PC-AH
		PC-AI
		PC-AJ
		PC-AK
		PC-AO
		PC-AU
		PC-AX
		PC-AY
		PC-AZ
		PC-BB
		PC-BH
		PC-BJ
		PC-BK
		PC-BL
		PC-BM
		PC-BO
		PC-BT
		PC-BU
		PC-BW
Loss of HTS Cooling	HTS	HTS-AK
		HTS-AL
		HTS-AN
Loss of Offsite Power and Both Turbines Trip	LOSP	LOSP-AF
		LOSP-AG
		LOSP-AH
		LOSP-AI

Table 5. List of Identified LBEs for Step 3

Initiating Event	Initiating Event ID	LBEs
Anticipated Transient Requiring Scram	RS	RS-AN
		RS-AO
		RS-AP
		RS-AR
		RS-AS
Small Steam Generator Tube Leak	SS	SS-BS
		SS-BT
Moderate Steam Generator Tube Leak	MS	MS-BV
		MS-BW
		MS-BX
		MS-BY
		MS-BZ
		MS-CC
		MS-CD
		MS-CE
		MS-CF
		MS-CG
		MS-CJ
		MS-CK

- Step 4 → in this step, only one HFE within the cut sets associated with the LBEs listed in Table 5 is set to its baseline failure probabilities. The remaining HFEs within a specific cut set are all set to 1.0E+00, i.e., guaranteed to fail. Similar to the previous step, DepHep4 is used in this step to automate the process. The result of assuming complete dependency between all HFEs can be seen in the change of the LBE frequency in Run 1 in Table 7.
- Step 5 → in this step, the HFE combinations are arranged in descending order with respect to their importance. The importance measure of choice for the current demonstration is a modified version of Birnbaum's importance measure, as discussed in section 4.1.3. The importance of the combination essentially assumes that only one operator action in the combination can be credited at its random failure rate, and the other is completely

dependent on the first HFE. This step identifies key human action combinations for each LBE in Table 5.

- Steps 6 and 7 → For this demonstration, it was assumed that all HFEs represent a single critical task, i.e., each HFE can be represented as a single node CRD. It should be noted that this is only for demonstration purposes, and a similar assumption would significantly reduce the failure probabilities of the quantified HFE.

Table 6. Dependency/Independency Assumptions Regarding Operator Actions

LBE	First Operator Action	Second Operator Action	Assumption
HTS-AL	OA-A-X63-2	OA-C-CR3-X8-A	Independent
	OA-A-X66-2	OA-C-CR3-X8-A	Independent
	OA-A-X57-1	OA-C-CR3-X8-A	Dependent
	OA-A-X60-1	OA-C-CR3-X8-A	Dependent
	OA-A-X63-1	OA-C-CR3-X8-A	Dependent
	OA-A-X66-1	OA-C-CR3-X8-A	Dependent
	OA-A-X57-2	OA-C-CR3-X8-A	Dependent
	OA-A-X60-2	OA-C-CR3-X8-A	Dependent
PC-AU	OA-A-X151-1	OA-A-X84-MT	Independent
	OA-A-X151-1	OA-C-A7	Independent
	OA-A-X84-MT	OA-C-A7	Dependent
RS-AP	OA-A-X151-1	OA-A-X79-MT	Independent
	OA-A-X151-1	OA-A-X78-MT	Independent
	OA-A-X151-1	OA-C-CR3-X8-A	Dependent
	OA-A-X151-1	OA-A-X81-MT	Dependent
MS-CG	OA-A-X151-1	OA-C-MOIST-DETECT-1	Dependent
	OA-A-X242-1	OA-C-MOIST-DETECT-1	Dependent
	OA-A-X240-1	OA-C-MOIST-DETECT-1	Dependent

- Step 8 → The assumptions made regarding the independence/dependence between different operator actions are listed in Table 6. Listed in Table 6 also is the LBE that identified these specific combinations. It should be noted that these combinations do not only impact these specific LBEs; however, their impacts are model-wide. Hence, any modification performed on any operator action may result in significant changes in other LBEs.

- Step 9 → The status of each PIF impacting the assumed CFMs is analyzed. Figure 84 to Figure 86 illustrate the assumptions made for each PIF; similar to the previous step, this is for demonstration purposes only and does not reflect the status of PIFs within the actual PRA sequence.
- Step 10 → Using the previous assumptions, Bayesian networks for the HFEs are built, as seen in the example networks in Figure 84 to Figure 86.

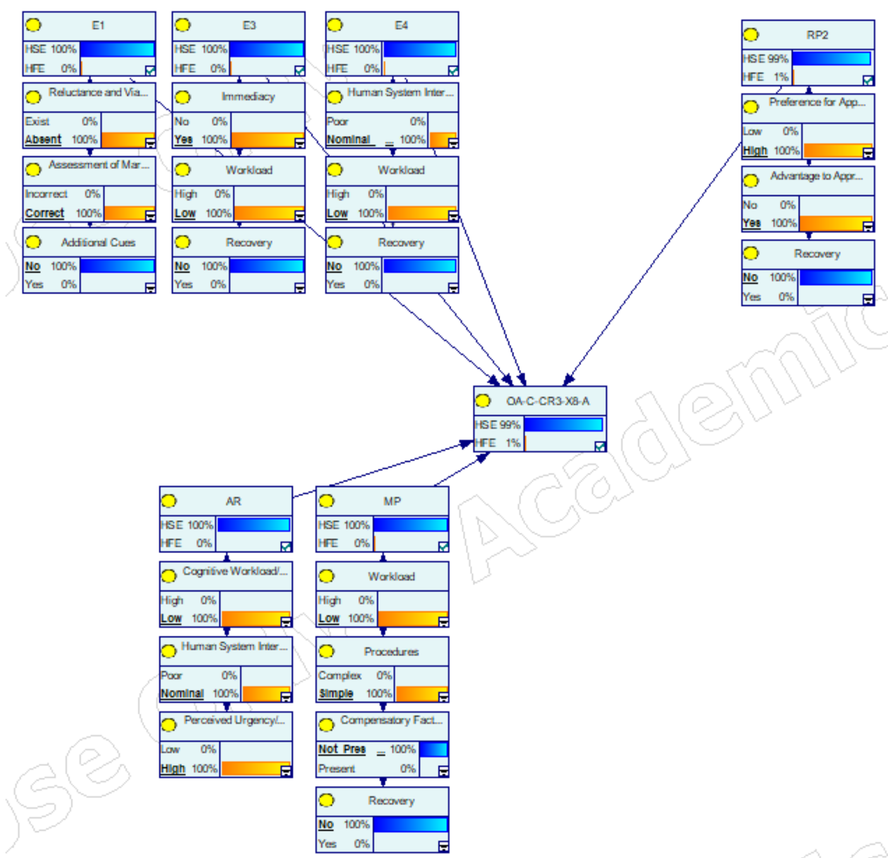

Figure 84. Independent Bayesian Network for OA-C-CR3-X8-A

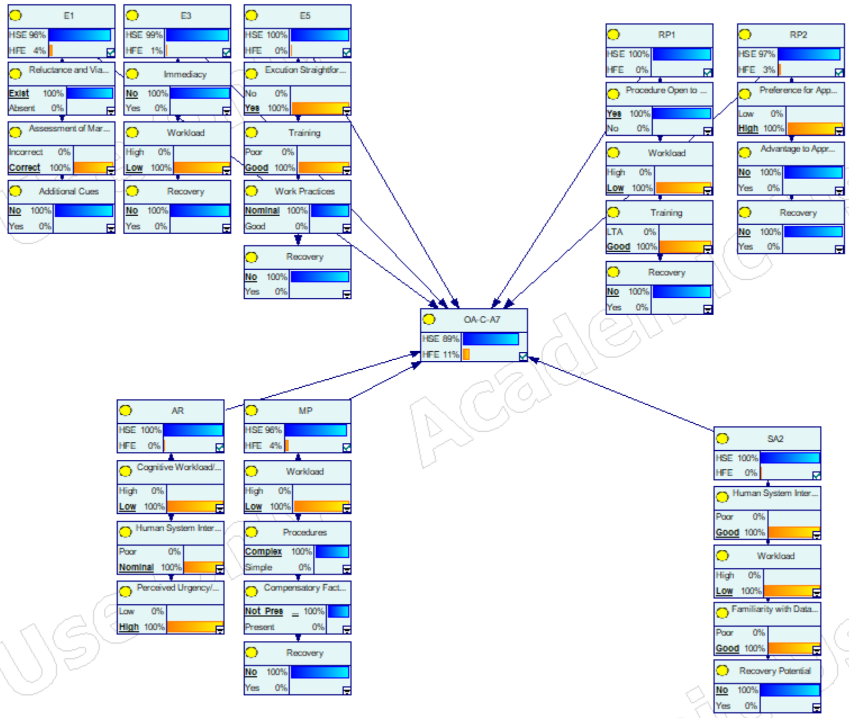

Figure 85. Independent Bayesian Network for OA-C-A7

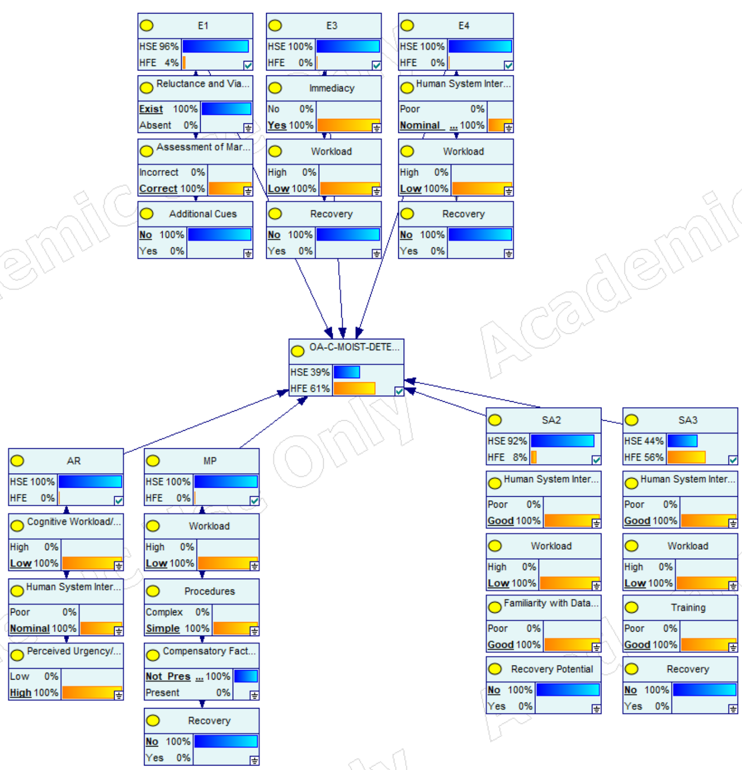

Figure 86. Independent Bayesian Network for OA-C-MOIST-DETECT-1

- Step 11 → In this step, the pre-initiator HFEs are not decomposed but are used as basic events. The Bayesian networks are then modified to include the dependency links with the assumed CFMs of the post-initiator HFE.
- Steps 12 and 13 → in this step, the failure of the pre-initiator HFE is assumed to result in an increase in the workload/stress level from low to high. The conditional probability tables are modified, and the Bayesian networks are quantified, as seen in the example networks given in Figure 87 to Figure 89. It should be noted that, for OA-A-X81-MT-HF, it was assumed that this would be performed outside of the main control room; hence, the IDHEAS-ECA software is used to quantify its dependent and independent fault tree basic events. The list of assumptions used to quantify this operator action are listed in Appendix E.

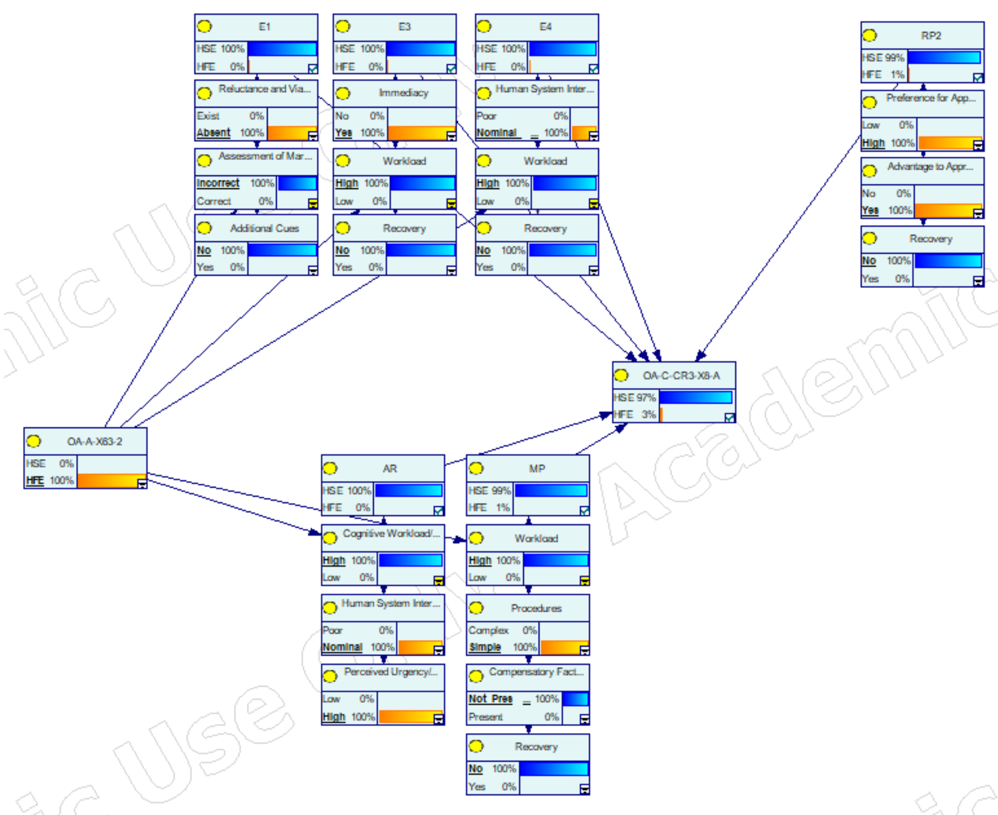

Figure 87. Dependent Bayesian Network for OA-C-CR3-X8-A

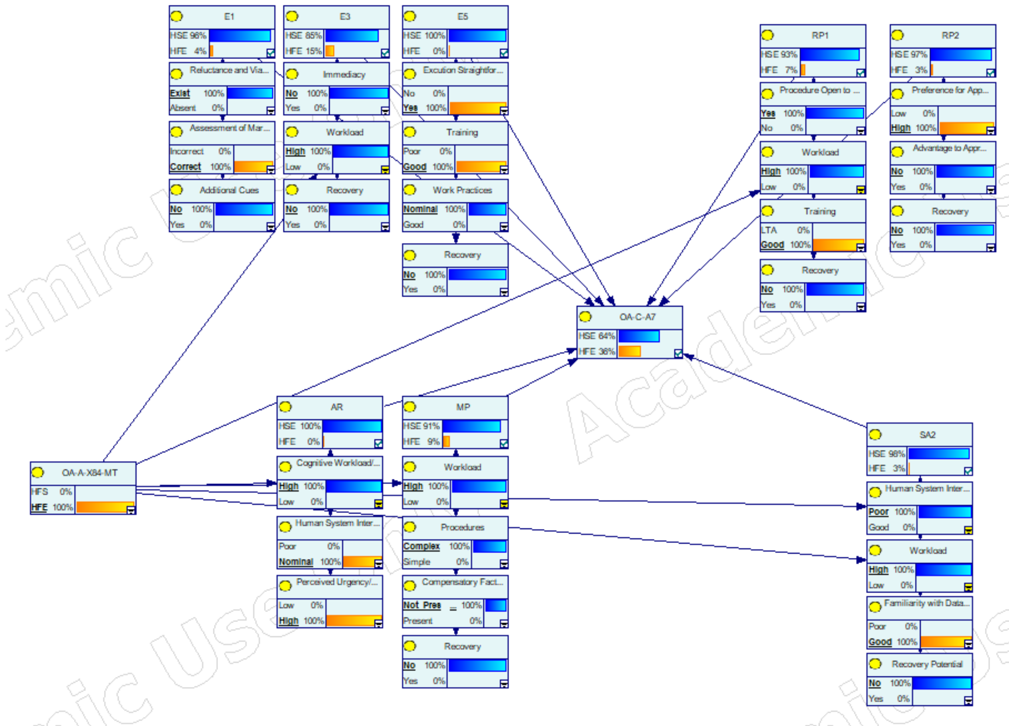

Figure 88. Dependent Bayesian Network for OA-C-A7

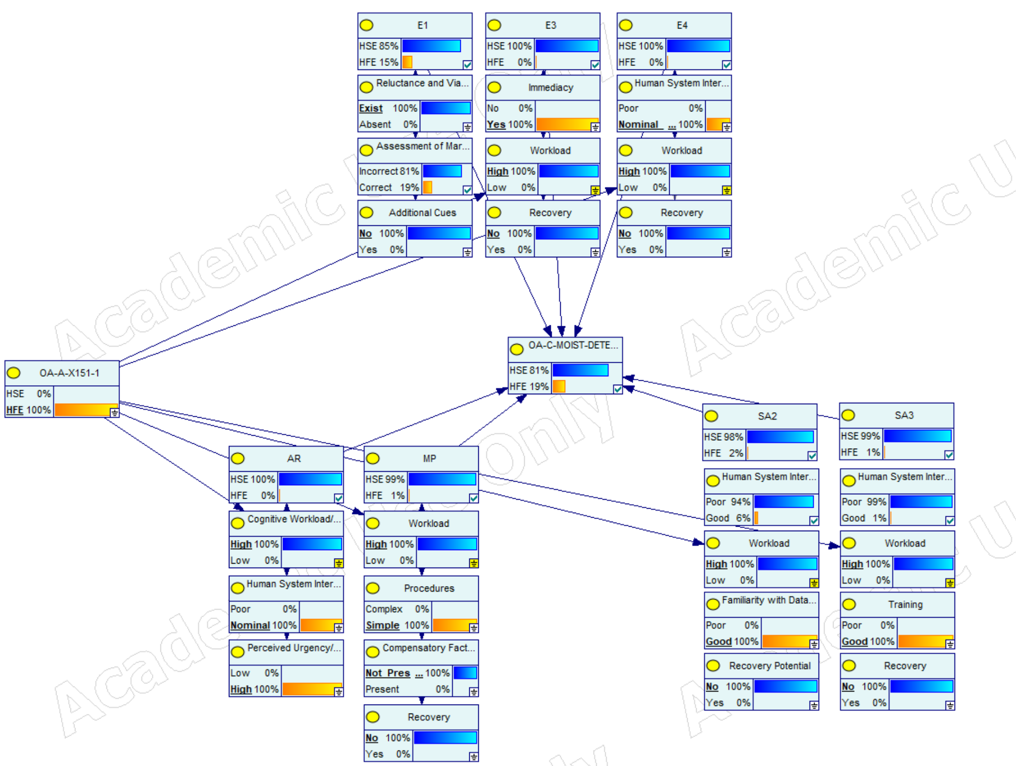

Figure 89. Dependent Bayesian Network for OA-C-MOIST-DETECT-1

- Step 14 → The human fault trees, presented in Figure 90 to Figure 93, are built and added to the PRA model for the MHTGR. The failure probabilities, both independent and dependent, of the CFMs, which are quantified in Steps 10 and 13, respectively, are used as the failure probabilities of the basic events within the human fault trees.

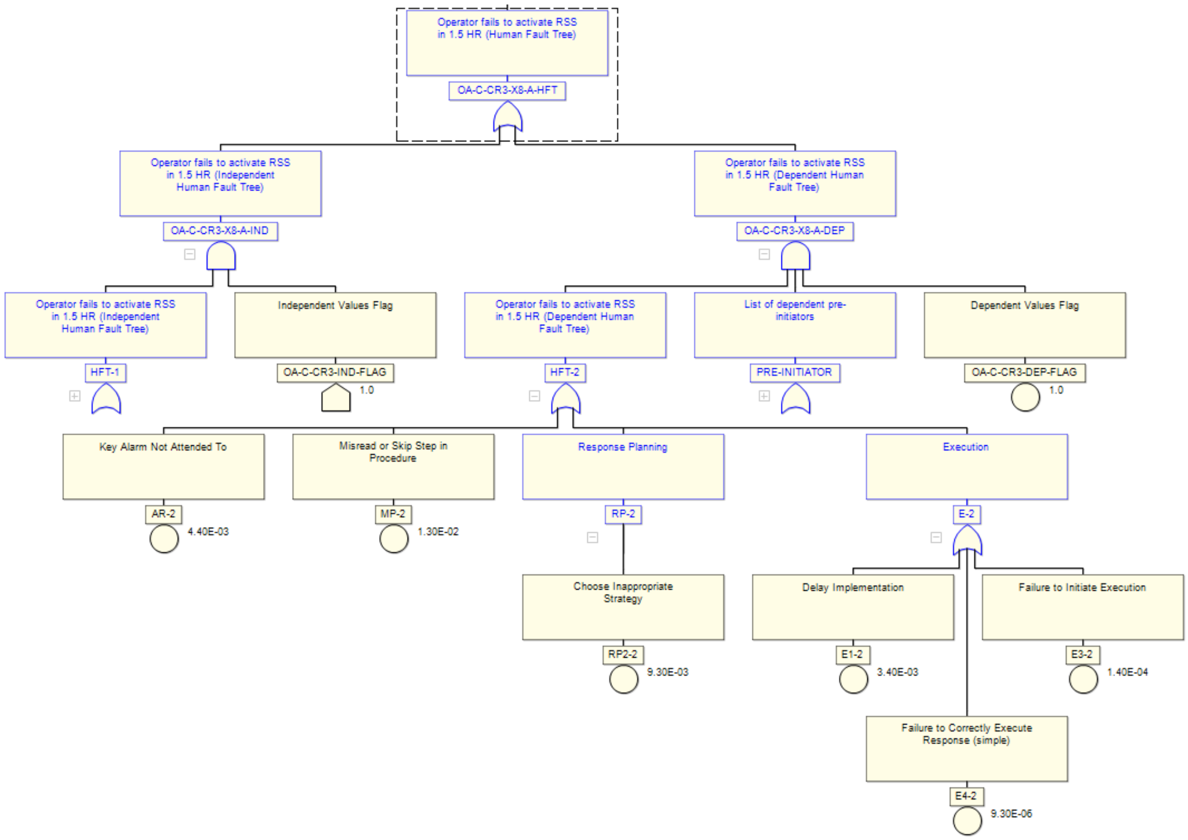

Figure 90. Human Fault Tree for OA-C-CR3-X8-A

- Step 15 → both independent and dependent HFTs are linked as described in 4.3.15 and as can be seen in Figure 90 to Figure 93. Flags are introduced to the HFT to differentiate between independent and dependent values for the failure probability. The ESQ model is quantified where the linked HFT is used. Both flags in the linked HFT are listed as mutually exclusive events, so any illogical cut sets are removed. It should be noted that, for this demonstration purposes, it was assumed that any pre-initiator HFE would have the same impact on the post-initiators, and all pre-initiators are listed within a separate gate, as seen in Figure 90 and Figure 92.

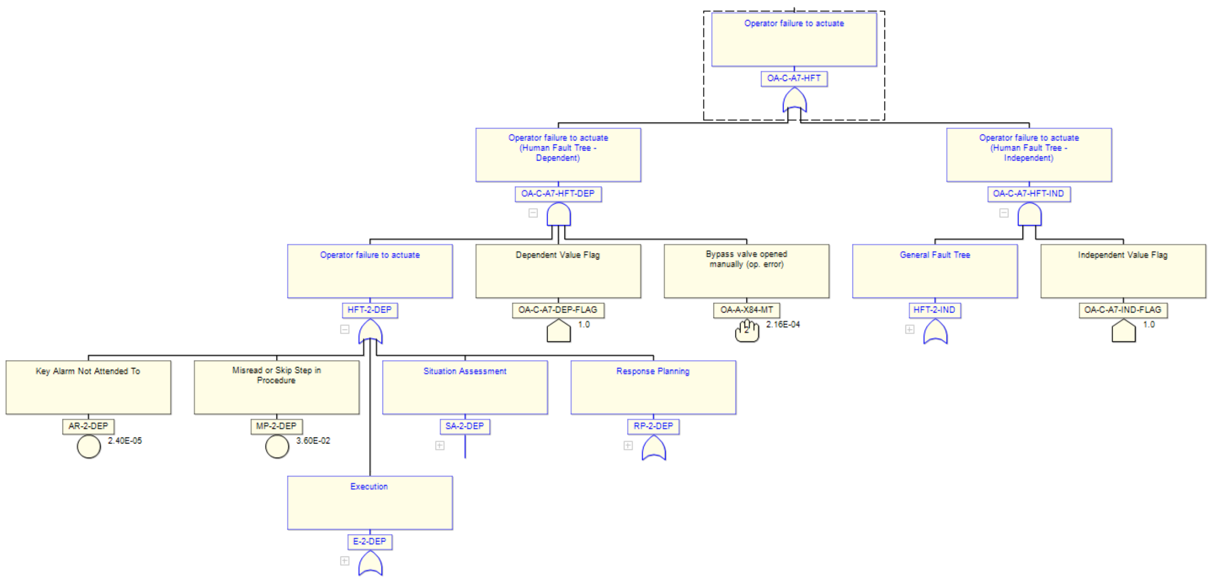

Figure 91. Human Fault Tree for OA-C-A7

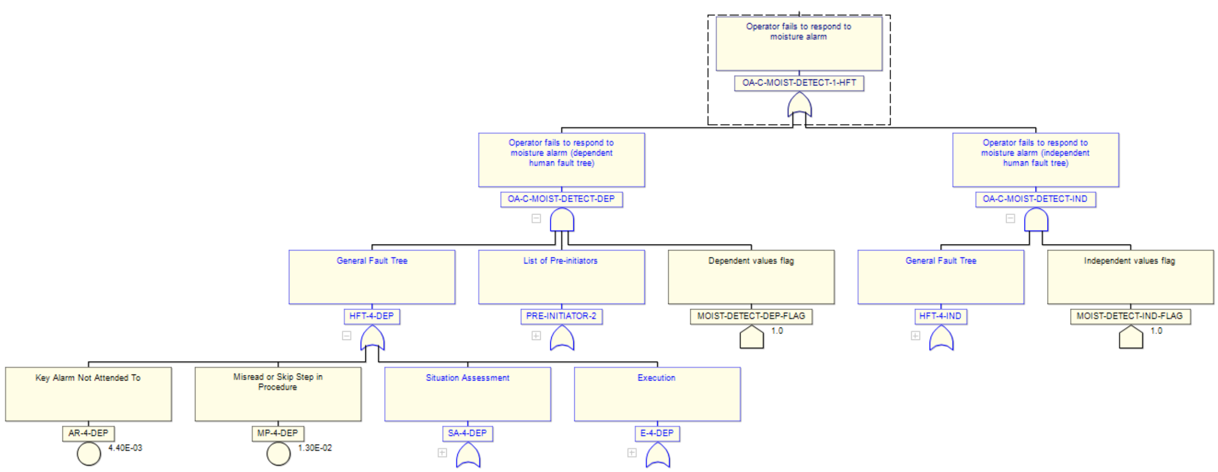

Figure 92. Human Fault Tree for OA-C-MOIST-DETECT-1

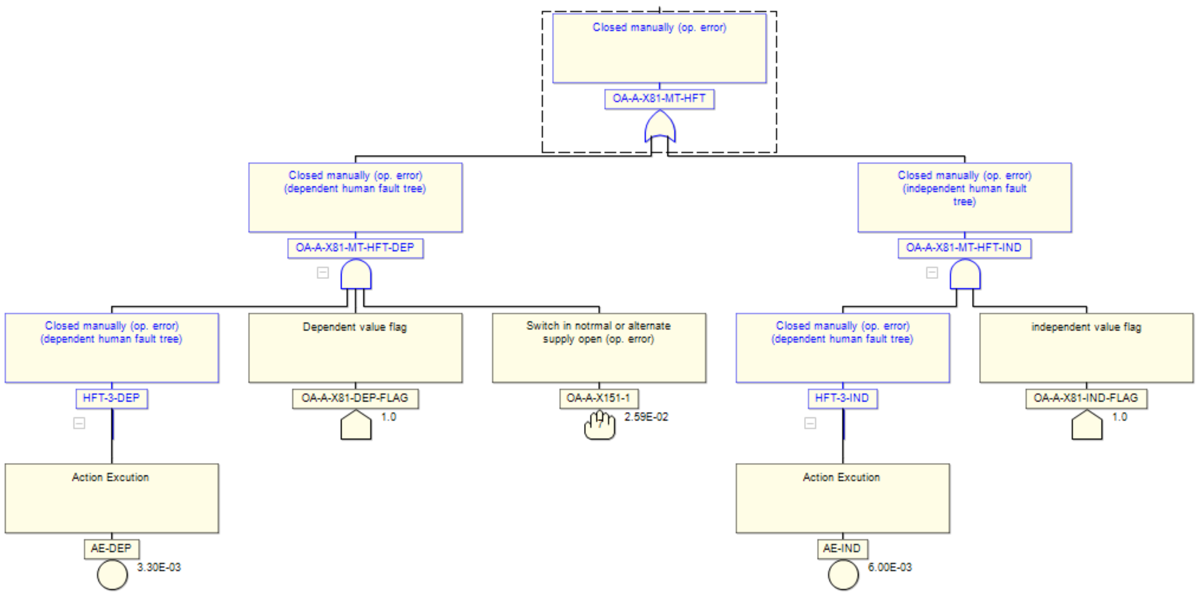

Figure 93. Human Fault Tree for OA-A-X81-MT-HF

5.1.3. Multi-module Considerations

As discussed in section 4.5, to incorporate multi-module implication into the PRA model, a simple approach to that employed by the MHTGR cannot be used. To showcase how a high-fidelity multi-module PRA model should be developed to adequately incorporate the dependencies within a shared control room, examples of how the MHTGR event trees should be modified are illustrated in Figure 94 and Figure 95.

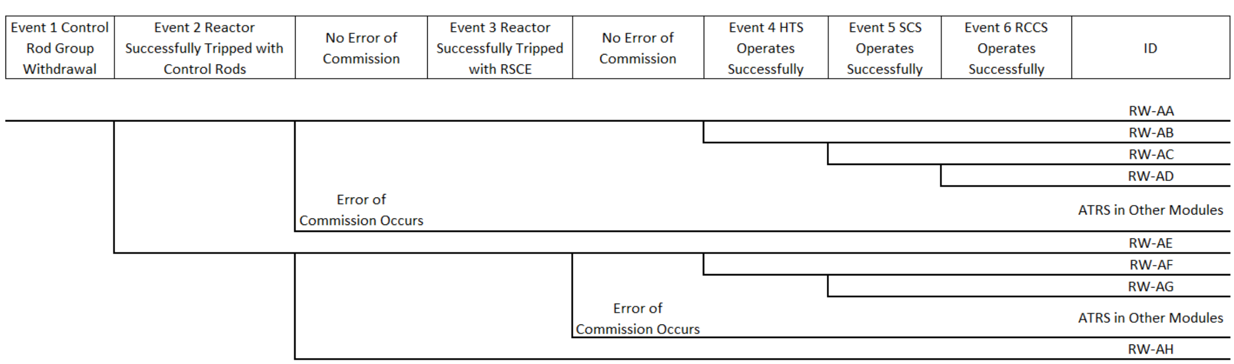

Figure 94. Modified Control Rod Group Withdrawal Initiating Event

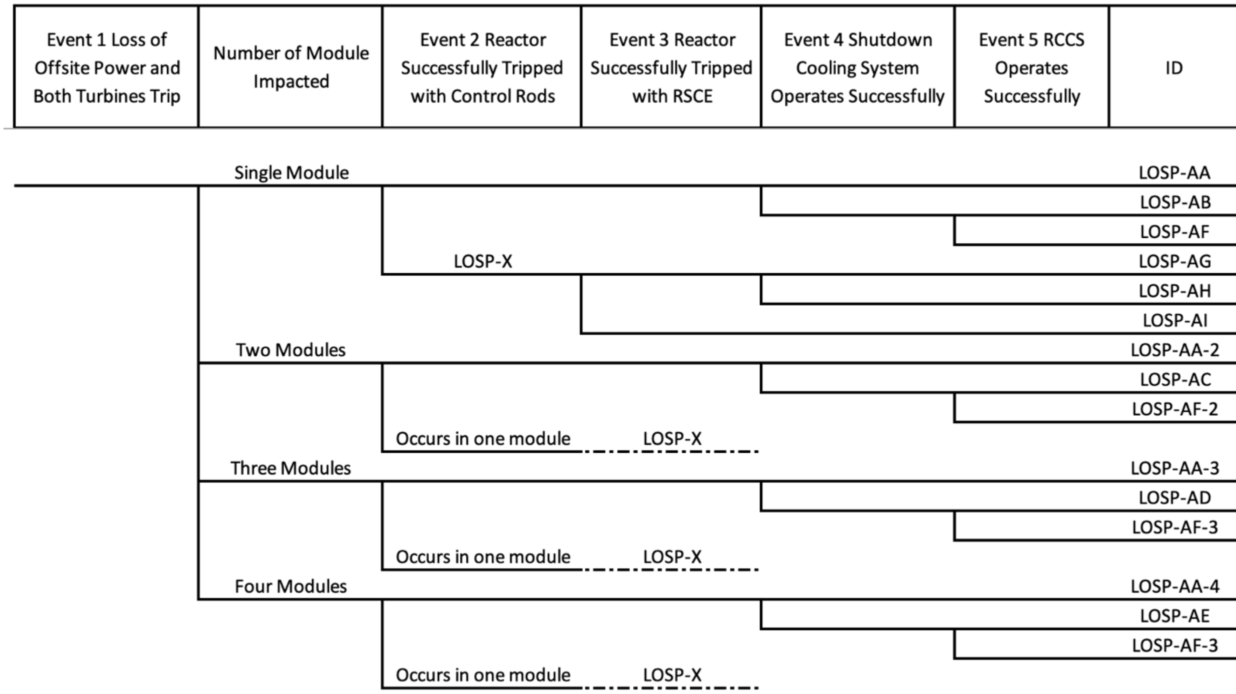

Figure 95. Modified Loss of Offsite Power and Both Turbines Trip Initiating Event

It should be noted that Figure 94 tries to capture the impact of errors of commissions following single-module initiating events. In contrast, Figure 95 attempts to explicitly capture the different types of the same operator action, for example, tripping a single module vs. four modules. By reordering the top events, Figure 73 vs Figure 95, any operator actions associated with successfully running the shutdown cooling system can be explicitly modeled. The dependency between failing to manually actuate the shutdown cooling system associated with LBE LOSP-AB, LOSP-AC, LOSP-AD, and LOSP-AE can be explicitly incorporated in the model along with any additional operator actions needed to realistically model the multi-module response.

5.1.4.Results and Limitations

The results of the framework implementation are listed in Table 7 for all the initiating events within the scope of this study, i.e., internal events. It should be noted that the baseline results represent the initial LBE frequencies quantified using the MHTGR model as listed in [80]-[82]. The results of Run 0 represent the LBE frequencies, assuming the failure of all operator actions, which allows the identification of LBEs that are sensitive to operator actions. On the other hand, the results of Run 1 represent the LBE frequencies assuming complete dependence between all operator actions within a cut set, i.e., crediting only one operator action per cut set. Finally, Run 2 represents the LBE frequencies after expanding the human failure basic events into linked human fault trees that explicitly model dependencies.

Starting from 115 different operator actions implemented in the MHTGR PRA model, the proposed framework reduced the number of operator actions to be assessed to only 18 pairs. This significant reduction in analysis load, as can be computed in equation (17) from the percentage of OA combinations explicitly modeled, can result in a significant speed-up in the dependency analysis while maintaining a high fidelity level and traceability of the work, assumptions, and connections performed.

$$Explicit\ Analysis\ Coverage = \frac{(18) * 100}{115C2} = \frac{(18) * 100}{6555} = 0.27\% \qquad (17)$$

It should be noted that Run 2 represents the end of a single iteration of the framework; as indicated in Figure 16, steps 4 onwards should be repeated until no changes in LBE categorization are observed. Moreover, some LBE frequencies increase to the extent that, despite not changing any categorizations, the mean frequency becomes close to the categorization limit that the 95th percentile may exceed categorization. These LBEs, flagged using asterisks in Table 7, are candidates to showcase the uncertainty treatment presented in section 4.6.2. However, due to the limited uncertainty parameter information available for the MHTGR, only the mean value of the LBE frequencies is quantified. However, an example of the uncertainty treatment will be presented for the G-PWR model in section 5.2.

Moreover, Run 1's result for some LBEs is higher than that of their Run 0 counterparts despite the fact that Run 0 fails all operator actions, whereas Run 1 credits one operator action. This discrepancy stems from the modeling decision of only failing post-initiator operator actions in Run 0, whereas Run 1 assumes complete dependency between all pre- and post-initiator operator actions. This discrepancy will be eliminated by only listing post-initiators within the DepHep input files.

Table 7. Implementation Results for the Modular High-Temperature Gas-Cooled Reactor

Initiating Event	**LBE**	**Baseline**	**Run 0**	**Run 1**	**Run 2**
Control Rod Group Withdrawal	RW-AA	1.00E-01	1.00E-01	-	1.00E-01
	RW-AB	6.66E-03	7.06E-03	-	6.66E-03
	RW-AC	3.88E-04	4.11E-04	-	3.88E-04
	RW-AD	< 1.0E-10	< 1.0E-10	-	< 1.0E-10
	RW-AE	1.09E-08	1.08E-05	1.09E-08	1.79E-07
	RW-AF	< 1.0E-10	7.20E-07	1.84E-08	3.23E-09
	RW-AG	< 1.0E-10	1.72E-08	-	< 1.0E-10
	RW-AH	1.65E-09	4.67E-06	2.87E-07*	2.61E-08
Primary Coolant Leak	PC-AA	1.79E-01	1.79E-01	-	1.79E-01
	PC-AB	4.73E-02	5.23E-02	-	4.92E-02
	PC-AC	1.17E-02	1.25E-02	-	1.17E-02
	PC-AD	3.75E-03	3.96E-03	-	3.75E-03
	PC-AE	6.83E-04	7.24E-04	1.09E-08	6.83E-04
	PC-AF	1.99E-04	6.98E-04	1.84E-08	3.69E-04
	PC-AG	< 1.0E-10	< 1.0E-10	-	< 1.0E-10
	PC-AH	1.96E-08	1.94E-05	1.96E-08	3.23E-07
	PC-AI	5.06E-09	6.17E-06	5.13E-07	8.04E-08
	PC-AJ	< 1.0E-10	1.30E-06	3.30E-08	6.45E-09
	PC-AK	< 1.0E-10	3.14E-07	1.97E-09	2.40E-10
	PC-AL	< 1.0E-10	3.24E-08	-	< 1.0E-10
	PC-AM	< 1.0E-10	3.38E-08	-	< 1.0E-10
	PC-AN	< 1.0E-10	< 1.0E-10	-	< 1.0E-10
	PC-AO	3.14E-09	8.38E-06	5.15E-07	4.76E-08
	PC-AP	4.16E-02	4.16E-02	-	4.16E-02
	PC-AQ	1.17E-02	1.30E-02	-	1.22E-02
	PC-AR	2.76E-03	2.94E-03	-	2.76E-03
	PC-AS	8.70E-04	9.21E-04	-	8.70E-04
	PC-AT	1.55E-04	1.64E-04	-	1.55E-04
	PC-AU	4.36E-05	1.59E-04	1.60E-03	8.22E-05

Table 7. Implementation Results for the Modular High-Temperature Gas-Cooled Reactor

Initiating Event	**LBE**	**Baseline**	**Run 0**	**Run 1**	**Run 2**
	PC-AV	< 1.0E-10	< 1.0E-10	-	< 1.0E-10
	PC-AW	4.53E-09	4.49E-06	4.53E-09	7.33E-08
	PC-AX	8.06E-10	1.43E-06	1.19E-07*	1.37E-08
	PC-AY	< 1.0E-10	2.84E-07	2.17E-09	< 1.0E-10
	PC-AZ	< 1.0E-10	4.57E-08	4.10E-10	< 1.0E-10
	PC-BA	< 1.0E-10	4.89E-09	-	< 1.0E-10
	PC-BB	6.86E-10	1.94E-06	1.19E-07	7.68E-09
	PC-BC	2.86E-02	2.86E-02	-	2.86E-02
	PC-BD	8.06E-03	9.01E-03	-	8.42E-03
	PC-BE	1.90E-03	2.03E-03	-	1.90E-03
	PC-BF	5.98E-04	6.33E-04	-	5.98E-04
	PC-BG	1.06E-04	1.12E-04	-	1.06E-04
	PC-BH	2.93E-05	1.09E-04	1.07E-03	5.57E-05
	PC-BI	< 1.0E-10	< 1.0E-10	-	< 1.0E-10
	PC-BJ	3.12E-09	3.09E-06	3.12E-09	4.97E-08
	PC-BK	4.80E-10	9.81E-07	8.18E-08	7.89E-09
	PC-BL	< 1.0E-10	1.93E-07	1.49E-09	< 1.0E-10
	PC-BM	< 1.0E-10	2.78E-08	2.70E-10	< 1.0E-10
	PC-BN	< 1.0E-10	3.37E-09	-	< 1.0E-10
	PC-BO	4.72E-10	1.34E-06	8.21E-08	5.04E-09
	PC-BP	7.80E-03	7.80E-03	-	7.80E-03
	PC-BQ	5.36E-04	5.70E-04	-	5.36E-04
	PC-BR	2.88E-05	3.05E-05	-	2.88E-05
	PC-BS	< 1.0E-10	< 1.0E-10	-	< 1.0E-10
	PC-BT	7.80E-10	8.42E-07	8.50E-10	1.22E-08
	PC-BU	< 1.0E-10	3.89E-08	2.98E-10	< 1.0E-10
	PC-BV	< 1.0E-10	1.67E-10	-	< 1.0E-10
	PC-BW	< 1.0E-10	3.64E-07	2.24E-08	1.20E-09
	PC-BX	2.60E-03	2.60E-03	-	2.60E-03
Loss of HTS Cooling	HTS-AA	9.68E-01	9.78E-01	-	9.68E-01
	HTS-AB	7.13E-01	7.50E-01	-	7.13E-01
	HTS-AC	7.25E-02	7.82E-02	-	7.25E-02
	HTS-AD	1.52E-02	1.66E-02	-	1.52E-02
	HTS-AE	8.58E-03	9.41E-03	-	8.58E-03
	HTS-AF	6.86E-02	7.52E-02	-	6.86E-02
	HTS-AG	1.98E-07	2.09E-07	-	1.98E-07
	HTS-AH	3.68E-09	3.68E-09	-	3.68E-09
	HTS-AI	2.00E-08	8.17E-08	-	4.22E-08
	HTS-AJ	8.59E-10	9.51E-09	-	2.33E-09
	HTS-AK	2.59E-07	3.24E-04	3.96E-04	4.21E-06

Table 7. Implementation Results for the Modular High-Temperature Gas-Cooled Reactor

Initiating Event	**LBE**	**Baseline**	**Run 0**	**Run 1**	**Run 2**
	HTS-AL	2.22E-09	7.10E-06	6.33E-05	8.05E-08
	HTS-AM	< 1.0E-10	< 1.0E-10	-	< 1.0E-10
	HTS-AN	3.66E-08	1.30E-04	6.65E-05	5.57E-07
Loss of Offsite Power and Both Turbine Trip	LOSP-AA	3.91E-03	3.91E-03	-	3.91E-03
	LOSP-AB	1.86E-04	1.86E-04	-	1.86E-04
	LOSP-AC	6.36E-06	< 1.0E-10	-	6.36E-06
	LOSP-AD	7.38E-06	3.72E-07	-	7.38E-06
	LOSP-AE	1.14E-04	1.77E-08	-	1.14E-04
	LOSP-AF	< 1.0E-10	1.61E-07	1.87E-10	< 1.0E-10
	LOSP-AG	3.45E-10	6.36E-06	3.76E-10	4.59E-09
	LOSP-AH	< 1.0E-10	7.39E-06	9.87E-09	1.16E-10
	LOSP-AI	< 1.0E-10	1.14E-04	9.10E-09	5.29E-10
Anticipated Transient Requiring Scram	RS-AA	1.62E+01	1.62E+01	-	1.62E+01
	RS-AB	2.43E+00	2.43E+00	-	2.43E+00
	RS-AC	8.08E+00	8.08E+00	-	8.08E+00
	RS-AD	1.32E+00	1.40E+00	-	1.33E+00
	RS-AE	4.98E-01	5.28E-01	-	4.98E-01
	RS-AF	6.52E-02	6.90E-02	-	6.53E-02
	RS-AG	1.14E-02	1.21E-02	-	1.14E-02
	RS-AH	5.82E-03	6.17E-03	-	5.82E-03
	RS-AI	4.47E-02	4.74E-02	-	4.47E-02
	RS-AJ	1.05E-07	1.10E-07	-	1.05E-07
	RS-AK	4.93E-10	4.93E-10	-	4.93E-10
	RS-AL	7.49E-09	9.11E-08	-	1.57E-08
	RS-AM	< 1.0E-10	6.40E-09	-	< 1.0E-10
	RS-AN	1.77E-06	1.75E-03	1.77E-06	2.92E-05
	RS-AO	1.05E-07	1.27E-04	1.37E-05	1.50E-06
	RS-AP	7.76E-10	6.42E-06	1.58E-03	6.56E-08
	RS-AQ	< 1.0E-10	< 1.0E-10	-	< 1.0E-10
	RS-AR	3.00E-07	7.56E-04	4.65E-05	4.95E-06
	RS-AS	5.08E-08	7.49E-04	4.65E-05	8.35E-07
Small Steam Generator Tube Leak	SS-AA	4.00E-01	4.00E-01	-	4.00E-01
	SS-AB	2.15E-02	2.15E-02	-	2.15E-02
	SS-AC	1.95E-08	1.95E-08	-	1.95E-08
	SS-AD	3.59E-05	3.59E-05	-	3.59E-05
	SS-AE	1.89E-06	1.89E-06	-	1.89E-06
	SS-AF	7.13E-08	7.13E-08	-	7.13E-08
	SS-AG	< 1.0E-10	< 1.0E-10	-	< 1.0E-10
	SS-AH	< 1.0E-10	< 1.0E-10	-	< 1.0E-10
	SS-AI	3.48E-04	3.48E-04	-	3.48E-04

Table 7. Implementation Results for the Modular High-Temperature Gas-Cooled Reactor

Initiating Event	LBE	Baseline	Run 0	Run 1	Run 2
	SS-AJ	1.86E-05	1.86E-05	-	1.86E-05
	SS-AK	< 1.0E-10	< 1.0E-10	-	< 1.0E-10
	SS-AL	7.11E-06	7.11E-06	-	7.11E-06
	SS-AM	3.57E-07	3.57E-07	-	3.57E-07
	SS-AN	< 1.0E-10	< 1.0E-10	-	< 1.0E-10
	SS-AO	1.42E-07	1.42E-07	-	1.42E-07
	SS-AP	3.12E-08	3.12E-08	-	3.12E-08
	SS-AQ	8.76E-10	8.76E-10	-	8.76E-10
	SS-AR	5.16E-10	5.16E-10	-	5.16E-10
	SS-AS	3.03E-05	3.03E-05	-	3.03E-05
	SS-AT	5.15E-05	5.15E-05	-	5.15E-05
	SS-AU	2.69E-06	2.69E-06	-	2.69E-06
	SS-AV	< 1.0E-10	< 1.0E-10	-	< 1.0E-10
	SS-AW	4.61E-09	4.61E-09	-	4.61E-09
	SS-AX	3.03E-05	3.03E-05	-	3.03E-05
	SS-AY	4.53E-08	4.53E-08	-	4.53E-08
	SS-AZ	1.12E-09	1.12E-09	-	1.12E-09
	SS-BA	< 1.0E-10	< 1.0E-10	-	< 1.0E-10
	SS-BB	< 1.0E-10	< 1.0E-10	-	< 1.0E-10
	SS-BC	3.03E-05	3.03E-05	-	3.03E-05
	SS-BD	4.36E-05	4.36E-05	-	4.36E-05
	SS-BE	2.30E-06	2.30E-06	-	2.30E-06
	SS-BF	< 1.0E-10	< 1.0E-10	-	< 1.0E-10
	SS-BG	3.91E-09	3.91E-09	-	3.91E-09
	SS-BH	3.26E-09	3.26E-09	-	3.26E-09
	SS-BI	< 1.0E-10	< 1.0E-10	-	< 1.0E-10
	SS-BJ	1.03E-04	1.03E-04	-	1.03E-04
	SS-BK	5.40E-06	5.40E-06	-	5.40E-06
	SS-BL	< 1.0E-10	< 1.0E-10	-	< 1.0E-10
	SS-BM	9.23E-09	9.23E-09	-	9.23E-09
	SS-BN	< 1.0E-10	< 1.0E-10	-	< 1.0E-10
	SS-BO	7.49E-09	7.49E-09	-	7.49E-09
	SS-BP	1.44E-04	1.44E-04	-	1.44E-04
	SS-BQ	7.74E-06	7.75E-06	-	7.74E-06
	SS-BR	1.29E-08	1.29E-08	-	1.29E-08
	SS-BS	4.00E-04	3.96E-01	4.00E-04	2.00E-02
	SS-BT	6.07E-06	4.42E-03	6.07E-06	2.28E-04
Moderate Steam Generator Tube Leak	MS-AA	4.00E-02	4.00E-02	-	4.00E-02
	MS-AB	2.15E-03	2.15E-03	-	2.15E-03
	MS-AC	8.61E-06	8.61E-06	-	8.61E-06

Table 7. Implementation Results for the Modular High-Temperature Gas-Cooled Reactor

Initiating Event	**LBE**	**Baseline**	**Run 0**	**Run 1**	**Run 2**
	MS-AD	2.05E-07	2.05E-07	-	2.05E-07
	MS-AE	1.39E-09	1.39E-09	-	1.39E-09
	MS-AF	3.59E-06	3.59E-06	-	3.59E-06
	MS-AG	1.82E-07	1.82E-07	-	1.82E-07
	MS-AH	6.14E-09	6.14E-09	-	6.14E-09
	MS-AI	< 1.0E-10	< 1.0E-10	-	< 1.0E-10
	MS-AJ	< 1.0E-10	< 1.0E-10	-	< 1.0E-10
	MS-AK	3.48E-05	3.48E-07	-	3.48E-05
	MS-AL	1.38E-06	1.36E-08	-	1.38E-06
	MS-AM	3.13E-10	< 1.0E-10	-	3.13E-10
	MS-AN	1.80E-06	1.59E-08	-	1.80E-06
	MS-AO	6.41E-08	< 1.0E-10	-	6.41E-08
	MS-AP	< 1.0E-10	< 1.0E-10	-	< 1.0E-10
	MS-AQ	7.10E-07	7.03E-09	-	7.10E-07
	MS-AR	2.78E-08	< 1.0E-10	-	2.78E-08
	MS-AS	3.31E-08	< 1.0E-10	-	3.31E-08
	MS-AT	1.41E-08	< 1.0E-10	-	1.41E-08
	MS-AU	3.03E-06	3.01E-08	-	3.03E-06
	MS-AV	< 1.0E-10	< 1.0E-10	-	3.85E-08
	MS-AW	4.64E-06	4.64E-06	-	4.64E-06
	MS-AX	1.83E-07	1.83E-07	-	1.83E-07
	MS-AY	< 1.0E-10	< 1.0E-10	-	< 1.0E-10
	MS-AZ	2.34E-07	2.34E-07	-	2.34E-07
	MS-BA	7.01E-09	7.01E-09	-	7.01E-09
	MS-BB	< 1.0E-10	< 1.0E-10	-	< 1.0E-10
	MS-BC	2.73E-06	2.73E-06	-	2.73E-06
	MS-BD	5.15E-07	5.15E-07	-	5.15E-07
	MS-BE	2.04E-08	2.04E-08	-	2.04E-08
	MS-BF	2.44E-08	2.44E-08	-	2.44E-08
	MS-BG	3.03E-07	3.03E-07	-	3.03E-07
	MS-BH	8.15E-08	8.15E-08	-	8.15E-08
	MS-BI	4.11E-09	< 1.0E-10	-	4.11E-09
	MS-BJ	< 1.0E-10	< 1.0E-10	-	< 1.0E-10
	MS-BK	< 1.0E-10	< 1.0E-10	-	< 1.0E-10
	MS-BL	< 1.0E-10	< 1.0E-10	-	< 1.0E-10
	MS-BM	< 1.0E-10	< 1.0E-10	-	< 1.0E-10
	MS-BN	< 1.0E-10	< 1.0E-10	-	< 1.0E-10
	MS-BO	3.03E-06	3.01E-08	-	3.03E-06
	MS-BP	< 1.0E-10	< 1.0E-10	-	3.01E-09
	MS-BQ	< 1.0E-10	< 1.0E-10	-	< 1.0E-10

Table 7. Implementation Results for the Modular High-Temperature Gas-Cooled Reactor

Initiating Event	LBE	Baseline	Run 0	Run 1	Run 2
	MS-BR	< 1.0E-10	< 1.0E-10	-	< 1.0E-10
	MS-BS	< 1.0E-10	< 1.0E-10	-	< 1.0E-10
	MS-BT	< 1.0E-10	< 1.0E-10	-	< 1.0E-10
	MS-BU	4.36E-06	4.36E-06	-	4.36E-06
	MS-BV	6.47E-05	3.96E-02	6.47E-05	1.83E-03
	MS-BW	2.56E-06	1.55E-03	2.56E-06	7.30E-05
	MS-BX	6.04E-10	4.41E-07	7.19E-10	2.01E-08
	MS-BY	3.38E-06	2.13E-03	1.07E-03	2.58E-04
	MS-BZ	1.24E-07	8.55E-05	4.22E-05	1.01E-05
	MS-CA	< 1.0E-10	2.14E-08	-	2.37E-09
	MS-CB	< 1.0E-10	1.37E-09	-	1.51E-10
	MS-CC	3.23E-05	1.98E-02	3.23E-05	9.19E-04
	MS-CD	1.28E-06	7.81E-04	1.28E-06	3.65E-05
	MS-CE	2.22E-10	2.20E-07	3.60E-10	9.85E-09
	MS-CF	1.67E-06	1.08E-03	5.33E-04	1.29E-04
	MS-CG	5.93E-08	4.26E-05	2.11E-05	5.01E-06
	MS-CH	< 1.0E-10	1.07E-08	-	9.73E-10
	MS-CI	< 1.0E-10	6.86E-10	-	< 1.0E-10
	MS-CJ	4.74E-09	3.00E-06	4.90E-09	1.53E-07
	MS-CK	7.22E-07	4.42E-04	7.22E-07	2.29E-05

5.2.Generic PWR PRA Model

The generic pressurized water reactor (G-PWR) PRA model was developed by INL to have a generic model that can be publicly used external to INL. The model does not represent any existing nuclear power plant; however, it was developed to support research and training purposes, including event trees, fault trees, and basic events needed to create a SAPHIRE risk model [91]. The Systems Analysis Programs for Hands-on Integrated Reliability Evaluations (SAPHIRE) tool has been developed and maintained by INL for the U.S. NRC. The primary approach to solving PRA models employed by SAPHIRE is the classical method of Boolean manipulation, generating minimal cut sets, quantifying top event probabilities, computing importance measures, and performing uncertainty quantification [92].

5.2.1.G-PWR Model Description

The G-PWR model is developed as a public data repository; three distinct types of data are used: event trees, fault trees, and basic events. The event trees incorporated in the G-PWR model represent a wide range of high-level sequences typical of PWRs. Event trees include different variations of seismic, flooding, internal fire, hurricane, tornado, loss of coolant accident, loss of component cooling water, loss of DC bus, loss of main feedwater, loss of offsite power, steam line breaks, and steam generator tube rupture event tress. Whenever possible, publicly available documents are used and referenced in building each part of the PRA model.

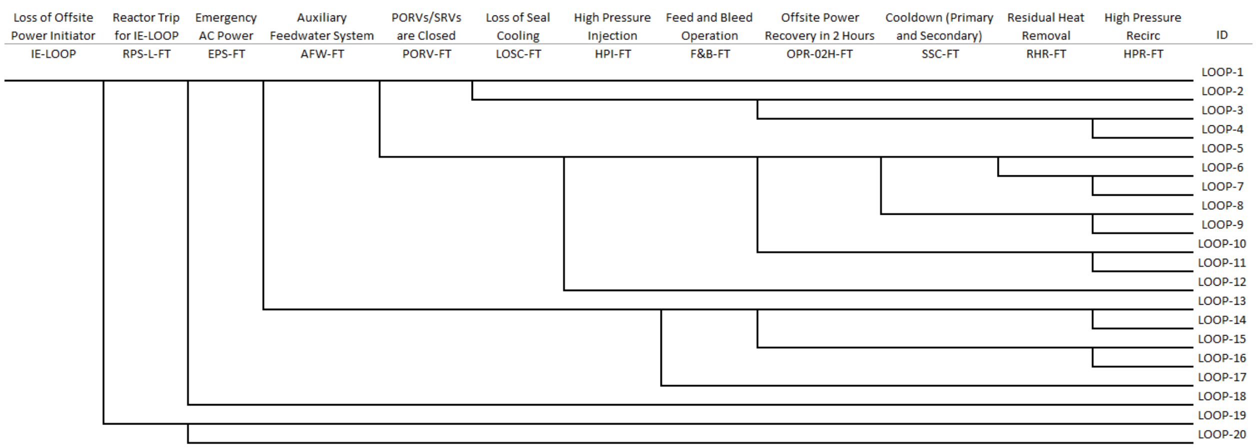

Figure 96. Generic PWR Loss of Offsite Power Event Tree

The G-PWR PRA model for a generic loss of offsite power is reproduced in CAFTA to demonstrate the proposed framework. The loss of offsite power event tree was chosen to represent a sitewide initiating event that could impact all units within a specific complex. The G-PWR event tree, however, only treated the event progression in terms of a single unit without expanding the scope to multiple units. The model includes one type of operator error basic event that reflects the post-initiator HFEs. It should be noted that, in reproducing the G-PWR model, the following modifications were made to the model:

- The flags of other initiating events, like seismic or flooding, are removed from the model to reduce the scope of a single hazard internal event.
- For each top event, only applicable failures following a loss of offsite power are included. In other words, if a flag indicates that a failure mode (fault sub-tree) is associated with other initiating events, this failure mode is not included in the CAFTA model.
- The averaged loss of offsite power initiating event frequency is used [93] instead of one of its subcategories.

5.2.2.Framework Implementation

After building the PRA model for the G-PWR in CAFTA, the ESQ model is quantified to produce the baseline model for the framework implementation. The results of the baseline quantification, along with all following quantifications, are presented in Table 8. The framework starts by using the baseline quantification and conducts the following modifications:

- Step 1 → the failure probability of all post-initiator HFE basic events is modified from its original value to 9.9E-01. The modified ESQ model is then quantified to produce the first run of the framework, Run 0 in Table 8.
- Step 2 → the updated LBE frequencies are compared against their baseline values to identify the LBEs most impacted by HFEs. As can be seen in Figure 97, LOOP-1, LOOP-5, LOOP-13, and LOOP-18 are insensitive to the changes in HFE probabilities, where the remaining LBEs see an increase in their frequency. The frequency of multiple LBEs increases from the uncategorized rare events to the BDBE region, making them good candidates for the next step in the analysis.
- Step 3 → the cut sets associated with LOOP-6, LOOP-7, LOOP-8, LOOP-9, LOOP-11, LOOP-14, LOOP-16, and LOOP-17 are investigated to identify different HFE

combinations using DepHep. The list of HFEs used in the G-PWR model, listed in Appendix F, is used in this step, along with the cut set files and the database of the PRA model.

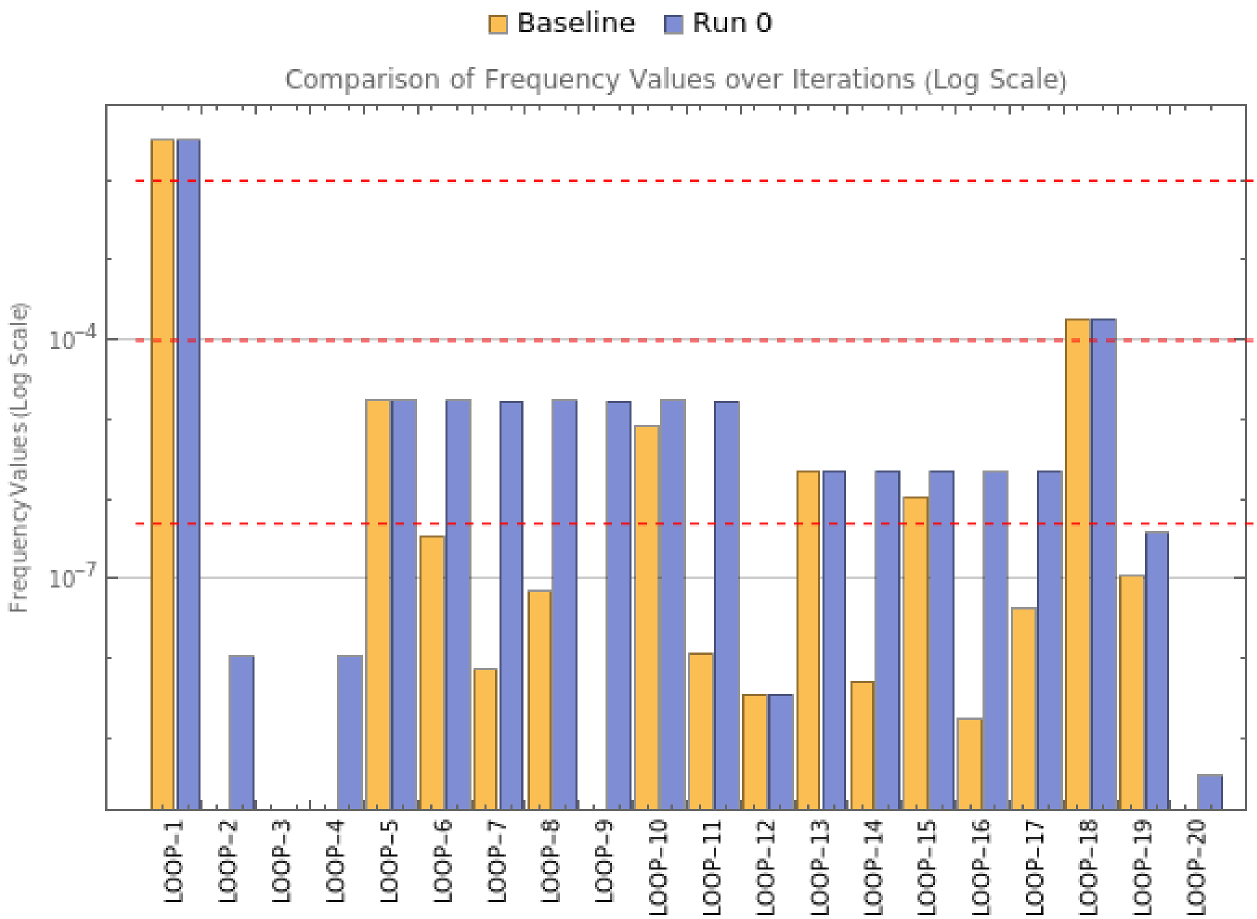

Figure 97. LOOP End State Frequency Comparison

- Step 4 → in this step, only one HFE within the LBE cut sets is set to its baseline failure probabilities. The remaining HFEs within a specific cut set are all set to 1.0E+00, i.e., guaranteed to fail. DepHep4 is used in this step to automate the process. The result of assuming complete dependency between all HFEs can be seen in the change of the LBE frequency in Run 1 in Table 8.

As shown in Table 8, the results of Run 1 showcase that, after assuming complete dependency between multiple HFEs within the same cut set, no significant changes are observed in the frequency of the associated LBEs. This insensitivity stems from the simplicity of the G-PWR model, which incorporates mainly one operator action per cut set.

5.2.3.Multi-Unit Considerations

As discussed in section 1.1, to incorporate multi-module implications into the PRA model, a simplified PRA model approach is used to capture the frequency impact of shared actions. To showcase how a simplified model should be quantified to adequately incorporate the shared operator action, the guidelines presented in section 1.1 are implemented, quantified, and listed in section 5.2.4. To conduct the analysis, it was assumed that operators failing to initiate and control RHR is a shared multi-unit action. However, it should be noted that this assumption is only for demonstration purposes and has no basis. As can be seen in Table 10, some LBE frequencies see a significant increase (around 50%) after implementing the guidelines, whereas others see a significant decrease (around 110%). This is due to the change from crediting four independent operator action failures to only crediting a single operator action.

5.2.4.Results and Limitations

The results of the framework implementation are listed in Table 8 for the averaged loss of offsite power initiating event of the G-PWR model. It should be noted that the baseline results represent the initial LBE frequencies quantified using the G-PWR model as listed in [91]. The results of Run 0 represent the LBE frequencies, assuming the failure of all operator actions, which allows the identification of LBEs that are sensitive to operator actions. On the other hand, the results of Run 1 represent the LBE frequencies assuming complete dependence between all operator actions within a cut set, i.e., crediting only one operator action per cut set. As can be seen, no LBE experiences a categorization shift after the assumption of complete dependency. This finalizes the analysis and showcases that no further detailed analysis is needed to incorporate dependencies.

Starting from 22 different operator actions implemented in the G-PWR PRA model, the proposed framework eliminated the need to conduct detailed dependency analysis on any pair. This elimination stems from the fact that no risk insights are expected following the completion of any detailed analysis. This significant reduction in analysis load, as can be computed in equation (18) by the number of OA combinations model, can result in a considerable speed up in the modeling while showcasing that no risk-significant dependencies are unanalyzed.

$$Explicit\ Model\ Coverage = \frac{(0) * 100}{22C2} = 0\% \tag{18}$$

It should be noted that some LBE frequencies increase to the extent that, despite not changing any categorizations, the mean frequency becomes close to the categorization limit that the 95th percentile may exceed categorization. This LBE, flagged using asterisks in Table 8, is a candidate to showcase the uncertainty treatment presented in section 4.6.2. By quantifying the different percentiles for this LBE, it can be seen that the 95th percentile exceeds the uncategorized rare events region in the BDBE region. Hence, as discussed in section 4.6.2, this LBE is considered within the scope of the following analysis in Run 2. However, no operator action combinations were identified in Run 2, which can be identified by comparing the results of Run 1 to that of the baseline. However, for this demonstration, this LBE is used to showcase how to treat uncertainty within the LBE frequencies.

Despite not having HFE combinations to analyze, this case study showcased what to expect from the final iteration of the proposed framework, where further detailed analysis would not yield any additional insights. It also demonstrated the framework's approach to accounting for the uncertainties associated with LBE frequencies.

Table 8. Implementation Results for the Generic Pressurized Water Reactor

Initiating Event	LBE	Baseline	Run 0	Run 1	Run 2
Loss of Offsite Power	LOOP-1	3.11E-02	3.11E-02	-	
	LOOP-2	< 1.00E-10	1.05E-08	-	
	LOOP-3	< 1.00E-10	< 1.00E-10	-	
	LOOP-4	< 1.00E-10	1.04E-08	-	
	LOOP-5	1.71E-05	1.71E-05	-	
	LOOP-6	3.42E-07	1.69E-05	3.43E-07*	-
	LOOP-7	7.10E-09	1.68E-05	3.35E-08	-
	LOOP-8	6.85E-08	1.69E-05	6.85E-08	-
	LOOP-9	< 1.00E-10	1.68E-05	1.75E-08	-
	LOOP-10	8.05E-06	1.69E-05	-	
	LOOP-11	1.14E-08	1.68E-05	2.55E-08	-
	LOOP-12	3.55E-09	3.55E-09	-	
	LOOP-13	2.23E-06	2.23E-06	-	
	LOOP-14	5.18E-09	2.21E-06	4.26E-08	-
	LOOP-15	1.04E-06	2.21E-06	-	
	LOOP-16	1.70E-09	2.19E-06	3.62E-08	-
	LOOP-17	4.20E-08	2.21E-06	7.79E-08	-
	LOOP-18	1.80E-04	1.80E-04	-	
	LOOP-19	1.06E-07	3.71E-07	-	
	LOOP-20	< 1.00E-10	3.38E-10	-	

Table 9. Uncertainty Analysis for LOOP-6 Run 1 Results

LBE	Parameter	Estimate	Confidence Range
LOOP-6	Point Estimate	3.424E-07	
	Mean	3.538E-07	[3.4E-07, 3.6E-07]
	5th Percentile	1.301E-07	[1.1E-07, 1.4E-07]
	Median	3.210E-07	[3.1E-07, 3.3E-07]
	95th Percentile	6.750E-07	[6.5E-07, 7.1E-07]

Table 10. Multi-unit Frequency Adjustment

Initiating Event	ID	Baseline (1 unit)	Failed MU OA	Success MU OA	Event Sequence Frequency (4 units)	Relative Percentage Frequency Change
Loss of Offsite Power	LOOP-1	3.11E-02	3.11E-02	3.11E-02	1.24E-01	
	LOOP-2	0.00E+00	1.10E-09	3.50E-10	2.15E-09	
	LOOP-3	0.00E+00	0.00E+00	0.00E+00	0.00E+00	
	LOOP-4	0.00E+00	1.10E-09	0.00E+00	1.10E-09	

Table 10. Multi-unit Frequency Adjustment

Initiating Event	ID	Baseline (1 unit)	Failed MU OA	Success MU OA	Event Sequence Frequency (4 units)	Relative Percentage Frequency Change
	LOOP-5	1.71E-05	1.71E-05	1.71E-05	6.84E-05	
	LOOP-6	3.42E-07	3.43E-07	3.43E-07	1.37E-06	
	LOOP-7	7.10E-09	1.54E-08	1.54E-08	6.16E-08	-117%
	LOOP-8	6.85E-08	6.85E-08	6.85E-08	2.74E-07	
	LOOP-9	0.00E+00	1.38E-10	1.38E-10	5.52E-10	
	LOOP-10	8.05E-06	1.71E-05	0.00E+00	1.71E-05	47%
	LOOP-11	1.14E-08	3.47E-08	0.00E+00	3.47E-08	24%
	LOOP-12	3.55E-09	7.16E-09	7.16E-09	2.86E-08	-102%
	LOOP-13	2.23E-06	2.24E-06	2.24E-06	8.96E-06	
	LOOP-14	5.18E-09	1.30E-08	1.25E-08	5.05E-08	-144%
	LOOP-15	1.04E-06	2.24E-06	0.00E+00	2.24E-06	46%
	LOOP-16	1.70E-09	1.30E-08	0.00E+00	1.30E-08	-91%
	LOOP-17	4.20E-08	4.95E-08	4.95E-08	1.98E-07	-18%
	LOOP-18	1.80E-04	1.80E-04	1.80E-04	7.21E-04	
	LOOP-19	1.06E-07	1.07E-07	1.07E-07	4.28E-07	-1%
	LOOP-20	0.00E+00	6.23E-10	6.23E-10	2.49E-09	

CHAPTER 6. CONCLUSIONS AND FUTURE WORK

6.1.Research Summary

Current human reliability analysis (HRA) methodologies face significant limitations in incorporating dependency between different operator actions. Generally, current methods fall into one of two categories. Multi-point continuum methodologies, like THERP, oversimplify dependencies by assuming each Human Failure Event (HFE) depends only on the preceding one. In contrast, Linked Bayesian Network methodologies rely heavily on expert elicitation, leading to potential biases. Both approaches often treat human failures as basic events, obscuring specific dependencies and improvements. Future advanced reactor designs introduce new challenges like shared control rooms and remote supervision.

The proposed framework for HFE dependency analysis integrates inputs from the Probabilistic Risk Assessment (PRA) model and follows a detailed 15-step process. It begins by setting all human error probabilities (HEP) to a high value to highlight the impact of HFEs within the PRA model. Key HFEs are identified by examining sequences with significant frequency changes and isolating sequences with multiple HFEs. Complete dependency is assumed among these multiple HFEs by setting subsequent HEPs to unity. Key HFE combinations significantly affecting LBE frequencies are then determined, while non-critical combinations are screened. This process involves developing crew response diagrams (CRD) and identifying critical tasks that are broken down into cognitive failure modes (CFM) and performance-influencing factors (PIFs).

Subsequent steps involve constructing Bayesian networks for each critical task, identifying dependency links, and modifying these networks to reflect the impacts of dependencies. This culminates in quantifying failure probabilities for CFMs and building human fault trees (HFT) for HFE combinations. The final step links these HFTs within the PRA model, accurately modeling conditional probabilities and dependencies. The framework aims to enhance the precision of HRA by providing a systematic approach to identify and quantify the dependencies among HFEs, critical tasks, and CFMs, thereby improving the overall reliability and risk assessment of complex systems. In multi-unit or multi-module sites, initiating events can affect either a single unit/module or multiple units/modules simultaneously. Single-unit events impact only one unit, while site-wide events affect all units. Current reactors often have separate control rooms but may share support systems, creating dependencies that need to be identified for accurate risk assessment. Building a multi-unit PRA model can involve modifying a single-unit model to reflect multi-unit risks or creating an explicit multi-unit model capturing all units' responses. For multi-module sites, advanced reactors may share systems and crews, necessitating a high-fidelity PRA model to accurately model operator action dependencies across modules. Simplified models are inadequate due to the complexity of these interdependencies, highlighting the need for detailed analysis to ensure precise risk assessment.

6.2. Future Work

The IDHEAS-ECA and IDHEAS At-power methodologies differ in their approach to failure probability quantification, with IDHEAS-ECA using expert-elicited adjustment factors rather than decision trees. This reintroduces uncertainties akin to those in conditional failure probability elicitation. Despite this, the proposed framework addresses these uncertainties by providing a pathway to incorporate decision trees. Therefore, while current uncertainties exist due to reliance on IDHEAS-ECA factors, the framework offers a straightforward method for future resolution. Future efforts may construct the decision trees associated with IDHEAS-ECA, which will allow for the construction of Bayesian networks similar to those used for IDHEAS At-power within the scope of this study.

The proposed framework does not address uncertainties related to the time and feasibility of operator actions, relying instead on the HRA model's feasibility analysis to determine whether actions can be realistically executed. This assessment happens during the HRA's Identification and Definition phase, screening out unfeasible actions early, with detailed analysis occurring as more information becomes available. IDHEAS At-Power and IDHEAS-ECA estimate time and time uncertainty for HFEs, but this study focused only on cognitive failures, leaving time uncertainty impacts dependencies between actions unaddressed. Hence, a critical recommendation for future improvement includes systematically evaluating the impact of time constraints on the dependency between different operator actions. Another open research topic is the impact of digital instrumentation and control (I&C) on the performance of varying operator actions. Failures of I&C, in general, present a direct path of failure of all operator actions that rely upon it. Such an improvement would open the door for realistic human performance simulation in codes like IDAC. Finally, errors of commission, which can significantly affect operator actions and plant states, are not explicitly modeled or assessed in the proposed framework. These errors, particularly relevant in multi-module PRA models, introduce significant uncertainty by potentially transforming single-module events into more complex multi-module events. As per the advanced non-light-water PRA standard, incorporating errors of commission within the PRA model constitutes multiple supporting requirements throughout different PRA elements. Hence, explicitly and systematically assessing error of commission to error of commission or error of omission to error of commission dependencies is a critical area of further research and improvement.

To finalize, this study presents a step towards adequate and complete representation of the impact of human errors throughout the PRA model. Future efforts should continue on the path set forward in this study, leading to a safe, economical, and reliable energy source.

CHAPTER 7. REFERENCES

[1] Reactor safety study. An assessment of accident risks in U. S. commercial nuclear power plants. Executive summary: main report. [PWR and BWR]. United States: N. p., 1975. Web. doi:10.2172/7134131.

[2] Swain, A. D. Human factors in design of reliable systems. United States: N. p., 1964. Web. doi:10.2172/4070176.

[3] Swain, A D. A method for performing a human-factors reliability analysis. United States: N. p., 1963. Web.

[4] Swain, A D. Human reliability assessment in nuclear reactor plants. United States: N. p., 1969. Web.

[5] Kyriakidis, M., Majumdar, A., & Ochieng, W. Y. (2018). The human performance railway operational index—A novel approach to assess human performance for railway operations. Reliability Engineering & System Safety, 170, 226–243. https://doi.org/10.1016/j.ress.2017.10.012

[6] Loh, T. Y., Brito, M. P., Bose, N., Xu, J., & Tenekedjiev, K. (2020). Human Error in Autonomous Underwater Vehicle Deployment: A System Dynamics Approach. Risk Analysis, 40(6), 1258–1278. https://doi.org/10.1111/risa.13467

[7] Selvik, J. T., & Bellamy, L. J. (2020). Addressing human error when collecting failure cause information in the oil and gas industry: A review of ISO 14224:2016. Reliability Engineering & System Safety, 194, 106418. https://doi.org/10.1016/j.ress.2019.03.025

[8] Lin, Q.-L., Wang, D.-J., Lin, W.-G., & Liu, H.-C. (2014). Human reliability assessment for medical devices based on failure mode and effects analysis and fuzzy linguistic theory. Safety Science, 62, 248–256. https://doi.org/10.1016/j.ssci.2013.08.022

[9] Bell, Julie, and Justin Holroyd. "Review of human reliability assessment methods." Health & Safety Laboratory 78 (2009).

[10] American Society of Mechanical Engineers. (2008). Standard for level 1/large early release frequency probabilistic risk assessment for nuclear power plant applications. American Society for Mechanical Engineers.

[11] American Society of Mechanical Engineers, & American Nuclear Society. (2021). Probabilistic risk assessment standard for advanced non-light water reactor nuclear power plants. ASME, American Society of Mechanical Engineers.

[12] NUREG-1792 "Good Practices for Implementing Human Reliability Analysis" (Final). (2005). 110.

[13] U.S. Nuclear Regulatory Commission. Office of Nuclear Regulatory Research. (2007). Regulatory Guide 1.200 an approach for determining the technical adequacy of probabilistic risk assessment results for risk-informed activities. [Washington, D.C.]: U.S. Nuclear Regulatory Commission, Office of Nuclear Regulatory Research

[14] NUREG-1842 "Evaluation of Human Reliability Analysis Methods Against Good Practices, Final Report." (2006). 288.

[15] Swain, A. D., & Guttmann, H. E. (1983). Handbook of human-reliability analysis with emphasis on nuclear power plant applications. Final report (NUREG/CR-1278, SAND-80-0200, 5752058; p. NUREG/CR-1278, SAND-80-0200, 5752058). https://doi.org/10.2172/5752058

[16] Swain, A. D. (1987). Accident Sequence Evaluation Program: Human reliability analysis procedure (NUREG/CR-4772; SAND-86-1996). Sandia National Labs.,

Albuquerque, NM (USA); Nuclear Regulatory Commission, Washington, DC (USA). Office of Nuclear Regulatory Research. https://doi.org/10.2172/6370593

[17] Gertman et al., "The SPAR-H human reliability analysis method, NUREG/CR-6883," Idaho National Laboratory, pre-pared for U. S. Nuclear Regulatory Commission Office of Nuclear Regulatory Research Washington, DC 205555-0001.

[18] NuScale Power, LLC Submittal of 'NuScale Control Room Staffing Plan,' TR-0420-69456, Revision 0.

[19] Beck, C. K., Cowan, F. P., & et. al. (1957). Theoretical Possibilities and Consequences of Major Accidents in Large Nuclear Power Plants (WASH-740, 4344308; p. WASH-740, 4344308). Brookhaven National Laboratory. https://doi.org/10.2172/4344308

[20] "Anticipated Transients Without Scram for Water-Cooled Power Reactors," WASH1270, U.S. Atomic Energy Commission (1973).

[21] "Anticipated Transients Without Scram for Light-Water Reactors," NUREG0460, vols. 1–3, U.S. Nuclear Regulatory Commission (1978).

[22] Kaplan, S., & Garrick, B. J. (1981). On The Quantitative Definition of Risk. Risk Analysis, 1(1), 11–27. https://doi.org/10.1111/j.1539-6924.1981.tb01350.x

[23] Probabilistic Risk Assessment (PRA). (n.d.). NRC Web. Retrieved August 23, 2022, from https://www.nrc.gov/about-nrc/regulatory/risk-informed/pra.html

[24] Lee, J. C., & McCormick, N. J. (2012). Risk and Safety Analysis of Nuclear Systems. John Wiley & Sons.

[25] Three Mile Island: A report to the commissioners and to the public. Volume I (NUREG/CR-1250(Vol.1)). (1979). Nuclear Regulatory Commission, Washington, DC (United States). Three Mile Island Special Inquiry Group. https://doi.org/10.2172/5395798

[26] PRA Implementation Plan (1994 to 1999). NRC Web. Retrieved July 29, 2022, from https://www.nrc.gov/about-nrc/regulatory/risk-informed/history/1994-1999.html

[27] Travers, W. D. (2000). Risk-Informed Regulation Implementation Plan. 6

[28] Reyes, L. A. (2007). Implementation And Update of The Risk-Informed and Performance-Based Plan. 26.

[29] International Nuclear Safety Advisory Group. (1992). Probabilistic Safety Assessment. INTERNATIONAL ATOMIC ENERGY AGENCY. https://www.iaea.org/publications/3789/probabilistic-safety-assessment

[30] Moe, W.L. (2019). NEI 18-04 Risk-Informed Performance-Based Technology Inclusive Guidance for Advanced Reactor Licensing Basis Development (INL/EXT-19-55375-Rev000). Idaho National Lab. (INL), Idaho Falls, ID (United States). https://doi.org/10.2172/1557649.

[31] Moe, W., & Afzali, A. (2020). Modernization of Technical Requirements for Licensing of Advanced Non-Light Water Reactors: Probabilistic Risk Assessment Approach (INL/EXT--20-60395, SC--29980-101-Rev.01, 1700670; p. INL/EXT--20-60395, SC--29980-101-Rev.01, 1700670). https://doi.org/10.2172/1700670.

[32] Reckley, W. (2020). Guidance for a Technology-inclusive, Risk-informed, and Performance-based Methodology to Inform the Licensing Basis and Content of Applications for Licenses, Certifications, and Approvals for Non-Light-Water Reactors (Guidance ML20091L698; p. 31). U.S. Nuclear Regulatory Commission. https://www.nrc.gov/docs/ML2009/ML20091L698.pdf

[33] Reactor safety study. An assessment of accident risks in U. S. commercial nuclear power plants. Appendix III and IV. United States: N. p., 1975. Web. https://www.nrc.gov/docs/ML0706/ML070610293.pdf.

[34] Implications of the accident at Chernobyl for safety regulation of commercial nuclear power plants in the United States: Volume 1, Main report: Final report. United States: N. p., 1989. Web. doi:10.2172/6300378.

[35] Internationale Atomenergie-Organisation (2015). The Fukushima Daiichi accident. International Atomic Energy Agency.

[36] R. Boring and D. Gertman, "Atomistic and holistic approaches to human reliability analysis in the US nuclear power industry:" Safety and Reliability, vol. 25, pp. 21–37, Jun. 2005, doi: 10.1080/09617353.2005.11690802.

[37] Hamza, M., & Diaconeasa, M. A. (2023). Investigating the applicability of human reliability analysis methods during early design stages of non-light-water nuclear power plants. Progress in Nuclear Energy, 161, 104716. https://doi.org/10.1016/j.pnucene.2023.104716

[38] Ekanem, N. J. (2013). A Model-Based Human Reliability Analysis Methodology (Phoenix Method) [PhD]. http://drum.lib.umd.edu/handle/1903/14831

[39] Mosleh, S-H. Shen, D. L. Kelly, J. H. Oxstrand, and K. M. Groth, "A Model-Based Human Reliability Analysis Methodology," in Proc. 2012 Probabilistic Safety Assessment and Management (PSAM 11) Int. Conf., Helsinki, Finland, 2012.

[40] Wakefield, D.J., Parry, G.W., Hannaman, G.W., & Spurgin, A.J. (1990). SHARP1: A revised systematic human action reliability procedure, Report Summary.

[41] Wakefield, D.J., Parry, G.W., Hannaman, G.W., & Spurgin, A.J. (1993). SHARP1: A revised systematic human action reliability procedure, Main Report.

[42] Čepin, M. (2008). Importance of human contribution within the human reliability analysis (IJS-HRA). *Journal of Loss Prevention in the Process Industries*, *21*(3), 268–276. https://doi.org/10.1016/j.jlp.2007.04.012

[43] Čepin, M. (2007). Comparison of Methods for Dependency Determination between Human Failure Events within Human Reliability Analysis. Proceedings of the International Conference Nuclear Energy for New Europe, Portorož, Slovenia, Sept. 10-13, 2007.

[44] Čepin, M. (2008). DEPEND-HRA—A method for consideration of dependency in human reliability analysis. *Reliability Engineering & System Safety*, *93*(10), 1452–1460. https://doi.org/10.1016/j.ress.2007.10.004

[45] Su, X., Mahadevan, S., Xu, P., & Deng, Y. (2015). Dependence Assessment in Human Reliability Analysis Using Evidence Theory and AHP. Risk Analysis, 35(7), 1296–1316. https://doi.org/10.1111/risa.12347

[46] Zio E, Baraldi P, Librizzi M, Podofillini L, Dang V. A fuzzy set-based approach for modeling dependence among human errors. Fuzzy Sets and Systems, 2009; 160:1947–1964.

[47] Podofillini L, Dang V, Zio E, Baraldi P, Librizzi M. Using expert models in human reliability analysis—A dependence assessment method based on fuzzy logic. Risk Analysis, 2010;30:1277–1297.

[48] Abrishami, S., Khakzad, N., Hosseini, S. M., & van Gelder, P. (2020). BN-SLIM: A Bayesian Network methodology for human reliability assessment based on Success

Likelihood Index Method (SLIM). Reliability Engineering & System Safety, 193, 106647. https://doi.org/10.1016/j.ress.2019.106647

[49] Liu, J., Zou, Y., Wang, W., Zio, E., Yuan, C., Wang, T., & Jiang, J. (2022). A Bayesian belief network framework for nuclear power plant human reliability analysis accounting for dependencies among performance shaping factors. *Reliability Engineering & System Safety*, *228*, 108766. https://doi.org/10.1016/j.ress.2022.108766

[50] Wang, Z., Zeng, S., Guo, J., & Che, H. (2021). A Bayesian network for reliability assessment of man-machine phased-mission system considering the phase dependencies of human cognitive error. *Reliability Engineering & System Safety*, *207*, 107385. https://doi.org/10.1016/j.ress.2020.107385

[51] Yontay, P., & Pan, R. (2016). A computational Bayesian approach to dependency assessment in system reliability. *Reliability Engineering & System Safety*, *152*, 104–114. https://doi.org/10.1016/j.ress.2016.03.005

[52] Diaconeasa, M. A. (2017). Integration of Qualitative and Quantitative Hybrid Causal Logic into a Simulation-based Platform for Probabilistic Risk Assessment of Nuclear Power Plants [PhD, University of California, Los Angeles]. https://escholarship.org/uc/item/9wc84881

[53] Yang, J.-E. (2018). Multi-unit risk assessment of nuclear power plants: Current status and issues. Nuclear Engineering and Technology, 50(8), 1199–1209. https://doi.org/10.1016/j.net.2018.09.010

[54] Modarres, M., Zhou, T., & Massoud, M. (2017). Advances in multi-unit nuclear power plant probabilistic risk assessment. Reliability Engineering & System Safety, 157, 87–100. https://doi.org/10.1016/j.ress.2016.08.005

[55] Arigi, A. M., Park, G., & Kim, J. (2020). Dependency analysis method for human failure events in multi-unit probabilistic safety assessments. Reliability Engineering & System Safety, 203, 107112. https://doi.org/10.1016/j.ress.2020.107112

[56] Zhang, S., Tong, J., & Zhao, J. (2016). An integrated modeling approach for event sequence development in multi-unit probabilistic risk assessment. Reliability Engineering & System Safety, 155, 147–159. https://doi.org/10.1016/j.ress.2016.07.008

[57] Le Duy, T. D., Vasseur, D., & Serdet, E. (2016). Probabilistic Safety Assessment of twin-unit nuclear sites: Methodological elements. Reliability Engineering & System Safety, 145, 250–261. https://doi.org/10.1016/j.ress.2015.07.014

[58] Schroer, S., & Modarres, M. (2013). An event classification schema for evaluating site risk in a multi-unit nuclear power plant probabilistic risk assessment. Reliability Engineering & System Safety, 117, 40–51. https://doi.org/10.1016/j.ress.2013.03.005

[59] Kim, I. S., Jang, M., & Kim, S. R. (2017). Holistic Approach to Multi-Unit Site Risk Assessment: Status and Issues. Nuclear Engineering and Technology, 49(2), 286–294. https://doi.org/10.1016/j.net.2017.01.003

[60] Zhou, T., Modarres, M., & Droguett, E. L. (2019). Multi-unit risk aggregation with consideration of uncertainty and bias in risk metrics. Reliability Engineering & System Safety, 188, 473–482. https://doi.org/10.1016/j.ress.2019.04.001

[61] Le Duy, T. D., & Vasseur, D. (2018). A practical methodology for modeling and estimation of common cause failure parameters in multi-unit nuclear PSA model. Reliability Engineering & System Safety, 170, 159–174. https://doi.org/10.1016/j.ress.2017.10.018

[62] eVinci™ Microreactor | Westinghouse Electric Company. (n.d.). Retrieved June 13, 2024, from https://www.westinghousenuclear.com/energy-systems/evinci-microreactor/

[63] Nuclear—Remote-controlled reactors | ORNL. (n.d.). Retrieved June 13, 2024, from https://www.ornl.gov/news/nuclear-remote-controlled-reactors

[64] MARVEL Microreactor Reaches Final Design Step. (n.d.). Energy.Gov. Retrieved June 13, 2024, from https://www.energy.gov/ne/articles/marvel-microreactor-reaches-final-design-step

[65] Stevens, Kaeley Renee, Oncken, Joseph Eugene, Bryan, Haydn C, Gutowska, Izabela, Ulrich, Thomas A, Boring PhD, Ronald Laurids, & Culler, Megan Jordan. Opportunities and Challenges for Remote Microreactor Operations. United States.

[66] Fleming Lindsley, Elizabeth Scott, Nyre-Yu, Megan, & Luxat, David Lyle. Human Factors Considerations for Automating Microreactors. United States. https://doi.org/10.2172/1763526

[67] 10 CFR Part 50—Domestic Licensing of Production and Utilization Facilities. Retrieved June 13, 2024, from https://www.ecfr.gov/current/title-10/part-50

[68] Johnson, M. R. Operator Staffing for Small or Multi-Module Nuclear Power Plant Facilities.

[69] Human Factors Engineering (Final Safety Evaluation Report Chapter 18; NuScale US600 Safety Evaluations). NuScale Power, Inc. Retrieved June 13, 2024, from https://www.nrc.gov/docs/ML2002/ML20023B605.pdf

[70] Probabilistic Risk Assessment and Severe Accident Evaluation (Final Safety Evaluation Report Chapter 19; NuScale US600 Safety Evaluations). NuScale Power, Inc. Retrieved June 13, 2024, from https://www.nrc.gov/docs/ML2020/ML20205L410.pdf

[71] Xing, J., Chang, J., & DeJesus, J. NUREG-2198, “The General Methodology of an Integrated Human Event Analysis System (IDHEAS-G).”

[72] NUREG-2199, Vol. 1, “An Integrated Human Event Analysis System (IDHEAS) for Nuclear Power Plant Internal Events At-Power Application—Volume 1.”. 317.

[73] Xing, J. NUREG-2256, “Integrated Human Event Analysis System for Event and Condition Assessment (IDHEAS-ECA).”

[74] Xing, J. RIL 2021-14—Integrated Human Event Analysis System Dependency Analysis Guidance.

[75] Ma, Z., Kvarfordt, K., & Wierman, T. (2022). Industry-Average Performance for Components and Initiating Events at U.S. Commercial Nuclear Power Plants: 2020 Update (INL/EXT-21-65055-Rev000, 1847110; p. INL/EXT-21-65055-Rev000, 1847110). https://doi.org/10.2172/1847110

[76] Lindeman, A. (2020). EPRI/NRC-RES Fire Human Reliability Analysis Guidelines—Qualitative Analysis for Main Control Room Abandonment Scenarios (NUREG-1921). Electric Power Research Institute (EPRI).

[77] Kolaczkowski, A., Forester, J., Gallucci, R., & Bongarra, J. (2007). Demonstrating the Feasibility and Reliability of Operator Manual Actions in Response to Fire (NUREG-1852). Sandia National Laboratories.

[78] A. J. Neylan, D. V. Graf, and A. C. Millunzi, “The modular high temperature gas-cooled reactor (MHTGR) in the U.S.,” Nuclear Engineering and Design, vol. 109, no. 1, pp. 99–105, Sep. 1988, doi: 10.1016/0029-5493(88)90146-X

[79] C. J. Everline, E. A. Bellis, and J. Vasquez, “Probabilistic risk assessment of the modular HTGR plant. Revision 1,” GA Technologies, Inc., San Diego, CA (United States), Report DOE/HTGR--86-011-Rev.1, Jun. 1986. doi:10.2172/455545
[80] GA TECHNOLOGIES INC., (1987). Probabilistic risk assessment of the modular HTGR plant. Revision 3 (Report DOE/HTGR--86-011-Rev.3). GA Technologies, Inc., San Diego, CA (United States). DOE-HTGR-86-011, Rev.3, Vol. 1
[81] GA TECHNOLOGIES INC., (1987). GA Proprietary Supplement Probabilistic Risk Assessment For The Standard Modular High Temperature Gas-Cooled Reactor (Report DOE/HTGR--86-011-Rev.3). GA Technologies, Inc., San Diego, CA (United States). DOE-HTGR-86-011, Rev. 3, Vol. 2
[82] Fleming, K. N., et a1., "HTGR Accident Initiation and Progression Analysis Status Report Phase II Assessment," GA Report GA-A15000, April 1978.
[83] Jang, S., & Jae, M. (2020). A development of methodology for assessing the inter-unit common cause failure in multi-unit PSA model. Reliability Engineering & System Safety, 203, 107012. https://doi.org/10.1016/j.ress.2020.107012
[84] DeJesus Segarra, J., Bensi, M., & Modarres, M. (2021). A Bayesian Network Approach for Modeling Dependent Seismic Failures in a Nuclear Power Plant Probabilistic Risk Assessment. Reliability Engineering & System Safety, 213, 107678. https://doi.org/10.1016/j.ress.2021.107678
[85] Bensi, M., Kiureghian, A. D., & Straub, D. (2013). Efficient Bayesian network modeling of systems. Reliability Engineering & System Safety, 112, 200–213. https://doi.org/10.1016/j.ress.2012.11.017
[86] Langseth, H., Nielsen, T. D., Rumí, R., & Salmerón, A. (2009). Inference in hybrid Bayesian networks. *Reliability Engineering & System Safety*, *94*(10), 1499–1509. https://doi.org/10.1016/j.ress.2009.02.027
[87] Earthperson, A., Pandit, P. M., Diaconeasa, M. A., (2024). Quantifying Safety System Unavailability Margins via Inverse Estimation of Event Sequence Frequencies. American Nuclear Society Advanced Reactor Safety.
[88] Cimock, M., Szetu, P., (2002) An Approach to Assessing the Impact of Human Error Dependency on Plant Risk for the Palisades Nuclear Power Plant PSA. American Nuclear Society Probabilistic Safety Assessment 2002.
[89] Applied Reliability Engineering, Inc., Dependent Human Error Analysis Program – DepHep 3 User Manual.
[90] Holmes, D. E. (Ed.). (2008). Innovations in Bayesian Networks: Theory and Applications. Springer-Verlag. https://www.springer.com/gp/book/9783540850656
[91] Smith, C. (2021). Generic Pressurized Water Reactor Model for SAPHIRE (INL/EXT-21-62553-Rev000, 1804754; p. INL/EXT-21-62553-Rev000, 1804754). https://doi.org/10.2172/1804754
[92] Hamza, M., Tezbasaran, A., Aras, E., Farag, A. S., Diaconeasa, M. A. (2023). Model Exchange Methodology Between Probabilistic Risk Assessment Tools: SAPHIRE and CAFTA Case Study. 10.13182/PSA23-41025.
[93] Ma, Zhegang, Wierman, Thomas E., and Kvarfordt, Kellie J. Industry-Average Performance for Components and Initiating Events at U.S. Commercial Nuclear Power Plants: 2020 Update. United States: N. p., 2021. Web. doi:10.2172/1847110.

APPENDICES

Appendix A. IDHEAS At-Power Decision Trees

In this Appendix, the decision trees associated with quantifying the conditional failure probabilities of the different crew failure modes in the Integrated Human Event Analysis System (IDHEAS) for Nuclear Power Plant Internal Events At-Power Application (IDHEAS At-Power) is presented. Figure 98 gives the decision tree for the alarm response where Figure 99 to Figure 103 give the decision trees for the situation assessment different crew failure modes. Figure 104 and Figure 105 present the decision trees associated with the response planning phase. Finally, Figure 106 to Figure 110 and Figure 111 illustrates the decision trees of the Execution phase and misreading a step in procedure, respectively. All these figures are extracted from [72].

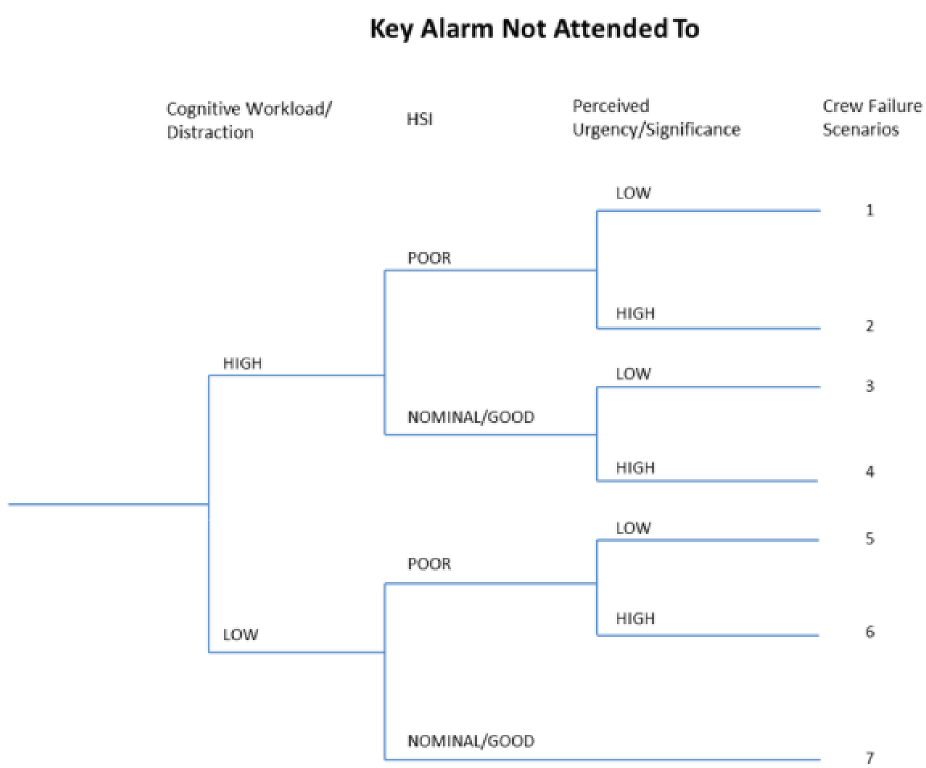

Figure 98. Decision Tree for CFM "Key Alarm Not Attended to"

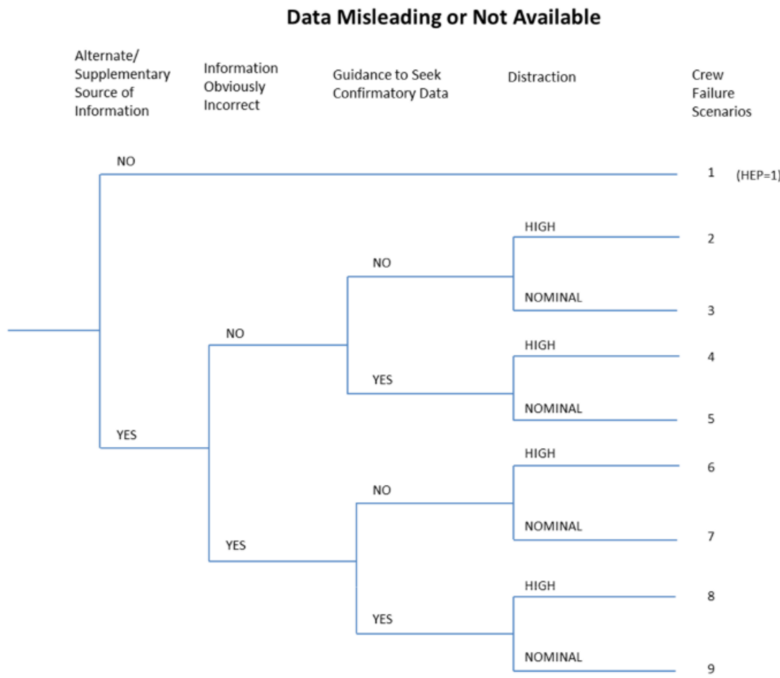

Figure 99. Decision Tree for CFM "Data Misleading or Not Available"

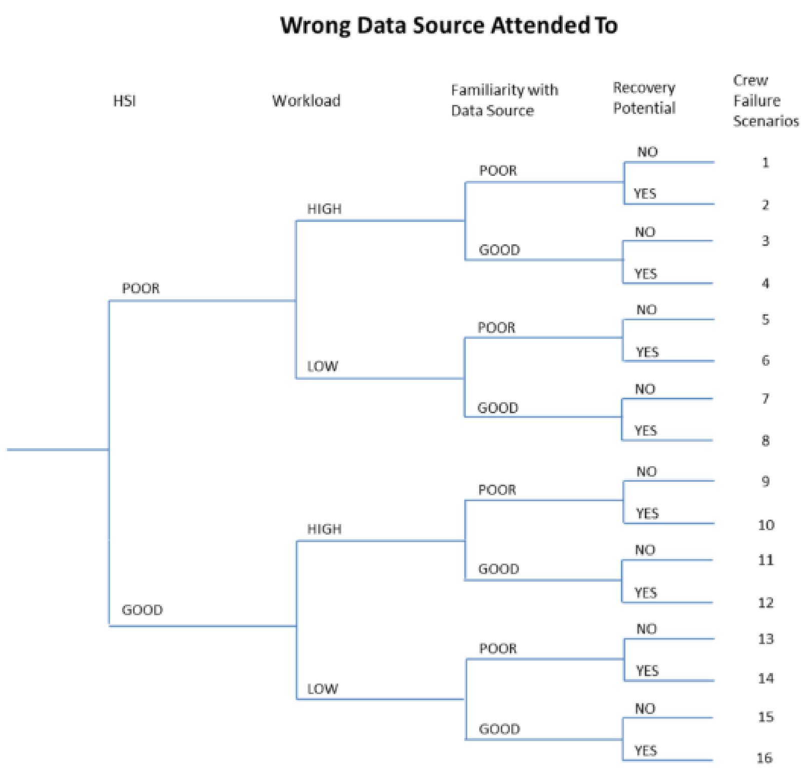

Figure 100. Decision Tree for CFM "Wrong Data Source Attended to"

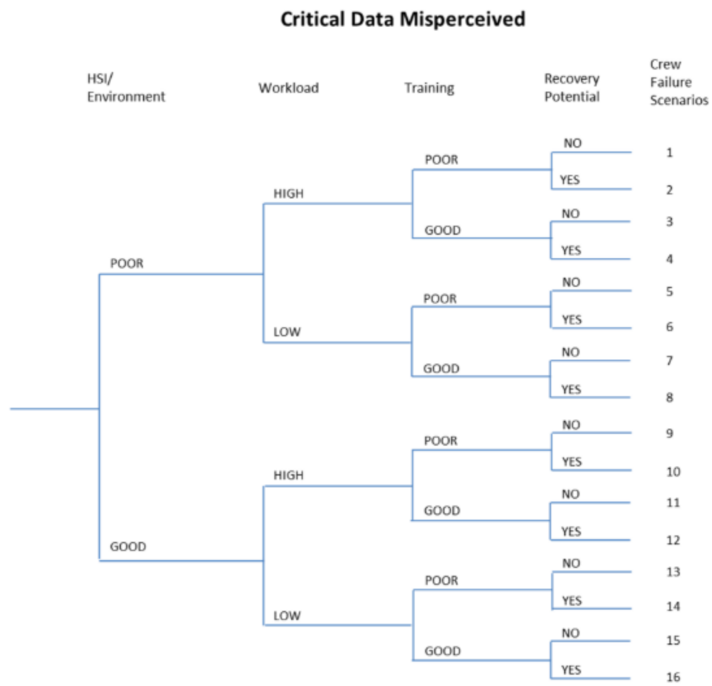

Figure 101. Decision Tree for CFM "Critical Data Misperceived"

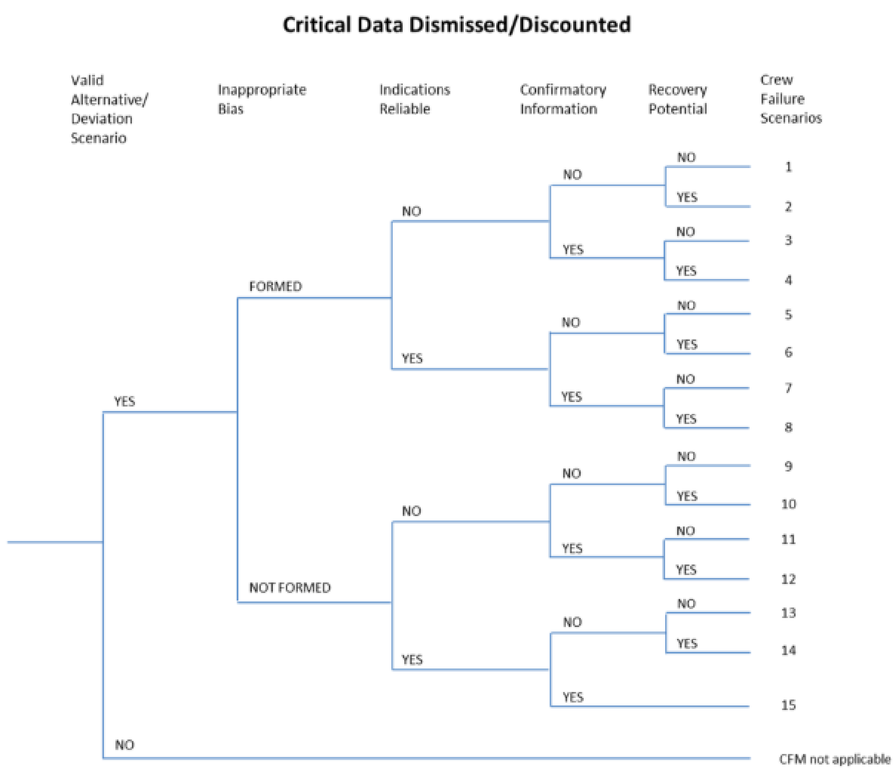

Figure 102. Decision Tree for CFM "Critical Data Dismissed/Discounted"

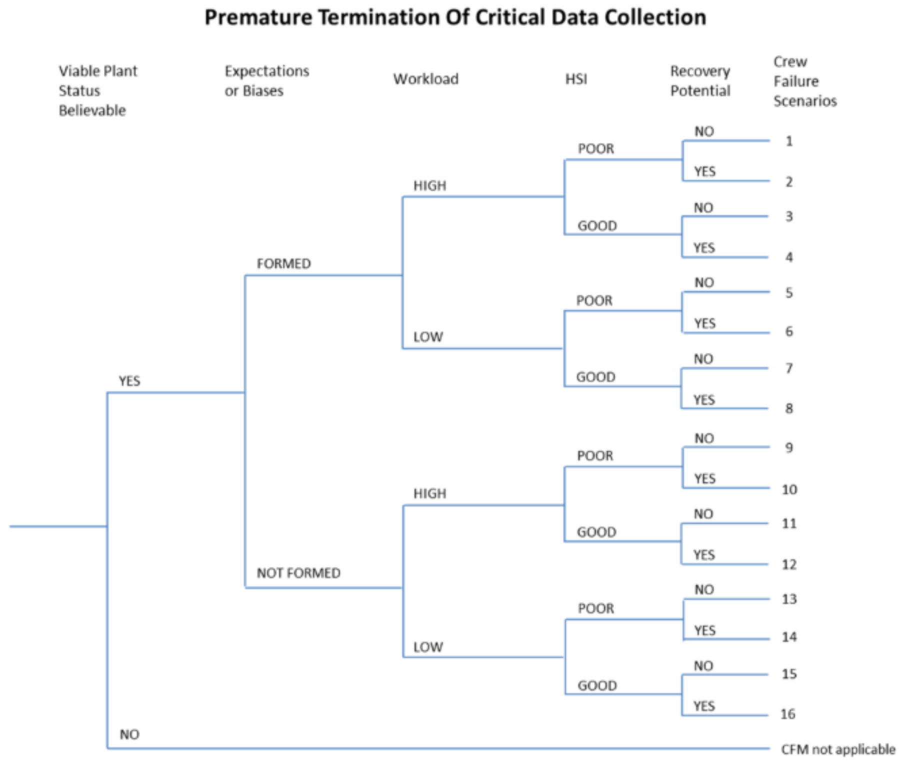

Figure 103. Decision Tree for CFM "Premature Termination of Critical Data Collection"

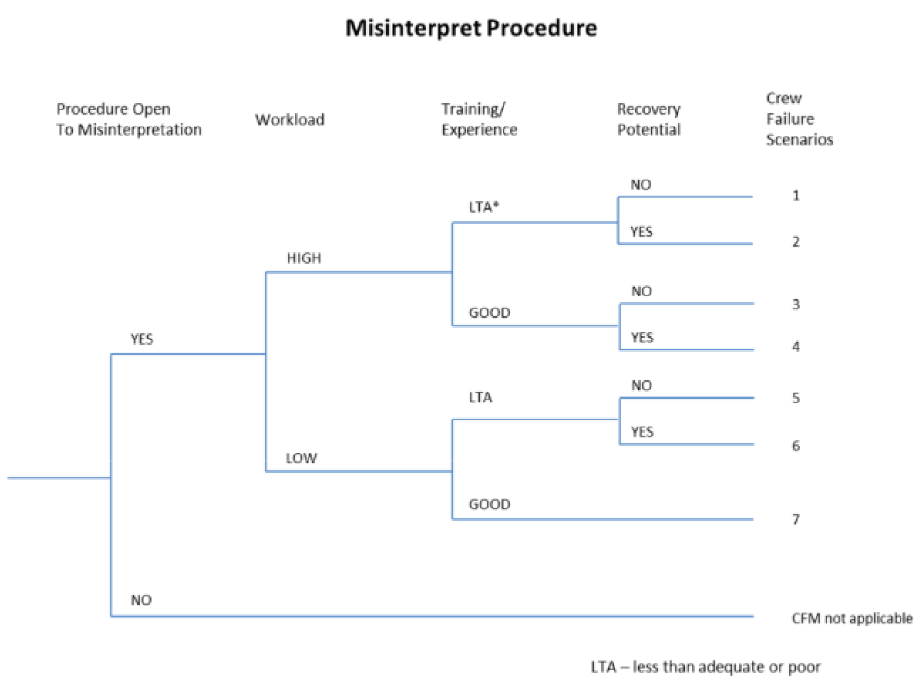

Figure 104. Decision Tree for CFM "Misinterpret Procedure"

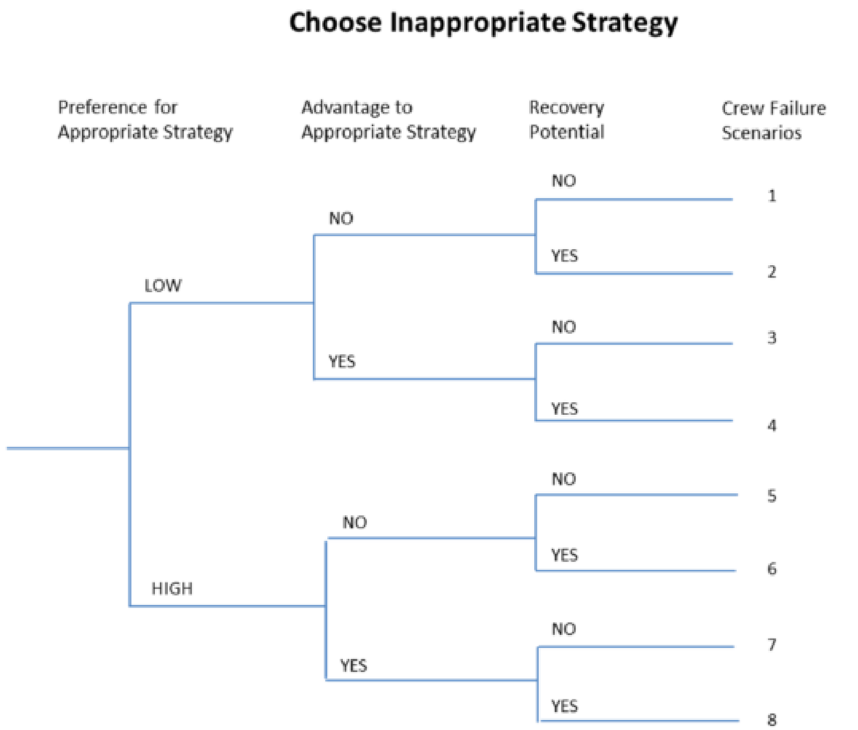

Figure 105. Decision Tree for CFM "Choose Inappropriate Strategy"

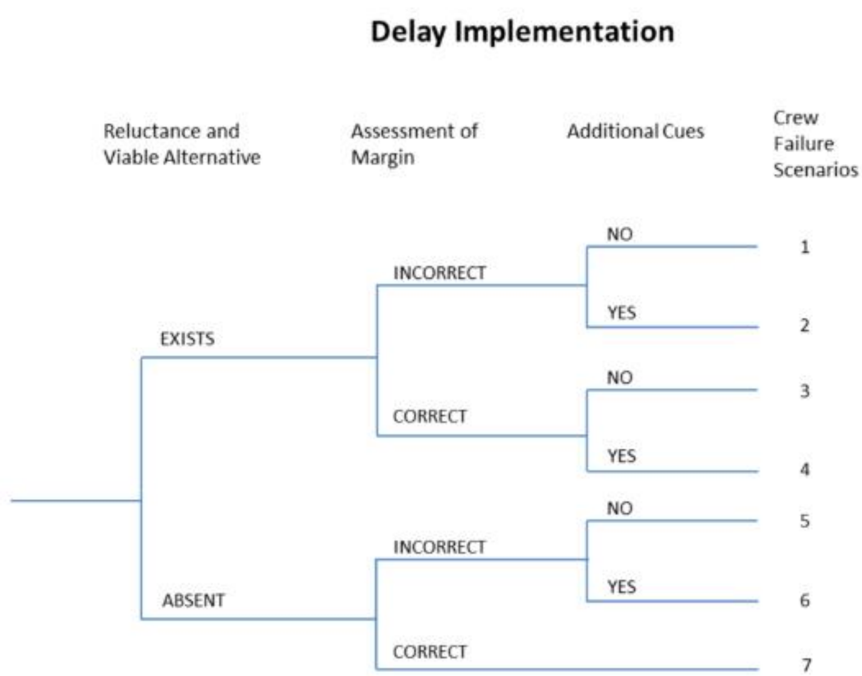

Figure 106. Decision Tree for CFM "Delay Implementation"

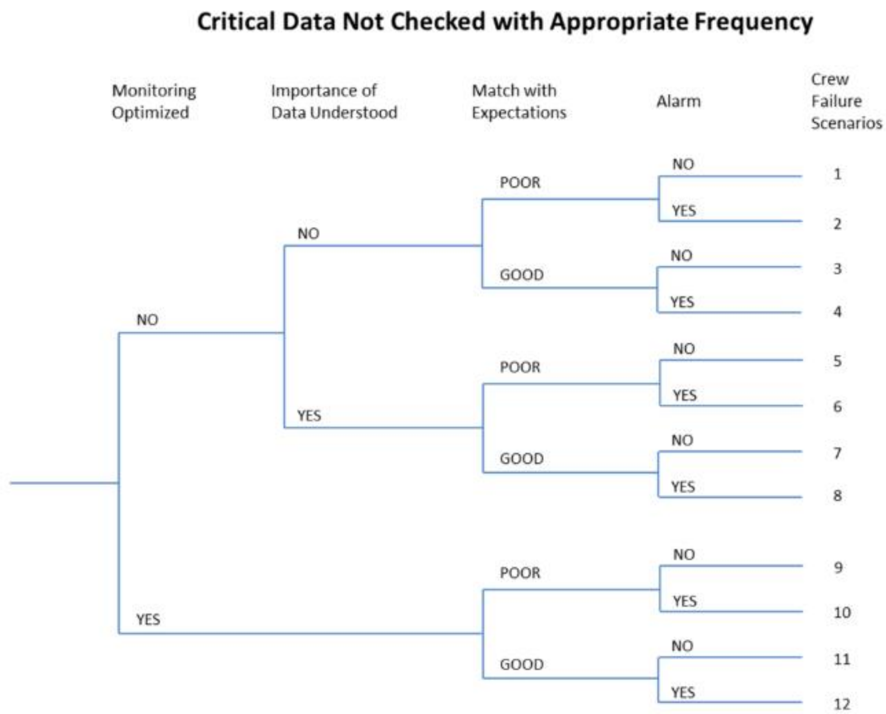

Figure 107. Decision Tree for CFM "Critical Data No Checked with Appropriate Frequency"

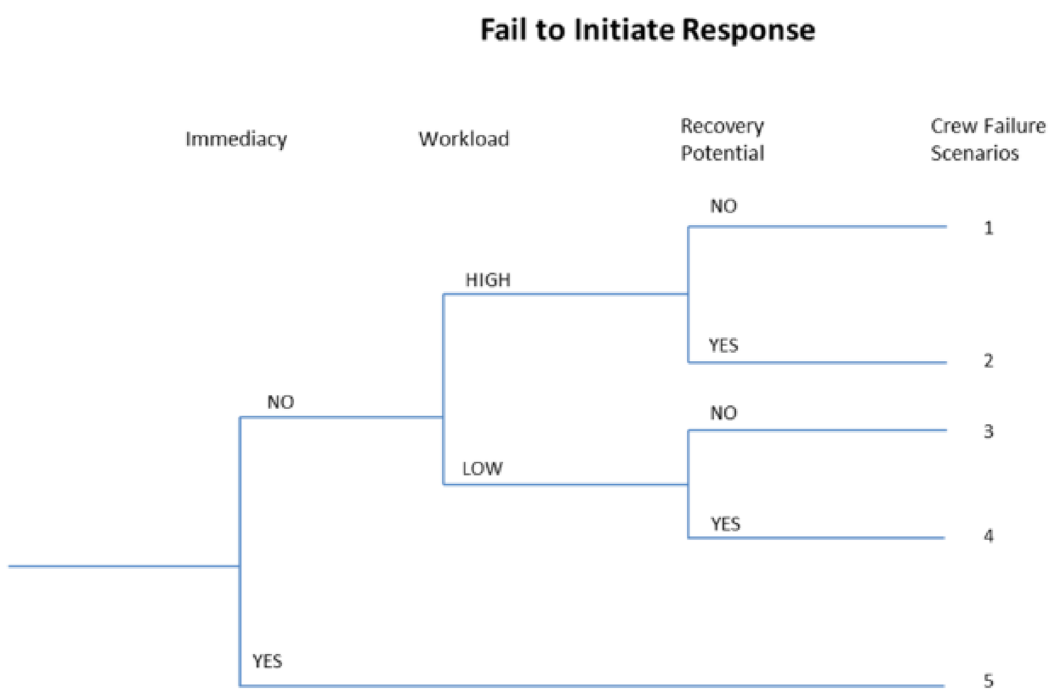

Figure 108. Decision Tree for CFM "Fail to Initiate Response"

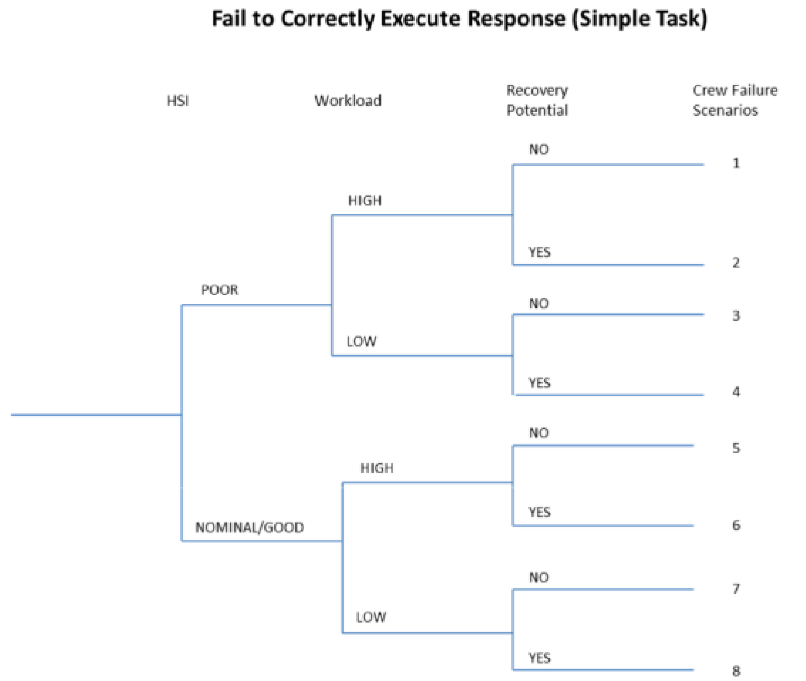

Figure 109. Decision Tree for CFM "Fail to Correctly Execute Response (Simple Task)"

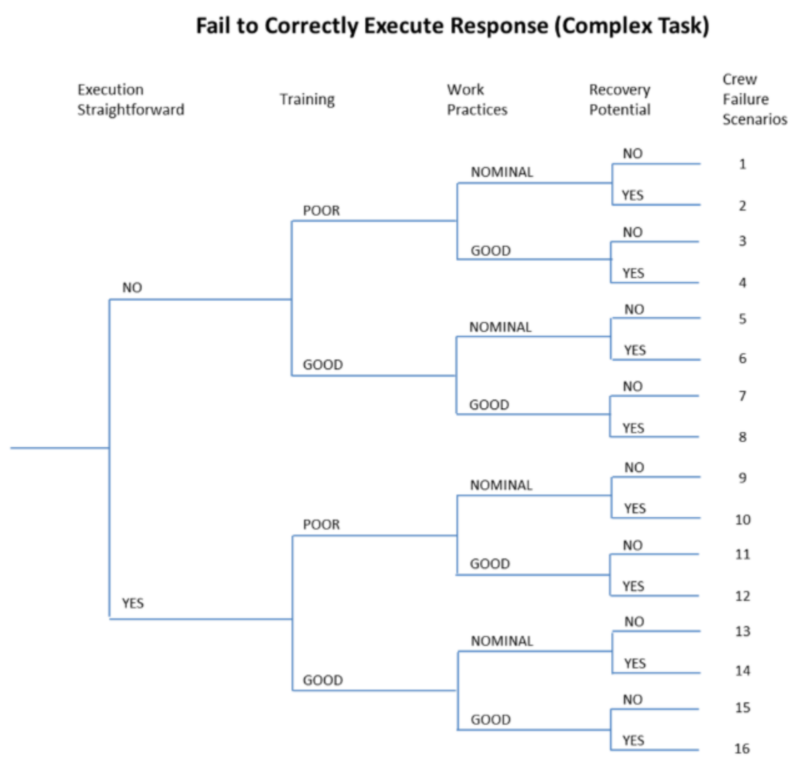

Figure 110. Decision Tree for CFM "Fail to Correctly Execute Response (Complex Task)"

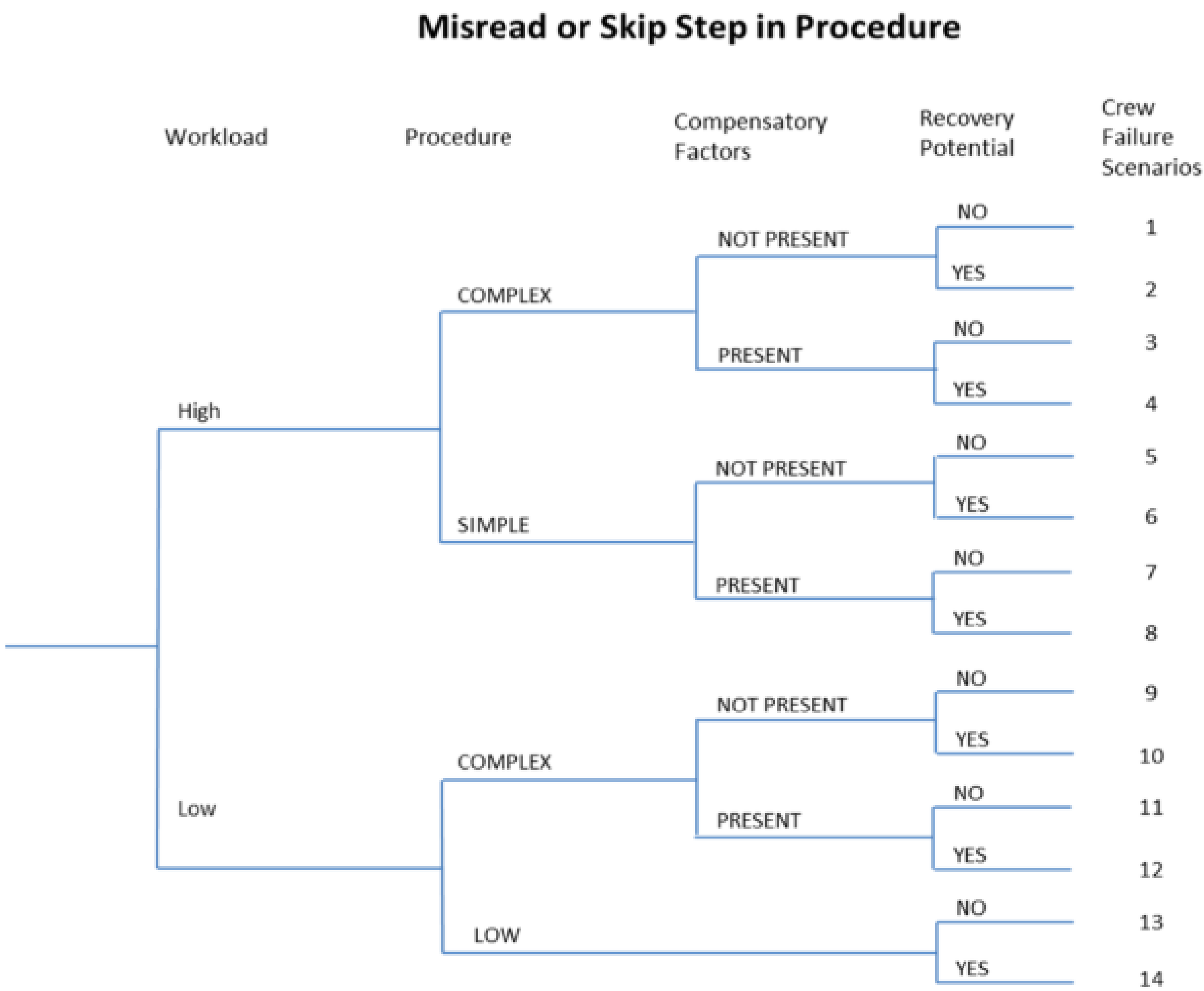

Figure 111. Decision Tree for CFM "Misread or Skip Step in Procedure"

Appendix B. Inverse-Canopy Input Codes

B.a. Inverse-Canopy Input Code for CFM AR

```
!pip install inverse-canopy==0.0.20
from inverse_canopy import InverseCanopy
import tensorflow as tf
import numpy as np

tunable = {
 'num_samples': 5000000,      # number of monte carlo samples
 'learning_rate': 0.05,    # the gradient update rate
 'dtype': tf.float64,     # use 64-bit floats
 'epsilon': 1e-30,        # useful for avoiding log(0 + epsilon) type errors
 'max_steps': 5000,       # maximum steps, regardless of convergence
 'patience': 50,          # number of steps to wait before early stopping if the loss does not improve
 'initiating_event_frequency': 4.26E-01,
 'freeze_initiating_event': True,
}

## encoding scheme
#
# Distraction High/Low -> 0/1
# HSI Poor/Nominal -> 0/1
# Perceived Urgency Low/High -> 0/1
#
## all events are described in terms of the downward branching event.

conditional_events = {
    'names': ['Stub IE', '1', '2', '3', '4', '5', '6'],
    'bounds': {
        'mean': {
            'min': 1e-14,
            'max': 1.00,
        },
        'std': {
            'min': 1e-10,
            'max': 1e8,
        },
     },
    'initial': {
       'mean': 5e-1,
       'std': 1e8,
    }
}

end_states = {

    'AR-1': {
        'sequence': [1, 0, 0, np.nan, 0, np.nan, np.nan],
        'probability': 2.50E-01,
    },

    'AR-2': {
        'sequence': [1, 0, 0, np.nan, 1, np.nan, np.nan],
        'probability': 9.80E-02,
    },

    'AR-3': {
        'sequence': [1, 0, 1, np.nan, np.nan, 0, np.nan],
        'probability': 6.50E-02,
```

```
    },

    'AR-4': {
        'sequence': [1, 0, 1, np.nan, np.nan, 1, np.nan],
        'probability': 4.40E-03,
    },

    'AR-5': {
        'sequence': [1, 1, np.nan, 0, np.nan, np.nan, 0],
        'probability': 7.30E-03,
    },

    'AR-6': {
        'sequence': [1, 1, np.nan, 0, np.nan, np.nan, 1],
        'probability': 9.60E-04,
    },

    'AR-7': {
        'sequence': [1, 1, np.nan, 1, np.nan, np.nan, np.nan],
        'probability': 2.40E-05,
    },

}

model = InverseCanopy(conditional_events, end_states, tunable)
model.fit(steps=tunable['max_steps'], patience=tunable['patience'], learning_rate=tunable['learning_rate'])
model.summarize(show_metrics=False)

```

B.b. Inverse-Canopy Input Code for CFM SA-1

```
!pip install inverse-canopy==0.0.20
from inverse_canopy import InverseCanopy
import tensorflow as tf
import numpy as np

tunable = {
 'num_samples': 5000000,      # number of monte carlo samples
 'learning_rate': 0.05,     # the gradient update rate
 'dtype': tf.float64,     # use 64-bit floats
 'epsilon': 1e-30,        # useful for avoiding log(0 + epsilon) type errors
 'max_steps': 5000,       # maximum steps, regardless of convergence
 'patience': 50,          # number of steps to wait before early stopping if the loss does not improve
 'initiating_event_frequency': 2e+0,
 'freeze_initiating_event': True,
}

## encoding scheme
#
# Distraction High/Low -> 0/1
# HSI Poor/Nominal -> 0/1
# Perceived Urgency Low/High -> 0/1
#
## all events are described in terms of the downward branching event.

conditional_events = {
    'names': ['Stub IE', '1', '2', '3', '4', '5', '6', '7', '8'],
    'bounds': {
        'mean': {
            'min': 1e-14,
```

```
            'max': 1.00,
        },
        'std': {
            'min': 1e-10,
            'max': 1e8,
        },
     },
    'initial': {
       'mean': 5e-1,
       'std': 1e8,
    }
}

end_states = {

    'SA1-1': {
        'sequence': [1, 0, np.nan, np.nan, np.nan, np.nan, np.nan, np.nan, np.nan],
        'probability': 1e+0,
    },

    'SA1-2': {
        'sequence': [1, 1, 0, 0, np.nan, 0, np.nan, np.nan, np.nan],
        'probability': 3.6e-1,
    },

    'SA1-3': {
        'sequence': [1, 1, 0, 0, np.nan, 1, np.nan, np.nan, np.nan],
        'probability': 3.2e-1,
    },

    'SA1-4': {
        'sequence': [1, 1, 0, 1, np.nan, np.nan, 0, np.nan, np.nan],
        'probability': 1.5e-1,
    },

    'SA1-5': {
        'sequence': [1, 1, 0, 1, np.nan, np.nan, 1, np.nan, np.nan],
        'probability': 9.6e-3,
    },

    'SA1-6': {
        'sequence': [1, 1, 1, np.nan, 0, np.nan, np.nan, 0, np.nan],
        'probability': 1.1e-1,
    },

    'SA1-7': {
        'sequence': [1, 1, 1, np.nan, 0, np.nan, np.nan, 1, np.nan],
        'probability': 1.2e-2,
    },

    'SA1-8': {
        'sequence': [1, 1, 1, np.nan, 1, np.nan, np.nan, np.nan, 0],
        'probability': 3.1e-2,
    },

    'SA1-9': {
        'sequence': [1, 1, 1, np.nan, 1, np.nan, np.nan, np.nan, 1],
        'probability': 3.4e-3,
    },

}

model = InverseCanopy(conditional_events, end_states, tunable)
model.fit(steps=tunable['max_steps'], patience=tunable['patience'],
learning_rate=tunable['learning_rate'])
```

```
model.summarize(show_metrics=False)

```

B.c. Inverse-Canopy Input Code for CFM SA-2

```
!pip install inverse-canopy==0.0.20
from inverse_canopy import InverseCanopy
import tensorflow as tf
import numpy as np

tunable = {
 'num_samples': 5000000,      # number of monte carlo samples
 'learning_rate': 0.05,    # the gradient update rate
 'dtype': tf.float64,     # use 64-bit floats
 'epsilon': 1e-30,        # useful for avoiding log(0 + epsilon) type errors
 'max_steps': 5000,       # maximum steps, regardless of convergence
 'patience': 50,          # number of steps to wait before early stopping if the loss does not improve
 'initiating_event_frequency': 2.09e-1,
 'freeze_initiating_event': True,
}

## encoding scheme
#
# Distraction High/Low -> 0/1
# HSI Poor/Nominal -> 0/1
# Perceived Urgency Low/High -> 0/1
#
## all events are described in terms of the downward branching event.

conditional_events = {
    'names': ['Stub IE', '1', '2', '3', '4', '5', '6', '7', '8', '9', '10', '11', '12', '13', '14', '15'],
    'bounds': {
        'mean': {
            'min': 1e-14,
            'max': 1.00,
        },
        'std': {
            'min': 1e-10,
            'max': 1e8,
        },
     },
    'initial': {
       'mean': 5e-1,
       'std': 1e8,
    }
}

end_states = {

    'SA2-1': {
        'sequence': [1, 0, 0, np.nan, 0, np.nan, np.nan, np.nan, 0, np.nan, np.nan, np.nan, np.nan, np.nan, np.nan, np.nan],
        'probability': 8.20E-02,
    },

    'SA2-2': {
        'sequence': [1, 0, 0, np.nan, 0, np.nan, np.nan, np.nan, 1, np.nan, np.nan, np.nan, np.nan, np.nan, np.nan, np.nan],
        'probability': 3.90E-02,
    },
```

```

    'SA2-3': {
        'sequence': [1, 0, 0, np.nan, 1, np.nan, np.nan, np.nan, np.nan, 0, np.nan, np.nan, np.nan, np.nan, np.nan, np.nan],
        'probability': 2.50E-02,
    },

    'SA2-4': {
        'sequence': [1, 0, 0, np.nan, 1, np.nan, np.nan, np.nan, np.nan, 1, np.nan, np.nan, np.nan, np.nan, np.nan, np.nan],
        'probability': 4.20E-03,
    },

    'SA2-5': {
        'sequence': [1, 0, 1, np.nan, np.nan, 0, np.nan, np.nan, np.nan, np.nan, 0, np.nan, np.nan, np.nan, np.nan, np.nan],
        'probability': 3.30E-02,
    },

    'SA2-6': {
        'sequence': [1, 0, 1, np.nan, np.nan, 0, np.nan, np.nan, np.nan, np.nan, 1, np.nan, np.nan, np.nan, np.nan, np.nan],
        'probability': 5.40E-03,
    },

    'SA2-7': {
        'sequence': [1, 0, 1, np.nan, np.nan, 1, np.nan, np.nan, np.nan, np.nan, np.nan, 0, np.nan, np.nan, np.nan, np.nan],
        'probability': 7.20E-03,
    },

    'SA2-8': {
        'sequence': [1, 0, 1, np.nan, np.nan, 1, np.nan, np.nan, np.nan, np.nan, np.nan, 1, np.nan, np.nan, np.nan, np.nan],
        'probability': 1.20E-03,
    },

    'SA2-9': {
        'sequence': [1, 1, np.nan, 0, np.nan, np.nan, 0, np.nan, np.nan, np.nan, np.nan, np.nan, 0, np.nan, np.nan, np.nan],
        'probability': 6.20E-03,
    },

    'SA2-10': {
        'sequence': [1, 1, np.nan, 0, np.nan, np.nan, 0, np.nan, np.nan, np.nan, np.nan, np.nan, 1, np.nan, np.nan, np.nan],
        'probability': 8.30E-04,
    },

    'SA2-11': {
        'sequence': [1, 1, np.nan, 0, np.nan, np.nan, 1, np.nan, np.nan, np.nan, np.nan, np.nan, np.nan, 0, np.nan, np.nan],
        'probability': 2.00E-03,
    },

    'SA2-12': {
        'sequence': [1, 1, np.nan, 0, np.nan, np.nan, 1, np.nan, np.nan, np.nan, np.nan, np.nan, np.nan, 1, np.nan, np.nan],
        'probability': 3.20E-04,
    },

    'SA2-13': {
        'sequence': [1, 1, np.nan, 1, np.nan, np.nan, np.nan, 0, np.nan, np.nan, np.nan, np.nan, np.nan, np.nan, 0, np.nan],
        'probability': 2.00E-03,
```

```
    },

    'SA2-14': {
        'sequence': [1, 1, np.nan, 1, np.nan, np.nan, np.nan, 0, np.nan, np.nan, np.nan, np.nan, np.nan, np.nan, 1, np.nan],
        'probability': 3.20E-04,
    },

    'SA2-15': {
        'sequence': [1, 1, np.nan, 1, np.nan, np.nan, np.nan, 1, np.nan, np.nan, np.nan, np.nan, np.nan, np.nan, np.nan, 0],
        'probability': 5.20E-04,
    },

    'SA2-16': {
        'sequence': [1, 1, np.nan, 1, np.nan, np.nan, np.nan, 1, np.nan, np.nan, np.nan, np.nan, np.nan, np.nan, np.nan, 1],
        'probability': 5.20E-05,
    },

}

model = InverseCanopy(conditional_events, end_states, tunable)
model.fit(steps=tunable['max_steps'], patience=tunable['patience'], learning_rate=tunable['learning_rate'])
model.summarize(show_metrics=False)

```

B.d. Inverse-Canopy Input Code for CFM SA-3

```
!pip install inverse-canopy==0.0.20
from inverse_canopy import InverseCanopy
import tensorflow as tf
import numpy as np

tunable = {
 'num_samples': 5000000,      # number of monte carlo samples
 'learning_rate': 0.05,     # the gradient update rate
 'dtype': tf.float64,      # use 64-bit floats
 'epsilon': 1e-30,         # useful for avoiding log(0 + epsilon) type errors
 'max_steps': 5000,        # maximum steps, regardless of convergence
 'patience': 50,           # number of steps to wait before early stopping if the loss does not improve
 'initiating_event_frequency': 6.48E-01,
 'freeze_initiating_event': True,
}

## encoding scheme
#
# Distraction High/Low -> 0/1
# HSI Poor/Nominal -> 0/1
# Perceived Urgency Low/High -> 0/1
#
## all events are described in terms of the downward branching event.

conditional_events = {
    'names': ['Stub IE', '1', '2', '3', '4', '5', '6', '7', '8', '9', '10', '11', '12', '13', '14', '15'],
    'bounds': {
        'mean': {
            'min': 1e-14,
            'max': 1.00,
```

```
            },
            'std': {
                'min': 1e-10,
                'max': 1e8,
            },
         },
        'initial': {
           'mean': 5e-1,
           'std': 1e8,
        }
}

end_states = {

    'SA3-1': {
        'sequence': [1, 0, 0, np.nan, 0, np.nan, np.nan, np.nan, 0, np.nan, np.nan, np.nan, np.nan, np.nan, np.nan, np.nan],
        'probability': 5.60E-01,
    },

    'SA3-2': {
        'sequence': [1, 0, 0, np.nan, 0, np.nan, np.nan, np.nan, 1, np.nan, np.nan, np.nan, np.nan, np.nan, np.nan, np.nan],
        'probability': 5.70E-02,
    },

    'SA3-3': {
        'sequence': [1, 0, 0, np.nan, 1, np.nan, np.nan, np.nan, np.nan, 0, np.nan, np.nan, np.nan, np.nan, np.nan, np.nan],
        'probability': 1.10E-02,
    },

    'SA3-4': {
        'sequence': [1, 0, 0, np.nan, 1, np.nan, np.nan, np.nan, np.nan, 1, np.nan, np.nan, np.nan, np.nan, np.nan, np.nan],
        'probability': 5.70E-03,
    },

    'SA3-5': {
        'sequence': [1, 0, 1, np.nan, np.nan, 0, np.nan, np.nan, np.nan, np.nan, 0, np.nan, np.nan, np.nan, np.nan, np.nan],
        'probability': 6.50E-03,
    },

    'SA3-6': {
        'sequence': [1, 0, 1, np.nan, np.nan, 0, np.nan, np.nan, np.nan, np.nan, 1, np.nan, np.nan, np.nan, np.nan, np.nan],
        'probability': 1.30E-03,
    },

    'SA3-7': {
        'sequence': [1, 0, 1, np.nan, np.nan, 1, np.nan, np.nan, np.nan, np.nan, np.nan, 0, np.nan, np.nan, np.nan, np.nan],
        'probability': 1.30E-04,
    },

    'SA3-8': {
        'sequence': [1, 0, 1, np.nan, np.nan, 1, np.nan, np.nan, np.nan, np.nan, np.nan, 1, np.nan, np.nan, np.nan, np.nan],
        'probability': 2.60E-05,
    },

    'SA3-9': {
        'sequence': [1, 1, np.nan, 0, np.nan, np.nan, 0, np.nan, np.nan, np.nan, np.nan, np.nan, 0, np.nan, np.nan, np.nan],
```

```
        'probability': 5.70E-03,
    },

    'SA3-10': {
        'sequence': [1, 1, np.nan, 0, np.nan, np.nan, 0, np.nan, np.nan, np.nan, np.nan, np.nan, 1, np.nan, np.nan, np.nan],
        'probability': 1.30E-04,
    },

    'SA3-11': {
        'sequence': [1, 1, np.nan, 0, np.nan, np.nan, 1, np.nan, np.nan, np.nan, np.nan, np.nan, np.nan, 0, np.nan, np.nan],
        'probability': 1.60E-04,
    },

    'SA3-12': {
        'sequence': [1, 1, np.nan, 0, np.nan, np.nan, 1, np.nan, np.nan, np.nan, np.nan, np.nan, np.nan, 1, np.nan, np.nan],
        'probability': 3.40E-05,
    },

    'SA3-13': {
        'sequence': [1, 1, np.nan, 1, np.nan, np.nan, np.nan, 0, np.nan, np.nan, np.nan, np.nan, np.nan, np.nan, 0, np.nan],
        'probability': 1.30E-04,
    },

    'SA3-14': {
        'sequence': [1, 1, np.nan, 1, np.nan, np.nan, np.nan, 0, np.nan, np.nan, np.nan, np.nan, np.nan, np.nan, 1, np.nan],
        'probability': 1.30E-05,
    },

    'SA3-15': {
        'sequence': [1, 1, np.nan, 1, np.nan, np.nan, np.nan, 1, np.nan, np.nan, np.nan, np.nan, np.nan, np.nan, np.nan, 0],
        'probability': 1.30E-05,
    },

    'SA3-16': {
        'sequence': [1, 1, np.nan, 1, np.nan, np.nan, np.nan, 1, np.nan, np.nan, np.nan, np.nan, np.nan, np.nan, np.nan, 1],
        'probability': 1.30E-05,
    },

}

model = InverseCanopy(conditional_events, end_states, tunable)
model.fit(steps=tunable['max_steps'], patience=tunable['patience'], learning_rate=tunable['learning_rate'])
model.summarize(show_metrics=False)

```

B.e. Inverse-Canopy Input Code for CFM SA-4

```
!pip install inverse-canopy==0.0.20
from inverse_canopy import InverseCanopy
import tensorflow as tf
import numpy as np

tunable = {
 'num_samples': 5000000,      # number of monte carlo samples
 'learning_rate': 0.05,    # the gradient update rate
```

```
    'dtype': tf.float64,      # use 64-bit floats
    'epsilon': 1e-30,         # useful for avoiding log(0 + epsilon) type errors
    'max_steps': 5000,        # maximum steps, regardless of convergence
    'patience': 50,           # number of steps to wait before early stopping if the loss does not improve
    'initiating_event_frequency': 8.98E-01,
    'freeze_initiating_event': True,
}

## encoding scheme
#
# Distraction High/Low -> 0/1
# HSI Poor/Nominal -> 0/1
# Perceived Urgency Low/High -> 0/1
#
## all events are described in terms of the downward branching event.

conditional_events = {
    'names': ['Stub IE', '1', '2', '3', '4', '5', '6', '7', '8', '9', '10', '11', '12', '13', '14', '15'],
    'bounds': {
        'mean': {
            'min': 1e-14,
            'max': 1.00,
        },
        'std': {
            'min': 1e-10,
            'max': 1e8,
        },
     },
    'initial': {
       'mean': 5e-1,
       'std': 1e8,
    }
}

end_states = {

    'SA4-1': {
        'sequence': [1, 0, 0, 0, np.nan, 0, np.nan, np.nan, np.nan, 0, np.nan, np.nan, np.nan, np.nan, np.nan, np.nan],
        'probability': 4.90E-01,
    },

    'SA4-2': {
        'sequence': [1, 0, 0, 0, np.nan, 0, np.nan, np.nan, np.nan, 1, np.nan, np.nan, np.nan, np.nan, np.nan, np.nan],
        'probability': 5.00E-02,
    },

    'SA4-3': {
        'sequence': [1, 0, 0, 0, np.nan, 1, np.nan, np.nan, np.nan, np.nan, 0, np.nan, np.nan, np.nan, np.nan, np.nan],
        'probability': 4.50E-02,
    },

    'SA4-4': {
        'sequence': [1, 0, 0, 0, np.nan, 1, np.nan, np.nan, np.nan, np.nan, 1, np.nan, np.nan, np.nan, np.nan, np.nan],
        'probability': 4.50E-03,
    },

    'SA4-5': {
        'sequence': [1, 0, 0, 1, np.nan, np.nan, 0, np.nan, np.nan, np.nan, np.nan, 0, np.nan, np.nan, np.nan, np.nan],
```

```
        'probability': 2.50E-01,
    },

    'SA4-6': {
        'sequence': [1, 0, 0, 1, np.nan, np.nan, 0, np.nan, np.nan, np.nan, np.nan, 1, np.nan, np.nan, np.nan, np.nan],
        'probability': 2.50E-02,
    },

    'SA4-7': {
        'sequence': [1, 0, 0, 1, np.nan, np.nan, 1, np.nan, np.nan, np.nan, np.nan, np.nan, 0, np.nan, np.nan, np.nan],
        'probability': 2.50E-02,
    },

    'SA4-8': {
        'sequence': [1, 0, 0, 1, np.nan, np.nan, 1, np.nan, np.nan, np.nan, np.nan, np.nan, 1, np.nan, np.nan, np.nan],
        'probability': 2.50E-03,
    },

    'SA4-9': {
        'sequence': [1, 0, 1, np.nan, 0, np.nan, np.nan, 0, np.nan, np.nan, np.nan, np.nan, np.nan, 0, np.nan, np.nan],
        'probability': 3.30E-03,
    },

    'SA4-10': {
        'sequence': [1, 0, 1, np.nan, 0, np.nan, np.nan, 0, np.nan, np.nan, np.nan, np.nan, np.nan, 1, np.nan, np.nan],
        'probability': 3.30E-04,
    },

    'SA4-11': {
        'sequence': [1, 0, 1, np.nan, 0, np.nan, np.nan, 1, np.nan, np.nan, np.nan, np.nan, np.nan, np.nan, 0, np.nan],
        'probability': 3.10E-04,
    },

    'SA4-12': {
        'sequence': [1, 0, 1, np.nan, 0, np.nan, np.nan, 1, np.nan, np.nan, np.nan, np.nan, np.nan, np.nan, 1, np.nan],
        'probability': 3.10E-05,
    },

    'SA4-13': {
        'sequence': [1, 0, 1, np.nan, 1, np.nan, np.nan, np.nan, 0, np.nan, np.nan, np.nan, np.nan, np.nan, np.nan, 0],
        'probability': 1.60E-03,
    },

    'SA4-14': {
        'sequence': [1, 0, 1, np.nan, 1, np.nan, np.nan, np.nan, 0, np.nan, np.nan, np.nan, np.nan, np.nan, np.nan, 1],
        'probability': 1.60E-04,
    },

    'SA4-15': {
        'sequence': [1, 0, 1, np.nan, 1, np.nan, np.nan, np.nan, 1, np.nan, np.nan, np.nan, np.nan, np.nan, np.nan, np.nan],
        'probability': 1.30E-05,
    },

    'SA4-16': {
```

```
        'sequence': [1, 1, np.nan, np.nan, np.nan, np.nan, np.nan, np.nan, np.nan, np.nan, np.nan, np.nan, np.nan, np.nan, np.nan, np.nan],
        'probability': 0.00E+00,
    },

}

model = InverseCanopy(conditional_events, end_states, tunable)
model.fit(steps=tunable['max_steps'], patience=tunable['patience'], learning_rate=tunable['learning_rate'])
model.summarize(show_metrics=False)

```

B.f. Inverse-Canopy Input Code for CFM SA-5

```
!pip install inverse-canopy==0.0.20
from inverse_canopy import InverseCanopy
import tensorflow as tf
import numpy as np

tunable = {
 'num_samples': 3000000,      # number of monte carlo samples
 'learning_rate': 0.05,    # the gradient update rate
 'dtype': tf.float64,     # use 64-bit floats
 'epsilon': 1e-30,        # useful for avoiding log(0 + epsilon) type errors
 'max_steps': 430,       # maximum steps, regardless of convergence
 'patience': 250,          # number of steps to wait before early stopping if the loss does not improve
 'initiating_event_frequency': 6.48E-01,
 'freeze_initiating_event': True,
}

## encoding scheme
#
# Distraction High/Low -> 0/1
# HSI Poor/Nominal -> 0/1
# Perceived Urgency Low/High -> 0/1
#
## all events are described in terms of the downward branching event.

conditional_events = {
    'names': ['Stub IE', '1', '2', '3', '4', '5', '6', '7', '8', '9', '10', '11', '12', '13', '14', '15'],
    'bounds': {
        'mean': {
            'min': 1e-14,
            'max': 1.00,
        },
        'std': {
            'min': 1e-10,
            'max': 1e8,
        },
     },
    'initial': {
       'mean': 5e-1,
       'std': 1e8,
    }
}

end_states = {

    'SA3-1': {
```

```
        'sequence': [1, 0, 0, np.nan, 0, np.nan, np.nan, np.nan, 0, np.nan, np.nan, np.nan, np.nan, np.nan, np.nan, np.nan],
        'probability': 5.60E-01,
    },

    'SA3-2': {
        'sequence': [1, 0, 0, np.nan, 0, np.nan, np.nan, np.nan, 1, np.nan, np.nan, np.nan, np.nan, np.nan, np.nan, np.nan],
        'probability': 5.70E-02,
    },

    'SA3-3': {
        'sequence': [1, 0, 0, np.nan, 1, np.nan, np.nan, np.nan, np.nan, 0, np.nan, np.nan, np.nan, np.nan, np.nan, np.nan],
        'probability': 1.10E-02,
    },

    'SA3-4': {
        'sequence': [1, 0, 0, np.nan, 1, np.nan, np.nan, np.nan, np.nan, 1, np.nan, np.nan, np.nan, np.nan, np.nan, np.nan],
        'probability': 5.70E-03,
    },

    'SA3-5': {
        'sequence': [1, 0, 1, np.nan, np.nan, 0, np.nan, np.nan, np.nan, np.nan, 0, np.nan, np.nan, np.nan, np.nan, np.nan],
        'probability': 6.50E-03,
    },

    'SA3-6': {
        'sequence': [1, 0, 1, np.nan, np.nan, 0, np.nan, np.nan, np.nan, np.nan, 1, np.nan, np.nan, np.nan, np.nan, np.nan],
        'probability': 1.30E-03,
    },

    'SA3-7': {
        'sequence': [1, 0, 1, np.nan, np.nan, 1, np.nan, np.nan, np.nan, np.nan, np.nan, 0, np.nan, np.nan, np.nan, np.nan],
        'probability': 1.30E-04,
    },

    'SA3-8': {
        'sequence': [1, 0, 1, np.nan, np.nan, 1, np.nan, np.nan, np.nan, np.nan, np.nan, 1, np.nan, np.nan, np.nan, np.nan],
        'probability': 2.60E-05,
    },

    'SA3-9': {
        'sequence': [1, 1, np.nan, 0, np.nan, np.nan, 0, np.nan, np.nan, np.nan, np.nan, np.nan, 0, np.nan, np.nan, np.nan],
        'probability': 5.70E-03,
    },

    'SA3-10': {
        'sequence': [1, 1, np.nan, 0, np.nan, np.nan, 0, np.nan, np.nan, np.nan, np.nan, np.nan, 1, np.nan, np.nan, np.nan],
        'probability': 1.30E-04,
    },

    'SA3-11': {
        'sequence': [1, 1, np.nan, 0, np.nan, np.nan, 1, np.nan, np.nan, np.nan, np.nan, np.nan, np.nan, 0, np.nan, np.nan],
        'probability': 1.60E-04,
    },

```

```
    'SA3-12': {
        'sequence': [1, 1, np.nan, 0, np.nan, np.nan, 1, np.nan, np.nan, np.nan, np.nan, np.nan, np.nan, 1, np.nan, np.nan],
        'probability': 3.40E-05,
    },

    'SA3-13': {
        'sequence': [1, 1, np.nan, 1, np.nan, np.nan, np.nan, 0, np.nan, np.nan, np.nan, np.nan, np.nan, np.nan, 0, np.nan],
        'probability': 1.30E-04,
    },

    'SA3-14': {
        'sequence': [1, 1, np.nan, 1, np.nan, np.nan, np.nan, 0, np.nan, np.nan, np.nan, np.nan, np.nan, np.nan, 1, np.nan],
        'probability': 1.30E-05,
    },

    'SA3-15': {
        'sequence': [1, 1, np.nan, 1, np.nan, np.nan, np.nan, 1, np.nan, np.nan, np.nan, np.nan, np.nan, np.nan, np.nan, 0],
        'probability': 1.30E-05,
    },

    'SA3-16': {
        'sequence': [1, 1, np.nan, 1, np.nan, np.nan, np.nan, 1, np.nan, np.nan, np.nan, np.nan, np.nan, np.nan, np.nan, 1],
        'probability': 1.30E-05,
    },

}

model = InverseCanopy(conditional_events, end_states, tunable)
model.fit(steps=tunable['max_steps'], patience=tunable['patience'], learning_rate=tunable['learning_rate'])
model.summarize(show_metrics=False)

```

B.g. Inverse-Canopy Input Code for CFM RP-1

```
!pip install inverse-canopy==0.0.20
from inverse_canopy import InverseCanopy
import tensorflow as tf
import numpy as np

tunable = {
 'num_samples': 4000000,      # number of monte carlo samples
 'learning_rate': 0.05,     # the gradient update rate
 'dtype': tf.float64,     # use 64-bit floats
 'epsilon': 1e-30,        # useful for avoiding log(0 + epsilon) type errors
 'max_steps': 5000,       # maximum steps, regardless of convergence
 'patience': 250,          # number of steps to wait before early stopping if the loss does not improve
 'initiating_event_frequency': 4.18E-01,
 'freeze_initiating_event': True,
}

## encoding scheme
#
# Distraction High/Low -> 0/1
# HSI Poor/Nominal -> 0/1
# Perceived Urgency Low/High -> 0/1
```

```
#
## all events are described in terms of the downward branching event.

conditional_events = {
    'names': ['Stub IE', '1', '2', '3', '4', '5', '6', '7'],
    'bounds': {
        'mean': {
            'min': 1e-14,
            'max': 1.00,
        },
        'std': {
            'min': 1e-10,
            'max': 1e8,
        },
     },
    'initial': {
       'mean': 5e-1,
       'std': 1e8,
    }
}

end_states = {

    'RP1-1': {
        'sequence': [1, 0, 0, 0, np.nan, 0, np.nan, np.nan],
        'probability': 2.3e-1,
    },

    'RP1-2': {
        'sequence': [1, 0, 0, 0, np.nan, 1, np.nan, np.nan],
        'probability': 3.3e-2,
    },

    'RP1-3': {
        'sequence': [1, 0, 0, 1, np.nan, np.nan, 0, np.nan],
        'probability': 7.3e-2,
    },

    'RP1-4': {
        'sequence': [1, 0, 0, 1, np.nan, np.nan, 1, np.nan],
        'probability': 5.3e-3,
    },

    'RP1-5': {
        'sequence': [1, 0, 1, np.nan, 0, np.nan, np.nan, 0],
        'probability': 7.3e-2,
    },

    'RP1-6': {
        'sequence': [1, 0, 1, np.nan, 0, np.nan, np.nan, 1],
        'probability': 3.6e-3,
    },

    'RP1-7': {
        'sequence': [1, 0, 1, np.nan, 1, np.nan, np.nan, np.nan],
        'probability': 1.6e-4,
    },

    'RP1-8': {
        'sequence': [1, 1, np.nan, np.nan, np.nan, np.nan, np.nan, np.nan],
        'probability': 0,
    },


}
```

```

model = InverseCanopy(conditional_events, end_states, tunable)
model.fit(steps=tunable['max_steps'], patience=tunable['patience'], learning_rate=tunable['learning_rate'])
model.summarize(show_metrics=False)

```

B.h. Inverse-Canopy Input Code for CFM RP-2

```
!pip install inverse-canopy==0.0.20
from inverse_canopy import InverseCanopy
import tensorflow as tf
import numpy as np

tunable = {
 'num_samples': 4000000,      # number of monte carlo samples
 'learning_rate': 0.05,     # the gradient update rate
 'dtype': tf.float64,     # use 64-bit floats
 'epsilon': 1e-30,        # useful for avoiding log(0 + epsilon) type errors
 'max_steps': 5000,       # maximum steps, regardless of convergence
 'patience': 250,          # number of steps to wait before early stopping if the loss does not improve
 'initiating_event_frequency': 8.03E-01,
 'freeze_initiating_event': True,
}

## encoding scheme
#
# Distraction High/Low -> 0/1
# HSI Poor/Nominal -> 0/1
# Perceived Urgency Low/High -> 0/1
#
## all events are described in terms of the downward branching event.

conditional_events = {
    'names': ['Stub IE', '1', '2', '3', '4', '5', '6', '7'],
    'bounds': {
        'mean': {
            'min': 1e-14,
            'max': 1.00,
        },
        'std': {
            'min': 1e-10,
            'max': 1e8,
        },
     },
    'initial': {
       'mean': 5e-1,
       'std': 1e8,
    }
}

end_states = {

    'RP2-1': {
        'sequence': [1, 0, 0, np.nan, 0, np.nan, np.nan, np.nan],
        'probability': 5.20E-01,
    },

    'RP2-2': {
        'sequence': [1, 0, 0, np.nan, 1, np.nan, np.nan, np.nan],
        'probability': 8.20E-02,
    },
```

```

    'RP2-3': {
        'sequence': [1, 0, 1, np.nan, np.nan, 0, np.nan, np.nan],
        'probability': 1.40E-01,
    },

    'RP2-4': {
        'sequence': [1, 0, 1, np.nan, np.nan, 1, np.nan, np.nan],
        'probability': 1.40E-02,
    },

    'RP2-5': {
        'sequence': [1, 1, np.nan, 0, np.nan, np.nan, 0, np.nan],
        'probability': 3.30E-02,
    },

    'RP2-6': {
        'sequence': [1, 1, np.nan, 0, np.nan, np.nan, 1, np.nan],
        'probability': 3.30E-03
    },

    'RP2-7': {
        'sequence': [1, 1, np.nan, 1, np.nan, np.nan, np.nan, 0],
        'probability': 9.30E-03,
    },

    'RP2-8': {
        'sequence': [1, 1, np.nan, 1, np.nan, np.nan, np.nan, 1],
        'probability': 9.30E-04,
    },


}

model = InverseCanopy(conditional_events, end_states, tunable)
model.fit(steps=tunable['max_steps'], patience=tunable['patience'], learning_rate=tunable['learning_rate'])
model.summarize(show_metrics=False)

```

B.i. Inverse-Canopy Input Code for CFM E-1

```
!pip install inverse-canopy==0.0.20
from inverse_canopy import InverseCanopy
import tensorflow as tf
import numpy as np

tunable = {
 'num_samples': 4000000,      # number of monte carlo samples
 'learning_rate': 0.05,    # the gradient update rate
 'dtype': tf.float64,     # use 64-bit floats
 'epsilon': 1e-30,        # useful for avoiding log(0 + epsilon) type errors
 'max_steps': 5000,       # maximum steps, regardless of convergence
 'patience': 250,          # number of steps to wait before early stopping if the loss does not improve
 'initiating_event_frequency': 2.29E-01,
 'freeze_initiating_event': True,
}

## encoding scheme
#
# Distraction High/Low -> 0/1
# HSI Poor/Nominal -> 0/1
```

```
# Perceived Urgency Low/High -> 0/1
#
## all events are described in terms of the downward branching event.

conditional_events = {
    'names': ['Stub IE', '1', '2', '3', '4', '5', '6'],
    'bounds': {
        'mean': {
            'min': 1e-14,
            'max': 1.00,
        },
        'std': {
            'min': 1e-10,
            'max': 1e8,
        },
     },
    'initial': {
       'mean': 5e-1,
       'std': 1e8,
    }
}

end_states = {

    'E1-1': {
        'sequence': [1, 0, 0, np.nan, 0, np.nan, np.nan],
        'probability': 1.70E-01,
    },

    'E1-2': {
        'sequence': [1, 0, 0, np.nan, 1, np.nan, np.nan],
        'probability': 1.10E-02,
    },

    'E1-3': {
        'sequence': [1, 0, 1, np.nan, np.nan, 0, np.nan],
        'probability': 3.80E-02,
    },

    'E1-4': {
        'sequence': [1, 0, 1, np.nan, np.nan, 1, np.nan],E1
        'probability': 6.50E-03,
    },

    'E1-5': {
        'sequence': [1, 1, np.nan, 0, np.nan, np.nan, 0],
        'probability': 3.40E-03,
    },

    'E1-6': {
        'sequence': [1, 1, np.nan, 0, np.nan, np.nan, 1],
        'probability': 2.20E-04,
    },

    'E1-7': {
        'sequence': [1, 1, np.nan, 1, np.nan, np.nan, np.nan],
        'probability': 1.70E-05,
    },


}

model = InverseCanopy(conditional_events, end_states, tunable)
model.fit(steps=tunable['max_steps'], patience=tunable['patience'],
learning_rate=tunable['learning_rate'])
```

```
model.summarize(show_metrics=False)

```

B.j. Inverse-Canopy Input Code for CFM E-2

```
!pip install inverse-canopy==0.0.20
from inverse_canopy import InverseCanopy
import tensorflow as tf
import numpy as np

tunable = {
 'num_samples': 4000000,      # number of monte carlo samples
 'learning_rate': 0.05,    # the gradient update rate
 'dtype': tf.float64,     # use 64-bit floats
 'epsilon': 1e-30,        # useful for avoiding log(0 + epsilon) type errors
 'max_steps': 5000,       # maximum steps, regardless of convergence
 'patience': 250,          # number of steps to wait before early stopping if the loss does not improve
 'initiating_event_frequency': 5.26E-01,
 'freeze_initiating_event': True,
}

## encoding scheme
#
# Distraction High/Low -> 0/1
# HSI Poor/Nominal -> 0/1
# Perceived Urgency Low/High -> 0/1
#
## all events are described in terms of the downward branching event.

conditional_events = {
    'names': ['Stub IE', '1', '2', '3', '4', '5', '6', '7', '8', '9', '10', '11', '12'],
    'bounds': {
        'mean': {
            'min': 1e-14,
            'max': 1.00,
        },
        'std': {
            'min': 1e-10,
            'max': 1e8,
        },
     },
    'initial': {
       'mean': 5e-1,
       'std': 1e8,
    }
}

end_states = {

    'E2-1': {
        'sequence': [1, 0, 0, 0, np.nan, np.nan, 0, np.nan, np.nan, np.nan, np.nan, np.nan, np.nan],
        'probability': 4.30E-01,
    },

    'E2-2': {
        'sequence': [1, 0, 0, 0, np.nan, np.nan, 1, np.nan, np.nan, np.nan, np.nan, np.nan, np.nan],
        'probability': 1.00E-02,
    },

```

```
    'E2-3': {
        'sequence': [1, 0, 0, 1, np.nan, np.nan, np.nan, 0, np.nan, np.nan, np.nan, np.nan, np.nan],
        'probability': 3.20E-02,
    },

    'E2-4': {
        'sequence': [1, 0, 0, 1, np.nan, np.nan, np.nan, 1, np.nan, np.nan, np.nan, np.nan, np.nan],
        'probability': 8.50E-03,
    },

    'E2-5': {
        'sequence': [1, 0, 1, np.nan, 0, np.nan, np.nan, np.nan, np.nan, 0, np.nan, np.nan, np.nan],
        'probability': 1.40E-02,
    },

    'E2-6': {
        'sequence': [1, 0, 1, np.nan, 0, np.nan, np.nan, np.nan, np.nan, 1, np.nan, np.nan, np.nan],
        'probability': 3.20E-04,
    },

    'E2-7': {
        'sequence': [1, 0, 1, np.nan, 1, np.nan, np.nan, np.nan, np.nan, np.nan, 0, np.nan, np.nan],
        'probability': 1.30E-02,
    },

    'E2-8': {
        'sequence': [1, 0, 1, np.nan, 1, np.nan, np.nan, np.nan, np.nan, np.nan, 1, np.nan, np.nan],
        'probability': 2.30E-03,
    },

    'E2-9': {
        'sequence': [1, 1, np.nan, np.nan, np.nan, 0, np.nan, np.nan, np.nan, np.nan, 0, np.nan],
        'probability': 1.30E-02,
    },

    'E2-10': {
        'sequence': [1, 1, np.nan, np.nan, np.nan, 0, np.nan, np.nan, np.nan, np.nan, 1, np.nan],
        'probability': 2.50E-04,
    },

    'E2-11': {
        'sequence': [1, 1, np.nan, np.nan, np.nan, 1, np.nan, np.nan, np.nan, np.nan, np.nan, 0],
        'probability': 2.30E-03,
    },

    'E2-12': {
        'sequence': [1, 1, np.nan, np.nan, np.nan, 1, np.nan, np.nan, np.nan, np.nan, np.nan, 1],
        'probability': 4.90E-05,
    },


}

model = InverseCanopy(conditional_events, end_states, tunable)
```

```
model.fit(steps=tunable['max_steps'], patience=tunable['patience'], learning_rate=tunable['learning_rate'])
model.summarize(show_metrics=False)

```

B.k. Inverse-Canopy Input Code for CFM E-3

```
!pip install inverse-canopy==0.0.20
from inverse_canopy import InverseCanopy
import tensorflow as tf
import numpy as np

tunable = {
 'num_samples': 4000000,      # number of monte carlo samples
 'learning_rate': 0.05,    # the gradient update rate
 'dtype': tf.float64,     # use 64-bit floats
 'epsilon': 1e-30,        # useful for avoiding log(0 + epsilon) type errors
 'max_steps': 5000,       # maximum steps, regardless of convergence
 'patience': 250,          # number of steps to wait before early stopping if the loss does not improve
 'initiating_event_frequency': 1.75E-01,
 'freeze_initiating_event': True,
}

## encoding scheme
#
# Distraction High/Low -> 0/1
# HSI Poor/Nominal -> 0/1
# Perceived Urgency Low/High -> 0/1
#
## all events are described in terms of the downward branching event.

conditional_events = {
    'names': ['Stub IE', '1', '2', '3', '4'],
    'bounds': {
        'mean': {
            'min': 1e-14,
            'max': 1.00,
        },
        'std': {
            'min': 1e-10,
            'max': 1e8,
        },
     },
    'initial': {
       'mean': 5e-1,
       'std': 1e8,
    }
}

end_states = {

    'E3-1': {
        'sequence': [1, 0, 0, 0, np.nan],
        'probability': 1.50E-01,
    },

    'E3-2': {
        'sequence': [1, 0, 0, 1, np.nan],
        'probability': 1.60E-02,
    },

    'E3-3': {
```

```
        'sequence': [1, 0, 1, np.nan, 0],
        'probability': 8.20E-03,
    },

    'E3-4': {
        'sequence': [1, 0, 1, np.nan, 1],
        'probability': 8.20E-04,
    },

    'E3-5': {
        'sequence': [1, 1, np.nan, np.nan, np.nan],
        'probability': 1.40E-04,
    },


}

model = InverseCanopy(conditional_events, end_states, tunable)
model.fit(steps=tunable['max_steps'], patience=tunable['patience'], learning_rate=tunable['learning_rate'])
model.summarize(show_metrics=False)

```

B.l. Inverse-Canopy Input Code for CFM E-4

```
!pip install inverse-canopy==0.0.20
from inverse_canopy import InverseCanopy
import tensorflow as tf
import numpy as np

tunable = {
 'num_samples': 4000000,      # number of monte carlo samples
 'learning_rate': 0.05,    # the gradient update rate
 'dtype': tf.float64,     # use 64-bit floats
 'epsilon': 1e-30,        # useful for avoiding log(0 + epsilon) type errors
 'max_steps': 5000,       # maximum steps, regardless of convergence
 'patience': 250,          # number of steps to wait before early stopping if the loss does not improve
 'initiating_event_frequency': 7.92E-02,
 'freeze_initiating_event': True,
}

## encoding scheme
#
# Distraction High/Low -> 0/1
# HSI Poor/Nominal -> 0/1
# Perceived Urgency Low/High -> 0/1
#
## all events are described in terms of the downward branching event.

conditional_events = {
    'names': ['Stub IE', '1', '2', '3', '4', '5', '6', '7'],
    'bounds': {
        'mean': {
            'min': 1e-14,
            'max': 1.00,
        },
        'std': {
            'min': 1e-10,
            'max': 1e8,
        },
     },
    'initial': {
```

```
        'mean': 5e-1,
        'std': 1e8,
    }
}

end_states = {

    'E4-1': {
        'sequence': [1, 0, 0, np.nan, 0, np.nan, np.nan, np.nan],
        'probability': 3.30E-02,
    },

    'E4-2': {
        'sequence': [1, 0, 0, np.nan, 1, np.nan, np.nan, np.nan],
        'probability': 6.60E-03,
    },

    'E4-3': {
        'sequence': [1, 0, 1, np.nan, np.nan, 0, np.nan, np.nan],
        'probability': 3.30E-02,
    },

    'E4-4': {
        'sequence': [1, 0, 1, np.nan, np.nan, 1, np.nan, np.nan],
        'probability': 6.60E-03,
    },

    'E4-5': {
        'sequence': [1, 1, np.nan, 0, np.nan, np.nan, 0, np.nan],
        'probability': 9.30E-06,
    },

    'E4-6': {
        'sequence': [1, 1, np.nan, 0, np.nan, np.nan, 1, np.nan],
        'probability': 1.60E-06,
    },

    'E4-7': {
        'sequence': [1, 1, np.nan, 1, np.nan, np.nan, np.nan, 0],
        'probability': 9.30E-06,
    },

    'E4-8': {
        'sequence': [1, 1, np.nan, 1, np.nan, np.nan, np.nan, 1],
        'probability': 1.60E-06,
    },


}

model = InverseCanopy(conditional_events, end_states, tunable)
model.fit(steps=tunable['max_steps'], patience=tunable['patience'], learning_rate=tunable['learning_rate'])
model.summarize(show_metrics=False)

```

B.m. Inverse-Canopy Input Code for CFM E-5

```
!pip install inverse-canopy==0.0.20
from inverse_canopy import InverseCanopy
import tensorflow as tf
import numpy as np

```

```
tunable = {
 'num_samples': 1150000,      # number of monte carlo samples
 'learning_rate': 0.05,    # the gradient update rate
 'dtype': tf.float64,     # use 64-bit floats
 'epsilon': 1e-30,        # useful for avoiding log(0 + epsilon) type errors
 'max_steps': 474,       # maximum steps, regardless of convergence
 'patience': 250,          # number of steps to wait before early stopping if the loss does not improve
 'initiating_event_frequency': 1.99E-01,
 'freeze_initiating_event': True,
}

## encoding scheme
#
# Distraction High/Low -> 0/1
# HSI Poor/Nominal -> 0/1
# Perceived Urgency Low/High -> 0/1
#
## all events are described in terms of the downward branching event.

conditional_events = {
    'names': ['Stub IE', '1', '2', '3', '4', '5', '6', '7', '8', '9', '10', '11', '12', '13', '14', '15'],
    'bounds': {
        'mean': {
            'min': 1e-14,
            'max': 1.00,
        },
        'std': {
            'min': 1e-10,
            'max': 1e8,
        },
     },
    'initial': {
       'mean': 5e-1,
       'std': 1e8,
    }
}

end_states = {

    'E5-1': {
        'sequence': [1, 0, 0, np.nan, 0, np.nan, np.nan, np.nan, 0, np.nan, np.nan, np.nan, np.nan, np.nan, np.nan, np.nan],
        'probability': 1.00E-01,
    },

    'E5-2': {
        'sequence': [1, 0, 0, np.nan, 0, np.nan, np.nan, np.nan, 1, np.nan, np.nan, np.nan, np.nan, np.nan, np.nan, np.nan],
        'probability': 1.60E-02,
    },

    'E5-3': {
        'sequence': [1, 0, 0, np.nan, 1, np.nan, np.nan, np.nan, np.nan, 0, np.nan, np.nan, np.nan, np.nan, np.nan, np.nan],
        'probability': 5.10E-02,
    },

    'E5-4': {
        'sequence': [1, 0, 0, np.nan, 1, np.nan, np.nan, np.nan, np.nan, 1, np.nan, np.nan, np.nan, np.nan, np.nan, np.nan],
        'probability': 5.10E-03,
    },

```

```
    'E5-5': {
        'sequence': [1, 0, 1, np.nan, np.nan, 0, np.nan, np.nan, np.nan, np.nan, 0, np.nan, np.nan, np.nan, np.nan, np.nan],
        'probability': 9.60E-03,
    },

    'E5-6': {
        'sequence': [1, 0, 1, np.nan, np.nan, 0, np.nan, np.nan, np.nan, np.nan, 1, np.nan, np.nan, np.nan, np.nan, np.nan],
        'probability': 9.60E-04,
    },

    'E5-7': {
        'sequence': [1, 0, 1, np.nan, np.nan, 1, np.nan, np.nan, np.nan, np.nan, np.nan, 0, np.nan, np.nan, np.nan, np.nan],
        'probability': 3.80E-03,
    },

    'E5-8': {
        'sequence': [1, 0, 1, np.nan, np.nan, 1, np.nan, np.nan, np.nan, np.nan, np.nan, 1, np.nan, np.nan, np.nan, np.nan],
        'probability': 3.80E-04,
    },

    'E5-9': {
        'sequence': [1, 1, np.nan, 0, np.nan, np.nan, 0, np.nan, np.nan, np.nan, np.nan, np.nan, 0, np.nan, np.nan, np.nan],
        'probability': 9.60E-03,
    },

    'E5-10': {
        'sequence': [1, 1, np.nan, 0, np.nan, np.nan, 0, np.nan, np.nan, np.nan, np.nan, np.nan, 1, np.nan, np.nan, np.nan],
        'probability': 1.30E-04,
    },

    'E5-11': {
        'sequence': [1, 1, np.nan, 0, np.nan, np.nan, 1, np.nan, np.nan, np.nan, np.nan, np.nan, np.nan, 0, np.nan, np.nan],
        'probability': 9.80E-04,
    },

    'E5-12': {
        'sequence': [1, 1, np.nan, 0, np.nan, np.nan, 1, np.nan, np.nan, np.nan, np.nan, np.nan, np.nan, 1, np.nan, np.nan],
        'probability': 5.70E-05,
    },

    'E5-13': {
        'sequence': [1, 1, np.nan, 1, np.nan, np.nan, np.nan, 0, np.nan, np.nan, np.nan, np.nan, np.nan, np.nan, 0, np.nan],
        'probability': 8.00E-04,
    },

    'E5-14': {
        'sequence': [1, 1, np.nan, 1, np.nan, np.nan, np.nan, 0, np.nan, np.nan, np.nan, np.nan, np.nan, np.nan, 1, np.nan],
        'probability': 8.00E-05,
    },

    'E5-15': {
        'sequence': [1, 1, np.nan, 1, np.nan, np.nan, np.nan, 1, np.nan, np.nan, np.nan, np.nan, np.nan, np.nan, np.nan, 0],
        'probability': 8.00E-05,
    },
```

```
    'E5-16': {
        'sequence': [1, 1, np.nan, 1, np.nan, np.nan, np.nan, 1, np.nan, np.nan, np.nan, np.nan, np.nan, np.nan, np.nan, 1],
        'probability': 1.00E-05,
    },
}
model = InverseCanopy(conditional_events, end_states, tunable)
model.fit(steps=tunable['max_steps'], patience=tunable['patience'], learning_rate=tunable['learning_rate'])
model.summarize(show_metrics=False)
```

B.n. Inverse-Canopy Input Code for CFM MP

```
!pip install inverse-canopy==0.0.20
from inverse_canopy import InverseCanopy
import tensorflow as tf
import numpy as np
tunable = {
 'num_samples': 5000000,      # number of monte carlo samples
 'learning_rate': 0.05,     # the gradient update rate
 'dtype': tf.float64,     # use 64-bit floats
 'epsilon': 1e-30,        # useful for avoiding log(0 + epsilon) type errors
 'max_steps': 5000,       # maximum steps, regardless of convergence
 'patience': 50,          # number of steps to wait before early stopping if the loss does not improve
 'initiating_event_frequency': 1.88E-01,
 'freeze_initiating_event': True,
}
## encoding scheme
#
# Distraction High/Low -> 0/1
# HSI Poor/Nominal -> 0/1
# Perceived Urgency Low/High -> 0/1
#
## all events are described in terms of the downward branching event.
conditional_events = {
    'names': ['Stub IE', '1', '2', '3', '4', '5', '6', '7', '8', '9', '10', '11', '12', '13'],
    'bounds': {
        'mean': {
            'min': 1e-14,
            'max': 1.00,
        },
        'std': {
            'min': 1e-10,
            'max': 1e8,
        },
     },
    'initial': {
       'mean': 5e-1,
       'std': 1e8,
    }
}
end_states = {
    'MP-1': {
```

```
        'sequence': [1, 0, 0, np.nan, 0, np.nan, np.nan, 0, np.nan, np.nan, np.nan, np.nan, np.nan, np.nan],
        'probability': 9.40E-02,
    },

    'MP-2': {
        'sequence': [1, 0, 0, np.nan, 0, np.nan, np.nan, 1, np.nan, np.nan, np.nan, np.nan, np.nan, np.nan],
        'probability': 1.30E-02,
    },

    'MP-3': {
        'sequence': [1, 0, 0, np.nan, 1, np.nan, np.nan, np.nan, 0, np.nan, np.nan, np.nan, np.nan, np.nan],
        'probability': 1.90E-02,
    },

    'MP-4': {
        'sequence': [1, 0, 0, np.nan, 1, np.nan, np.nan, np.nan, 1, np.nan, np.nan, np.nan, np.nan, np.nan],
        'probability': 2.70E-03,
    },

    'MP-5': {
        'sequence': [1, 0, 1, np.nan, np.nan, 0, np.nan, np.nan, np.nan, 0, np.nan, np.nan, np.nan, np.nan],
        'probability': 1.30E-02,
    },

    'MP-6': {
        'sequence': [1, 0, 1, np.nan, np.nan, 0, np.nan, np.nan, np.nan, 1, np.nan, np.nan, np.nan, np.nan],
        'probability': 1.90E-03,
    },

    'MP-7': {
        'sequence': [1, 0, 1, np.nan, np.nan, 1, np.nan, np.nan, np.nan, np.nan, 0, np.nan, np.nan, np.nan],
        'probability': 1.00E-03,
    },

    'MP-8': {
        'sequence': [1, 0, 1, np.nan, np.nan, 1, np.nan, np.nan, np.nan, np.nan, 1, np.nan, np.nan, np.nan],
        'probability': 1.50E-04,
    },

    'MP-9': {
        'sequence': [1, 1, np.nan, 0, np.nan, np.nan, 0, np.nan, np.nan, np.nan, np.nan, 0, np.nan, np.nan],
        'probability': 3.60E-02,
    },

    'MP-10': {
        'sequence': [1, 1, np.nan, 0, np.nan, np.nan, 0, np.nan, np.nan, np.nan, np.nan, 1, np.nan, np.nan],
        'probability': 5.10E-03,
    },

    'MP-11': {
        'sequence': [1, 1, np.nan, 0, np.nan, np.nan, 1, np.nan, np.nan, np.nan, np.nan, np.nan, 0, np.nan],
        'probability': 1.30E-03,
    },

```

```
    'MP-12': {
        'sequence': [1, 1, np.nan, 0, np.nan, np.nan, 1, np.nan, np.nan, np.nan, np.nan, np.nan, 1, np.nan],
        'probability': 9.70E-05,
    },

    'MP-13': {
        'sequence': [1, 1, np.nan, 1, np.nan, np.nan, np.nan, np.nan, np.nan, np.nan, np.nan, np.nan, np.nan, 0],
        'probability': 8.20E-04,
    },

    'MP-14': {
        'sequence': [1, 1, np.nan, 1, np.nan, np.nan, np.nan, np.nan, np.nan, np.nan, np.nan, np.nan, np.nan, 1],
        'probability': 1.20E-04,
    },

}

model = InverseCanopy(conditional_events, end_states, tunable)
model.fit(steps=tunable['max_steps'], patience=tunable['patience'], learning_rate=tunable['learning_rate'])
model.summarize(show_metrics=False)

```

Appendix C. IDHEAS At-Power Bayesian Networks Conditional Probability

Table 11. Conditional Probability Tabel for CFM AR

PIF			Human Success Probability	Human Failure Probability
Cognitive Work	Human System Interface	Perceived Urgency		
High	Poor	Low	7.50E-01	2.50E-01
		High	9.02E-01	9.80E-02
	Nominal	Low	9.35E-01	6.50E-02
		High	9.96E-01	4.40E-03
Low	Poor	Low	9.93E-01	7.30E-03
		High	9.99E-01	9.60E-04
	Nominal	Low	1.00E+00	2.40E-05
		High	1.00E+00	2.40E-05

Table 12. Conditional Probability Tabel for CFM SA-1

PIF				Human Success Probability	Human Failure Probability
Alternate / Supplementary Source of Information	Information Obviously incorrect	Guidance to Seek Confirmatory Data	Distraction		
No	No	No	High	0.00E+00	1.00E+00
			Nominal	0.00E+00	1.00E+00
		Yes	High	0.00E+00	1.00E+00
			Nominal	0.00E+00	1.00E+00
	Yes	No	High	0.00E+00	1.00E+00
			Nominal	0.00E+00	1.00E+00
		Yes	High	0.00E+00	1.00E+00
			Nominal	0.00E+00	1.00E+00
Yes	No	No	High	6.40E-01	3.60E-01
			Nominal	6.80E-01	3.20E-01
		Yes	High	8.50E-01	1.50E-01
			Nominal	9.90E-01	9.60E-03
	Yes	No	High	8.90E-01	1.10E-01
			Nominal	9.88E-01	1.20E-02
		Yes	High	9.69E-01	3.10E-02
			Nominal	9.98E-01	2.40E-03

Table 13. Conditional Probability Tabel for CFM SA-2

PIF

Human System Interface	Workload	Familiarity with Data Source	Recovery	**Human Success Probability**	**Human Failure Probability**
Poor	High	Poor	No	9.18E-01	8.20E-02
			Yes	9.61E-01	3.90E-02
		Good	No	9.75E-01	2.50E-02
			Yes	9.96E-01	4.20E-03
	Low	Poor	No	9.67E-01	3.30E-02
			Yes	9.95E-01	5.40E-03
		Good	No	9.93E-01	7.20E-03
			Yes	9.99E-01	1.20E-03
Good	High	Poor	No	9.94E-01	6.20E-03
			Yes	9.99E-01	8.30E-04
		Good	No	9.98E-01	2.00E-03
			Yes	1.00E+00	3.20E-04
	Low	Poor	No	9.98E-01	2.00E-03
			Yes	1.00E+00	3.20E-04
		Good	No	9.99E-01	5.20E-04
			Yes	1.00E+00	5.20E-05

Table 14. Conditional Probability Tabel for CFM SA-3

PIF				**Human Success Probability**	**Human Failure Probability**
Human System Interface	Workload	Training	Recovery		
Poor	High	Poor	No	4.40E-01	5.60E-01
			Yes	9.43E-01	5.70E-02
		Good	No	9.89E-01	1.10E-02
			Yes	9.94E-01	5.70E-03
	Low	Poor	No	9.94E-01	6.50E-03
			Yes	9.99E-01	1.30E-03
		Good	No	1.00E+00	1.30E-04
			Yes	1.00E+00	2.60E-05
Good	High	Poor	No	9.94E-01	5.70E-03
			Yes	1.00E+00	1.30E-04
		Good	No	1.00E+00	1.60E-04
			Yes	1.00E+00	3.40E-05
	Low	Poor	No	1.00E+00	1.30E-04
			Yes	1.00E+00	1.30E-05
		Good	No	1.00E+00	1.30E-05
			Yes	1.00E+00	1.30E-05

Table 15. Conditional Probability Tabel for CFM SA-4

PIF					Human Success Probability	Human Failure Probability
Valid Alternative Scenario	Inappropriate Biase	Indication Reliable	Confirmatory Information	Recovery		
Yes	Formed	No	No	No	5.10E-01	4.90E-01
				Yes	9.50E-01	5.00E-02
			Yes	No	9.55E-01	4.50E-02
				Yes	9.96E-01	4.50E-03
		Yes	No	No	7.50E-01	2.50E-01
				Yes	9.75E-01	2.50E-02
			Yes	No	9.75E-01	2.50E-02
				Yes	9.98E-01	2.50E-03
	Not Formed	No	No	No	9.97E-01	3.30E-03
				Yes	1.00E+00	3.30E-04
			Yes	No	1.00E+00	3.10E-04
				Yes	1.00E+00	3.10E-05
		Yes	No	No	9.98E-01	1.60E-03
				Yes	1.00E+00	1.60E-04
			Yes	No	1.00E+00	1.30E-05
				Yes	1.00E+00	1.30E-05
No	Formed	No	No	No	1.00E+00	0.00E+00
				Yes	1.00E+00	0.00E+00
			Yes	No	1.00E+00	0.00E+00
				Yes	1.00E+00	0.00E+00
		Yes	No	No	1.00E+00	0.00E+00
				Yes	1.00E+00	0.00E+00
			Yes	No	1.00E+00	0.00E+00
				Yes	1.00E+00	0.00E+00
	Not Formed	No	No	No	1.00E+00	0.00E+00
				Yes	1.00E+00	0.00E+00
			Yes	No	1.00E+00	0.00E+00
				Yes	1.00E+00	0.00E+00
		Yes	No	No	1.00E+00	0.00E+00
				Yes	1.00E+00	0.00E+00
			Yes	No	1.00E+00	0.00E+00
				Yes	1.00E+00	0.00E+00

Table 16. Conditional Probability Tabel for CFM SA-5

PIF					Human Success Probability	Human Failure Probability
Visible Plant Status Believable	Expectations or Biases	Workload	Human System Interface	Recovery		

Yes	Formed	High	Poor	No	8.90E-01	1.10E-01
				Yes	9.87E-01	1.30E-02
			Good	No	9.49E-01	5.10E-02
				Yes	9.95E-01	5.10E-03
		Low	Poor	No	9.24E-01	7.60E-02
				Yes	9.92E-01	7.60E-03
			Good	No	9.92E-01	8.20E-03
				Yes	9.99E-01	8.20E-04
	Not Formed	High	Poor	No	9.87E-01	1.30E-02
				Yes	9.99E-01	1.30E-03
			Good	No	9.96E-01	4.10E-03
				Yes	1.00E+00	4.10E-04
		Low	Poor	No	9.96E-01	4.20E-03
				Yes	1.00E+00	4.20E-04
			Good	No	1.00E+00	3.50E-04
				Yes	1.00E+00	3.50E-05
No	Formed	High	Poor	No	1.00E+00	0.00E+00
				Yes	1.00E+00	0.00E+00
			Good	No	1.00E+00	0.00E+00
				Yes	1.00E+00	0.00E+00
		Low	Poor	No	1.00E+00	0.00E+00
				Yes	1.00E+00	0.00E+00
			Good	No	1.00E+00	0.00E+00
				Yes	1.00E+00	0.00E+00
	Not Formed	High	Poor	No	1.00E+00	0.00E+00
				Yes	1.00E+00	0.00E+00
			Good	No	1.00E+00	0.00E+00
				Yes	1.00E+00	0.00E+00
		Low	Poor	No	1.00E+00	0.00E+00
				Yes	1.00E+00	0.00E+00
			Good	No	1.00E+00	0.00E+00
				Yes	1.00E+00	0.00E+00

Table 17. Conditional Probability Tabel for CFM RP-1

PIF				**Human Success Probability**	**Human Failure Probability**
Procedures Open to Misinterpretation	Workload	Training	Recovery		
Yes	High	Less than Adequate	No	7.70E-01	2.30E-01
			Yes	9.67E-01	3.30E-02
		Good	No	9.27E-01	7.30E-02
			Yes	9.95E-01	5.30E-03
	Low	Less than Adequate	No	9.27E-01	7.30E-02
			Yes	9.96E-01	3.60E-03

		Good	No	1.00E+00	1.60E-04
			Yes	1.00E+00	1.60E-04
No	High	Less than Adequate	No	1.00E+00	0.00E+00
			Yes	1.00E+00	0.00E+00
		Good	No	1.00E+00	0.00E+00
			Yes	1.00E+00	0.00E+00
	Low	Less than Adequate	No	1.00E+00	0.00E+00
			Yes	1.00E+00	0.00E+00
		Good	No	1.00E+00	0.00E+00
			Yes	1.00E+00	0.00E+00

Table 18. Conditional Probability Tabel for CFM RP-2

PIF			**Human Success Probability**	**Human Failure Probability**
Preference for Appropriate Strategy	Advantage to Appropriate Strategy	Recovery		
Low	No	No	4.80E-01	5.20E-01
		Yes	9.18E-01	8.20E-02
	Yes	No	8.60E-01	1.40E-01
		Yes	9.86E-01	1.40E-02
High	No	No	9.67E-01	3.30E-02
		Yes	9.97E-01	3.30E-03
	Yes	No	9.91E-01	9.30E-03
		Yes	9.99E-01	9.30E-04

Table 19. Conditional Probability Tabel for CFM E-1

PIF			**Human Success Probability**	**Human Failure Probability**
Reluctance and Viable Alternative	Assessment of Margin	Additional Cues		
Exist	Incorrect	No	8.30E-01	1.70E-01
		Yes	9.89E-01	1.10E-02
	Correct	No	9.62E-01	3.80E-02
		Yes	9.94E-01	6.50E-03
Absent	Incorrect	No	9.97E-01	3.40E-03
		Yes	1.00E+00	2.20E-04
	Correct	No	1.00E+00	1.70E-05
		Yes	1.00E+00	1.70E-05

Table 20. Conditional Probability Tabel for CFM E-2

PIF				**Human Success Probability**	**Human Failure Probability**
Monitoring Optimized	Importance of Data Understood	Match with Expectation	Alarm		
No	No	Poor	No	5.70E-01	4.30E-01

			Yes	9.90E-01	1.00E-02
		Good	No	9.68E-01	3.20E-02
			Yes	9.92E-01	8.50E-03
	Yes	Poor	No	9.86E-01	1.40E-02
			Yes	1.00E+00	3.20E-04
		Good	No	9.87E-01	1.30E-02
			Yes	9.98E-01	2.30E-03
Yes	No	Poor	No	9.87E-01	1.30E-02
			Yes	1.00E+00	2.50E-04
		Good	No	9.98E-01	2.30E-03
			Yes	1.00E+00	4.90E-05
	Yes	Poor	No	9.87E-01	1.30E-02
			Yes	1.00E+00	2.50E-04
		Good	No	9.98E-01	2.30E-03
			Yes	1.00E+00	4.90E-05

Table 21. Conditional Probability Tabel for CFM E-3

PIF			**Human Success Probability**	**Human Failure Probability**
Immediacy	Workload	Recovery		
No	High	No	8.50E-01	1.50E-01
		Yes	9.84E-01	1.60E-02
	Low	No	9.92E-01	8.20E-03
		Yes	9.99E-01	8.20E-04
Yes	High	No	1.00E+00	1.40E-04
		Yes	1.00E+00	1.40E-04
	Low	No	1.00E+00	1.40E-04
		Yes	1.00E+00	1.40E-04

Table 22. Conditional Probability Tabel for CFM E-4

PIF			**Human Success Probability**	**Human Failure Probability**
Human System Interface	Workload	Recovery		
Poor	High	No	9.67E-01	3.30E-02
		Yes	9.93E-01	6.60E-03
	Low	No	9.67E-01	3.30E-02
		Yes	9.93E-01	6.60E-03
Nominal/Good	High	No	1.00E+00	9.30E-06
		Yes	1.00E+00	1.60E-06
	Low	No	1.00E+00	9.30E-06
		Yes	1.00E+00	1.60E-06

Table 23. Conditional Probability Tabel for CFM E-5

PIF				Human Success Probability	Human Failure Probability
Execution Straightforward	Training	Work Practices	Recovery		
No	Poor	Nominal	No	9.00E-01	1.00E-01
			Yes	9.84E-01	1.60E-02
		Good	No	9.49E-01	5.10E-02
			Yes	9.95E-01	5.10E-03
	Good	Nominal	No	9.90E-01	9.60E-03
			Yes	9.99E-01	9.60E-04
		Good	No	9.96E-01	3.80E-03
			Yes	1.00E+00	3.80E-04
Yes	Poor	Nominal	No	9.90E-01	9.60E-03
			Yes	1.00E+00	1.30E-04
		Good	No	9.99E-01	9.80E-04
			Yes	1.00E+00	5.70E-05
	Good	Nominal	No	9.99E-01	8.00E-04
			Yes	1.00E+00	8.00E-05
		Good	No	1.00E+00	8.00E-05
			Yes	1.00E+00	1.00E-05

Table 24. Conditional Probability Tabel for CFM MP

PIF				Human Success Probability	Human Failure Probability
Workload	Procedures	Compensatory Factors	Recovery		
High	Complex	Not Present	No	9.06E-01	9.40E-02
			Yes	9.87E-01	1.30E-02
		Present	No	9.81E-01	1.90E-02
			Yes	9.97E-01	2.70E-03
	Simple	Not Present	No	9.87E-01	1.30E-02
			Yes	9.98E-01	1.90E-03
		Present	No	9.99E-01	1.00E-03
			Yes	1.00E+00	1.50E-04
Low	Complex	Not Present	No	9.64E-01	3.60E-02
			Yes	9.95E-01	5.10E-03
		Present	No	9.99E-01	1.30E-03
			Yes	1.00E+00	9.70E-05
	Simple	Not Present	No	9.99E-01	8.20E-04
			Yes	1.00E+00	1.20E-04
		Present	No	9.99E-01	8.20E-04
			Yes	1.00E+00	1.20E-04

Appendix D. DepHep4 HFE Combination Identification Results

Table 25. DepHep4 HFE Combinations for Event Sequence HTS-AL

Index	Pairs	Triplets	Quadruples
1	OA-A-X63-2,OA-C-CR3-X8-A	OA-A-X151-1-MT,OA-A-X86-1,OA-C-CR3-X8-A	OA-A-X102,OA-A-X151-1-MT,OA-A-X78,OA-C-CR3-X8-A
2	OA-A-X66-2,OA-C-CR3-X8-A	OA-A-X44-1,OA-A-X54-2-1,OA-C-CR3-X8-A	OA-A-X151-1-MT,OA-A-X78,OA-A-X92,OA-C-CR3-X8-A
3	OA-A-X57-1,OA-C-CR3-X8-A	OA-A-X151-1-MT,OA-A-X66-2,OA-C-CR3-X8-A	OA-A-X151-1-MT,OA-A-X78,OA-A-X96,OA-C-CR3-X8-A
4	OA-A-X60-1,OA-C-CR3-X8-A	OA-A-X44-1,OA-A-X48-1,OA-C-CR3-X8-A	OA-A-X102,OA-A-X151-1-MT,OA-A-X79,OA-C-CR3-X8-A
5	OA-A-X63-1,OA-C-CR3-X8-A	OA-A-X44-2,OA-A-X48-2,OA-C-CR3-X8-A	OA-A-X151-1-MT,OA-A-X79,OA-A-X92,OA-C-CR3-X8-A
6	OA-A-X66-1,OA-C-CR3-X8-A	OA-A-X151-1-MT,OA-A-X88-2,OA-C-CR3-X8-A	OA-A-X151-1-MT,OA-A-X79,OA-A-X96,OA-C-CR3-X8-A
7	OA-A-X57-2,OA-C-CR3-X8-A	OA-A-X151-1-MT,OA-A-X86-2,OA-C-CR3-X8-A	OA-A-X102,OA-A-X151-1-MT,OA-A-X81,OA-C-CR3-X8-A
8	OA-A-X60-2,OA-C-CR3-X8-A	OA-A-X151-1-MT,OA-A-X88-1,OA-C-CR3-X8-A	OA-A-X151-1-MT,OA-A-X81,OA-A-X92,OA-C-CR3-X8-A
9	OA-A-X57-1,OA-A-X151-1-MT	OA-A-X51-1-2,OA-A-X51-2-2,OA-C-CR3-X8-A	OA-A-X151-1-MT,OA-A-X81,OA-A-X96,OA-C-CR3-X8-A
10	OA-A-X60-1,OA-A-X151-1-MT	OA-A-X102,OA-A-X81,OA-C-CR3-X8-A	OA-A-X151-1-MT,OA-A-X88-1,OA-A-X88-2,OA-C-CR3-X8-A
11	OA-A-X63-1,OA-A-X151-1-MT	OA-A-X79,OA-A-X92,OA-C-CR3-X8-A	OA-A-X151-1-MT,OA-A-X86-2,OA-A-X88-1,OA-C-CR3-X8-A
12	OA-A-X66-1,OA-A-X151-1-MT	OA-A-X78,OA-A-X92,OA-C-CR3-X8-A	OA-A-X151-1-MT,OA-A-X86-1,OA-A-X88-2,OA-C-CR3-X8-A
13	OA-A-X57-2,OA-A-X151-1-MT	OA-A-X242-1,OA-A-X84,OA-C-CR3-X8-A	OA-A-X151-1-MT,OA-A-X86-1,OA-A-X86-2,OA-C-CR3-X8-A
14	OA-A-X60-2,OA-A-X151-1-MT	OA-A-X151-1-MT,OA-A-X48-2,OA-C-CR3-X8-A	OA-A-X151-1-MT,OA-A-X66-1,OA-A-X66-2,OA-C-CR3-X8-A
15	OA-A-X63-2,OA-A-X151-1-MT	OA-A-X151-1-MT,OA-A-X44-2,OA-C-CR3-X8-A	OA-A-X151-1-MT,OA-A-X63-2,OA-A-X66-1,OA-C-CR3-X8-A

16	OA-A-X66-2,OA-A-X151-1-MT	OA-A-X151-1-MT,OA-A-X54-1-1,OA-C-CR3-X8-A	OA-A-X151-1-MT,OA-A-X60-2,OA-A-X66-1,OA-C-CR3-X8-A
17	OA-A-X79,OA-C-CR3-X8-A	OA-A-X63-1,OA-A-X66-2,OA-C-CR3-X8-A	OA-A-X151-1-MT,OA-A-X57-2,OA-A-X66-1,OA-C-CR3-X8-A
18	OA-A-X81,OA-C-CR3-X8-A	OA-A-X63-1,OA-A-X63-2,OA-C-CR3-X8-A	OA-A-X151-1-MT,OA-A-X63-1,OA-A-X66-2,OA-C-CR3-X8-A
19	OA-A-X78,OA-C-CR3-X8-A	OA-A-X57-2,OA-A-X66-1,OA-C-CR3-X8-A	OA-A-X151-1-MT,OA-A-X63-1,OA-A-X63-2,OA-C-CR3-X8-A
20	OA-A-X81,OA-A-X151-1-MT		OA-A-X151-1-MT,OA-A-X60-2,OA-A-X63-1,OA-C-CR3-X8-A
21	OA-A-X79,OA-A-X151-1-MT		OA-A-X151-1-MT,OA-A-X57-2,OA-A-X63-1,OA-C-CR3-X8-A
22	OA-A-X78,OA-A-X151-1-MT		OA-A-X51-1-2,OA-A-X51-2-2,OA-A-X57-1,OA-C-CR3-X8-A
23	OA-A-X86-1,OA-C-CR3-X8-A	OA-A-X57-1,OA-A-X60-2,OA-C-CR3-X8-A	OA-A-X51-1-2,OA-A-X54-2-2,OA-A-X57-1,OA-C-CR3-X8-A
24	OA-A-X88-1,OA-C-CR3-X8-A	OA-A-X57-1,OA-A-X57-2,OA-C-CR3-X8-A	OA-A-X51-2-2,OA-A-X54-1-2,OA-A-X57-1,OA-C-CR3-X8-A
25	OA-A-X86-2,OA-C-CR3-X8-A	OA-A-X151-1-MT,OA-A-X60-2,OA-C-CR3-X8-A	OA-A-X54-1-2,OA-A-X54-2-2,OA-A-X57-1,OA-C-CR3-X8-A
26	OA-A-X88-2,OA-C-CR3-X8-A	OA-A-X151-1-MT,OA-A-X63-2,OA-C-CR3-X8-A	OA-A-X151-1-MT,OA-A-X60-1,OA-A-X66-2,OA-C-CR3-X8-A
27	OA-A-X88-2,OA-A-X151-1-MT	OA-A-X151-1-MT,OA-A-X51-1-2,OA-C-CR3-X8-A	OA-A-X151-1-MT,OA-A-X60-1,OA-A-X63-2,OA-C-CR3-X8-A
28	OA-A-X86-2,OA-A-X151-1-MT	OA-A-X151-1-MT,OA-A-X54-2-1,OA-C-CR3-X8-A	OA-A-X151-1-MT,OA-A-X60-1,OA-A-X60-2,OA-C-CR3-X8-A
29	OA-A-X88-1,OA-A-X151-1-MT	OA-A-X151-1-MT,OA-A-X51-2-1,OA-C-CR3-X8-A	OA-A-X151-1-MT,OA-A-X57-2,OA-A-X60-1,OA-C-CR3-X8-A
30	OA-A-X86-1,OA-A-X151-1-MT	OA-A-X151-1-MT,OA-A-X54-2-2,OA-C-CR3-X8-A	OA-A-X151-1-MT,OA-A-X57-1,OA-A-X66-2,OA-C-CR3-X8-A
31	OA-A-X44-2,OA-C-CR3-X8-A	OA-A-X57-2,OA-A-X60-1,OA-C-CR3-X8-A	OA-A-X151-1-MT,OA-A-X57-1,OA-A-X63-2,OA-C-CR3-X8-A
32	OA-A-X48-2,OA-C-CR3-X8-A	OA-A-X57-1,OA-A-X66-2,OA-C-CR3-X8-A	OA-A-X151-1-MT,OA-A-X57-1,OA-A-X60-2,OA-C-CR3-X8-A
33	OA-A-X44-1,OA-C-CR3-X8-A	OA-A-X151-1-MT,OA-A-X66-1,OA-C-CR3-X8-A	OA-A-X151-1-MT,OA-A-X57-1,OA-A-X57-2,OA-C-CR3-X8-A
34	OA-A-X48-1,OA-C-CR3-X8-A	OA-A-X57-1,OA-A-X63-2,OA-C-CR3-X8-A	OA-A-X151-1-MT,OA-A-X44-1,OA-A-X48-1,OA-C-CR3-X8-A
35	OA-A-X48-1,OA-A-X151-1-MT	OA-A-X51-2-2,OA-A-X63-1,OA-C-CR3-X8-A	OA-A-X151-1-MT,OA-A-X44-2,OA-A-X48-2,OA-C-CR3-X8-A

36	OA-A-X44-1,OA-A-X151-1-MT	OA-A-X54-2-1,OA-A-X60-2,OA-C-CR3-X8-A	OA-A-X151-1-MT,OA-A-X48-1,OA-A-X54-1-1,OA-C-CR3-X8-A
37	OA-A-X48-2,OA-A-X151-1-MT	OA-A-X51-2-1,OA-A-X60-2,OA-C-CR3-X8-A	OA-A-X151-1-MT,OA-A-X48-1,OA-A-X51-1-1,OA-C-CR3-X8-A
38	OA-A-X44-2,OA-A-X151-1-MT	OA-A-X54-2-2,OA-A-X60-1,OA-C-CR3-X8-A	OA-A-X51-1-1,OA-A-X51-2-1,OA-A-X57-2,OA-C-CR3-X8-A
39	OA-A-X84,OA-C-CR3-X8-A	OA-A-X44-2,OA-A-X54-2-2,OA-C-CR3-X8-A	OA-A-X51-1-1,OA-A-X54-2-1,OA-A-X57-2,OA-C-CR3-X8-A
40	OA-A-X51-1-2,OA-C-CR3-X8-A	OA-A-X60-2,OA-A-X63-1,OA-C-CR3-X8-A	OA-A-X51-2-1,OA-A-X54-1-1,OA-A-X57-2,OA-C-CR3-X8-A
41	OA-A-X54-1-2,OA-C-CR3-X8-A	OA-A-X57-2,OA-A-X63-1,OA-C-CR3-X8-A	OA-A-X54-1-1,OA-A-X54-2-1,OA-A-X57-2,OA-C-CR3-X8-A
42	OA-A-X51-1-1,OA-C-CR3-X8-A	OA-A-X151-1-MT,OA-A-X57-1,OA-C-CR3-X8-A	OA-A-X151-1-MT,OA-A-X48-2,OA-A-X54-1-2,OA-C-CR3-X8-A
43	OA-A-X54-1-1,OA-C-CR3-X8-A	OA-A-X60-1,OA-A-X66-2,OA-C-CR3-X8-A	OA-A-X151-1-MT,OA-A-X48-2,OA-A-X51-1-2,OA-C-CR3-X8-A
44	OA-A-X51-2-2,OA-C-CR3-X8-A	OA-A-X60-1,OA-A-X63-2,OA-C-CR3-X8-A	OA-A-X151-1-MT,OA-A-X44-1,OA-A-X54-2-1,OA-C-CR3-X8-A
45	OA-A-X54-2-2,OA-C-CR3-X8-A	OA-A-X151-1-MT,OA-A-X60-1,OA-C-CR3-X8-A	OA-A-X151-1-MT,OA-A-X44-1,OA-A-X51-2-1,OA-C-CR3-X8-A
46	OA-A-X51-2-1,OA-C-CR3-X8-A	OA-A-X60-1,OA-A-X60-2,OA-C-CR3-X8-A	OA-A-X151-1-MT,OA-A-X44-2,OA-A-X54-2-2,OA-C-CR3-X8-A
47	OA-A-X54-2-1,OA-C-CR3-X8-A	OA-A-X151-1-MT,OA-A-X63-1,OA-C-CR3-X8-A	OA-A-X151-1-MT,OA-A-X44-2,OA-A-X51-2-2,OA-C-CR3-X8-A
48	OA-A-X84,OA-A-X151-1-MT		OA-A-X151-1-MT,OA-A-X54-1-1,OA-A-X54-2-1,OA-C-CR3-X8-A
49	OA-A-X151-1,OA-C-CR3-X8-A	OA-A-X88-1,OA-A-X88-2,OA-C-CR3-X8-A	OA-A-X151-1-MT,OA-A-X51-2-1,OA-A-X54-1-1,OA-C-CR3-X8-A
50	OA-A-X88-1,OA-A-X88-2	OA-A-X44-2,OA-A-X51-2-2,OA-C-CR3-X8-A	OA-A-X151-1-MT,OA-A-X51-1-1,OA-A-X54-2-1,OA-C-CR3-X8-A
51	OA-A-X86-2,OA-A-X88-1	OA-A-X48-1,OA-A-X54-1-1,OA-C-CR3-X8-A	OA-A-X151-1-MT,OA-A-X51-1-1,OA-A-X51-2-1,OA-C-CR3-X8-A

52	OA-A-X86-1,OA-A-X88-2	OA-A-X48-1,OA-A-X51-1-1,OA-C-CR3-X8-A	OA-A-X151-1-MT,OA-A-X54-1-2,OA-A-X54-2-2,OA-C-CR3-X8-A
53	OA-A-X86-1,OA-A-X86-2	OA-A-X48-2,OA-A-X54-1-2,OA-C-CR3-X8-A	OA-A-X151-1-MT,OA-A-X51-2-2,OA-A-X54-1-2,OA-C-CR3-X8-A
54	OA-A-X81,OA-A-X96	OA-A-X44-2,OA-A-X60-1,OA-C-CR3-X8-A	OA-A-X51-1-2,OA-A-X51-2-2,OA-A-X60-1,OA-C-CR3-X8-A
55	OA-A-X81,OA-A-X92	OA-A-X44-1,OA-A-X57-2,OA-C-CR3-X8-A	OA-A-X51-1-2,OA-A-X54-2-2,OA-A-X60-1,OA-C-CR3-X8-A
56	OA-A-X79,OA-A-X96	OA-A-X54-2-1,OA-A-X66-2,OA-C-CR3-X8-A	OA-A-X51-2-2,OA-A-X54-1-2,OA-A-X60-1,OA-C-CR3-X8-A
57	OA-A-X79,OA-A-X92	OA-A-X51-2-1,OA-A-X66-2,OA-C-CR3-X8-A	OA-A-X54-1-2,OA-A-X54-2-2,OA-A-X60-1,OA-C-CR3-X8-A
58	OA-A-X78,OA-A-X96	OA-A-X51-2-2,OA-A-X66-1,OA-C-CR3-X8-A	OA-A-X151-1-MT,OA-A-X51-1-2,OA-A-X54-2-2,OA-C-CR3-X8-A
59	OA-A-X78,OA-A-X92	OA-A-X54-2-1,OA-A-X63-2,OA-C-CR3-X8-A	OA-A-X151-1-MT,OA-A-X51-1-2,OA-A-X51-2-2,OA-C-CR3-X8-A
60	OA-A-X54-1-1,OA-A-X151-1-MT	OA-A-X51-2-2,OA-A-X60-1,OA-C-CR3-X8-A	OA-A-X44-1,OA-A-X48-1,OA-A-X66-2,OA-C-CR3-X8-A
61	OA-A-X51-1-1,OA-A-X151-1-MT	OA-A-X54-2-1,OA-A-X57-2,OA-C-CR3-X8-A	OA-A-X44-2,OA-A-X48-2,OA-A-X66-1,OA-C-CR3-X8-A
62	OA-A-X54-1-2,OA-A-X151-1-MT	OA-A-X51-2-1,OA-A-X57-2,OA-C-CR3-X8-A	OA-A-X44-1,OA-A-X48-1,OA-A-X63-2,OA-C-CR3-X8-A
63	OA-A-X51-1-2,OA-A-X151-1-MT	OA-A-X54-2-2,OA-A-X57-1,OA-C-CR3-X8-A	OA-A-X44-2,OA-A-X48-2,OA-A-X63-1,OA-C-CR3-X8-A
64	OA-A-X54-2-1,OA-A-X151-1-MT	OA-A-X51-2-2,OA-A-X57-1,OA-C-CR3-X8-A	OA-A-X44-1,OA-A-X48-1,OA-A-X60-2,OA-C-CR3-X8-A
65	OA-A-X51-2-1,OA-A-X151-1-MT	OA-A-X54-1-1,OA-A-X66-2,OA-C-CR3-X8-A	OA-A-X44-2,OA-A-X48-2,OA-A-X60-1,OA-C-CR3-X8-A
66	OA-A-X54-2-2,OA-A-X151-1-MT	OA-A-X51-1-1,OA-A-X66-2,OA-C-CR3-X8-A	OA-A-X44-1,OA-A-X48-1,OA-A-X57-2,OA-C-CR3-X8-A
67	OA-A-X51-2-2,OA-A-X151-1-MT	OA-A-X54-1-2,OA-A-X66-1,OA-C-CR3-X8-A	OA-A-X44-2,OA-A-X48-2,OA-A-X57-1,OA-C-CR3-X8-A
68	OA-A-X66-1,OA-A-X66-2	OA-A-X48-2,OA-A-X51-1-2,OA-C-CR3-X8-A	OA-A-X44-1,OA-A-X54-2-1,OA-A-X66-2,OA-C-CR3-X8-A
69	OA-A-X63-2,OA-A-X66-1	OA-A-X54-1-1,OA-A-X54-2-1,OA-C-CR3-X8-A	OA-A-X44-1,OA-A-X51-2-1,OA-A-X66-2,OA-C-CR3-X8-A
70	OA-A-X60-2,OA-A-X66-1	OA-A-X51-2-1,OA-A-X54-1-1,OA-C-CR3-X8-A	OA-A-X51-1-1,OA-A-X51-2-1,OA-A-X60-2,OA-C-CR3-X8-A

71	OA-A-X57-2,OA-A-X66-1	OA-A-X51-1-1,OA-A-X54-2-1,OA-C-CR3-X8-A	OA-A-X51-1-1,OA-A-X54-2-1,OA-A-X60-2,OA-C-CR3-X8-A
72	OA-A-X63-1,OA-A-X66-2	OA-A-X51-1-1,OA-A-X51-2-1,OA-C-CR3-X8-A	OA-A-X51-2-1,OA-A-X54-1-1,OA-A-X60-2,OA-C-CR3-X8-A
73	OA-A-X63-1,OA-A-X63-2	OA-A-X54-1-2,OA-A-X54-2-2,OA-C-CR3-X8-A	OA-A-X54-1-1,OA-A-X54-2-1,OA-A-X60-2,OA-C-CR3-X8-A
74	OA-A-X60-2,OA-A-X63-1	OA-A-X51-2-2,OA-A-X54-1-2,OA-C-CR3-X8-A	OA-A-X44-2,OA-A-X54-2-2,OA-A-X66-1,OA-C-CR3-X8-A
75	OA-A-X57-2,OA-A-X63-1	OA-A-X51-1-2,OA-A-X54-2-2,OA-C-CR3-X8-A	OA-A-X44-2,OA-A-X51-2-2,OA-A-X66-1,OA-C-CR3-X8-A
76	OA-A-X60-1,OA-A-X66-2	OA-A-X81,OA-A-X96,OA-C-CR3-X8-A	OA-A-X44-1,OA-A-X54-2-1,OA-A-X63-2,OA-C-CR3-X8-A
77	OA-A-X60-1,OA-A-X63-2	OA-A-X81,OA-A-X92,OA-C-CR3-X8-A	OA-A-X44-1,OA-A-X51-2-1,OA-A-X63-2,OA-C-CR3-X8-A
78	OA-A-X60-1,OA-A-X60-2	OA-A-X79,OA-A-X96,OA-C-CR3-X8-A	OA-A-X44-2,OA-A-X54-2-2,OA-A-X63-1,OA-C-CR3-X8-A
79	OA-A-X57-2,OA-A-X60-1	OA-A-X102,OA-A-X79,OA-C-CR3-X8-A	OA-A-X44-2,OA-A-X51-2-2,OA-A-X63-1,OA-C-CR3-X8-A
80	OA-A-X57-1,OA-A-X66-2	OA-A-X78,OA-A-X96,OA-C-CR3-X8-A	OA-A-X44-1,OA-A-X54-2-1,OA-A-X60-2,OA-C-CR3-X8-A
81	OA-A-X57-1,OA-A-X63-2	OA-A-X102,OA-A-X78,OA-C-CR3-X8-A	OA-A-X44-1,OA-A-X51-2-1,OA-A-X60-2,OA-C-CR3-X8-A
82	OA-A-X57-1,OA-A-X60-2	OA-A-X151-1-MT,OA-A-X48-1,OA-C-CR3-X8-A	OA-A-X44-2,OA-A-X54-2-2,OA-A-X60-1,OA-C-CR3-X8-A
83	OA-A-X57-1,OA-A-X57-2	OA-A-X151-1-MT,OA-A-X44-1,OA-C-CR3-X8-A	OA-A-X44-2,OA-A-X51-2-2,OA-A-X60-1,OA-C-CR3-X8-A
84	OA-A-X102,OA-C-CR3-X8-A	OA-A-X66-1,OA-A-X66-2,OA-C-CR3-X8-A	OA-A-X44-1,OA-A-X54-2-1,OA-A-X57-2,OA-C-CR3-X8-A
85	OA-A-X92,OA-C-CR3-X8-A	OA-A-X63-2,OA-A-X66-1,OA-C-CR3-X8-A	OA-A-X44-1,OA-A-X51-2-1,OA-A-X57-2,OA-C-CR3-X8-A
86	OA-A-X96,OA-C-CR3-X8-A	OA-A-X60-2,OA-A-X66-1,OA-C-CR3-X8-A	OA-A-X51-1-2,OA-A-X51-2-2,OA-A-X63-1,OA-C-CR3-X8-A
87	OA-A-X96,OA-A-X151-1-MT		OA-A-X51-1-2,OA-A-X54-2-2,OA-A-X63-1,OA-C-CR3-X8-A
88	OA-A-X92,OA-A-X151-1-MT		OA-A-X51-2-2,OA-A-X54-1-2,OA-A-X63-1,OA-C-CR3-X8-A
89	OA-A-X102,OA-A-X151-1-MT		OA-A-X54-1-2,OA-A-X54-2-2,OA-A-X63-1,OA-C-CR3-X8-A
90	OA-A-X151-1-MT,OA-C-CR3-X8-A	OA-A-X44-1,OA-A-X51-2-1,OA-C-CR3-X8-A	OA-A-X44-2,OA-A-X54-2-2,OA-A-X57-1,OA-C-CR3-X8-A

91	OA-A-X44-1,OA-A-X48-1	OA-A-X151-1-MT,OA-A-X51-1-1,OA-C-CR3-X8-A	OA-A-X44-2,OA-A-X51-2-2,OA-A-X57-1,OA-C-CR3-X8-A
92	OA-A-X44-2,OA-A-X48-2	OA-A-X151-1-MT,OA-A-X54-1-2,OA-C-CR3-X8-A	OA-A-X48-1,OA-A-X54-1-1,OA-A-X66-2,OA-C-CR3-X8-A
93	OA-A-X44-1,OA-A-X54-2-1	OA-A-X151-1-MT,OA-A-X51-2-2,OA-C-CR3-X8-A	OA-A-X48-1,OA-A-X51-1-1,OA-A-X66-2,OA-C-CR3-X8-A
94	OA-A-X44-1,OA-A-X51-2-1	OA-A-X48-1,OA-A-X66-2,OA-C-CR3-X8-A	OA-A-X48-2,OA-A-X54-1-2,OA-A-X66-1,OA-C-CR3-X8-A
95	OA-A-X44-2,OA-A-X54-2-2	OA-A-X48-2,OA-A-X66-1,OA-C-CR3-X8-A	OA-A-X48-2,OA-A-X51-1-2,OA-A-X66-1,OA-C-CR3-X8-A
96	OA-A-X44-2,OA-A-X51-2-2	OA-A-X48-1,OA-A-X63-2,OA-C-CR3-X8-A	OA-A-X48-1,OA-A-X54-1-1,OA-A-X63-2,OA-C-CR3-X8-A
97	OA-A-X48-1,OA-A-X54-1-1	OA-A-X48-2,OA-A-X63-1,OA-C-CR3-X8-A	OA-A-X48-1,OA-A-X51-1-1,OA-A-X63-2,OA-C-CR3-X8-A
98	OA-A-X48-1,OA-A-X51-1-1	OA-A-X48-1,OA-A-X60-2,OA-C-CR3-X8-A	OA-A-X48-2,OA-A-X54-1-2,OA-A-X63-1,OA-C-CR3-X8-A
99	OA-A-X48-2,OA-A-X54-1-2	OA-A-X48-2,OA-A-X60-1,OA-C-CR3-X8-A	OA-A-X48-2,OA-A-X51-1-2,OA-A-X63-1,OA-C-CR3-X8-A
100	OA-A-X48-2,OA-A-X51-1-2	OA-A-X151-1-MT,OA-B-X172,OA-C-CR3-X8-A	OA-A-X48-1,OA-A-X54-1-1,OA-A-X60-2,OA-C-CR3-X8-A
101	OA-A-X54-1-1,OA-A-X54-2-1	OA-A-X151-1-MT,OA-B-X98,OA-C-CR3-X8-A	OA-A-X48-1,OA-A-X51-1-1,OA-A-X60-2,OA-C-CR3-X8-A
102	OA-A-X51-2-1,OA-A-X54-1-1	OA-A-X48-1,OA-A-X57-2,OA-C-CR3-X8-A	OA-A-X51-1-1,OA-A-X51-2-1,OA-A-X63-2,OA-C-CR3-X8-A
103	OA-A-X51-1-1,OA-A-X54-2-1	OA-A-X48-2,OA-A-X57-1,OA-C-CR3-X8-A	OA-A-X51-1-1,OA-A-X54-2-1,OA-A-X63-2,OA-C-CR3-X8-A
104	OA-A-X51-1-1,OA-A-X51-2-1	OA-A-X44-1,OA-A-X66-2,OA-C-CR3-X8-A	OA-A-X51-2-1,OA-A-X54-1-1,OA-A-X63-2,OA-C-CR3-X8-A
105	OA-A-X54-1-2,OA-A-X54-2-2	OA-A-X44-2,OA-A-X66-1,OA-C-CR3-X8-A	OA-A-X54-1-1,OA-A-X54-2-1,OA-A-X63-2,OA-C-CR3-X8-A
106	OA-A-X51-2-2,OA-A-X54-1-2	OA-A-X44-1,OA-A-X63-2,OA-C-CR3-X8-A	OA-A-X48-2,OA-A-X54-1-2,OA-A-X60-1,OA-C-CR3-X8-A
107	OA-A-X51-1-2,OA-A-X54-2-2	OA-A-X44-2,OA-A-X63-1,OA-C-CR3-X8-A	OA-A-X48-2,OA-A-X51-1-2,OA-A-X60-1,OA-C-CR3-X8-A
108	OA-A-X51-1-2,OA-A-X51-2-2	OA-A-X44-1,OA-A-X60-2,OA-C-CR3-X8-A	OA-A-X48-1,OA-A-X54-1-1,OA-A-X57-2,OA-C-CR3-X8-A
109	OA-A-X102,OA-A-X81	OA-A-X44-2,OA-A-X57-1,OA-C-CR3-X8-A	OA-A-X48-1,OA-A-X51-1-1,OA-A-X57-2,OA-C-CR3-X8-A
110	OA-A-X102,OA-A-X79	OA-A-X54-2-2,OA-A-X66-1,OA-C-CR3-X8-A	OA-A-X48-2,OA-A-X54-1-2,OA-A-X57-1,OA-C-CR3-X8-A
111	OA-A-X102,OA-A-X78	OA-A-X51-2-1,OA-A-X63-2,OA-C-CR3-X8-A	OA-A-X48-2,OA-A-X51-1-2,OA-A-X57-1,OA-C-CR3-X8-A

112	OA-A-X242-1,OA-C-CR3-X8-A	OA-A-X151-1-MT,OA-A-X57-2,OA-C-CR3-X8-A	OA-A-X54-1-1,OA-A-X54-2-1,OA-A-X66-2,OA-C-CR3-X8-A
113	OA-A-X48-1,OA-A-X66-2	OA-A-X51-1-2,OA-A-X66-1,OA-C-CR3-X8-A	OA-A-X51-2-1,OA-A-X54-1-1,OA-A-X66-2,OA-C-CR3-X8-A
114	OA-A-X48-2,OA-A-X66-1	OA-A-X54-1-1,OA-A-X63-2,OA-C-CR3-X8-A	OA-A-X51-1-1,OA-A-X54-2-1,OA-A-X66-2,OA-C-CR3-X8-A
115	OA-A-X48-1,OA-A-X63-2	OA-A-X51-1-1,OA-A-X63-2,OA-C-CR3-X8-A	OA-A-X51-1-1,OA-A-X51-2-1,OA-A-X66-2,OA-C-CR3-X8-A
116	OA-A-X48-2,OA-A-X63-1	OA-A-X54-1-2,OA-A-X63-1,OA-C-CR3-X8-A	OA-A-X54-1-2,OA-A-X54-2-2,OA-A-X66-1,OA-C-CR3-X8-A
117	OA-A-X48-1,OA-A-X60-2	OA-A-X51-1-2,OA-A-X63-1,OA-C-CR3-X8-A	OA-A-X51-2-2,OA-A-X54-1-2,OA-A-X66-1,OA-C-CR3-X8-A
118	OA-A-X48-2,OA-A-X60-1	OA-A-X54-1-1,OA-A-X60-2,OA-C-CR3-X8-A	OA-A-X51-1-2,OA-A-X51-2-2,OA-A-X66-1,OA-C-CR3-X8-A
119	OA-A-X48-1,OA-A-X57-2	OA-A-X51-1-2,OA-A-X60-1,OA-C-CR3-X8-A	OA-A-X51-1-2,OA-A-X54-2-2,OA-A-X66-1,OA-C-CR3-X8-A
120	OA-A-X48-2,OA-A-X57-1	OA-A-X54-1-1,OA-A-X57-2,OA-C-CR3-X8-A	-
121	OA-A-X44-1,OA-A-X66-2	OA-A-X51-1-1,OA-A-X57-2,OA-C-CR3-X8-A	-
122	OA-A-X44-2,OA-A-X66-1	OA-A-X54-1-2,OA-A-X57-1,OA-C-CR3-X8-A	-
123	OA-A-X44-1,OA-A-X63-2	OA-A-X51-1-2,OA-A-X57-1,OA-C-CR3-X8-A	-
124	OA-A-X44-2,OA-A-X63-1	OA-A-X151-1-MT,OA-A-X81,OA-C-CR3-X8-A	-
125	OA-A-X44-1,OA-A-X60-2	OA-A-X151-1-MT,OA-A-X79,OA-C-CR3-X8-A	-
126	OA-A-X44-2,OA-A-X60-1	OA-A-X151-1-MT,OA-A-X78,OA-C-CR3-X8-A	-
127	OA-A-X44-1,OA-A-X57-2	OA-A-X240-1,OA-A-X242-1,OA-C-CR3-X8-A	-
128	OA-A-X44-2,OA-A-X57-1	OA-A-X151-1-MT,OA-A-X96,OA-C-CR3-X8-A	-
129	OA-A-X54-2-1,OA-A-X66-2	OA-A-X151-1-MT,OA-A-X92,OA-C-CR3-X8-A	-
130	OA-A-X51-2-1,OA-A-X66-2	OA-A-X102,OA-A-X151-1-MT,OA-C-CR3-X8-A	-
131	OA-A-X54-2-2,OA-A-X66-1	OA-A-X242-1,OA-A-X66-2,OA-C-CR3-X8-A	-
132	OA-A-X51-2-2,OA-A-X66-1	OA-A-X242-1,OA-A-X63-2,OA-C-CR3-X8-A	-
133	OA-A-X54-2-1,OA-A-X63-2	OA-A-X242-1,OA-A-X60-2,OA-C-CR3-X8-A	-
134	OA-A-X51-2-1,OA-A-X63-2	OA-A-X242-1,OA-A-X57-2,OA-C-CR3-X8-A	-

135	OA-A-X54-2-2,OA-A-X63-1	OA-A-X242-1,OA-A-X66-1,OA-C-CR3-X8-A	-
136	OA-A-X51-2-2,OA-A-X63-1	OA-A-X242-1,OA-A-X63-1,OA-C-CR3-X8-A	-
137	OA-A-X54-2-1,OA-A-X60-2	OA-A-X242-1,OA-A-X60-1,OA-C-CR3-X8-A	-
138	OA-A-X51-2-1,OA-A-X60-2	OA-A-X242-1,OA-A-X57-1,OA-C-CR3-X8-A	-
139	OA-A-X54-2-2,OA-A-X60-1	OA-A-X81,OA-B-X98,OA-C-CR3-X8-A	-
140	OA-A-X51-2-2,OA-A-X60-1	OA-A-X81,OA-B-X172,OA-C-CR3-X8-A	-
141	OA-A-X54-2-1,OA-A-X57-2	OA-A-X79,OA-B-X98,OA-C-CR3-X8-A	-
142	OA-A-X51-2-1,OA-A-X57-2	OA-A-X79,OA-B-X172,OA-C-CR3-X8-A	-
143	OA-A-X54-2-2,OA-A-X57-1	OA-A-X78,OA-B-X98,OA-C-CR3-X8-A	-
144	OA-A-X51-2-2,OA-A-X57-1	OA-A-X78,OA-B-X172,OA-C-CR3-X8-A	-
145	OA-A-X54-1-1,OA-A-X66-2	OA-A-X240-1,OA-A-X84,OA-C-CR3-X8-A	-
146	OA-A-X51-1-1,OA-A-X66-2	OA-A-X151-1-MT,OA-A-X84,OA-C-CR3-X8-A	-
147	OA-A-X54-1-2,OA-A-X66-1	OA-A-X242-1,OA-A-X88-1,OA-C-CR3-X8-A	-
148	OA-A-X51-1-2,OA-A-X66-1	OA-A-X242-1,OA-A-X86-1,OA-C-CR3-X8-A	-
149	OA-A-X54-1-1,OA-A-X63-2	OA-A-X242-1,OA-A-X88-2,OA-C-CR3-X8-A	-
150	OA-A-X51-1-1,OA-A-X63-2	OA-A-X242-1,OA-A-X86-2,OA-C-CR3-X8-A	-
151	OA-A-X54-1-2,OA-A-X63-1	-	-
152	OA-A-X51-1-2,OA-A-X63-1	-	-
153	OA-A-X54-1-1,OA-A-X60-2	-	-
154	OA-A-X51-1-1,OA-A-X60-2	-	-
155	OA-A-X54-1-2,OA-A-X60-1	-	-
156	OA-A-X51-1-2,OA-A-X60-1	-	-
157	OA-A-X54-1-1,OA-A-X57-2	-	-

158	OA-A-X51-1-1,OA-A-X57-2	-	-
159	OA-A-X54-1-2,OA-A-X57-1	-	-
160	OA-A-X51-1-2,OA-A-X57-1	-	-
161	OA-A-X81,OA-B-X98	-	-
162	OA-A-X81,OA-B-X172	-	-
163	OA-A-X79,OA-B-X98	-	-
164	OA-A-X79,OA-B-X172	-	-
165	OA-A-X78,OA-B-X98	-	-
166	OA-A-X78,OA-B-X172	-	-
167	OA-A-X240-1,OA-C-CR3-X8-A	OA-A-X86-1,OA-A-X86-2,OA-C-CR3-X8-A	-
168	OA-A-X240-1,OA-A-X242-1	-	-
169	OA-A-X242-1,OA-A-X84	OA-A-X54-2-2,OA-A-X63-1,OA-C-CR3-X8-A	-
170	OA-A-X242-1,OA-A-X66-2	-	-
171	OA-A-X242-1,OA-A-X63-2	-	-
172	OA-A-X242-1,OA-A-X60-2	-	-
173	OA-A-X242-1,OA-A-X57-2	-	-
174	OA-A-X242-1,OA-A-X66-1	-	-
175	OA-A-X242-1,OA-A-X63-1	-	-
176	OA-A-X242-1,OA-A-X60-1	-	-
177	OA-A-X242-1,OA-A-X57-1	-	-
178	OA-A-X240-1,OA-A-X84	-	-
179	OA-A-X242-1,OA-A-X88-1	-	-
180	OA-A-X242-1,OA-A-X86-1	-	-

181	OA-A-X242-1,OA-A-X88-2	-	-
182	OA-A-X242-1,OA-A-X86-2	-	-
183	OA-B-X172,OA-C-CR3-X8-A	OA-A-X86-2,OA-A-X88-1,OA-C-CR3-X8-A	-
184	OA-B-X98,OA-C-CR3-X8-A	OA-A-X86-1,OA-A-X88-2,OA-C-CR3-X8-A	-
185	OA-B-X172,OA-A-X151-1-MT	OA-A-X51-1-1,OA-A-X60-2,OA-C-CR3-X8-A	-
186	OA-B-X98,OA-A-X151-1-MT	OA-A-X54-1-2,OA-A-X60-1,OA-C-CR3-X8-A	-

Table 26. DepHep4 HFE Combinations for Event Sequence PC-AU

Index	Pairs	Triplets	Quadruples
1	OA-A-X151-1,OA-A-X84-MT	-	-
2	OA-A-X151-1,OA-C-A7	-	-
3	OA-A-X151-1,OA-A-X66-MT1	-	-
4	OA-A-X151-1,OA-A-X63-MT1	-	-
5	OA-A-X151-1,OA-A-X60-MT1	-	-
6	OA-A-X151-1,OA-A-X57-MT1	-	-
7	OA-A-X151-1,OA-A-X66-MT2	-	-
8	OA-A-X151-1,OA-A-X63-MT2	-	-
9	OA-A-X151-1,OA-A-X60-MT2	-	-
10	OA-A-X151-1,OA-A-X57-MT2	-	-
11	OA-A-X84-MT,OA-C-A7	-	-
12	OA-A-X151-1-MT,OA-C-A7	OA-A-X151-1,OA-A-X84-MT,OA-C-A7	-

Table 27. DepHep4 HFE Combinations for Event Sequence RS-AP

Index	Pairs	Triplets	Quadruples
1	OA-A-X151-1,OA-C-CR3-X8-A	OA-A-X151-1,OA-A-X60-MT1,OA-C-CR3-X8-A	OA-A-X151-1,OA-A-X57-MT1,OA-A-X57-MT2,OA-C-CR3-X8-A
2	OA-A-X151-1,OA-A-X81-MT	-	OA-A-X151-1,OA-A-X57-MT1,OA-A-X60-MT2,OA-C-CR3-X8-A

3	OA-A-X151-1,OA-A-X79-MT	-	OA-A-X151-1,OA-A-X57-MT1,OA-A-X63-MT2,OA-C-CR3-X8-A
4	OA-A-X151-1,OA-A-X78-MT	-	OA-A-X151-1,OA-A-X57-MT1,OA-A-X66-MT2,OA-C-CR3-X8-A
5	OA-A-X151-1,OA-A-X66-MT1	OA-A-X78-MT,OA-B-X172-MT,OA-C-CR3-X8-A	OA-A-X151-1,OA-A-X57-MT2,OA-A-X60-MT1,OA-C-CR3-X8-A
6	OA-A-X151-1,OA-A-X63-MT1	OA-A-X242-1,OA-A-X84-MT,OA-C-CR3-X8-A	OA-A-X151-1,OA-A-X60-MT1,OA-A-X60-MT2,OA-C-CR3-X8-A
7	OA-A-X151-1,OA-A-X60-MT1	OA-A-X240-1,OA-A-X242-1,OA-C-CR3-X8-A	OA-A-X151-1,OA-A-X60-MT1,OA-A-X63-MT2,OA-C-CR3-X8-A
8	OA-A-X151-1,OA-A-X57-MT1	OA-A-X151-1,OA-A-X84-MT,OA-C-CR3-X8-A	OA-A-X151-1,OA-A-X60-MT1,OA-A-X66-MT2,OA-C-CR3-X8-A
9	OA-A-X151-1,OA-A-X66-MT2	-	OA-A-X151-1,OA-A-X57-MT2,OA-A-X63-MT1,OA-C-CR3-X8-A
10	OA-A-X151-1,OA-A-X63-MT2	-	OA-A-X151-1,OA-A-X60-MT2,OA-A-X63-MT1,OA-C-CR3-X8-A
11	OA-A-X151-1,OA-A-X60-MT2	-	OA-A-X151-1,OA-A-X63-MT1,OA-A-X63-MT2,OA-C-CR3-X8-A
12	OA-A-X151-1,OA-A-X57-MT2	-	OA-A-X151-1,OA-A-X63-MT1,OA-A-X66-MT2,OA-C-CR3-X8-A
13	OA-A-X151-1,OA-B-X98-MT	-	OA-A-X151-1,OA-A-X57-MT2,OA-A-X66-MT1,OA-C-CR3-X8-A
14	OA-A-X151-1,OA-B-X172-MT	-	OA-A-X151-1,OA-A-X60-MT2,OA-A-X66-MT1,OA-C-CR3-X8-A
15	OA-A-X151-1,OA-A-X96-MT	-	OA-A-X151-1,OA-A-X63-MT2,OA-A-X66-MT1,OA-C-CR3-X8-A
16	OA-A-X151-1,OA-A-X92-MT	-	OA-A-X151-1,OA-A-X66-MT1,OA-A-X66-MT2,OA-C-CR3-X8-A
17	OA-A-X151-1,OA-A-X102-MT	-	OA-A-X102-MT,OA-A-X151-1,OA-A-X78-MT,OA-C-CR3-X8-A

18	OA-A-X151-1,OA-A-X88-2-MT	-	OA-A-X151-1,OA-A-X78-MT,OA-A-X92-MT,OA-C-CR3-X8-A
19	OA-A-X151-1,OA-A-X86-2-MT	-	OA-A-X151-1,OA-A-X78-MT,OA-A-X96-MT,OA-C-CR3-X8-A
20	OA-A-X151-1,OA-A-X88-1-MT	-	OA-A-X102-MT,OA-A-X151-1,OA-A-X79-MT,OA-C-CR3-X8-A
21	OA-A-X151-1,OA-A-X86-1-MT	-	OA-A-X151-1,OA-A-X79-MT,OA-A-X92-MT,OA-C-CR3-X8-A
22	OA-A-X151-1,OA-A-X84-MT	-	OA-A-X151-1,OA-A-X79-MT,OA-A-X96-MT,OA-C-CR3-X8-A
23	OA-B-X172-MT,OA-C-CR3-X8-A	OA-A-X151-1,OA-A-X57-MT1,OA-C-CR3-X8-A	OA-A-X102-MT,OA-A-X151-1,OA-A-X81-MT,OA-C-CR3-X8-A
24	OA-A-X78-MT,OA-C-CR3-X8-A	OA-A-X151-1,OA-A-X86-2-MT,OA-C-CR3-X8-A	OA-A-X151-1,OA-A-X81-MT,OA-A-X92-MT,OA-C-CR3-X8-A
25	OA-A-X81-MT,OA-C-CR3-X8-A	OA-A-X151-1,OA-B-X172-MT,OA-C-CR3-X8-A	OA-A-X151-1,OA-A-X81-MT,OA-A-X96-MT,OA-C-CR3-X8-A
26	OA-A-X79-MT,OA-C-CR3-X8-A	OA-A-X151-1,OA-A-X88-2-MT,OA-C-CR3-X8-A	OA-A-X151-1,OA-A-X86-1-MT,OA-A-X86-2-MT,OA-C-CR3-X8-A
27	OA-A-X66-MT2,OA-C-CR3-X8-A	OA-A-X102-MT,OA-A-X151-1,OA-C-CR3-X8-A	OA-A-X151-1,OA-A-X86-1-MT,OA-A-X88-2-MT,OA-C-CR3-X8-A
28	OA-A-X57-MT1,OA-C-CR3-X8-A	OA-A-X81-MT,OA-B-X98-MT,OA-C-CR3-X8-A	OA-A-X151-1,OA-A-X86-2-MT,OA-A-X88-1-MT,OA-C-CR3-X8-A
29	OA-A-X60-MT1,OA-C-CR3-X8-A	OA-A-X81-MT,OA-B-X172-MT,OA-C-CR3-X8-A	OA-A-X151-1,OA-A-X88-1-MT,OA-A-X88-2-MT,OA-C-CR3-X8-A
30	OA-A-X63-MT1,OA-C-CR3-X8-A	OA-A-X79-MT,OA-B-X98-MT,OA-C-CR3-X8-A	OA-A-X151-1,OA-A-X78-MT,OA-B-X172-MT,OA-C-CR3-X8-A
31	OA-A-X66-MT1,OA-C-CR3-X8-A	OA-A-X79-MT,OA-B-X172-MT,OA-C-CR3-X8-A	OA-A-X151-1,OA-A-X78-MT,OA-B-X98-MT,OA-C-CR3-X8-A
32	OA-A-X57-MT2,OA-C-CR3-X8-A	OA-A-X151-1,OA-A-X78-MT,OA-C-CR3-X8-A	OA-A-X151-1,OA-A-X79-MT,OA-B-X172-MT,OA-C-CR3-X8-A

33	OA-A-X60-MT2,OA-C-CR3-X8-A	OA-A-X151-1,OA-A-X96-MT,OA-C-CR3-X8-A	OA-A-X151-1,OA-A-X79-MT,OA-B-X98-MT,OA-C-CR3-X8-A
34	OA-A-X63-MT2,OA-C-CR3-X8-A	OA-A-X151-1,OA-A-X92-MT,OA-C-CR3-X8-A	OA-A-X151-1,OA-A-X81-MT,OA-B-X172-MT,OA-C-CR3-X8-A
35	OA-A-X92-MT,OA-C-CR3-X8-A	OA-A-X151-1,OA-A-X81-MT,OA-C-CR3-X8-A	OA-A-X151-1,OA-A-X81-MT,OA-B-X98-MT,OA-C-CR3-X8-A
36	OA-A-X102-MT,OA-C-CR3-X8-A	OA-A-X151-1,OA-A-X79-MT,OA-C-CR3-X8-A	-
37	OA-A-X96-MT,OA-C-CR3-X8-A	OA-A-X151-1,OA-A-X86-1-MT,OA-C-CR3-X8-A	-
38	OA-A-X88-2-MT,OA-C-CR3-X8-A	OA-A-X151-1,OA-A-X63-MT2,OA-C-CR3-X8-A	-
39	OA-A-X86-2-MT,OA-C-CR3-X8-A	OA-A-X151-1,OA-A-X60-MT2,OA-C-CR3-X8-A	-
40	OA-A-X88-1-MT,OA-C-CR3-X8-A	OA-A-X151-1,OA-A-X57-MT2,OA-C-CR3-X8-A	-
41	OA-A-X86-1-MT,OA-C-CR3-X8-A	OA-A-X151-1,OA-B-X98-MT,OA-C-CR3-X8-A	-
42	OA-A-X84-MT,OA-C-CR3-X8-A	OA-A-X78-MT,OA-B-X98-MT,OA-C-CR3-X8-A	-
43	OA-A-X151-1-MT,OA-C-CR3-X8-A	OA-A-X151-1,OA-A-X66-MT1,OA-C-CR3-X8-A	-
44	OA-A-X81-MT,OA-B-X98-MT	-	-
45	OA-A-X81-MT,OA-B-X172-MT	-	-
46	OA-A-X79-MT,OA-B-X98-MT	-	-
47	OA-A-X79-MT,OA-B-X172-MT	-	-
48	OA-A-X78-MT,OA-B-X98-MT	-	-

49	OA-A-X78-MT,OA-B-X172-MT	-	-
50	OA-A-X102-MT,OA-A-X78-MT	-	-
51	OA-A-X78-MT,OA-A-X92-MT	-	-
52	OA-A-X78-MT,OA-A-X96-MT	-	-
53	OA-A-X102-MT,OA-A-X79-MT	-	-
54	OA-A-X79-MT,OA-A-X92-MT	-	-
55	OA-A-X79-MT,OA-A-X96-MT	-	-
56	OA-A-X102-MT,OA-A-X81-MT	-	-
57	OA-A-X81-MT,OA-A-X92-MT	-	-
58	OA-A-X81-MT,OA-A-X96-MT	-	-
59	OA-A-X86-1-MT,OA-A-X86-2-MT	-	-
60	OA-A-X86-1-MT,OA-A-X88-2-MT	-	-
61	OA-A-X86-2-MT,OA-A-X88-1-MT	-	-
62	OA-A-X88-1-MT,OA-A-X88-2-MT	-	-
63	OA-A-X57-MT1,OA-A-X57-MT2	-	-
64	OA-A-X57-MT1,OA-A-X60-MT2	-	-
65	OA-A-X57-MT1,OA-A-X63-MT2	-	-
66	OA-A-X57-MT1,OA-A-X66-MT2	-	-

67	OA-A-X57-MT2,OA-A-X60-MT1	-	-
68	OA-A-X60-MT1,OA-A-X60-MT2	-	-
69	OA-A-X60-MT1,OA-A-X63-MT2	-	-
70	OA-A-X60-MT1,OA-A-X66-MT2	-	-
71	OA-A-X57-MT2,OA-A-X63-MT1	-	-
72	OA-A-X60-MT2,OA-A-X63-MT1	-	-
73	OA-A-X63-MT1,OA-A-X63-MT2	-	-
74	OA-A-X63-MT1,OA-A-X66-MT2	-	-
75	OA-A-X57-MT2,OA-A-X66-MT1	-	-
76	OA-A-X60-MT2,OA-A-X66-MT1	-	-
77	OA-A-X63-MT2,OA-A-X66-MT1	-	-
78	OA-A-X66-MT1,OA-A-X66-MT2	-	-
79	OA-A-X242-1,OA-C-CR3-X8-A	OA-A-X151-1,OA-A-X88-1-MT,OA-C-CR3-X8-A	-
80	OA-A-X242-1,OA-A-X84-MT		-
81	OA-A-X240-1,OA-C-CR3-X8-A	OA-A-X151-1,OA-A-X66-MT2,OA-C-CR3-X8-A	-
82	OA-A-X240-1,OA-A-X242-1	-	-

83	OA-B-X98-MT,OA-C-CR3-X8-A	OA-A-X151-1,OA-A-X63-MT1,OA-C-CR3-X8-A	-

Table 28. DepHep4 HFE Combinations for Event Sequence MS-CG

Index	Pairs	Triplets	Quadruples
1	OA-A-X151-1,OA-C-MOIST-DETECT-1	OA-A-X240-1,OA-A-X242-1,OA-C-MOIST-DETECT-1	-
2	OA-A-X242-1,OA-C-MOIST-DETECT-1	-	-
3	OA-A-X151-1-MT,OA-C-MOIST-DETECT-1	-	-
4	OA-A-X240-1,OA-C-MOIST-DETECT-1	-	-
5	OA-A-X240-1,OA-A-X242-1	-	-
6	OA-C-MOIST-DETECT-1,OA-C-Z20-1	-	-
7	A-A-X151-1,OA-C-MOIST-DETECT-1	-	-

Appendix E. IDHEAS-ECA Assumptions

Table 29 lists the assumptions made in quantifying the failure probability associated with the operator action OA-A-X81-MT-HF. It should be noted that this operator action has only the cognitive failure mode of action execution; hence, the attribute assumptions listed in Table 29 relates only to this CFM.

Table 29. IDHEAS-ECA Assumptions for OA-A-X81-MT-HF

Attribute	Assumptions for Independent HFT	Assumptions for Dependent HFT
Scenario Familiarity	SF0: No Impact	SF0: No Impact
Task Complexity	C31: Straightforward Procedure Execution with Many Steps	C31: Straightforward Procedure Execution with Many Steps
Environmental Factors	ENV0: No Impact	ENV0: No Impact
System and IC Transparency	SIC0: No Impact	SIC0: No Impact
Human-System Interface	HSI8: Similarity in Elements	HSI8: Similarity in Elements
Critical Tools and Parts	TP3: Tool Does Not Work Properly	TP3: Tool Does Not Work Properly
Training and Experience	TE5: Operator is Inexperienced	TE5: Operator is Inexperienced
Team Factors	-	TF2: Poor Command and Control
Mental Fatigue, Stress, and Time Pressure	-	MF2: Time Pressure due to Perceived Time Urgency
		MF6: Sudden Increase Workload from Low of a Long Period to High

Appendix F. G-PWR List of Operator Actions

Table 30. Generic Pressurized Water Reactor Operator Action List

Operator Action	Initial Failure Probability
OA-EPS-XHE-XM-DGSEQ	1.00E+00
OA-HPI-XHE-XM-FAB	2.00E-02
OA-HPR-XHE-XM-RC	1.00E-03
OA-OEP-XHE-XL-NR02H	4.70E-01
OA-PWR-XHE-XM-DEPRCS	4.00E-03
OA-RHR-XHE-XM-OPERATE	2.00E-02
OA-RPS-XHE-XM-NSIGNL	1.13E-01
OA-RPS-XHE-XM-SIGNL	9.95E-03
OA-SWS-XHE-XM-TRNC	1.00E-03
OP-CCW-XHE-XM-TRNC	1.00E-03